

City Research Online

City St George's, University of London

Citation: Wijeyeratne, Y. D. (2021). SCN5A-E1784K long QT and brugada overlap syndrome: phenotype, risk, genetic modifiers and functional characterisation. (Unpublished Doctoral thesis, St George's, University of London)

This is the accepted version of the paper.

This version of the publication may differ from the final published version. To cite this item please consult the publisher's version.

Permanent repository link: https://openaccess.city.ac.uk/id/eprint/37095/

Copyright and Reuse: Copyright and Moral Rights remain with the author(s) and/or copyright holders. Copies of full items can be used for personal research or study, educational, or not-for-profit purposes without prior permission or charge, unless otherwise indicated, provided that the authors, title and full bibliographic details are credited, a hyperlink and/or URL is given for the original metadata page and the content is not changed in any way. For full details of reuse please refer to City Research Online policy.

City Research Online: http://openaccess.city.ac.uk/ publications@citystgeorges.ac.uk

SCN5A-E1784K Long QT and Brugada Overlap Syndrome: Phenotype, Risk, Genetic Modifiers and Functional Characterisation

Yanushi Dullewe Wijeyeratne

BMedSci(Hons) BMBS MRCP

Submitted in partial fulfilment of the requirements of

the Degree of Doctor of Philosophy

St George's, University of London

2021

Declaration

I, Yanushi Dullewe Wijeyeratne, confirm that the research included within this thesis is my own work or that where it has been carried out in collaboration with, or supported by others, that this is duly acknowledged and my contribution indicated.

Previously published material is also acknowledged.

Signature:



Date: *16th November 2021*

This thesis is dedicated to all patients and their families with the SCN5A-E1784K mutation worldwide and to anyone affected by sudden death at a young age.

Abstract

Introduction: Long QT syndrome (LQTS) and Brugada syndrome (BrS) are inherited arrhythmia syndromes that cause sudden cardiac death. *SCN5A*-E1784K, the most common LQTS- and BrS-associated *SCN5A* mutation, has a variable phenotype that presents challenges in clinical management. Risk features in this mutation have not been reported, and while functional characteristics have been studied in heterologous cell lines, there is limited data in patient-specific models.

Aims: 1) To study clinical characteristics, risk features, common genetic variants and genetic risk scores associated with phenotype in a large international *SCN5A*-E1784K cohort, and 2) study phenotype-specific properties of this mutation *in vitro* using human induced pluripotent stem cell derived cardiomyocytes (hiPSC-CMs) from *SCN5A*-E1784K carriers with extremes of phenotype.

Methods: Single nucleotide polymorphisms (SNPs) previously associated with ECG traits were genotyped. Association of phenotypic characteristics with risk and common genetic variants were studied. Integration-free hiPSC-CMs were produced from dermal fibroblasts of *SCN5A*-E1784K carriers with extremes of phenotype and a healthy control. These cells were characterised. Nav1.5 expression and action potential characteristics were studied *in vitro*.

Results: Cardiac conduction (QRS duration) was the only independent marker of risk in *SCN5A*-E1784K. SNP associations with phenotype were inconsistent and varied with ethnicity. Genetic risk scores were, however, associated with BrS phenotype and QRS duration transethnically. Integration-free hiPSC lines were

derived from two *SCN5A*-E1784K carriers with extremes of phenotype and each line was differentiated to hiPSC-CMs, laying the foundation for future work. There was a trend towards reduced $Na_v1.5$ expression in the BrS line compared to the LQT3 line and the control line. Electrophysiological results were limited by cellular heterogeneity.

Discussion: This project has provided insight into clinical features of risk, common genetic modifiers of phenotype, and genetic mechanisms of BrS/LQTS genotype/phenotype correlation in *SCN5A*-E1784K. These findings, and planned future work, can help guide personalised patient management in clinic.

Acknowledgements

During the past five years, I have had the privilege to meet and be supported by so many incredible colleagues who have inspired, mentored and guided me. This project has been challenging, not least because of the mastery of some extremely specialised multidisciplinary skills that were required of me for the success of the project, from clinical genetics to derivation of human induced pluripotent stem cells and cellular differentiation, through to learning of the intricate skills required to carry out single cell electrophysiology. It has been a steep and challenging learning curve that also required long and arduous hours in the lab on consecutive days, particularly as I maintained and differentiated my stem cell cultures. Despite the challenges and intensive hours, I am immensely grateful for all the learning opportunities and training I received throughout this project.

This study has enabled me to develop a wide range of highly specialist and transferrable skills that I will be able to use for my future development as a clinician scientist. I was fortunate to train in these skills within three proficient institutions and with highly supportive supervisors, and to collaborate with world leaders in the field. The logistics of the study also presented unique opportunities but also challenges, including cross-site working, as well as single handedly setting up, developing standard operating procedures and running a stem cell culture facility from scratch at St George's, University of London with close supervision and support from my supervisors and collaborators. Setting up a stem cell culture facility as part of my PhD was an invaluable opportunity and it has taught me many valuable skills on setting up and running a laboratory that I can carry for the future.

My indebted gratitude will always remain with my Primary Supervisor, Prof Elijah Behr for the steadfast support, guidance and mentorship you have given me ever since I started as an Academic Clinical Fellow at St George's Hospital in 2012. Prof Behr introduced me to a whole new area of research that fascinated me, and I am grateful for all the opportunities I have been given over the years to contribute to ground-breaking and multifaceted international projects that have enabled me to develop my inner strengths and further discover myself as a researcher. A massive thank you to my co-supervisors Prof Andrew Tinker and Prof Chris Denning for your supervision and guidance over the past four years, and for supporting and welcoming me into your labs to carry out the cellular reprogramming, differentiation and cellular characterisation. My heartfelt gratitude extends to Prof Tristan McKay, who first introduced me to stem cell biology, and who encouraged and mentored me during the early inception phase of this project. I would also like to dearly thank Prof Juan Carlos Kaski, Prof John Camm and Prof Dot Bennett for always supporting me in my endeavours. Thank you also to Prof Iain Greenwood and Dr Maite Tome for all the feedback you provided to me after my MPhil to PhD transfer viva.

I want to express my humblest gratitude to all the patients and families who have contributed to this study by consenting to the use of their clinical data and DNA. A special mention to the families I had the privilege to meet when you took time out of your schedules to attend hospital in order to donate blood and skin biopsies for this study. This study would not have been the same without each and every one of you who contributed to this study.

Further, I wish to thank all my colleagues who have helped and supported me along the way. Through this project, I have had the privilege of working with so many fantastic clinical academics, as well as clinical colleagues and academic colleagues

in multiple hospitals and basic science labs across the country, and overseas. Thank you to all my colleagues in the Cardiology Clinical Academic group at St George's, University of London, past and present, for your comradeship and support over the years. Thank you to Professor Sanjay Sharma and Dr Michael Papadakis for the large patient groups you contributed to this study. I would like to especially thank my predecessors, Dr Martina Muggenthaler, Dr Hari Raju, and Dr Anthony Li who helped to set up various aspects of this project in the early months of its inception. A special mention to the late Dr Velislav Batchvarov, a dear colleague that sadly passed away in 2019, who was a true fountain of knowledge and who taught me much about the intricacies of ECG data analyses. Thank you to my student, Margarida Almeida for all your hard work and dedication during your year at St George's, and for your always maintaining your reliability and dependability in the lab. Thank you to Dr Kate Hawkins who taught me stem cell culture when I was first introduced to the field, and to Joe Fenn, who supported me in flow cytometry. My sincere gratitude extends to Dr Angeliki Asimaki and Gregory Perry who supported me through many arduous hours of immunostaining. Thank you to Jo Eggleton, Natalie Fayers, Derilyn Frusher, Alex Grayling, staff within the Joint Research and Enterprise Office and all the other administrative and support staff within St George's, University of London who provided vital support for my project on various levels over the years.

My heartfelt gratitude goes to Dr Stephen Harmer, Dr Mustafa Hassan, Dr Muriel Nobles, Dr Qadeer Aziz, Dr Mark Specterman, Dr Keat-Eng Ng and all my dear colleagues at The William Harvey Research Institute at Queen Mary, University of London for all your teaching and support in cardiac cellular electrophysiology and other related aspects of the project. Thank you for always warmly welcoming me as part of your group. A special thank you to Dr Duncan Miller for teaching me the

principles of cardiac differentiation and for helping me acquire pilot data for this project when I first started. I am thankful to Maria Barbadillo-Munoz, Dr Spandan Kalra, Dr Gary Duncan, Dr Divya Mirrington and everyone in the stem cell research group at University of Nottingham who supported me to learn stem cell reprogramming and differentiation during my time at Nottingham. I will cherish the times I spent in each lab, the enriching experiences and the lessons learnt along the way.

An enormous thank you to Dr Michael Tanck at the Amsterdam Medical Centre for all the bioinformatics training, statistical supervision, and the immense statistical support you've provided throughout the study. Thank you for hosting me in your department, for all the statistical training you provided for me during my time in Amsterdam, and for all your remote support at other times. Thank you to Prof Connie Bezzina for your ongoing collaboration for further work arising from this study. My sincere gratitude also to Dr Alison Muir and Prof Pascal McKeown at Belfast Health and Social Care Trust who facilitated my recruitment of a large patient cohort from your clinics, and for all your warmth and hospitality during my numerous visits to Belfast. My gratitude also to all other national and international study collaborators from elsewhere in the UK (Dr Ed Petzer and Dr Stephen Page), Ireland (Dr Joe Galvin), France (Prof Vincent Probst and colleagues; Dr Isabelle Denjoy), Germany (Prof Martin Borggrefe; Prof Christian Veltmann), Italy (Prof Peter Schwartz; Dr Lia Crotti and colleagues), USA (Prof Dan Roden; Prof Michael Ackerman; Dr David Tester; Dr Martijn Bos and colleagues); Japan (Prof Naomasa Makita; Prof Wataru Shimizu, Dr Takeshi Aiba; Prof Minoru Horie; Dr Seiko Ohno and colleagues) for your collaboration and participation in this study through patient recruitment and data collection, and for being part of this global, multicentre endeavour.

A special mention to Prof Stan Heptinstall and all my dear colleagues in the Platelets Group at University of Nottingham who instilled the love of research in me since Medical School and foundation training, and for nurturing my passion for translational bench research during my early years in clinical academia. You were my foundation in research, thank you!

This study would not have been possible without the continued charitable support of the Robert Lancaster Memorial Fund through St George's, University of London. My heartfelt gratitude to the Lancaster family and for all the patrons of the Robert Lancaster Memorial Fund for the financial support provided throughout the study.

Thank you to all my clinical supervisors and clinical colleagues at St George's Hospital and King's College Hospital for all your understanding and support as I navigated the fine balance of writing my thesis whilst in full-time clinical practice on the NHS frontline since 2019. A particular thank you to Dr Nick Bunce for all your support and mentorship during my early years in clinical academia at St George's Hospital. Thank you also to Dr Brian Clapp and Dr Dan Sado for all your support. During the past two years, it was a mammoth challenge to complete my thesis during unprecedented times when I was redeployed on multiple occasions to provide medical care to COVID patients, including redeployment to a COVID Intensive Care Unit. A particular thank you to Dr Francis Murgatroyd at King's College Hospital for paving the way for me to have time during my clinical duties during the past year, which was also the first year of my Electrophysiology subspecialty training, at a particularly busy time for the NHS. Your support in securing my study leave enabled me to complete my thesis within the timeframe. The comradeship of my fellow colleagues as we worked together in the frontline has

been invaluable to enable me to successfully navigate the fine balance between clinical service and completion of my thesis.

To all those who supported me in every little way along my journey, thank you from the bottom of my heart. I am forever grateful for everything you've done even though you may not be mentioned individually.

Most importantly, a colossal thank you to my parents for your unending support, care and affection over the years. Your unfaltering warmth, love and encouragement have sustained me throughout my life. I would not be here presenting this thesis if not for all of your everlasting support. I would like to extend my enormous gratitude to my dear grandparents for all their love and inspiration over the years. A massive thank you to my husband Anuruddha for all your patience, support and love as I was challenging myself to complete the thesis within a tight timeframe alongside my clinical commitments. Thank you also to my parents-in-law. Finally, a very special mention to our darling daughter Hoshika who was born a few days after my thesis was submitted!

Personal Contribution

I designed the study; collected data for the cohort studies; analysed the raw data including ECGs from all subjects recruited for the study; and managed the inter-observer variability. Simple analyses of the clinical cohort data were done by me. Genetic statistical analyses and the survival analysis presented in this thesis were carried out in collaboration with Dr Michael Tanck, a world expert in this field. Whilst Dr Tanck trained me in R-based analyses, the more sophisticated statistical analyses presented in Chapters 3-6 has been carried out in close collaboration with Dr Tanck.

I handled the ethics for the clinical, genetic and functional arms of the study, including annual reports and extension to the study to enable future work; recruited patients for hiPSC studies; carried out skin biopsies and harvested dermal fibroblasts; carried out fibroblast culture, expansion and cryopreservation to build fibroblast banks; reprogrammed the fibroblasts to hiPSCs; set up a stem cell culture lab at SGUL; isolated single clones of hiPSCs, expanded and cryopreserved the lines to build hiPSC banks; prepared the cells for karyotyping; stained and fixed the cells for imaging; carried out confocal microscopy with support from the SGUL Imaging Facility; differentiated the hiPSCs to cardiomyocytes and optimised the seeding densities for differentiation; fixed and stained the hiPSC-CMs for flow cytometry and imaging; carried out flow cytometry and analysed the results; carried out confocal microscopy with support from the SGUL Imaging Facility and analysed the results; harvested RNA and protein; stored cDNA and protein from the hiPSC-CMs for future studies; and carried out single cell patch clamping (current clamp for action potential recordings and voltage clamp for I_{Na} recordings).

Table of Contents

Declaration 1

Abstract 3

Acknowledgements 5

Personal Contribution 11

Table of Contents 12

Abbreviations 19

Publications During PhD 21

Peer-reviewed publications 21

Book chapters 27

Published Abstracts at International Conferences 27

Chapter 1: Background 28

The cardiac action potential 29

Cardiac conduction 31

SCN5A and the cardiac sodium channel 32

Studying sodium current kinetics 36

SCN5A-E1784K 39

Proposed mechanism of mixed phenotype in SCN5A-E1784K 41

Sudden cardiac death 42

Inherited arrhythmia syndromes 43

Common considerations in clinical genetics 43
Brugada syndrome 47
Clinical diagnosis 47
Molecular genetics and genotype-phenotype correlation 52
Common Genetic Variation 53
Pathophysiology of BrS and cardiac structural changes 54
Prognosis of BrS 56
Mechanisms of arrhythmia in BrS and their relevance to therapeutic considerations 57
Long QT syndrome 59
Clinical diagnosis 60
Electrocardiographic features of LQTS 62
Pathophysiology 68
Molecular genetics and genotype-phenotype correlation 69
Genetic modifiers 70
Human induced pluripotent stem cell-derived cardiomyocytes (hiPSC-CM) 71
hiPSC-CM models to study disease 75
Novelty of this thesis 76
Chapter 2: Study Design 79
Hypotheses 80
Rationale for the study 80
Objectives 80

Research governance....81
Participating centres....81
Chapter 3: Clinical Characterisation of *SCN5A*-E1784K....84
Introduction....85
Methods....86
Definitions applied....88
Results....91
Cohort demographics....92
Clinical evaluation....93
ECG characteristics....93
Disease phenotypes....100
Therapies....102
Events and follow up....103
Event-free Interval Analysis....108
Discussion....114
Cohort demographics....114
ECG characteristics....114
Therapies....115
Events and survival analysis – impact of cardiac conduction....115
Limitations....117
Chapter 4: ECG Trait SNPs Associations with Phenotype....120
Introduction....121

Methods 121
Recruitment and case selection 121
Clinical evaluation 122
SNP selection 122
SNP genotyping 126
Statistical analyses 126
Results 127
Population characteristics 127
SNP interactions and frequencies 130
Associations with ECG traits 132
Discussion 136
Limitations 137
Chapter 5: Genetic Risk Scores for PR interval, QRS duration and QTc 139
Introduction 140
Methods 140
Statistical analyses 141
Results 143
PR interval 144
QRS duration 145
QT interval 146
Discussion 157
Limitations 160

Chapter 6: *SCN5A* Mutation Type and a Genetic Risk Score Associate Variably with Brugada Syndrome Phenotype in *SCN5A* Families 161

Introduction 162

Methods 163

Recruitment and case selection 163

Clinical evaluation 163

Classification of variant pathogenicity and subsets 164

SNP selection 167

SNP genotyping 167

Statistical analyses 168

Results 170

Clinical characteristics 170

SCN5A mutation associations 173

Brugada Syndrome Genetic Risk Score 175

Discussion 180

A BrS-GRS and variability in BrS phenotype within affected families 181

Association of rare SCN5A variation with BrS phenotype and common variants 183

Genotype-phenotype mismatch in BrS and its implications 183

Future perspective: an optimised BrS-GRS 185

Limitations 185

Conclusions 186

Chapter 7: Functional characterisation 188

Introduction 189
Justification of the proposed functional work in the context of Chapters 3-6 190
Justification of the proposed functional work in the context of existing literature 191
Methods 193
General lab procedures 193
hiPSC reprogramming and characterisation 194
Differentiation into hiPSC-CMs and characterisation 199
Results 207
Recruitment for hiPSC studies and harvesting of dermal fibroblasts 207
Cellular reprogramming and clonal isolation 209
Karyotyping 212
Growth curves 214
Immunostaining of hiPSC 215
hiPSC differentiation to cardiomyocytes 216
FACS assessment of purity of hiPSC-CM differentiation 217
Immunostaining of hiPSC-CM 218
Preliminary electrophysiological characterisation 225
Discussion 226
hiPSC reprogramming and validation 227
Cardiomyocyte differentiation and validation 227
Electrophysiological characterisation 228

Limitations 229

Future work: Planned electrophysiological characterisation 231

Chapter 8: Summary and Future Work 233

Summary 234

Planned future work 236

Detailed clinical characterisation 237

GWAS and whole genome sequencing 237

Haplotype analyses 241

Functional characterisation using hiPSC-CM models 242

References 245

Appendices 273

Appendix 1: ECG trait GRSs in wild-type individuals 274

Appendix 2: ECG trait GRS meta-analyses 275

Appendix 3: Reagents 276

List of reagents 276

Preparation of reagents 278

Abbreviations

ACMG	American College of Medical Genetics
AP	Action potential
APD	Action potential duration
BrS	Brugada syndrome
BrS-GRS	Brugada syndrome genetic risk score
BSA	Bovine serum albumin
CM	Cardiomyocyte
ECG	Electrocardiogram
FBS	Foetal bovine serum
EP	Electrophysiological
FGF	Fibroblast growth factor
GEE	Generalised estimated equation
GRS	Genetic risk score
GSA	Global screening array
GWAS	Genome-wide association study
HDF	Human dermal fibroblast
hiPSC	Human induced pluripotent stem cells
hiPSC-CM	Human induced pluripotent stem cell-derived cardiomyocytes
ICC	Inherited Cardiac Conditions
KASP	Kompetitive Allele Specific PCR
KSR	KnockOut™ Serum Replacement
LD	Linkage disequilibrium
LQT1	Long QT syndrome 1

LQT2	Long QT syndrome 2
LQT3	Long QT syndrome 3
LQTS	Long QT syndrome
NEAA	Non-essential Amino Acids
OOHCA	Out of hospital cardiac arrest
OR	Odds ratio
PCR	Polymerase chain reaction
PFA	Paraformaldehyde
QC	Quality control
SCD	SCD
SD	Standard deviation
SE	Standard error
SNP	Single nucleotide polymorphism
VT	Ventricular tachycardia
VF	Ventricular fibrillation
WT	Wild-type

Publications During PhD

Peer-reviewed publications

Wijeyeratne YD, Tanck MW, Mizusawa Y, Batchvarov V, Barc J, Crotti L, Bos JM, Tester DJ, Muir A, Veltmann C, Ohno S, Page SP, Galvin J, Tadros R, Muggenthaler M, Raju H, Denjoy I, Schott JJ, Gourraud JB, Skoric-Milosavljevic D, Nannenberg EA, Redon R, Papadakis M, Kyndt F, Dagradi F, Castelletti S, Torchio M, Meitinger T, Lichtner P, Ishikawa T, Wilde AAM, Takahashi K, Sharma S, Roden DM, Borggrefe MM, McKeown PP, Shimizu W, Horie M, Makita N, Aiba T, Ackerman MJ, Schwartz PJ, Probst V, Bezzina CR, Behr ER. SCN5A Mutation Type and a Genetic Risk Score Associate Variably With Brugada Syndrome Phenotype in SCN5A Families. Circ Genom Precis Med 2020;13(6):e002911.

Lahrouchi N, Tadros R, Crotti L, Mizusawa Y, Postema PG, Beekman L, Walsh R, Hasegawa K, Barc J, Ernsting M, Turkowski KL, Mazzanti A, Beckmann BM, Shimamoto K, Diamant UB, **Wijeyeratne YD**, Kucho Y, Robyns T, Ishikawa T, Arbelo E, Christiansen M, Winbo A, Jabbari R, Lubitz SA, Steinfurt J, Rudic B, Loeys B, Shoemaker MB, Weeke PE, Pfeiffer R, Davies B, Andorin A, Hofman N, Dagradi F, Pedrazzini M, Tester DJ, Bos JM, Sarquella-Brugada G, Campuzano Ó, Platonov PG, Stallmeyer B, Zumhagen S, Nannenberg EA, Veldink JH, van den Berg LH, Al-Chalabi A, Shaw CE, Shaw PJ, Morrison KE, Andersen PM, Müller-Nurasyid M, Cusi D, Barlassina C, Galan P, Lathrop M, Munter M, Werge T, Ribasés M, Aung T, Khor CC, Ozaki M, Lichtner P, Meitinger T, van Tintelen JP, Hoedemaekers Y, Denjoy I, Leenhardt A, Napolitano C, Shimizu W, Schott JJ, Gourraud JB, Makiyama T, Ohno S, Itoh H, Krahn AD, Antzelevitch C, Roden DM, Saenen J, Borggrefe M, Odening KE, Ellinor PT, Tfelt-Hansen J, Skinner JR, van den Berg MP, Olesen MS, Brugada J, Brugada R, Makita N, Breckpot J, Yoshinaga

M, Behr ER, Rydberg A, Aiba T, Kääb S, Priori SG, Guicheney P, Tan HL, Newton-Cheh C, Ackerman MJ, Schwartz PJ, Schulze-Bahr E, Probst V, Horie M, Wilde AA, Tanck MWT, Bezzina CR. Transethnic Genome-Wide Association Study Provides Insights in the Genetic Architecture and Heritability of Long QT Syndrome. Circulation 2020;142(4):324-338. Erratum in: Circulation 2020;142(4):e66.

Roberts JD, Asaki SY, Mazzanti A, Bos JM, Tuleta I, Muir AR, Crotti L, Krahn AD, Kutyifa V, Shoemaker MB, Johnsrude CL, Aiba T, Marcondes L, Baban A, Udupa S, Dechert B, Fischbach P, Knight LM, Vittinghoff E, Kukavica D, Stallmeyer B, Giudicessi JR, Spazzolini C, Shimamoto K, Tadros R, Cadrin-Tourigny J, Duff HJ, Simpson CS, Roston TM, **Wijeyeratne YD**, El Hajjaji I, Yousif MD, Gula LJ, Leong-Sit P, Chavali N, Landstrom AP, Marcus GM, Dittmann S, Wilde AAM, Behr ER, Tfelt-Hansen J, Scheinman MM, Perez MV, Kaski JP, Gow RM, Drago F, Aziz PF, Abrams DJ, Gollob MH, Skinner JR, Shimizu W, Kaufman ES, Roden DM, Zareba W, Schwartz PJ, Schulze-Bahr E, Etheridge SP, Priori SG, Ackerman MJ. An International MultiCenter Evaluation of Type 5 Long QT Syndrome: A Low Penetrant Primary Arrhythmic Condition. Circulation 2020;141(6):429-439.

Lahrouchi N, Raju H, Lodder EM, Papatheodorou S, Miles C, Ware JS, Papadakis M, Tadros R, Cole D, Skinner JR, Crawford J, Love DR, Pua CJ, Soh BY, Bhalshankar JD, Govind R, Tfelt-Hansen J, Winkel BG, van der Werf C, **Wijeyeratne YD**, Mellor G, Till J, Cohen M, TomeEsteban M, Sharma S, Wilde AAM, Cook SA, Sheppard MN, Bezzina CR, Behr ER. The yield of postmortem genetic testing in sudden death cases with structural findings at autopsy. Eur J Hum Genet 2020;28(1):17-22.

Milman A, Andorin A, Postema PG, Gourraud JB, Sacher F, Mabo P, Kim SH, Maeda S, Takahashi Y, Kamakura T, Aiba T, Conte G, Juang JJM, Leshem E,

Michowitz Y, Fogelman R, Hochstadt A, Mizusawa Y, Giustetto C, Arbelo E, Huang Z, Corrado D, Delise P, Allocca G, Takagi M, **Wijeyeratne YD**, Mazzanti A, Brugada R, Casado-Arroyo R, Champagne J, Calo L, Sarquella-Brugada G, Jespersen CH, Tfelt-Hansen J, Veltmann C, Priori SG, Behr ER, Yan GX, Brugada J, Gaita F, Wilde AAM, Brugada P, Kusano KF, Hirao K, Nam GB, Probst V, Belhassen B. Ethnic differences in patients with Brugada syndrome and arrhythmic events: New insights from Survey on Arrhythmic Events in Brugada Syndrome. Heart Rhythm. 2019;16(10):1468-1474.

Michowitz Y, Milman A, Andorin A, Sarquella-Brugada G, Gonzalez Corcia MC, Gourraud JB, Conte G, Sacher F, Juang JJM, Kim SH, Leshem E, Mabo P, Postema PG, Hochstadt A, **Wijeyeratne YD**, Denjoy I, Giustetto C, Mizusawa Y, Huang Z, Jespersen CH, Maeda S, Takahashi Y, Kamakura T, Aiba T, Arbelo E, Mazzanti A, Allocca G, Brugada R, Casado-Arroyo R, Champagne J, Priori SG, Veltmann C, Delise P, Corrado D, Brugada J, Kusano KF, Hirao K, Calo L, Takagi M, Tfelt-Hansen J, Yan GX, Gaita F, Leenhardt A, Behr ER, Wilde AAM, Nam GB, Brugada P, Probst V, Belhassen B. Characterization and Management of Arrhythmic Events in Young Patients With Brugada Syndrome. J Am Coll Cardiol 2019;73(14):1756-1765.

Milman A, Hochstadt A, Andorin A, Gourraud JB, Sacher F, Mabo P, Kim SH, Conte G, Arbelo E, Kamakura T, Aiba T, Napolitano C, Giustetto C, Denjoy I, Juang JJM, Maeda S, Takahashi Y, Leshem E, Michowitz Y, Rahkovich M, Jespersen CH, **Wijeyeratne YD**, Champagne J, Calo L, Huang Z, Mizusawa Y, Postema PG, Brugada R, Wilde AAM, Yan GX, Behr ER, TfeltHansen J, Hirao K, Veltmann C, Leenhardt A, Corrado D, Gaita F, Priori SG, Kusano KF, Takagi M, Delise P, Brugada J, Brugada P, Nam GB, Probst V, Belhassen B. Time-to-first appropriate shock in patients implanted prophylactically with an implantable cardioverter

defibrillator: data from the Survey on Arrhythmic Events in Brugada Syndrome (SABRUS). Europace 2019;21(5):796-802.

Baruteau AE, Kyndt F, Behr ER, Vink AS, Lachaud M, Joong A, Schott JJ, Horie M, Denjoy I, Crotti L, Shimizu W, Bos JM, Stephenson EA, Wong L, Abrams DJ, Davis AM, Winbo A, Dubin AM, Sanatani S, Liberman L, Kaski JP, Rudic B, Kwok SY, Rieubland C, Tfelt-Hansen J, Van Hare GF, Guyomarc'h-Delasalle B, Blom NA, **Wijeyeratne YD**, Gourraud JB, Le Marec H, Ozawa J, Fressart V, Lupoglazoff JM, Dagradi F, Spazzolini C, Aiba T, Tester DJ, Zahavich LA, Beauséjour-Ladouceur V, Jadhav M, Skinner JR, Franciosi S, Krahn AD, Abdelsayed M, Ruben PC, Yung TC, Ackerman MJ, Wilde AA, Schwartz PJ, Probst V. SCN5A mutations in 442 neonates and children: genotype-phenotype correlation and identification of higher-risk subgroups. Eur Heart J 2018;39(31):2879-2887.

Milman A, Gourraud JB, Andorin A, Postema PG, Sacher F, Mabo P, Conte G, Giustetto C, Sarquella-Brugada G, Hochstadt A, Kim SH, Juang JJM, Maeda S, Takahashi Y, Kamakura T, Aiba T, Leshem E, Michowitz Y, Rahkovich M, Mizusawa Y, Arbelo E, Huang Z, Denjoy I, **Wijeyeratne YD**, Napolitano C, Brugada R, Casado-Arroyo R, Champagne J, Calo L, TfeltHansen J, Priori SG, Takagi M, Veltmann C, Delise P, Corrado D, Behr ER, Gaita F, Yan GX, Brugada J, Leenhardt A, Wilde AAM, Brugada P, Kusano KF, Hirao K, Nam GB, Probst V, Belhassen B. Gender differences in patients with Brugada syndrome and arrhythmic events: Data from a survey on arrhythmic events in 678 patients. Heart Rhythm 2018;15(10):1457-1465.

Michowitz Y, Milman A, Sarquella-Brugada G, Andorin A, Champagne J, Postema PG, CasadoArroyo R, Leshem E, Juang JJ, Giustetto C, Tfelt-Hansen J, **Wijeyeratne YD**, Veltmann C, Corrado D, Kim SH, Delise P, Maeda S, Gourraud

JB, Sacher F, Mabo P, Takahashi Y, Kamakura T, Aiba T, Conte G, Hochstadt A, Mizusawa Y, Rahkovich M, Arbelo E, Huang Z, Denjoy I, Napolitano C, Brugada R, Calo L, Priori SG, Takagi M, Behr ER, Gaita F, Yan GX, Brugada J, Leenhardt A, Wilde AAM, Brugada P, Kusano KF, Hirao K, Nam GB, Probst V, Belhassen B. Fever-Related Arrhythmic Events in the Multicenter Survey on Arrhythmic Events in Brugada Syndrome (SABRUS). Heart Rhythm 2018;15(9):1394-1401.

Papadakis M, Papatheodorou E, Mellor G, Raju H, Bastiaenen R, **Wijeyeratne Y**, Wasim S, Ensam B, Finocchiaro G, Gray B, Malhotra A, D'Silva A, Edwards N, Cole D, Attard V, Batchvarov VN, Tome-Esteban M, Homfray T, Sheppard MN, Sharma S, Behr ER. The Diagnostic Yield of Brugada Syndrome After Sudden Death With Normal Autopsy. J Am Coll Cardiol 2018; 71(11):1204-1214.

Milman A, Andorin A, Gourraud JB, Postema PG, Sacher F, Mabo P, Kim SH, Juang JJM, Maeda S, Takahashi Y, Kamakura T, Aiba T, Conte G, Sarquella-Brugada G, Leshem E, Rahkovich M, Hochstadt A, Mizusawa Y, Arbelo E, Huang Z, Denjoy I, Giustetto C, **Wijeyeratne YD**, Napolitano C, Michowitz Y, Brugada R, Casado-Arroyo R, Champagne J, Calo L, Tfelt-Hansen J, Priori SG, Takagi M, Veltmann C, Delise P, Corrado D, Behr ER, Gaita F, Yan GX, Brugada J, Leenhardt A, Wilde AAM, Brugada P, Kusano KF, Hirao K, Nam GB, Probst V, Belhassen B. Profile of patients with Brugada syndrome presenting with their first documented arrhythmic event: Data from the Survey on Arrhythmic Events in Brugada Syndrome. Heart Rhythm 2018;15(5):716-724.

Milman A, Andorin A, Gourraud JB, Sacher F, Mabo P, Kim SH, Maeda S, Takahashi Y, Kamakura T, Aiba T, Conte G, Juang JJM, Leshem E, Rahkovich M, Hochstadt A, Mizusawa Y, Postema PG, Arbelo E, Huang Z, Denjoy I, Giustetto C, **Wijeyeratne YD**, Napolitano C, Michowitz Y, Brugada R, Casado-Arroyo R,

Champagne J, Calo L, Sarquella-Brugada G, Tfelt-Hansen J, Priori SG, Takagi M, Veltmann C, Delise P, Corrado D, Behr ER, Gaita F, Yan GX, Brugada J, Leenhardt A, Wilde AAM, Brugada P, Kusano KF, Hirao K, Nam GB, Probst V, Belhassen B. Age of First Arrhythmic Event in Brugada Syndrome: Data From the SABRUS (Survey on Arrhythmic Events in Brugada Syndrome) in 678 Patients. Circ Arrhythm Electrophysiol 2017; 10(12). pii: e005222.

Roberts JD, Krahn AD, Ackerman MJ, Rohatgi RK, Moss AJ, Nazer B, Tadros R, Gerull B, Sanatani S, **Wijeyeratne YD**, Baruteau AE, Muir AR, Pang B, Cadrin-Tourigny J, Talajic M, Rivard L, Tester DJ, Liu T, Whitman IR, Wojciak J, Conacher S, Gula LJ, Leong-Sit P, Manlucu J, Green MS, Hamilton R, Healey JS, Lopes CM, Behr ER, Wilde AA, Gollob MH, Scheinman MM. Loss-of-Function KCNE2 Variants: True Monogenic Culprits of Long-QT Syndrome or Proarrhythmic Variants Requiring Secondary Provocation? Circ Arrhythm Electrophysiol 2017; 10(8). pii: e005282.

Lahrouchi N, Raju H, Lodder EM, Papatheodorou E, Ware JS, Papadakis M, Tadros R, Cole D, Skinner JR, Crawford J, Love DR, Pua CJ, Soh BY, Bhalshankar JD, Govind R, Tfelt-Hansen J, Winkel BG, van der Werf C, **Wijeyeratne YD**, Mellor G, Till J, Cohen MC, Tome-Esteban M, Sharma S, Wilde AAM, Cook SA, Bezzina CR, Sheppard MN, Behr ER. Utility of Post-Mortem Genetic Testing in Cases of Sudden Arrhythmic Death Syndrome. J Am Coll Cardiol 2017; 69(17):2134-45.

Bastiaenen R, Cox AT, Castelletti S, **Wijeyeratne YD**, Colbeck N, Pakroo N, Ahmed H, Bunce N, Anderson L, Moon JC, Prasad S, Sharma S, Behr ER. Late gadolinium enhancement in Brugada syndrome: A marker for subtle underlying cardiomyopathy? Heart Rhythm 2016; 2. pii: S1547-5271(16)31159-6.

Wijeyeratne YD, Behr ER. Sudden death and cardiac arrest without phenotype - the utility of genetic testing. Trends Cardiovasc Med 2016; pii: S1050-1738(16)30134-7.

Mellor G, Nelson CP, Robb C, Raju H, **Wijeyeratne Y**, Hengstenberg C, Reinhard W, Papadakis M, Sharma S, Samani NJ, Behr ER. The Prevalence and Significance of the Early Repolarization Pattern in Sudden Arrhythmic Death Syndrome Families. Circ Arrhythm Electrophysiol 2016;9(6).pii:e003960.

Book chapters

Wijeyeratne YD, Behr ER. Long QT syndrome. In: Clinical Cardiogenetics, 2nd ed. 2019. Springer. Pp 155-173.

Published Abstracts at International Conferences

Wijeyeratne YD, Tanck MW, Muir A, Bos JM, Denjoy I, Galvin J, Page S, Ohno S, Veltmann C, Crotti L, Roden D, Makita N, Probst V, Aiba T, Behr ER. A genetic risk score predicts Brugada syndrome phenotype in SCN5A overlap syndrome. Eur Heart J 2018;39(suppl 1). ehy563.P3815.

Chapter 1: Background

The cardiac action potential

The human ventricular cardiac action potential consists of five distinct phases determined by distinct ionic currents (Figure 1).

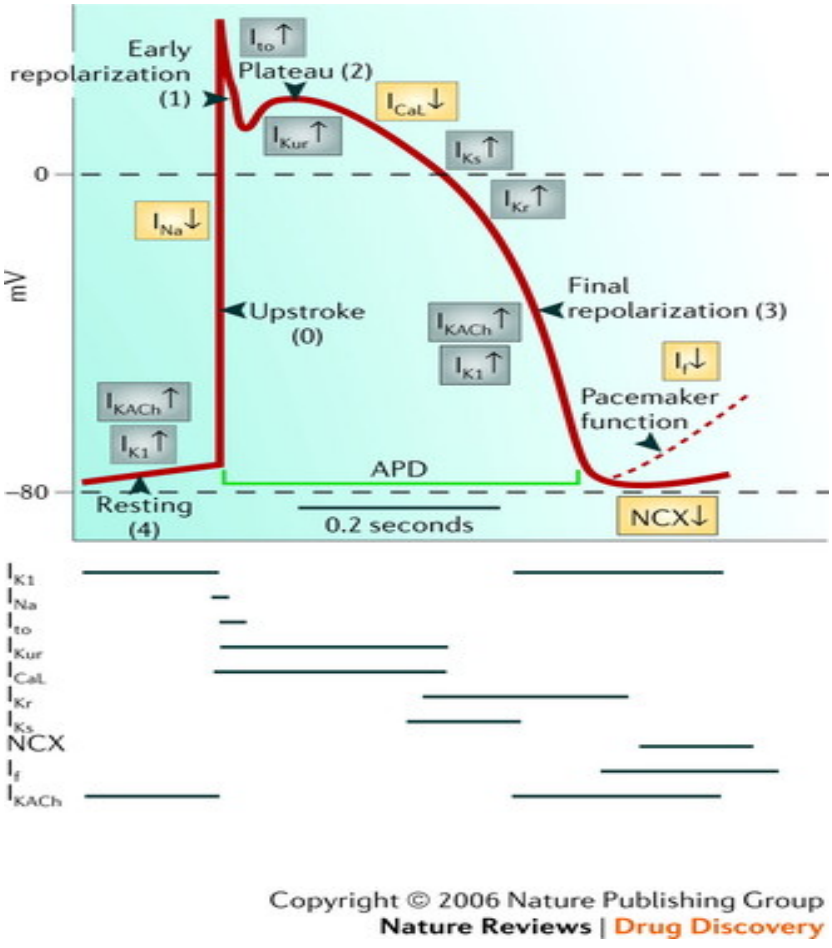


Figure 1. The cardiac action potential. Reproduced with permission from Nature Reviews.[1]

Phase 0 of the ventricular action potential is the rapid depolarising upstroke, when the membrane potential shifts into a positive voltage range. This phase is critical to the rapid propagation of the cardiac impulse (conduction velocity, θ = 1 m/s). Phase 0 is regulated by the voltage-gated sodium channels $Na_v1.5$, that generate the inward sodium current I_{Na}. It is followed by transient rapid repolarisation of the cell membrane (phase 1), due to inactivation of I_{Na} and activation of a transient outward voltage-gated K^+ current. This is known as the I_{to} current, which consists of a fast $I_{to,f}$ and a slower $I_{to,s}$ component. The I_{to} current is responsible for the characteristic

notch in the adult human ventricular cardiomyocyte action potential, and sets the potential for the next phase of the action potential. This is followed by the plateau phase of the action potential, also known as phase 2, which is the longest phase of the action potential.[1–3]

Phase 2 is unique among excitable cells and marks the phase of calcium entry into the cell. During phase 2 of the action potential, the depolarisation of the cell membrane activates voltage-gated Ca^{2+} channels (CaV). This triggers the influx of Ca^{2+}, known as the $I_{ca,L}$ current. As the CaV channels inactivate, outward rapid and slow K^+ currents (I_{Kr} and I_{Ks}) dominate. These drive further repolarisation of the cell membrane in the latter part of phase 3. This restores the membrane potential to its resting value. Meanwhile, inward rectifying K^+ channels (that mediate I_{Kr}) contribute to the late phase 3 and for maintenance of the resting membrane potential (RMP) in phase 4 of the action potential. The RMP is stable at approximately -90mV in adult cardiomyocytes.[1,2]

Cardiac potassium channels are membrane-spanning proteins that enable the passive movement of K+ ions along its electromechanical gradient across the cell membrane.[4] The human ether-a-go-go-related gene (hERG) encodes I_{Kr}, while the KCNQ1 and KCNE1 genes together encode the I_{Ks} current.[5] As well as regulating the resting membrane potential, potassium channels regulate the frequency of pacemaker cells and the shape of the cardiac action potential. I_{Kr} and I_{Ks} are voltage-gated channels. Potassium channels are formed by co-assembly of pore-forming α-subunits that surround a water-filled pore and accessory β-subunits. Over eighty K^+ channel-related genes have been cloned and characterised in humans.[4]

The action potentials of atrial cells, pacemaker cells in the sinoatrial node and cells of the atrioventricular node are markedly different to that of ventricular

cardiomyocytes. In pacemaker cells, the membrane potential at the onset of phase 4 is more depolarised (-50 to -65mV). The depolarisation is more gradual, merging into phase 0. This results in slow propagation of the action potential in nodal regions (θ = 0.1 - 0.2 m/s).[1] Action potentials of atrial cardiomyocytes have a less negative resting potential and a shorter action potential duration resulting in a more triangular shape with a shortened plateau phase (phase 2). However, the return to the resting membrane potential is slower in phase 3 and is described as a gradual terminal repolarisation. There is also heterogeneity in atrial cells , with some having a more distinct spike and plateau phase.[6]

Cardiac conduction

The cardiac action potential initiates within primary pacemaker cells of the heart in the sinoatrial node. The cardiac pacemaker cells are characterised as having no true resting potential, but instead generate spontaneous action potentials. In the centre of SA node, there are characteristic 'P' cells (or 'typical nodal' cells), which are thought to be the leading pacemaker cells. These cells contain only a few organised myofilaments running in all directions (as opposed to being organised into myofibrils), and contain relatively fewer mitochondria and little sarcoplasmic reticulum.[7] The cardiac action potential then propagates rapidly through the atria to the atrioventricular (AV) node, utilising specialised conducting tissue including Bachmann's Bundle, which is one of the main pathways of inter-atrial conduction.[8] The AV node delays the impulse reaching the ventricles, allowing the ventricles to fill during diastole before contraction is initiated. The relatively long refractory period results in temporal non-excitability, which protects the ventricles from rapid atrial arrhythmias. Furthermore, the AV nodal region is composed of several domains of myocardial cells of different architecture, interspersed with connective tissue and nerves, that together form a complex heterogeneous anatomical structure on the

dorsal wall of the human heart.[9] Complex patterning of four different connexin isoforms, comprising the gap junctions, with single channel conductance ranging from ultralow to high explains the dual pathway electrophysiology of the AV node. This is associated with poor electrical coupling between myocytes[10] and contributes to slow AV nodal conduction velocity.

The slow conduction velocity of the AV node is also, in part, the result of the small diameter of nodal myocytes, and the complex arrangement of the myocytes separated by extensive connective tissue (whereby the action potential has to follow a more tortuous path through the AV node). In addition, it results from the low expression of $Na_v1.5$ within the AV nodal cells, resulting in a slow upstroke velocity of the action potential within the AV node. All of these factors together contribute to the slowing of conduction within the AV node. Impulses then propagate down the Bundle of His and the Purkinje fibres and depolarise the ventricular myocardium.

SCN5A and the cardiac sodium channel

The human cardiac sodium channel, $Na_v1.5$, responsible for the inward sodium current, was first cloned, sequenced and functionally expressed in 1992. It was found to be a 2016 amino acid protein that is homologous to other members of the sodium channel multigene family, and absent in non-cardiac tissue.[11] $Na_v1.5$ denotes that it is a voltage-dependent transmembrane protein and is the fifth member of subfamily 1 of the sodium channel family. [12] $Na_v1.5$ is the predominant cardiac sodium channel expressed in cardiomyocytes and is a voltage-gated, tetrodotoxin (TTX)-insensitive, rapidly activating and inactivating transmembrane protein responsible for rapid depolarisation of cardiomyocytes (phase 0 of the cardiac action potential, Figure 2). TTX is a non-protein toxin that is a selective sodium channel blocker in neurological tissue.[13] As well as initiation of the cardiac

action potential, the cardiac sodium channel also controls the action potential duration and conduction of electrical impulses through the myocardium.[14]

The *SCN5A* gene on chromosome 3 encodes the α-subunit of $Na_v1.5$. It is highly conserved among species and is relatively large with 28 exons.[13] $Na_v1.5$ is composed of this principal (α) subunit that comprises four pore-forming transmembrane homologous domains attached by cytoplasmic linker sequences, with intracellular N and C termini.[15] The four structurally homologous domains (DI to DIV) are linked to each other by intracellular linkers. Each domain contains six transmembrane segments (S1 to S6), that are connected to each other by extracellular and intracellular loops. The four domains fold to form an ion-conducting pore.[13] $Na_v1.5$ is preferentially expressed in the intercalated disc and interacts with proteins that regulate its biosynthesis, trafficking, cell membrane localisation and stability, gating and degradation. Post-translational modifications of $Na_v1.5$ regulate its activity and/or trafficking.[13,16] Figure 2 illustrates the structure of *SCN5A* and $Na_v1.5$.

Between S5 and S6 of the 6 transmembrane segments in each domain, there are extracellular loops called P-loops that control ion selectivity and permeability. The P-loops are highly conserved pore-forming regions between S5 and S6 of each domain.[16] Depolarisation of the plasma membrane by electrical impulses from adjacent cells triggers an outward motion of the positively charged S4 segments. This leads to fast activation (channel opening) and rapid flow of sodium ions into the cells during phase 0 of the cardiac action potential. This is followed by channel closing, which is made up of two distinct conformational states: fast inactivation and slow inactivation.[13] Fast inactivation is directly coupled to $Na_v1.5$ activation, starting as activation proceeds and takes only milliseconds. It occurs via a 'ball and chain' mechanism where the 'ball', which occludes the pore, is represented by an interdomain linker loop that interrupts the flow of ions across the channel.

Conversely, slow inactivation is not coupled to activation, does not start during activation progression, and can be sustained for as long as a few seconds. The slow inactivation mechanism is induced by conformational modifications that directly involve the pore structure, while the entrance to the pore is unaffected.[16] $Na_v1.5$ can be activated again only after recovery from inactivation. This is a time-and voltage-dependent process that occurs during phase 1-4 (the repolarization and resting phases of the action potential) as depicted in Figure 1.[13]

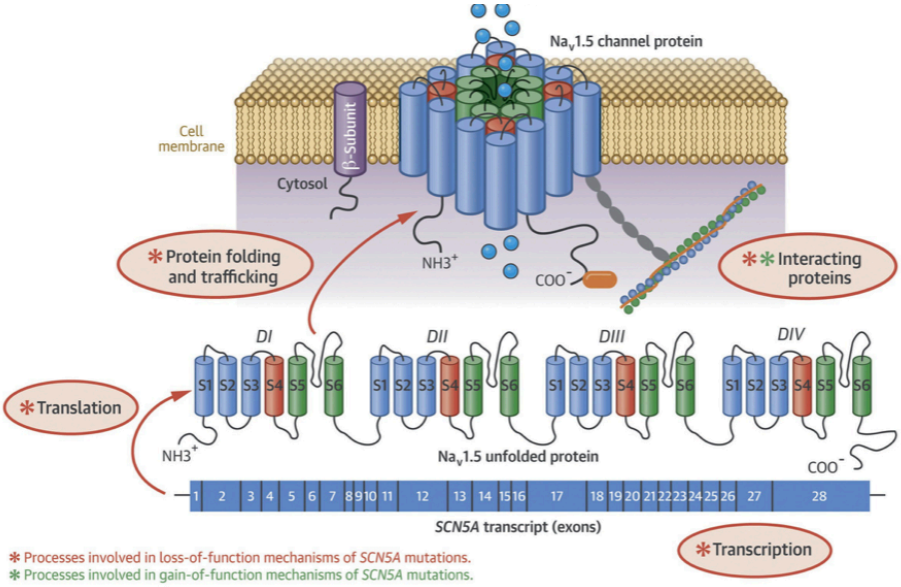


Figure 2. Diagrammatic representation of *SCN5A* and $Na_v1.5$ (figure adapted with permission from Wilde *et al*, 2018)[13]

Recovery from slow inactivation requires longer than recovery from fast inactivation. A small fraction (<1%) of $Na_v1.5$ can remain open or reactivate prematurely during plateau phase2 and repolarization phase 3. This can mediate a 'late sodium current' (I_{NaL}). The late current may also be referred to as the 'window current'. Thus I_{Na} continues to flow through $Na_v1.5$ in ventricular cells as well as Purkinje fibres.[17] The late current occurs transiently in a phase when the plasma membrane is still sufficiently depolarised to reactivate some sodium channels (those that have

recovered from inactivation) and before the plasma membrane reaches a voltage that is too negative to activate the channels. It is subject to regulatory pathways including phosphorylation and nitrosylation. The mechanisms for late I_{Na} are multiple but is generally thought of as a manifestation of incomplete inactivation.[18] In healthy individuals, the voltage range for the late sodium current is narrow and very small in magnitude.[13]

Sodium loading during the action potential therefore occurs in two phases: an intense phase lasting only a few milliseconds and a weak phase lasting hundreds of milliseconds. Even though the late current is only 1–2% at most in magnitude compared with the peak current, it lasts for 50–100 times longer, so the net sodium loading by the two phases during the complete cardiac cycle is comparable.[17] *SCN5A* mutations can disrupt gating properties of $Na_v1.5$ including activation, inactivation and/or recovery from inactivation. The balance of this interaction of certain *SCN5A* mutations on the gating properties of $Na_v1.5$ affect the disease phenotype.[13] I_{NaL} may contribute to arrhythmia in two ways: by causing repolarisation failure (early afterdepolarisations), and by triggering late afterdepolarisations attributable to calcium oscillations in sodium–calcium overload conditions.[17]

The cardiac sodium channel locus *SCN10A*, that is adjacent to *SCN5A ,* has also been implicated in genome-wide association studies as a modulator of cardiac electrophysiology.[19–22] *SCN10A* encodes $Na_v1.8$ and is mainly expressed in the dorsal root ganglia and the retina, but it is also expressed within the heart, particularly the cardiac conduction system. It has been shown that a highly specific Nav1.8 channel blocker can selectively block the late sodium current in mouse and rabbit ventricular cardiomyocytes, suggesting that *SCN10A* expression also

contributes to the late sodium current in the heart.[23] However, human studies are needed.

Loss of function mutations in *SCN5A* have been shown to lower expression of *SCN5A* or lead to production of defective $Na_v1.5$ and cause BrS and/or conduction disease, while gain of function mutations lead to more sodium influx into cardiomyocytes through abnormal channel gating, leading to conditions like LQTS. Increased intracellular sodium causes QT prolongation by lengthening phase 2 of the cardiac action potential and thereby the action potential duration.

The LQT3 subtype of LQTS, caused by mutations in *SCN5A,* was first described in 1995.[24] Overlap syndromes, where the same mutation can cause either BrS, LQTS, or both, may have both loss of function and gain of function effects. The first such reported overlap syndrome was an insertion mutation in *SCN5A*–1795insD, which is a Dutch founder mutation. The most common *SCN5A* overlap syndrome worldwide is *SCN5A*-E1784K, that can cause a mixed BrS and LQTS phenotype with variable severity. Other conditions that can be caused by mutations in *SCN5A* include dilated cardiomyopathy, familial atrial fibrillation, sick sinus syndrome, premature cardiac conduction disease (Lev-Lenègre syndrome), and a arrhythmia syndrome described relatively recently called multifocal ectopic premature Purkinje-related complexes (due to a sodium channel mutation that results in hyperexcitability of the Purkinje system).[13]

Studying sodium current kinetics

Sodium current kinetics can be studied by whole-cell patch clamp, using a voltage clamp. Protocols that can be used for studying sodium current kinetics, including how to measure fast and slow inactivation are illustrated below. As demonstrated,

several overlapping protocols can be used to study various aspects of sodium current kinetics (Figures 3-7).



Figure 3. Example of a protocol for measuring INa activation, fast inactivation and characterisation of voltage dependency of peak INa and late INa. Steady-state activation and inactivation curves would be fitted by using a Boltzmann equation: I/Imax=A/{1.0+exp[(V1/2V)/k]}, in which V1/2 is half-maximum (in)activation potential and k was the slope factor.[25]

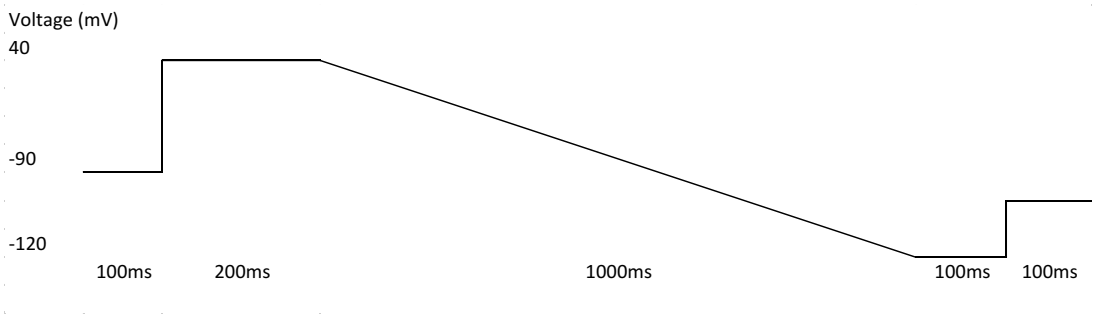


Figure 4. Example of a ramp protocol for isolating late I_{Na}. [26,27]

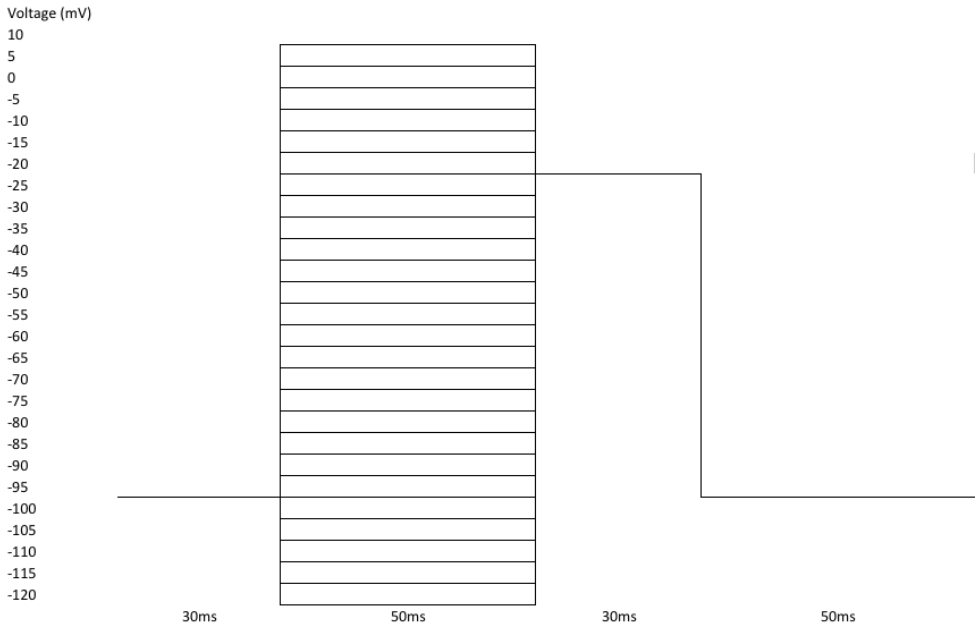


Figure 5. An example of a protocol for assessing voltage dependence of INa steady state inactivation (slow inactivation). Pre-pulses ranging from -120 to 10mV can be applied for a period of 50 msec followed by a 30 msec depolarising step to -20mV. Peak currents (I) are normalised to the maximal values (Imax) obtained at a holding potential of -120mV and plotted against the conditioning pulse potential.[28] Currents can be determined at -20mV preceded by a conditional step ranging from -120 to -20mV[25,29]

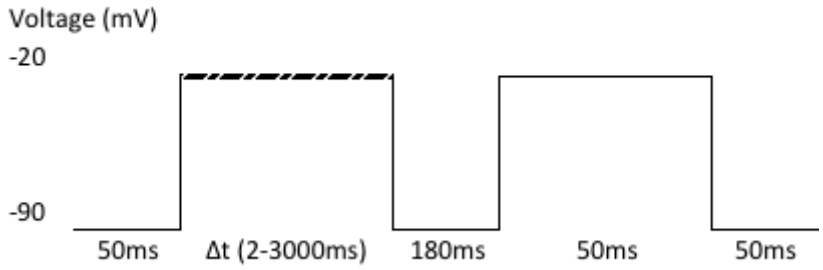


Figure 6. Further example of a protocol for studying development of slow inactivation.[27]

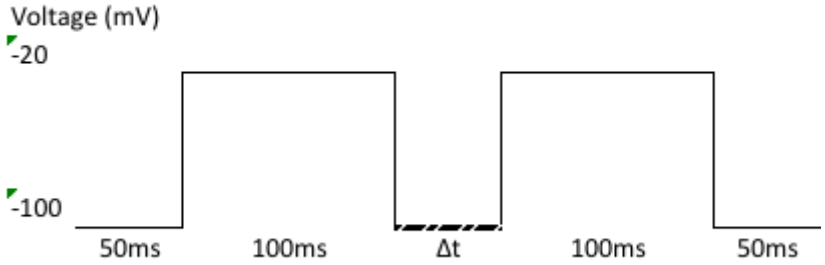


Figure 7. Recovery from inactivation can be measured using a 2-step pulse protocol to -20mV, by which the interpulse interval varies between 1 and 1000ms. Currents at the second pulse were normalised to currents at the first pulse and plotted against the interval between the 2 pulses. Recovery from inactivation and the speed of current inactivation will be fitted with a biexponential function y= y0+ Af{1exp[t/sf]}+ As{1exp[t/ss]}),where Af and As represent the amplitudes of the fast and slow components and sf and ss indicate the time constants of fast and slow components, respectively.[25]

SCN5A-E1784K

The p.E1784K (glutamine to lysine substitution at position 1784) missense mutation in *SCN5A* (c.5350G>A; ClinVar ID: 9377), is an overlap syndrome which can cause LQTS, BrS and/or conduction disease. It is the most common LQT3 mutation, accounting for up to a third of unrelated cases, as well as the mutation most

commonly associated with BrS (3% of unrelated cases) and is absent in the gnomAD database.[30,31] *SCN5A*-E1784K exhibits incomplete penetrance and can manifest as a variable, mixed clinical phenotype of LQTS, BrS and conduction disorders, even amongst affected individuals from the same pedigree.[32] It can predispose affected individuals to the risk of potentially fatal ventricular arrhythmias, particularly Torsades de Pointes but also monomorphic VT and VF. The variation in phenotype presents a challenge in clinical practice as risk stratification and the optimal management of these patients is unclear. Class Ib antiarrhythmic drugs have been shown to be beneficial at shortening the QTc if prolonged. Mexiletine, in particular, has been shown to reduce arrhythmic events in patients with LQT3, including *SCN5A*-E1784K[33–36] However, predicting the risk of sudden cardiac death (SCD) in individual patients with the mutation is difficult and the propensity for drug interaction is greater where there is a mixed clinical phenotype. Conversely, the variation in phenotype in individuals with the same known *SCN5A* genotype does, however, also make it an optimal target to study the role of potential genetic modifiers that may affect phenotypic expression not only in patients with this mutation, but also potentially in patients carrying other *SCN5A* mutations.[37]

The biophysical properties of *SCN5A*-E1784K have been already studied in heterologous *in vitro* models. The mutation was shown to be associated with a negative shift of steady-state sodium channel inactivation, resulting in a diminished inward sodium current, together with destabilised fast channel inactivation leading to a persistence of the late inward sodium current. Reduced sodium current can accentuate differences in action potential duration between the endocardium and epicardium, resulting in a favourable substrate for re-entrant tachyarrhythmias.[32] The reduced peak sodium current was also shown to result in delayed cardiac repolarisation and enhanced tonic block by class IC drugs. [32,38] It is, however, as yet unknown what electrophysiological differences cause different carriers of this

mutation (even within the same pedigree) to have different clinical phenotypes. The differences could be due to common genetic variation, demographic factors (gender, ethnicity) and/or environmental influences prenatally, during childhood or adolescence. Furthermore, in our experience, genotype-phenotype mismatch has been observed, with mutation-negative family members demonstrating a positive ajmaline challenge, or mutation-positive individuals not showing any manifestation of phenotype. Ajmaline is a class IA antiarrhythmic that is a potent competitive inhibitor of myocardial sodium channels and can unmask BrS.

Proposed mechanism of mixed phenotype in SCN5A-E1784K

The mechanism of action of modifier genes of the BrS and LQTS phenotypes are likely to be broadly different. I propose that that biophysical effects of *SCN5A*-E1784K may be influenced by common genetic variation such that *SCN5A*-E1784K carriers with the LQTS phenotype may have prolonged action potential duration (APD) and *SCN5A*-E1784K carriers with the BrS phenotype may have a reduced peak sodium current density. The plausibility of this suggested mechanism is supported by evidence of similar competing mechanisms that have been shown in other ion channel disorders with mixed phenotype. One such example is the L-type calcium channel (LTCC).[39] Mutations and polymorphisms in LTCC genes can reduce the LTCC peak current and prolong the LTCC window current.[40] $Ca_v1.2$ forms the α subunit of LTCC and is encoded by *CACNA1C*. Gain-of-function mutations in *CACNA1C* are associated with Timothy syndrome (LQT8). However, loss-of-function mutations in the α and β subunits of the cardiac LTCC have been shown to be associated with BrS, short QT intervals and risk of sudden death.[39,41,42]

Sudden cardiac death

Sudden cardiac death (SCD) is an important public health problem. Despite medical advances and progress in prevention and treatment, SCD remains a leading cause of mortality and morbidity worldwide and accounts for approximately half of all deaths from cardiovascular disease.[43] In the UK, every year up to 100,000 people suffer SCD with the NHS ambulance services treating approximately 30,000 out of hospital cardiac arrests (OOHCA) annually. Reported survival rates are poor, with successful initial resuscitation rates ranging from 13 to 37%, and survival to hospital discharge being under 12%, although there is a lack of available systematic data.[44–46] Inherited cardiac conditions confer an annual risk of SCD up to 1%, depending on the phenotype and severity of the underlying condition.[47] Sudden arrhythmic death syndromes (SADS), where the heart at post mortem is structurally normal and toxicology is negative, are estimated to account for 0.5% sudden unexplained deaths / 100,000 / year in adult Caucasians aged 16-64, although under-recording and mis-recording of SADS deaths have been found.[48,49] The true estimated rate of SADS deaths in UK may be as high as 1.34 deaths / 100,000 / year in Caucasians aged 4-64.[47,50] Overall, the annual incidence of SADS in the population is 0.16 per 100,000.[50]

Sudden cardiac death is distressing at any age, but sudden death in young, otherwise healthy individuals, is particularly devastating. A structurally normal heart is seen in up to 60% of all SCDs in young people and up to nearly a quarter of cases in athletes.[51] Evaluation of blood relatives can identify an underlying genetic cardiac condition in up to half of SADS deaths.[52–54] Up to 90% of SADS victims have no preceding symptoms or known risk factors for sudden death.[51] This highlights the importance of predicting risk in this population to prevent untimely sudden cardiac death.

Inherited arrhythmia syndromes

Long QT syndrome (LQTS), Brugada syndrome (BrS) and catecholaminergic polymorphic ventricular tachycardia (CPVT) are inherited arrhythmia syndromes that predispose affected individuals to fatal arrhythmias that lead to SCD. These conditions affect the electrical properties of myocardial tissue but are classically associated with no structural cardiac abnormalities, although evidence is emerging that BrS may be within the spectrum of subtle structural heart disease.[55,56]

LQTS and BrS are the most prevalent inherited arrhythmia syndromes globally and are responsible for 20-30% of unexpected SCD in the young.[57] LQTS is characterised by delayed cardiac repolarisation that manifests as a prolonged QT interval, Torsades de Pointes, syncope and SCD. The population prevalence is approximately 1:2000 to 1:5000.[58] BrS is characterised by the hallmark type 1 Brugada ECG pattern and predisposition to fatal ventricular arrhythmias. The type 1 Brugada ECG pattern may be transient and can be provoked by sodium channel blocking agents (class Ia and Ic antiarrhythmic drugs). The population prevalence is estimated to be 1:2000 in Western populations but is more common in South East Asia (up to 1: 500).[59]

Common considerations in clinical genetics

This section is adapted from a peer-reviewed clinical review co-authored by me.[60]

Genetic diagnostic yields in inherited arrhythmia syndromes are never 100%, even for the best characterised diseases, so a negative test does not exclude disease. For example, yield of disease-causing or pathogenic variants (also known as ‘mutations’) from genetic testing in definite cases of LQTS is 80-85%, while it is only 20-25% in BrS.[61] Determining variant pathogenicity (AKA variant calling) can be

challenging. Advances in sequencing, including the use of next generation sequencing (NGS), have led to increasing gene panel sizes and enabled simultaneous sequencing of the entire exome, thereby increasing the potential yield of genetic testing. This has also led to the discovery of an increasing number of variants of unknown or uncertain significance (VUS) compromising diagnostic sensitivity, the so-called 'signal-to-noise' ratio.[62,63] The signal-to-noise ratio is a more recently employed terminology and is the expected yield of rare genetic variants in disease cases divided by the background rate of rare genetic variants in controls. This provides a sense of the positive predictive value of a 'positive' genetic test result.[61] However, more established terms to describe this concept would be detection rate (sensitivity) and false positive rate (1-specificity). For genetic testing targeted to phenotype, it has been estimated that the specificity for disease-specific genetic testing can be exceedingly low for conditions such as arrhythmogenic cardiomyopathy, but better for LQTS.[61] In commercialised disease-specific gene panels that include minor disease-associated genes, where each gene may be responsible for <1% of the disease in question, the false positive rate worsens dramatically because of the frequency of background variation in these minor genes.[61]

The role of genetic testing should always be to complement, rather than replace or supersede, clinical evaluation. It is best suited to supporting diagnosis in the setting of a clear phenotype. Genetic yields are never 100%, so a negative test does not exclude disease. The exception is cascade genetic screening where a clear phenotype and pathogenic mutation has been identified in a family, in which case predictive testing is possible. Larger NGS panels increase the background genetic noise and reduce the signal-to-noise ratio with many rare variants often being missense and/or private to a family and pathogenicity unknown: the VUS. Large gene panels can be used to complement clinical screening. Incorrectly calling a

variant as pathogenic can have major clinical, psychological and financial consequences for the affected family members. Where a VUS is found, pathogenicity should be clarified through segregation analysis in the family after appropriate counselling (the variant could be 'private' within the family), along with regular review of the scientific literature.[64]

Rare variants are often missense or private to a specific family and are therefore often VUSs. A VUS can have significant implications for family members if it is used inappropriately to diagnose disease in relatives. Inappropriate genetic diagnosis and subsequent management has led to the coining of the term 'genetic purgatory' for such errors in interpretation that may often lead to incorrect therapeutics.[65] In this context, this term has been described as the situation where a genetic test-ordering physician and their patients and families become trapped in a diagnostic dilemma when a VUS has been found. It can cause avoidable suffering and psychological distress for families because of inappropriate handling of the VUS such as using the finding for predictive genetic testing or making radical treatment recommendations based on the presence or absence of a 'probable mutation'.[65] The use of VUSs should therefore be restricted to determination of pathogenicity through segregation analysis and clarification of sporadic (*de novo*) or germline mutations. The variant should also undergo regular rigorous review in case the scientific literature changes and pathogenicity can be accurately ascribed or excluded. Consensus guidelines have been developed by the American College of Medical Genetics (ACMG) to set standards on determining the pathogenicity of variants (pathogenic, likely pathogenic, benign or likely benign).[64] These are based upon: 1) the absence of the variant in a healthy control population; 2) co-segregation of phenotype with genotype in large families, or presence of a *de novo* variant (both paternity and maternity confirmed) in the proband with no family history; 3) severity of the type of mutation (for example nonsense, frameshift mutation or deletion vs. missense

mutation) and location of the variant within the genome (for example a critical and well established functional domain); 4) prior description of the variant in the literature; 5) amino acid conservation and evidence from *in silico* modelling tools; 6) *in vitro* or *in vivo* functional expression studies demonstrating the variant's biophysical effect(s).[62,64]

Miscalling of less common, but not extremely rare, variants as causative has added to problems with interpretation of genetic results. This is most apparent when historical studies utilising small controls have labelled certain variants as causative but when examined in modern data sets appear to be too common to be truly pathogenic of a monogenic disorder. For example, marked overrepresentation of variants previously associated with several inherited cardiac ion channelopathies have been identified in a large exome database provided by the Exome Sequencing Project.[66–68] These may represent predisposing genetic factors or benign background variation that may be ethnically specific, and must be taken into account before assigning pathogenicity.[69–71] In order to minimise the chances of incorrectly assigning pathogenicity, the number of ethnically matched controls in such studies should exceed as much as possible the prevalence of the disorder in the population studied. Thus, if a VUS has close to this prevalence in a healthy control it is highly unlikely to be pathogenic in its own right. Collaborative datasets including the ClinGen and ClinVar partnership, the Exome Variant Server and gnomAD (previously released as ExAC) databases attempt to address these issues.[72,73] ClinVar and ClinGen aim to centralise the data available on genomic variation and pathogenicity whilst ExAC provided exome data for over 60,000 individuals of different ethnicity. The ExAC database has now been superseded by the Genome Aggregation Database (gnomAD). This is a resource developed by an international collaboration of clinicians and scientists, with the goal of aggregating and harmonising both exome and genome sequencing data from an extensive array

of large-scale sequencing studies, making summary data available for the wider scientific community.[74]

Mutations in *SCN5A* constitute the most prevalent BrS genotype but a pathogenic variant is only identified in 20% of cases.[75] *SCN5A* mutations are also responsible for the LQT3 subtype of LQTS and account for 5-10% of LQTS probands.[76] Variable expression is common in both LQTS and BrS pedigrees, suggesting that genetic modifiers may play an important role in phenotype.[75] Common genetic variation has been associated with BrS, independent of *SCN5A* status.[77] The monogenic role of *SCN5A* in BrS has also been questioned, as wild-type individuals from mutation-positive pedigrees have been found to have the type 1 Brugada ECG pattern.[75] This will be discussed further in the following sections.

Brugada syndrome

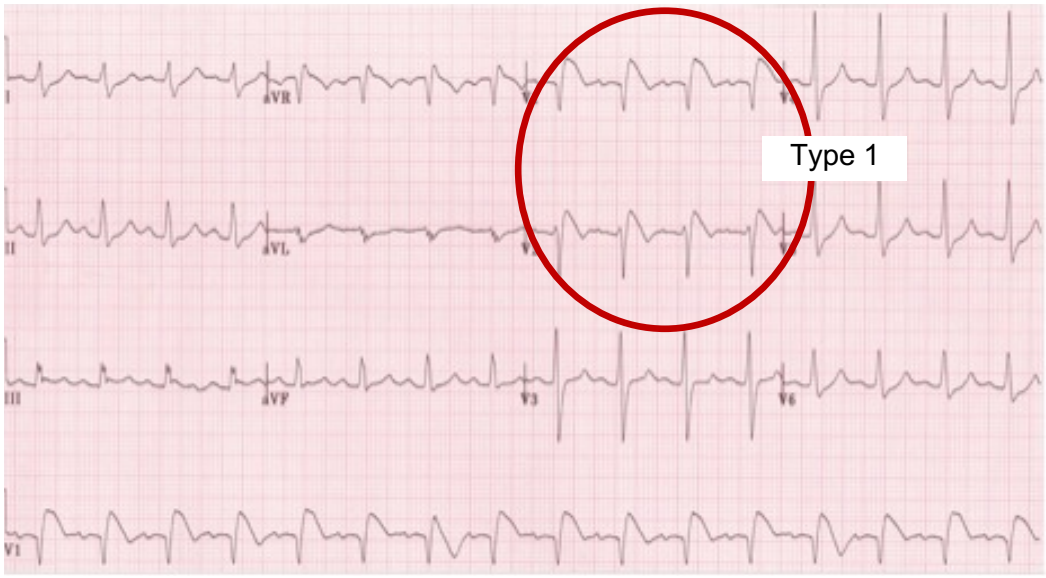
Brugada syndrome (BrS) can lead to ventricular arrhythmia and sudden cardiac death in otherwise apparently healthy young adults. It was first described in 1992 as a distinct clinical and electrocardiographic syndrome presenting with structurally normal heart, right bundle branch block, persistent ST segment elevation and sudden cardiac death.[78] It can predispose affected individuals to VF or polymorphic VT. The population prevalence worldwide is estimated to be approximately 1:2000, although its prevalence in Western European populations may be lower.[79]

Clinical diagnosis

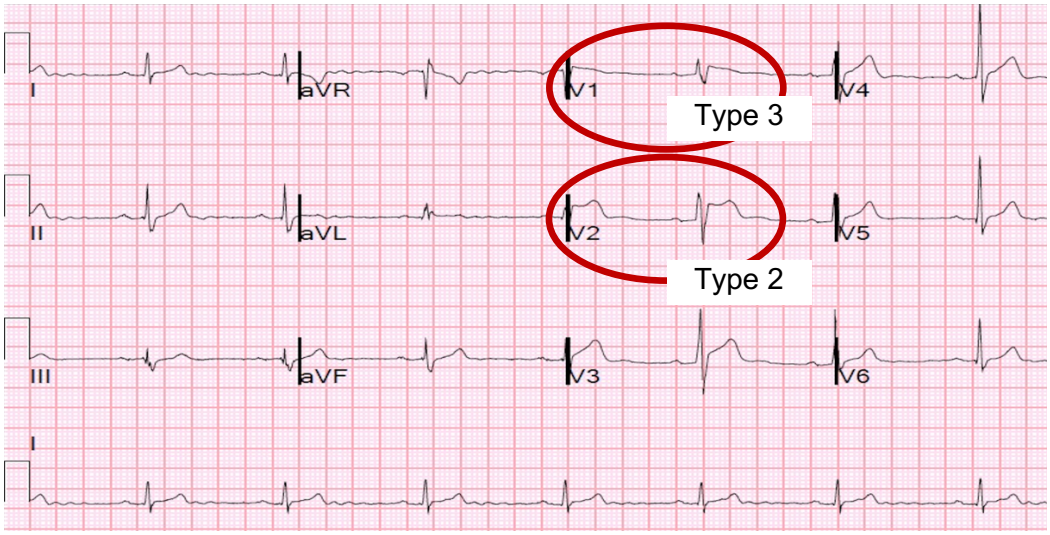
The diagnosis of BrS can be challenging. Affected individuals may be asymptomatic or suffer from syncope or seizures / nocturnal agonal respiration, although the first presentation may often be sudden death or sudden cardiac arrest. The clue to the initial clinical diagnosis of BrS is an abnormal surface ECG. The syndrome is

characterised by partial right bundle branch block and the presence or inducibility of characteristic J point elevation of >2mm or 0.2mV at its peak with coved-shaped ST elevation (little or no isoelectric separation with the J point) and T wave inversion in the right precordial leads (the type 1 Brugada ECG pattern).[78,80] The spectrum of Brugada ECG patterns also constitute the type 2 and type 3 Brugada ECG patterns. The type 2 Brugada ECG pattern also has high J point elevation ≥ 2mm or 0.2mV, but in this case, the J wave amplitude gives rise to a gradually descending ST segment elevation that remains ≥ 1mm above the baseline, followed by a positive or biphasic T wave that results in a 'saddle-back' configuration. The type 3 Brugada pattern is ST segment / J point elevation in the right precordial leads of <1mm of saddle-back type, coved type, or both.[81] However, only the type 1 Brugada pattern is diagnostic. Figure 8 shows examples of type 1, 2 and 3 Brugada ECG patterns.

The ECG characteristics of BrS are often dynamic and affected by certain drugs, autonomic tone, electrolyte disturbances, changes in body temperature and exercise. Affected individuals may have either a characteristic Brugada ECG pattern or baseline ECG values within the expected range in healthy population. It has been described that, upon intensive follow up, patients with a Brugada ECG may at some point in their lives, show a completely normal ECG.[82] This dynamic Brugada ECG pattern makes clinical diagnosis of the condition challenging, as an affected patient with a type 1 ECG pattern may not demonstrate that pattern during clinical evaluation.



(a)



(b)

Figure 8. Type 1 (Figure 3a leads V1 and V2), type 2 (Figure 3b lead V2) and type 3 (Figure 3b lead V1) Brugada ECG patterns. Only Figure 1a is diagnostic.

Expert consensus statements have recommended using a diagnostic challenge with a sodium channel blocker (class 1 antiarrhythmic drug) such as ajmaline to unmask the type 1 Brugada pattern.[59] Ajmaline has a short half-life, can be infused intravenously, and its effects are rapidly reversible. These properties make it useful in challenging the myocardium to unmask the electrophysiologic abnormalities

diagnostic of BrS. The peak effect from the drug is seen at one to two minutes after stopping the infusion after which the ECG gradually returns to baseline within approximately 10-20 minutes.[83] Systematic use of ajmaline diagnostic testing when evaluating first degree relatives of SCD victims has resulted in the diagnosis of BrS in 28% of families and 15% of relatives where there has been an unexplained sudden death / sudden arrhythmic death syndrome (SADS) in the family.[54] Within these families with a positive diagnosis of BrS, 42% of individual family members were found to be affected. These data suggest higher than expected prevalence of BrS as a cause of SADS.

There however remain several concerns with this approach. In the absence of a genetic gold standard test to diagnose BrS, it is unclear whether there is over-diagnosis of the condition by classifying people with positive ajmaline test as affected by the condition. Hasdemir *et al* attempted to determine the prevalence of the drug-induced type 1 Brugada ECG pattern (concealed BrS) in patients presenting with atrioventricular node re-entrant tachycardia, AVNRT (i.e. similar pre-test probability of an inherited cardiac condition compared to the general population). A drug-induced type 1 Brugada ECG pattern was uncovered in 26 of 96 patients with AVNRT (27%) of AVNRT patients and 4.5% of control subjects. Their findings suggested that spontaneous AVNRT and drug-induced type 1 Brugada ECG pattern can co-exist, particularly in females, and that this phenomenon may have a genetic predisposition.[84] There are limited data on the influence of genetic factors affecting the ECG responses seen with ajmaline (see below). Moreover, it is unknown whether changes seen during ajmaline testing are attributable to the variability in pharmacokinetic behaviour of ajmaline between individuals rather than being a true reflection of underlying disease. Fibrosis and pre-existing conduction properties in healthy as well as affected individuals may influence the ajmaline response.

A more recent consensus statement recommends only carrying out a class 1 antiarrhythmic drug challenge when the likelihood of the condition is clinically plausible. The 2016 HRS/EHRA/APHRS/SOLAECE J-Wave Syndrome Consensus Report proposed a scoring system for BrS diagnosis that takes into account electrocardiographic recordings, genetic results, clinical characteristics, and family history (Table 1). Validation of this scoring system by Kawada *et al* also proposed using it as a dynamic scoring system over a person's lifetime, thereby showing some potential as a risk prediction tool.[85–87]

I. ECG (12 lead or Ambulatory)	**Points**
A. Spontaneous type 1 Brugada ECG pattern on standard or high leads	3.5
B. Fever-induced type 1 Brugada ECG pattern on standard or high leads	3
C. Type 2 or type 3 Brugada ECG pattern that converts to a type 1 pattern with a provocative sodium channel blocker drug challenge	2
II. Clinical history	
A. Unexplained cardiac arrest or documented VF / polymorphic VT	3
B. Nocturnal agonal respiration	2
C. Suspected arrhythmic syncope	2
D. Syncope or unclear mechanism or unclear aetiology	1
E. Atrial flutter or atrial fibrillation in patients <30 years without an alternative aetiology	0.5
III. Family history	
A. First or second degree relative with a definitive diagnosis of BrS	2
B. Suspected SCD due to BrS (in the presence of fever, nocturnal death or in the presence of BrS aggravating drugs, for example) in a first or second degree relative	1
C. Unexplained SCD <45 years in a first or second degree relative with negative autopsy	0.5
IV. Genetic test result	
A. Probable pathogenic mutation in BrS-susceptibility	0.5

Table 1. Shanghai Score System for the Diagnosis of BrS (adapted from the 2016 HRS/EHRA/APHRS/SOLAECE J-Wave Syndrome Consensus Report). A score >3.5 points suggests

probable or definite BrS, whereas a score of 2 – 3 points should raise the suspicion of possible BrS. Points should only be allocated once for the highest score within each category (I – IV).[85]

Molecular genetics and genotype-phenotype correlation

BrS tends to show an autosomal dominant pattern of inheritance with low penetrance. More than 20 genes have been reported to cause BrS, although the evidence supporting causality is limited.[88] Evidence-based semiquantitative scoring of genetic and experimental evidence for gene-disease associations by the National Institutes of Health Clinical Genome Resource Consortium found that, of 21 genes previously curated for clinical validity, only the *SCN5A* gene, encoding the alpha subunit of the cardiac sodium channel, was found to have definitive evidence supporting causation. All the other genes were reclassified as disputed with regard to any assertions of disease causality in BrS.[89,90] However, despite its causal association with the Brugada phenotype, only 20-25% of Brugada cases have mutations in the *SCN5A* gene and *SCN5A* mutations exhibit incomplete penetrance and variable expression.[88,91] Incomplete penetrance is when some individuals who have the same genetic condition express the disease phenotype whilst others have no demonstrable phenotype. Variable expression is where the severity of the phenotype / clinical manifestation of a pathogenic variant varies between different individuals carrying the same pathogenic variant. Furthermore, the causal association in the case of *SCN5A* is less clear in some families, where genotype-phenotype mismatch is evident: in one study involving large families with known *SCN5A* mutations, it was found that some family members who developed the type 1 Brugada pattern, mostly in response to sodium channel blocker provocation, did not in fact carry the *SCN5A* mutation that was known to be present in their family.[75] Such genotype-phenotype mismatch may be accounted for by:

- an alternative genetic aetiology to BrS:
    - additional rare genetic variants and/or

    - common genetic variation
- *SCN5A* mutations acting as a modifier upon the phenotype rather than being directly causal.
- differences in the pharmacodynamic (PD) and pharmacokinetic (PK) properties of ajmaline in individual patients resulting in 'false positive' manifestations of the type 1 Brugada ECG pattern on provocation testing.
- underlying subtle structural properties influencing the Brugada phenotype as described above.

SCN5A mutations can also affect disease severity in BrS. In some families, the presence of *SCN5A* mutations have been associated with a higher prevalence of conduction abnormalities on ECG and a higher risk of cardiac events.[92,93]

Common Genetic Variation

A genome-wide association study (GWAS) aims to study common genetic variants or single nucleotide polymorphisms (SNPs) found in the general population, that can affect phenotypic expression of certain diseases. It involves comparing tagging SNPs across the genomes from a large number of individuals with the disease of interest compared to healthy controls, to identify common genetic markers that associate with the presence or severity of disease. Through a GWAS, three SNPs at the *SCN5A/SCN10A* locus and near the *HEY2* gene were associated with the BrS phenotype.[77] Bezzina *et al* found that there was a large cumulative effect of the three loci on disease susceptibility. The GWAS studied Caucasian probands and was validated in a Japanese population and Bezzina *et al* also demonstrated further evidence for the functional consequences of *HEY2* in affecting conduction and action potential velocity were demonstrated in animal models.[77] A study attempting to validate these SNPs in 190 unrelated Taiwanese BrS patients showed that the

cumulative risk of BrS-related SNPs were similar to that in Caucasian BrS patients. Interestingly, BrS patients without *SCN5A* mutations had more risk alleles than BrS patients with *SCN5A* mutations.[94] These findings provided the first substantial evidence that common genetic variation can have a strong impact on the expression of the BrS phenotype. Evidence from more functional studies subsequently emerged that the *HEY2* gene can modulate cardiac transmural ion channel patterning in ventricular cardiomyocytes and electrical heterogeneity across the right ventricle in transcriptomic studies in human hearts and animal models of BrS respectively.[25]

The emergence of evidence of increasing risk with increasing alleles raised the possibility of a potential genetic risk score (GRS, also known as polygenic risk score) for BrS. A GRS or polygenic risk score is an estimate of an individual's genetic liability to a trait or disease, calculated according to their genotype profile.[95] In 2019, genetic factors were shown to underlie the variability of cardiac electrical responses to sodium channel blocking drugs. Tadros *et al* demonstrated that a Brugada syndrome genetic risk score, family history and baseline ECG can predict the development of a diagnostic drug-induced type 1 Brugada ECG pattern with clinically relevant accuracy.[96]

Pathophysiology of BrS and cardiac structural changes

BrS has traditionally been associated with a structurally healthy heart. Despite this, fibrofatty changes and regional contractile abnormalities in the right ventricle have been described.[97,98] Patients with a spontaneous type 1 Brugada ECG pattern have been shown to have larger RVOT (right ventricular outflow tract) dimensions and slightly lower overall left and right ventricular ejection fractions compared to healthy controls.[99] Further, RVOT contraction delays have been demonstrated in patients

with BrS using equilibrium radionuclide angiography.[100] It is unclear whether any structural changes associated with the condition, provide a substrate for the abnormal electrophysiology; or rather represent contractile abnormalities and cardiac adaptation as a response to the abnormal depolarisation / repolarisation.[101] Some patients with BrS have left ventricular mid-wall late gadolinium enhancement on cardiac MRI that is consistent with an underlying cardiomyopathic process.[55] Due to emerging evidence, it has been proposed that BrS should be regarded as a condition within the spectrum of arrhythmogenic cardiomyopathy.[102]

BrS is associated with defects in cardiac sodium channel expression, resulting in a reduction the influx of sodium ions (I_{NA}) into myocardial cells. The exact mechanism of how this leads to the characteristic ECG changes is debatable. The primary repolarization theory was the first proposed hypothesis and is based on abnormal shortening of the epicardial action potential duration in affected individuals. An alternative theory is the depolarization disorder model where it is speculated that a conduction delay in the RVOT may be responsible, possibly due to a local structural abnormality.[103–105] Postema *et al* have demonstrated electrophysiological evidence of conduction slowing with substrates of discontinuous conduction in the RV of BrS patients.[106] Regional RVOT conduction delay and the presence of slow-conduction zones provide further evidence for an arrhythmogenic substrate in the RVOT in BrS.[107] In 2011, Nademanee *et al* showed that patients with the typical type 1 Brugada ECG pattern and inducible VT / VF show features of depolarisation delay over the anterior aspect of the RVOT that were corrected with catheter ablation.[56,108] Conduction slowing in the RVOT associated with interstitial fibrosis has also been demonstrated in the explanted heart from a patient with BrS undergoing cardiac transplantation.[109] Furthermore, BrS has been shown to be associated with epicardial surface and interstitial fibrosis and reduced gap junction expression in the right ventricular outflow tract in post-mortem hearts. These areas correlate with

areas of abnormal potentials on intracardiac electrograms *in vivo* in living patients, and ablation at these sites abolished the Brugada phenotype and risk of life-threatening arrhythmias. In the same study, it was also demonstrated that BrS is associated with increased collagen throughout the heart, providing further evidence that abnormal myocardial structure and conduction have an important role in the pathophysiology of BrS.[56]

Prognosis of BrS

The annual incidence of arrhythmic events for BrS patients who haven't had prior aborted SCD ranges from 0.5% to 4%, depending on the series, but it is not known whether this annual event rate is consistent over longer periods of follow up.[79] In a landmark study of BrS patients recruited from a number of European tertiary centres, the documented arrhythmic event rate (SCD, appropriate ICD shocks or sustained ventricular tachyarrhythmias) per year was 7.7% in patients with aborted SCD, 1.9% in patients with syncope, and 0.5% in asymptomatic patients.[110] A spontaneous type 1 Brugada ECG pattern and arrhythmic syncope were predictors of arrhythmic events, while gender, family history of SCD, presence of an *SCN5A* mutation or inducibility of tachyarrhythmia during electrophysiological study were not predictors of arrhythmic events.[110] Risk of SCD was higher in patients with the spontaneous type 1 Brugada ECG, as opposed to asymptomatic patients who only have an inducible ECG with ajmaline. Interestingly, in a recent series of 177 female patients, it has been shown that atrial fibrillation and a positive genetic test were risk factors for future arrhythmic events.[111] These findings need to be validated in larger numbers of patients.

A collaborative multicentre international study of 678 patients with documented arrhythmic events with BrS, where I am a co-author, found that the first appropriate

therapy in those with primary prevention ICDs occurred during the first five years in 76.6% of patients.[112] Seventy five percent of BrS patients who received a primary prevention ICD with a class II indication according to the 2013 HRS/EHRA/APHRS guidelines, exhibited an arrhythmic event.[59,113] The vast majority (94%) of patients who had an arrhythmic event were aged between 16 and 70 years.[114] Those who had an arrhythmic event at a later age after implantation of a primary prevention ICD had a higher incidence of positive family history of sudden cardiac death and *SCN5A* mutations compared with those presenting with an aborted cardiac arrest. More work is required in predicting risk and accurate risk stratification of BrS patients, particularly in subsets of BrS patients such as those with overlap syndromes.

Mechanisms of arrhythmia in BrS and their relevance to therapeutic considerations

As described above, the underlying pathophysiology of BrS have been proposed as due to two different mechanisms: the repolarisation theory[115] and the depolarisation theory.[56,103] It is unclear if these two proposed mechanisms co-exist or are mutually exclusive.[116] There are however other observations that are relevant to clinical considerations.

Differences in sex-related cardiac electrophysiological characteristics may be responsible for gender differences in risk of arrhythmia in BrS.[117] Males are more likely to have a type 1 BrS ECG pattern and have a higher risk of arrhythmias. Females have lower expression of $KChIP_2$, which is the main accessory subunit of I_{to} in the ventricular myocardium.[118] Females also have been shown to have greater sinoatrial node automaticity and enhanced AV node conduction than males, that may also contribute to the lower incidence of arrhythmias in females.[117,119]

The risk of arrhythmia in BrS is greatest during sleep and nocturnal death is a classic feature of BrS. This is at least partly due to higher vagal tone and resultant bradycardia during sleep.[120] However, there is also evidence that patients with BrS have a higher incidence of sleep disordered breathing, even in the presence of normal body habitus. Comorbid sleep disordered breathing may contribute to the higher incidence of nocturnal death in BrS. Further, autonomic instability during rapid eye movement (REM) sleep and arousals from sleep could exacerbate the risk of arrhythmias nocturnally.[121]

Other environmental factors that increase the risk of arrhythmia in BrS include alcohol intake and fever. In one Japanese study, it has been shown that enhanced activity of an alcohol metabolising enzyme ADH1B was associated with arrhythmic events.[122] These findings need to be verified in larger populations and other ethnicities. It has been shown that fever can worsen the biophysical properties of defective ion channels, that might lead to further attenuation of I_{Na}.[123] Another possibility is that, in heterozygote patients, the effect of fever on the wild-type channels (that become less efficient at high temperatures) may be responsible for fever-induced arrhythmias, but only in the presence of other factors that affect depolarisation and repolarisation reserve, such as heterozygosity with loss-of-function mutations.[124,125]

The only class 1 recommendations for treatment of BrS are lifestyle modifications (avoidance of drugs that may induce or aggravate ST-segment elevation in the right precordial leads; avoidance of excessive alcohol intake and immediate treatment of fever with antipyretic drugs), and ICD implantation as secondary prevention. Quinidine can be useful in suppressing recurrent arrhythmias in patients with BrS, and isoprenaline may suppress electrical storms related to BrS.[59] Quinidine is a class I antiarrhythmic agent (blocking I_{Na}), but it also blocks I_{to} amongst other

potassium currents. Unlike other class I antiarrhythmics that are proarrhythmic in BrS, it is plausible that inhibition of I_{to} by quinidine (that thereby restores electrical homogeneity) may contribute to its antiarrhythmic properties in BrS. Quinidine also prolongs ventricular refractoriness, and exerts an anticholinergic effect, both of which may also contribute to its utility in BrS.[126] Although isoprenaline is generally proarrhythmic, it is effective in electrical storms related to BRs and prevents recurrences of VF. This is due to beta-adrenergic stimulation and reduction in vagal tone with isoprenaline that reduce I_{to} and increase I_{CaL}. This may result in restoration of the dome of cardiac action potentials, reducing the degree of local and transmural heterogeneity and arrhythmogenicity.[127]

Long QT syndrome

This section is adapted from the chapter co-authored by me as first author for the book 'Clinical Cardiogenetics'.

Long QT syndrome (LQTS) is an inherited arrhythmia syndrome predisposing to life-threatening ventricular arrhythmias and sudden death. It is caused by prolongation of the repolarisation phase of the cardiac action potential, which may manifest as lengthening of the heart rate-corrected QT interval (QTc) on the surface electrocardiogram (ECG).

LQTS was first described as an autosomal recessive form with sensorineural deafness, the Jervell and Lange-Nielsen syndrome, and the autosomal dominant form, the Romano-Ward syndrome.[128–130] It was not until the 1990s that the molecular basis of the condition began to unravel through linkage studies and the subsequent identification of mutations in specific genes that encode cardiac ion channels.[24,131–134]

The prevalence of LQTS amongst Caucasians is estimated to be 1:2000-1:2500 based upon a large study of neonatal ECGs and targeted genetic testing in nearly 45,000 Italian infants.[135] The clinically diagnosed prevalence in the general population is however likely to be less than 1:2000. This is because of incomplete penetrance with a large proportion of mutation carriers remaining asymptomatic throughout life and escaping detection. In others, the first presentation may be a fatal cardiac arrhythmia and the diagnosis made post-mortem. Indeed LQTS is one of the most common causes of autopsy-negative sudden death (SADS), accounting for up to 20% of cases.[48,53,136] Patients with LQTS have been identified worldwide, although there is a paucity of cases reported among black ethnic groups.[59]

Clinical diagnosis

The principal clinical presentations of LQTS constitute arrhythmic events and distinct ECG features which may be detected incidentally or as a consequence of family screening. Symptomatic individuals may present with syncope (unexplained loss of consciousness without warning or preceding neurological symptoms), documented ventricular arrhythmias (VT / VF) and/or cardiac arrest. On evaluation, every effort must be made to distinguish true arrhythmic syncope from other likely aetiologies not relevant to a diagnosis of LQTS, although making such a distinction may often be challenging.

The occurrence of the initial cardiac event appears to be related to age, sex and the severity of QT prolongation. In particular, male children and female adults are at greater risk. Early data suggested that genotype may also predict risk. For example, early registry data indicated a higher incidence of lethal events in LQT3 despite therapy, especially at the first episode.[137] Cardiac events occur earlier in LQT1

males than females, and LQT1 patients typically experience cardiac events at a younger age, with the majority experiencing their first event (syncope, resuscitated cardiac arrest or sudden death) by the age of 20 years.[138] Other data, however, have suggested that LQT2 and LQT3 patients have the highest incidence of first cardiac event under the age of 40 years (42-45%) compared to LQT1 (30%).[139] The most recent data from the long QT registry suggest however that while the gene affected in an individual may influence the incidence of cardiac events, it plays less of a role in overall arrhythmic mortality than the above main factors. The exception is the female LQT2 carrier who is at higher risk than other genotypes.[140,141] The overall 10-year mortality of untreated, symptomatic LQTS patients is estimated at nearly 50%.[142]

Figure 9 summarises the current HRS/EHRA/APHRS consensus recommendations for diagnosis of LQTS. The international consensus risk score for probability of LQTS is summarised in Table 2. ESC guidelines that were published in 2015 recommended less stringent clinical diagnostic criteria (LQTS risk score>3; QTc≥480ms on repeated ECGs, or QTc≥460ms on repeated ECGs with unexplained syncope).[143] The presence of an unequivocally pathogenic LQTS mutation is sufficient to make the diagnosis according to both guidelines.

Expert Consensus Recommendations on LQTS Diagnosis

1. LQTS is diagnosed:
   a) in the presence of an LQTS risk score ≥3.5 (Table 2) in the absence of a secondary cause for QT prolongation and/or
   b) in the presence of an unequivocally pathogenic mutation in one of the LQTS genes or
   c) in the presence of a QT interval corrected for heart rate using Bazett's formula (QTc) ≥500 ms in repeated 12-lead electrocardiogram (ECG) and in the absence of a secondary cause for QT prolongation.

2. LQTS can be diagnosed in the presence of a QTc between 480–499 ms in repeated 12-lead ECGs in a patient with unexplained syncope in the absence of a secondary cause for QT prolongation and in the absence of a pathogenic mutation.

Figure 9. Current HRS/EHRA/APHRS Expert Consensus Recommendations on LQTS Diagnosis. Reproduced with permission from Priori *et al*, 2013.[59]

Electrocardiographic findings[a]			**Points**
A	QTc[b]	≥480 ms	3
		460–479 ms	2
		450–459 ms (male)	1
B	QTc[b] 4th minute of recovery from exercise stress test ≥480 ms		1
C	Torsades de pointes[c]		2
D	T-wave alternans		1
E	Notched T-wave in three leads		1
F	Low heart rate for age[d]		0.5
Clinical history			
A	Syncope	With stress	2
		Without stress	1
B	Congenital deafness		0.5
Family history			
A	Family members with definite LQTS[e]		1
B	Unexplained sudden cardiac death below age 30 among immediate family members[e]		0.5

Table 2. Schwartz LQTS risk score.[144] Reproduced with permission from Schwartz, P. J. & Ackerman, M. J. (2013).[145] SCORE: ≤1 point: low probability of LQTS. 1.5 to 3 points: intermediate probability of LQTS. ≥3.5 points high probability.

a In the absence of medications or disorders known to affect these electrocardiographic features.

b QTc calculated by Bazett's formula where QTc = QT/√RR.

c Mutually exclusive.

d Resting heart rate below the 2nd percentile for age.

e The same family member cannot be counted in A and B.

Electrocardiographic features of LQTS

Prolongation of the heart rate-corrected QT (QTc) interval is the hallmark of LQTS, but the QTc will vary and patients with prolonged QTc can intermittently be within normal limits. Other features to look for on the ECG include T wave morphology, T wave alternans, and evidence of sinus node dysfunction.

QT interval

The QT interval is defined as the time between the onset of the QRS complex and the end of the T wave. The end of the T wave has classically been defined as the intersection of a tangent to the steepest slope of the last limb of the T wave and the baseline, in lead II or V5/V6 (see Figure 10).[146] However, this method is not without its shortcomings, and it is easy to overestimate or underestimate the slope of the tangent. An alternative method is to use the visual end of the T wave. With either method, the end of the T wave can be difficult to determine in the presence of certain T wave morphologies, or if U waves are present and merge with the terminal part of the T wave. Generally, if the U wave is of low amplitude compared to the T wave it is unlikely to be part of the T wave and should not be measured (see figure 3). If both waves are of similar amplitude with a biphasic or notched appearance, then the U wave can be included in the measurement.[147] The only exception is Anderson-Tawil syndrome where the QT/U wave is routinely measured.[148] Another shortcoming of analogue surface ECGs is that the difference between normal and pathological QTc is below the minimum unit of measurement of intervals (40ms) on the ECG. This limitation can be at least partially overcome by using digital ECGs, and by using electronic calipers (eg. Cardio Calipers as used in this thesis) on scanned analogue ECGs that can be magnified to scale for making measurements.[149]

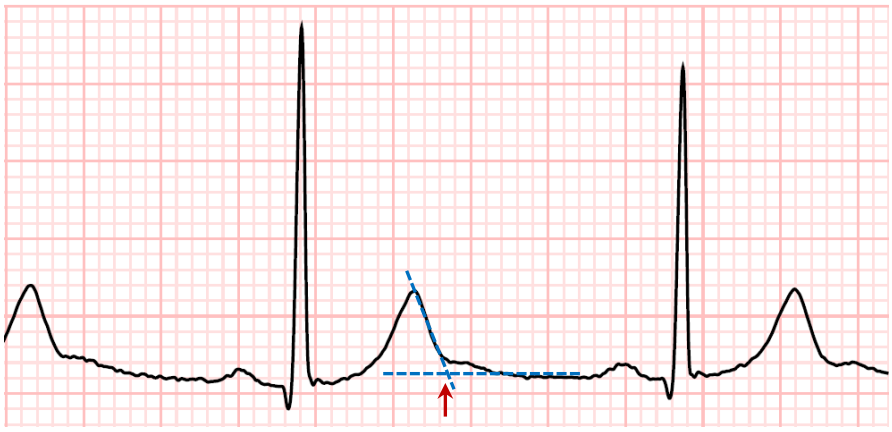


Figure 10. Determining the end of the T wave using the tangent method

The measured QT interval is then corrected for heart rate: the QTc. QTc is most commonly calculated using the Bazett's formula (QT interval/ $\sqrt{}$[R-R interval]) or occasionally Fredericia's (QT interval/ $\sqrt[3]{}$[R-R interval]), Framingham or Hodges formulae.50 Ideally the QT and RR intervals are measured on at least 3 separate beats and the mean values taken to minimise error due to sinus arrhythmia. Atrial fibrillation further complicates the time correction due to rhythm irregularity. Automated QTc measurements can be taken as a guide, but it is important that the QT interval is measured manually by a clinician with suitable expertise. Bazett's formula leads to an underestimation of the QTc at slow heart rates, while at fast heart rates there is under-correction of the QT interval leading to an overestimated QTc.

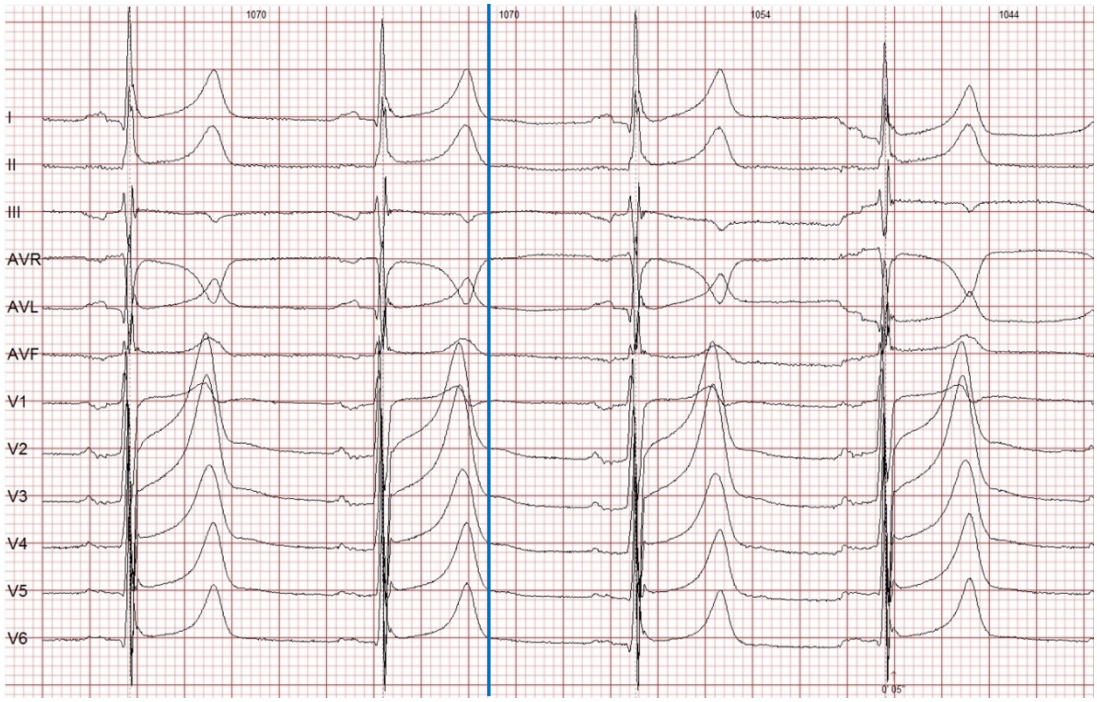
Furthermore, interventricular conduction delay and bundle branch block may lead to over-estimation of QTc. In left bundle branch block (LBBB), it has been proposed that a 'modified QTc' can be calculated to correct for the QRS prolongation, but this was based on a small study where 60 patients with sinus rhythm and narrow QRS underwent electrophysiological study with ventricular pacing at the right ventricular apex and right ventricular outflow tract to simulate LBBB.[150] It is important that the

physician is aware of these considerations when calculating the corrected QT interval.[151–153]

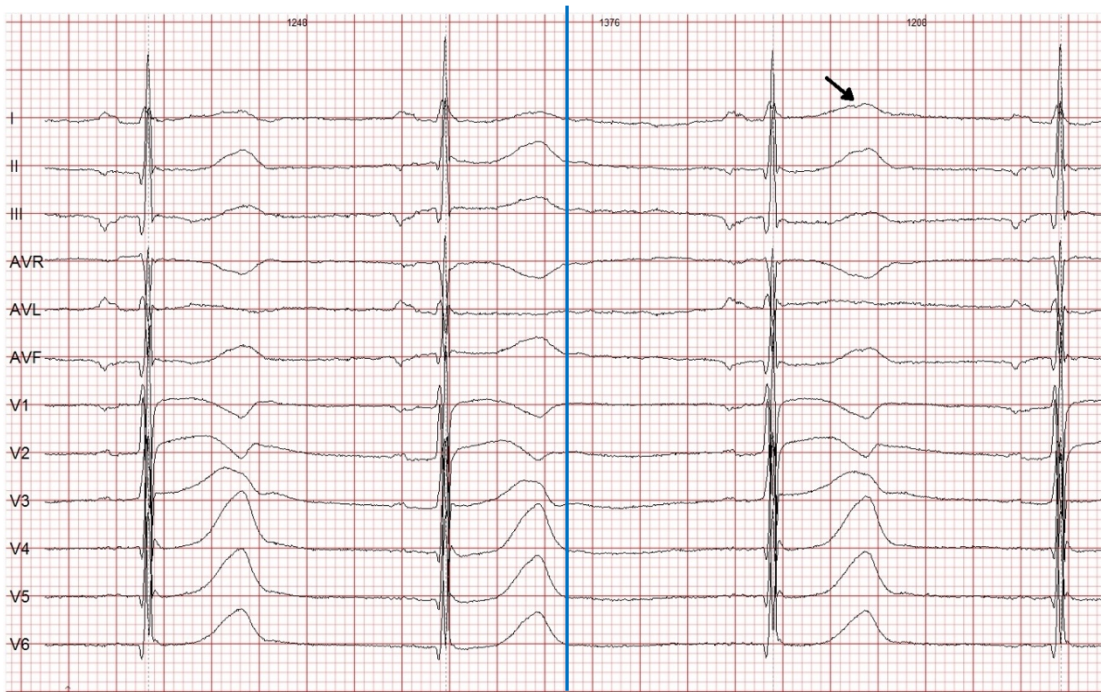
There is considerable overlap of QTc between unaffected individuals and LQTS patients in families and the general population. Many genetically confirmed LQTS patients may have QTc within the normal range due to variable penetrance: 30-40% of genotype-positive LQT1 patients, approximately 20% of LQT2 patients, and 10% of LQT3 patients do not have overt QT prolongation on the baseline ECG.[139] As a result, QTc on the surface ECG alone is not sufficient to diagnose LQTS in the vast majority of patients. An exception is if QTc is <400ms which has a negative predictive value of nearly 100%, and QTc>480ms has a high positive predictive value. In primary care, LQTS should be suspected if QTc>460ms in a child under the age of 15 years, QTc>450ms in an adult male, or if QTc>470ms in an adult female, and the patient should be referred for further evaluation.[154]

T wave morphology

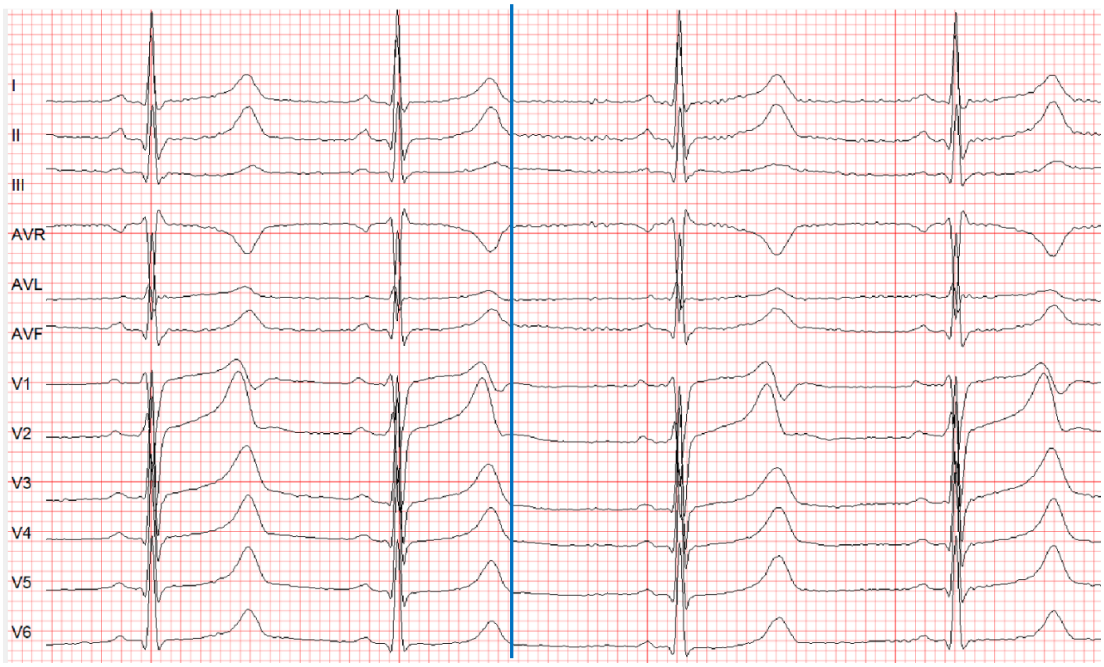
In addition to QTc prolongation, there are changes in T wave morphology in LQTS, with some morphologies being characteristically associated with mutations in certain genes. LQT1 (*KCNQ1*) is characterised by broad-based, often peaked T waves; LQT2 (*KCNH2*) by low amplitude, sometimes notched, T waves; and LQT3 (*SCN5A*) by late-onset T waves of normal duration and amplitude with a long isoelectric ST segment.[155] These characteristic morphologies, however, may not always be present and can even overlap.59 Examples of LQT1, LQT2, and LQT3 ECGs are shown in Figure 11.


1070
1070
1054
1044
I
II
III
AVR
AVL
AVF
V1
V2
V3
V4
V5
V6

a)


1248
1376
1208
I
II
III
AVR
AVL
AVF
V1
V2
V3
V4
V5
V6

b)



c)

Figure 11. Typical LQTS ECGs. a) LQT1 b) LQT2. The arrow shows a notched T wave not to be mistaken for a U wave and the whole T wave should be included in measurement. c) LQT3. The vertical blue lines indicate the end of the T wave for measuring the QT interval.

T wave alternans

T wave alternans is a beat-to-beat variation in the T wave morphology and ST segment secondary to regional heterogeneity of repolarisation. Macroscopic T wave alternans is one of the diagnostic criteria for LQTS and is a marker of high cardiac electrical instability. T wave alternans may be present at rest, but more commonly appears during periods of emotional stress or physical exertion.[156] It is associated with a propensity to life-threatening ventricular arrhythmias and high risk of cardiac events as it can precede TdP.[157]. More recently, microvolt T wave alternans, calculated from 24 hour continuous 12 lead ECG recordings, was shown to be prevalent in LQTS patients and a marker of arrhythmia risk.[158]

Post-ectopic QT prolongation

QT prolongation is common in post-ectopic sinus beats (see Figure 12).[159] QT prolongation of post-ectopic sinus beats > 480 ms should raise suspicion of LQTS which may be more apparent in LQT2.

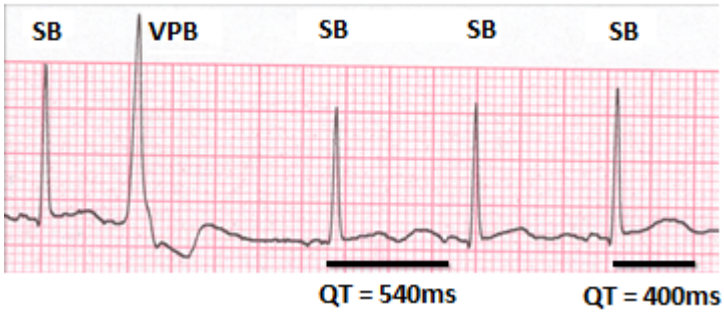


Figure 12. Post-ectopic QT prolongation in LQTS. SB = spontaneous beat and VPB = ventricular premature beat.

Sinus node dysfunction

Long sinus pauses or inappropriate sinus bradycardia indicative of sinus node dysfunction may be seen in patients with LQT3. [32,160] Incomplete penetrance of sinus node dysfunction in LQT3 may be manifest as exaggerated sinus arrhythmia, heart rates slower than would be expected for age in infants and children, or inappropriate sinus bradycardia.

Pathophysiology

LQTS is most frequently caused by loss of function mutations of genes encoding cardiac potassium channels responsible for I_{Ks} and I_{Kr}, the slow and rapid rectifying currents, resulting in reduced outward potassium currents and a longer action potential duration (APD). The ion channel dysfunction is secondary to two distinct biophysical mechanisms. One is the failure of assembly and trafficking of the channel to the cell membrane resulting in haploinsufficiency. The other is successful

trafficking to the membrane of defective channels with a dominant negative effect (where channel α-subunits are organised in tetramers and mutant protein acts antagonistically to the wild-type protein). Gain of function mutations affecting the cardiac sodium channel and its interacting proteins may lengthen the plateau phase of the APD by increasing the late inward sodium current (late I_{Na}) whilst gain of function mutations affecting the calcium channel (I_{CaL}) may also occasionally be associated.[161]

Molecular genetics and genotype-phenotype correlation

Advances in molecular genetics over the past 20 years have led to the discovery of mutations in a total of 15 genes causing LQTS and have provided insights into underlying molecular mechanisms. A mutation is identified in 80-85% of definite cases, but 15-20% of LQTS remains genetically elusive (no pathogenic variant identified despite standard clinical genetic testing). LQT1, LQT2, and LQT3, caused by mutations in *KCNQ1*, *KCNH2*, and *SCN5A* respectively, account for over 90% of genetically confirmed LQTS. Genes encoding β-subunits, membrane scaffolding proteins or proteins interacting with cardiac ion channels have been implicated in some rarer types of LQTS and have only been identified in a few families or isolated individuals.[61,161] More than 70% of cases of LQTS are caused by missense mutations, whilst the remainder comprise of frameshift (10%) and splice-site mutations and in-frame insertions and deletions.[162,163] Most reported mutations are exonic (in coding regions of the gene), but non-coding mutations that affect allele expression, and larger genomic rearrangements, have been described.[164]

Establishing the pathogenicity of variants is crucial as genetic screening has become an important tool in family screening. Identification of a VUS leads to diagnostic uncertainty with potential adverse psychological and economic

consequences to patients and families. Many studies implicating genetic variants with pathogenicity have relied on small control samples data without necessarily showing genotype-phenotype co-segregation.[165,166] A study of the Exome Variant Server in 2012, however, identified a much higher prevalence of previously LQTS-associated variants than expected in exome data from population studies, suggesting that caution must be exercised when interpreting the pathogenicity of variants in individuals and families.[66] In a further Danish population study, 33 genetic variants that were previously reported in LQTS patients were identified in 243 individuals from a sample of 7000 individuals from the general population. Ten variants were identified in 8 or more individuals included in this study. There were no associations with QTc prolongation, history of syncope, or mortality. Interestingly, the authors report that half of the identified variants also had functional studies supporting pathogenicity. The 33 variants called into question in this study only comprise <2.5% of all variants previously associated with LQTS, however these studies raise important questions about the true pathogenicity of some variants previously thought to be disease-causing.[165] In a recent transethnic GWAS, on which I am a co-author, we provided further insights into the genetic architecture of LQTS (see below).[167]

Genetic modifiers

Genetic loci, tagged by single nucleotide polymorphisms (SNPs), both in LQTS-associated genes as well as other genes, have been shown to be associated with QTc in the general population. [168–171] These are thought to influence variable penetrance and incomplete expression in some pedigrees. For example, variants in the *NOS1AP* gene in chromosome 1 has been shown to be associated with increased risk of sudden death in a South African population harbouring a founder mutation in *KCNQ1*.[172] More recently, *NOS1AP* SNPs were shown to be strongly

associated with QTc in patients with LQT2. There was also a trend for effect on risk of cardiac events in these patients. Furthermore, common genetic variation at *KCNQ1* were shown to be associated with risk of LQTS.[173] At this time these markers have not entered into routine clinical practice.

In a collaborative study led by University of Amsterdam for which I am a co-author, we found that common genetic variation plays an important role in the susceptibility to LQTS, and demonstrated overlap between genetic control of the QT interval in the general population and genetic factors contributing to LQTS susceptibility. Three loci were associated with LQTS at genome-wide statistical significance ($p<5x10^{-8}$) near *NOS1AP*, *KCNQ1* and *KLF12* in a transethnic meta-analysis in over 1600 unrelated LQTS patients of European or Japanese ancestry.[167] Around 15% of the overall susceptibility to LQTS was due to common genetic variation, and LQTS susceptibility showed a strong genome-wide genetic correlation with the QT-interval in the general population. A genetic risk score (GRS) was then calculated using common variants previously associated with the QT interval in the general population.[169] The GRS thus calculated was greater in LQTS cases compared to controls, and among LQTS probands, the GRS was greater in those who were genotype negative for the major LQTS genes. This study demonstrated interplay between common genetic variants and disease phenotype in LQTS, and was the first study to demonstrate evidence for a polygenic aetiology in genotype negative LQTS.[167]

Human induced pluripotent stem cell-derived cardiomyocytes (hiPSC-CM)

In 2006, Shinya Yamanaka and Kazutoshi Takahashi showed that differentiated cells can be reprogrammed to induced pluripotent stem cells capable of

differentiating to cells of all three germ layers by transfection with four factors, Oct3/4, Sox2, c-Myc and Klf4, under embryonic stem cell culture conditions.[174,175] Reprogramming readily harvested human somatic cells (such as fibroblasts) to human induced pluripotent stem cells (hiPSC) and subsequent differentiation to cardiomyocytes (CMs) *in vitro* provides a patient-specific model.[175–177] Using such patient-specific cells to study disease can help guide personalised risk stratification and management, a cornerstone of modern clinical practice.

Differentiation of cardiomyocytes from hiPSCs is critically dependent upon the careful regulation of Wnt / β catenin signalling pathway.[178] Wnt 3/3a play a critical role in early cardiac commitment, but non-canonical Wnt signalling is key for cardiomyocyte emergence. Wnt 11 and Wnt5a play a vital role in the final stages of cardiomyocyte differentiation.[179] However, the mechanisms remain unclear with regard to the timing of signalling pathways that regulate the Wnt in me endoderm specification to cardiac mesoderm. This leads to variability in differentiation efficiency and difficulty predicting consistency of hiPSC-CM generation.[178]

The electrophysiological properties of hiPSC-CMs have some crucial differences compared to adult human ventricular cardiomyocytes. The electrophysiological properties of hiPSC-CMs compared to mature human ventricular cardiomyocytes are depicted in Figure 13. *In vitro* differentiated cardiomyocytes currently exhibit an immature phenotype, resembling neonatal myocytes, and there can be intra-line and inter-line variability. Unlike human adult ventricular cardiomyocytes, hiPSC-CMs beat spontaneously. This is due to a more positive resting membrane potential (RMP). The more positive RMP is due to reduced I_{K1} and the presence of a pacemaker current or the “funny current”, I_f. The relatively depolarised resting membrane potential of iPSC-CMs leads to inactivation of the majority of $Na_v1.5$ channels. This renders available I_{Na} scarce during phase 0, reducing upstroke

velocity and subsequently leading to I_{to} inactivation, in turn reducing phase 1 repolarisation. Further, $I_{to,s}$ has been shown to be the dominant I_{to} current compared to $I_{to,f}$ in hiPSC-CMs, which is converse to the situation in adult human ventricular cardiomyocytes.[2] Despite these limitations, it has been demonstrated that hiPSC-CMs can be used as reliable models to study sodium currents and cardiac sodium channel disease in patients with *SCN5A* mutations.[27] These findings are reproducible in work carried out in Professor Tinker's and Professor Denning's laboratories.[180,181] However, no differences in sodium current compared to controls have been observed in patients with BrS who do not carry sodium channel mutations.[27,29] Thus focusing this study on cells from patients carrying the strongly pathogenic *SCN5A*-E1784K mutation maximises opportunities to observe electrophysiological differences that can be translated to clinical phenotype.

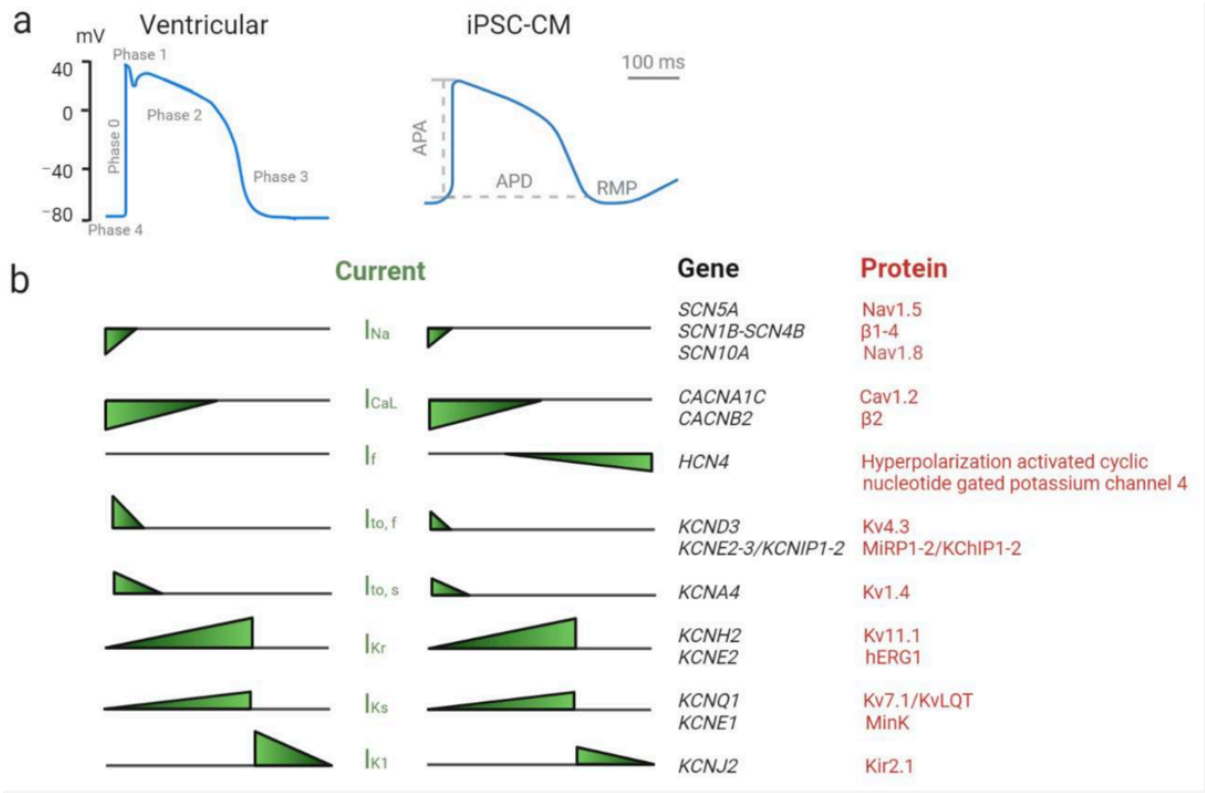


Figure 13. Schematic representation of adult human ventricular action potential (panel a) and underlying ionic currents (panel b) versus those of hiPSC-CMs. Panel b also illustrates the list of genes (in black) encoding alpha and beta ion channel

protein subunits (in red) that cooperate in the generation of the represented ion currents.[2] Reproduced with permission under the terms and conditions of the Creative Commons Attribution (CC BY) license (http://creativecommons.org/licenses/by/4.0/).

Integrating vs non-integrating strategies of reprogramming

Reprogramming methods of deriving hiPSCs from somatic cells may involve integrating vectors or non-integrating vectors. When integrating viral vectors such as retroviral and lentiviral vectors are used in reprogramming, the viral DNA translocates into the cellular nucleus and integrates into the host genome. In contrast, the genetic material of non-integrating vectors remains in the cytoplasm. Copy number variation, including likely pathogenic copy number variants, are a particular issue with integrating hiPSC lines. Further integrating hiPSC lines suffer from problems with single nucleotide variations and mosaicism than non-integrating lines.[182] These genomic aberrations make the use of integrating methods of reprogramming less attractive as a model for undertaking functional genetic studies.

One of the first so-called non-integrative approaches used to generate hiPSCs involved the use of adenoviruses that only resulted in transient expression of reprogramming factors. Adenoviruses are DNA viruses and still undergo integration events, but these are at a lower frequency than retroviral or lentiviral vectors. Genomic integration screening is still required for characterisation of adenoviral-derived hiPSCs to ensure that clones are indeed transgene-free, and reprogramming efficiency is also extremely low.[183] Several truly non-integrating methods of reprogramming exist – these include, Sendai viral, RNA transfection and episomal reprogramming.[184]

The reprogramming efficiency of all three methods of non-integrating reprogramming is in the range of 0.01-1%, with Sendai viral reprogramming having an efficiency of 0.1% with >90% reliability. The efficiency and high reliability are clear advantages of the Sendai viral method of reprogramming. There is complete absence of viral sequences in most lines at higher passages, although there is a relatively slow clearance of Sendai viral RNA. Alternative non-integrating strategies are the RNA method, which has advantages in the speed of colony emergency, high efficiency, low donor cell requirement, a complete lack of integration and low aneuploidy rate, but needs a higher workload. Further the reliability of RNA-based reprogramming is <50%, with particular issues reported when reprogramming fibroblasts from skin biopsies. Episomal reprogramming is highly reliable from both fibroblast and blood samples (CD34+ and peripheral blood mononuclear cells), however there are concerns about the genetic integrity of the resulting hiPSC lines due to the use of a *TP53* short hairpin RNA (shRNA) cassette.[184]

hiPSC-CM models to study disease

Human induced pluripotent stem cell-derived cardiomyocytes have several advantages over heterologous or animal models of human disease. Firstly, these are a true human model, derived directly from the subjects of interest. These cells have been shown to have a similar protein constitution to human cardiomyocytes and the full genomic background of the individual of interest from whom these are derived, are represented. It remains a scalable platform *in vitro* and single cells and monolayer models (2D) can be created. However, there are ongoing concerns about immaturity on a molecular, structural and electrophysiological level.[2] These will be described further in the Discussion sections of this thesis.

Several studies have demonstrated the use of hiPSC-CMs to study *in vitro* properties of inherited cardiac conditions, including the inherited arrhythmia syndromes LQTS and BrS.[29,185–188] The *in vitro* investigation of these models focus on ascertaining whether and how the electrophysiological properties of cardiomyocytes have been altered as a result of disease-causing mutations. Patch clamp allows study of single cell electrophysiology to make quantitative recordings of action potentials and ion currents in these cells, however, is limited by low throughput and single cells do not recapitulate the behaviour of the cells in a tissue or organ model. LQT1 was the first subtype of LQTS to be studied in hiPSC-CMs. I_{Ks} is challenging to study in hiPSC-CMs due to reduced total current density in these cells and late I_{Ks} onset during cardiomyocyte development. However, *in vitro* models of LQT1 were able to recapitulate the pathological phenotype with marked reductions in IKs peak current and arrhythmia susceptibility through effects on L-type Ca^{2+} current when compared to hiPSC-CMs from healthy donors or isogenic controls.[189–191] In LQT2 too, it has been shown that patient-specific hiPSC-CMs are able to predict clinical phenotype.[192] The overall magnitude of the I_{Na} current is lower in hiPSC-CMs compared to adult ventricular cardiomyocytes, but hiPSC-CM models of LQT3 have recapitulated abnormal action potential characteristics, increase in peak I_{Na}, calcium currents, arrhythmia risk and pharmacological response, despite limitations such as intra- and inter-line variability.[189,193]

Novelty of this thesis

There have, to date, been limited case series describing clinical characteristics of patients with *SCN5A*-E1784K.[32,38] This thesis describes a large cohort of patients with systematic data on phenotypic characteristics and comprises the world's largest cohort of patients collated thus far with this important mutation. It provides an opportunity to study clinical risk characteristics and common genetic variation

and their association with risk and phenotype. I describe a GRS using common variants to predict the risk of BrS phenotype in individuals from pedigrees with this mutation (Chapter 6).[194] There have been no prior studies on the impact of common genetic variation or a GRS on the expression of the LQT3 phenotype. Studying clinical characteristics of a large international cohort of carriers of this mutation and their unaffected relatives can offer unique insights into the clinical characteristics of this mutation and offers the opportunity to study for highly personalised medical management.

There has been one publication in the literature where *SCN5A*-E1784K was studied in patient-derived hiPSC-CMs.[195] Here, Okata *et al* studied hiPSC-cardiomyocytes from a single *SCN5A*-E1784K patient with BrS/LQTS overlap. They were able to recapitulate the LQT3 phenotype. However, the investigators were unable, initially, to recapitulate the BrS phenotype in hiPSC-cardiomyocytes derived from that patient, although they were able to do so after knockdown of *SCN3B*. They showed that expression of the beta-subunits of sodium channels is similar between embryonic hearts and iPSC-cardiomyocytes, but lower in adult hearts, and demonstrate through a heterologous expression system that *SCN3B* augments the otherwise reduced inward sodium current (I_{Na}) in cells transfected with *SCN5A*-E1784K.[195] Compared to the study reported by Okata *et al*, the novelty of this study lies within the strength of phenotypic data underlying the study. Detailed pedigree and phenotypic data had been collected on the largest international cohort of patients with this mutation, with access to several large pedigrees with multiple affected family members showing a wide spectrum of phenotypes. Multiple affected family members were recruited, enabling me to select patients with clear extremes of phenotype to take forward for functional characterisation using hiPSC-CMs. There have been no studies published to date of hiPSC-CMs derived from carriers of this mutation with phenotypic extremes.

Functional characterisation using patient-specific hiPSC models can offer important insights into the pathophysiology of both LQTS and BrS in patients with this mutation, and improve our understanding of the mechanisms of arrhythmia and phenotypic variability in LQTS/BrS overlap syndrome. This may be translated to better, more personalised patient management, which could improve clinical outcomes and thereby lead to patient benefit. There have been several advances in the protocols used, in line with recent advances in the field. Unlike the lentiviral method described by Okata *et al*, non-integrating Sendai virus was used to transfect the cells with the reprogramming vectors. Following this, the hiPSCs were cultured in a xeno-free and feeder-free medium, followed by a monolayer differentiation protocol using defined growth factors unlike the less specific mouse embryonic fibroblast feeder layer method for hiPSC culture and embryoid body differentiation described by the authors in the previous study.[195] The spontaneous differentiation of cardiomyocytes from pluripotent stem cells in embryoid bodies is inefficient, with a yield usually below 20%, is highly variable and cell line dependent. These variations can be minimised using a monolayer differentiation protocol.[177] Although the significance of these advances on the findings is uncertain, the newer protocols used in this thesis represent a more sophisticated model, reflecting the state of science in the hiPSC-CM field at the time. The *in vitro* properties of cells derived from mutation carriers with phenotypic extremes can offer insights into the pathophysiology of this mutation and pave the way for future research on potential therapeutic strategies, taking into account background genetic variation that may impact on phenotype.

Chapter 2: Study Design

Hypotheses

1. Common genetic variants and clinical markers associate with phenotype and risk in the cardiac sodium channel disease *SCN5A*-E1784K.
2. hiPSC-CMs derived from *SCN5A*-E1784K carriers with extremes of phenotype will recapitulate the clinical phenotype.

Rationale for the study

The study was inspired by the availability of a large, well-characterised patient cohort carrying by far the most common cardiac sodium channel mutation *SCN5A*-E1784K, that causes LQT3 and Brugada overlap disease with variable expression. There is an unmet need to improve our understanding of the pathophysiology of this mutation to identify clinical and genetic features associated with risk, not only in this, but in other cardiac ion channel diseases, through detailed clinical, genetic and functional characterisation.

Objectives

1) Study clinical characteristics and risk features that associate with outcome in a large international cohort of *SCN5A*-E1784K carriers.
2) Study common genetic variants that associate with phenotype and thus calculate genetic risk scores.
3) Produce and characterise hiPSC-CMs from *SCN5A*-E1784K carriers with extremes of LQTS and BrS phenotype, and compare to a healthy control cell line.

Research governance

The study was approved by the West London Research Ethics Committee and the St George's University of London and St George's Hospital NHS Trust Joint Research and Enterprise Office. The relevant ethics approval references are as follows:

- Clinical Evaluation and Genetic Tests for Inherited Heart Conditions (REC reference: 10/H0803/121; IRAS project ID: 53663)
- Functional Cardiomyocytes Derived from Patient-Specific Induced Pluripotent Stem Cells as a Novel Cellular Model for Studying Inherited Cardiac Diseases (REC reference: 13/LO/1447; IRAS project ID: 107616)

All international centres had ethical approval held locally for recruitment of participants and sharing of data for the study. Informed consent was obtained from all study participants. University of Nottingham and Queen Mary, University of London were approved study sites for cell reprogramming and differentiation.

Participating centres

Chapters 3-6 describe a large international multi-centre study. The complete list of participating centres was as follows:

1. Molecular and Clinical Sciences Research Institute, St George's University of London, London, United Kingdom; Cardiology Clinical Academic Group, St George's University Hospitals National Health Service (NHS) Foundation Trust, London, United Kingdom
2. Queen Mary, University of London, London, United Kingdom
3. University of Nottingham, Nottingham, United Kingdom

4. Belfast Health and Social Care Trust, Belfast, United Kingdom; Queen's University Belfast, Belfast, United Kingdom
5. Darent Valley Hospital, Dartford and Gravesham NHS Trust, Dartford, United Kingdom
6. Leeds Teaching Hospitals NHS Trust, Leeds, UK
7. Mater University and Private Hospitals, Dublin, Ireland
8. Amsterdam UMC, University of Amsterdam, Heart Center, Department of Clinical and Experimental Cardiology, Amsterdam Cardiovascular Sciences, Meibergdreef 9, Amsterdam, The Netherlands
9. L'institut du thorax, INSERM, CNRS, UNIV Nantes, Nantes, France; L'Institut du Thorax, Cardiologic Department and Reference Centre for Hereditary Arrhythmic Diseases, U1087 Nantes, France; CHU Nantes, Service de Génétique Médicale, Nantes, France; L'institut du thorax, CHU Nantes, Service de Cardiologie, Nantes, France
10. AP-HP, Hôpital Bichat, Département de Cardiologie et Centre de Référence des Maladies Cardiaques Héréditaires, Université Paris Diderot, Sorbonne Paris Cité, Paris, France INSERM U1166
11. Istituto Auxologico Italiano, IRCCS, Center for Cardiac Arrhythmias of Genetic Origin, Milan, Italy; Istituto Auxologico Italiano, IRCCS, Laboratory of Cardiovascular Genetics, Milan, Italy; Istituto Auxologico Italiano, IRCCS, Department of Cardiovascular, Neural and Metabolic Sciences, San Luca Hospital, Milan, Italy; Department of Medicine and Surgery, University of Milano-Bicocca, Milan, Italy
12. Rhythmology and Electrophysiology, Department of Cardiology and Angiology, Hannover Medical School, Hannover, Germany
13. Department of Medicine, University Medical Centre Mannheim (UMM), Faculty of Medicine Mannheim, University of Heidelberg, European Center for

AngioScience (ECAS), and DZHK (German Center for Cardiovascular Research) partner site Heidelberg/Mannheim, Mannheim, Germany

14. Helmholtz Zentrum München, Institute of Human Genetics, Neuherberg, Germany; Technische Universität München, Institute of Human Genetics, Munich, Germany; DZHK (German Centre for Cardiovascular Research), Partner Site Munich Heart Alliance, Munich, Germany
15. Departments of Cardiovascular Medicine (Division of Heart Rhythm Services), Pediatric and Adolescent Medicine (Division of Pediatric Cardiology), and Molecular Pharmacology & Experimental Therapeutics (Windland Smith Rice Sudden Death Genomics Laboratory), Mayo Clinic, USA
16. Vanderbilt University School of Medicine, Nashville, USA
17. Shiga University of Medical Science, Shiga, Japan
18. National Cerebral and Cardiovascular Center, Osaka, Japan
19. Kizawa memorial hospital, Gifu, Japan
20. Nippon Medical School, Tokyo, Japan

Chapter 3: Clinical Characterisation of *SCN5A*-E1784K

Introduction

There have been limited studies describing the phenotypic features of this mutation, despite it being the most common *SCN5A* mutation worldwide. The first case series describing the clinical characteristics of patients harbouring the cardiac sodium channel mutation *SCN5A*-E1784K was published in 2008.[32] Forty-one mutation carriers were studied. They reported a high prevalence of overlap of LQT3, BrS and sinus node disease among carriers of the mutation. The majority (>90%) were noted to have a LQT3 phenotype, approximately 20% BrS, and approximately 40% sinus node dysfunction, with variable degrees of overlap.[32] Another case series described 35 family members from a single European pedigree with the mutation, 17 of whom were *SCN5A*-E1784K positive. The *SCN5A*-E1784K positive family members were found to have QTc prolongation, and either BrS, cardiac conduction disease or both, with one family member also having sinus node dysfunction. Genotype-positive patients had longer PR interval, QRS duration and QTc compared to genotype-negative patients. None of the *SCN5A*-E1784K negative patients had a positive ajmaline test. Five of the genotype-positive family members developed VT / VF during follow up. In this case series of a single family, the authors found that the LQTS phenotype was present during all decades of life, whereas the cardiac conduction disease phenotype developed with increasing age. However, as this is a case series of a single pedigree, the generalisability of findings is questionable.[38]

In this chapter, I describe the clinical characteristics and risk markers observed in a large, well characterised international cohort of *SCN5A*-E1784K carriers and their relatives. To my knowledge, this is the largest cohort of carriers and wild-type (WT) relatives from pedigrees with this mutation described to date. Furthermore, the novelty of this study stems from the large, well characterised patient cohort recruited

to the study across a range of ethnicities. The phenotype data collected for the study was comprehensive and more extensive than any prior reported cohort or pedigrees with the *SCN5A*-E1784K mutation, despite this being the most commonly identified pathogenic variant in the voltage gated sodium channel $Na_v1.5$ among patients with BrS and those with LQT3.[13]

Methods

Recruitment and case selection

Study participants were recruited from sixteen Inherited Cardiac Conditions (ICC) specialist centres from United Kingdom, Ireland, France, Germany, Italy, USA and Japan participated. The complete list of participating centres is detailed in Chapter 2.

All participants were systematically recruited from families with *SCN5A*-E1784K under clinical care at the participating centres with suitable local ethics approval for the study. The *SCN5A*-E1784K mutation carrier status was determined before inclusion in the study. Upon identification of the probands, first- and second-degree relatives, whether hosting the mutation or not, were recruited.

Clinical parameters of the cohort studied

Comprehensive clinical data including initial presentation and follow-up data, presenting ECGs, details of any drug provocation tests, and pedigrees were collected. Data were also collected on the occurrence of all relevant cardiac symptoms at presentation and/or follow up.

ECG measurements included the presence of the Brugada ECG pattern, baseline PR interval, QRS duration, heart rate and rhythm, QRS angle and QTc (Bazett's formula). A minimum of two observers made independent manual measurements on the baseline ECG using electronic callipers (Cardio Calipers)[149], and where there was >5% discrepancy, the measurements were repeated and re-compared. If a discrepancy remained, a third observer made measurements and a mean was taken.

The data fields collected and counts of data that were completed for the study are shown in Table 3. After making manual measurements in the standardised manner described above, and data cleaning, data were inputted into the format shown in Table 4 ready for analyses.

Data field	Data count (n=336)	% (n/336)
Unique ID	336	100.0
Date of birth	336	100.0
Sex	336	100.0
Ethnicity	336	100.0
Family ID	336	100.0
Pedigree availability	336	100.0
SCN5A -E1784K status	336	100.0
ECG date	333	99.1
Baseline ECG availability for independent measurements	330	97.9
BrS code (0=negative drug challenge test; 1= spontaneous type 1 pattern; 2=positive drug challenge test)*	120	35.7
Was there an event (Yes/No)	336	100.0
Where there were event(s), event(s) experienced by study participant (arrhythmic syncope; ventricular tachycardia (VT); documented ventricular fibrillation (VF); aborted cardiac arrest; sudden death)	47	14.0
Date(s) of event(s) experienced by participant	47	14.0
Antiarrhythmic medication start date**	60	17.9
Beta blocker start date**	50	14.9
Mexiletine start date**	22	6.5
PPM date**	19	5.7
ICD date**	37	11.0
Last visit date	336	100

Table 3. Data fields collected and counts of data available. * Missing data for BrS code included those who did not undergo a drug challenge test to diagnose BrS. ** Centres completed the data sheet where therapies were given.

Data field
Unique ID
Date of birth
Sex
Ethnicity
Family ID
Father's ID
Mother's ID
SCN5A -E1784K status
BrS code (0=negative drug challenge test; 1= spontaneous type 1 pattern; 2=positive drug challenge test)
ECG date
PR interval
QRS duration
RR interval
QTcB
QRS axis
Event (0=No; 1=Yes)
Event-free interval
Lethal event (0=No; 1=Yes)
Lethal event-free interval
Antiarrhythmic medication start date
Beta blocker start date
Mexiletine start date
PPM date
ICD date
Duration of follow up

Table 4. Processed data set for analyses on R-Studio. To map pedigree data onto the data fields, for each individual, mother's ID and father's ID were derived based on the pedigree data collected. ECG data were derived from measurements made as described in methods. QTcB = corrected QT interval by Bazzett's formula.

Definitions applied

BrS phenotype was defined as the presence of either a spontaneous or drug-induced type 1 Brugada ECG pattern in at least one right precordial lead (in the standard or higher intercostal spaces).[59] Intravenous drug provocation tests (either ajmaline 1mg/kg, flecainide 2mg/kg or pilsicainide 1mg/kg) were performed at a pre-

determined rate as per local protocol. Prolonged QTc ('Long QT') was defined as >470ms for females and >450ms for males. Normal QRS axis was defined as -30 to +90 degrees. Conduction disease was defined as presence of left axis deviation (QRS axis < -30 degrees) and/or QRS duration > 120ms and/or PR interval > 200ms or the presence of higher degree AV block.

Relevant cardiac symptoms are referred here onwards as 'events' (sudden death, aborted cardiac arrest, documented ventricular fibrillation (VF), ventricular tachycardia (VT), or arrhythmic syncope) and lethal symptomatic events, referred here onwards as 'lethal events' (sudden death, aborted cardiac arrest or documented VF or VT). Arrhythmic syncope was defined as a clinical diagnosis that excluded vasovagal characteristics and supported an arrhythmic origin as determined by the cardiologist in the tertiary inherited cardiac conditions clinic from where the patient was recruited. Any events in the context of an electrophysiological (EP) study or a drug provocation test were excluded as these were provoked. Medications recorded were limited to antiarrhythmic drug use only.

Statistical analyses

All analyses were carried out using R (version 4.0.2) software and the rms, kinship2, coxme and survminer packages.[196–200] The coxme model is a cox mixed effect model for survival analysis. p-values <0.05 were considered statistically significant.

Categorical variables were described as count and percentage and compared using Fisher exact tests. Numerical variables were described as mean ± standard deviation (SD) or median and interquartile range (Q1-Q3: IQR) where appropriate. The numerical variables were compared using t-test or ANOVA for normally

distributed variables with equal variances, and Mann-Whitney or Kruskal-Wallis tests otherwise. Normality of the numerical variables was checked using histograms and the Shapiro-Wilk test. Equality of variances was tested using Levene's test.

The effects of variables on risk of events and lethal events (survival analyses) were calculated for single variables using a mixed effects Cox regression model for survival with correction for ethnicity and related observations (coxme() function). A kinship matrix was used for relatedness correction (this corrects for how much each individual in the pedigree is related to each other and makes the standard errors more robust for this analysis). This was constructed using pedigree information (kinship() function). The proportional hazard assumption was tested by visual inspection of the Kaplan-Meier curve, the Schoenfeld residuals plot and with a test for independence between covariates and time (using cox.zph() and ggcoxzph() functions).

The linearity assumption of continuous variables was checked by plotting the Martingale residuals against the continuous variable (ggcoxfunctional() function). In addition, the fit of a model assuming a nonlinear relationship (restricted cubic splines with 3 knots) was compared to that of a model assuming a linear relationship using a likelihood ratio test. For all models the discriminatory capacity was evaluated using Harrell's C statistic (interpreted as the area under the curve) for survival outcomes (rcorr.cens() function).

To correct for age-related differences in ECG traits (PR, QRS and QTc), a nonlinear relationship using restricted cubic splines (rcs() function) was fitted between age at the time of the ECG and the ECG parameters. The residuals from these models (i.e. PR.age, QRS.age and QTc.age) were used as variables in the subsequent analyses.

Possible ethnicity specific risk factors were investigated by comparing the fit of a model with the main variable and ethnicity effects with that of a model with main and the interaction effect using a likelihood ratio test. In case of a significant interaction, risks were estimated in the separate ethnicities. In case of multiple significant variables, an additional multivariable Cox regression analysis was performed with all significant ($p<0.05$) predictors with correction for ethnicity and relatedness. The same process was repeated for the risk of lethal events.

Results

The ethnicities, ECG characteristics and event status of the total cohort (at time of follow-up data collection) are described in Tables 5-6.

Variable	Total cohort n=336		Caucasian n=172 (51%)		Japanese n=80 (24%)		Other/mixed ethnicity n=80 (24%)		p-value
	N	%	N	%	N	%	N	%	
Male	148	44%	72	42%	41	51%	35	44%	0.3047
Medication	60	18%	44	26%	9	11%	7	9%	0.0015
Long QT	194	58%	94	55%	66	83%	34	43%	5.60E-07
Abnormal QRS axis	48	14%	22	13%	13	16%	13	16%	0.6575
Left axis deviation	18	5%	9	5%	4	5%	5	6%	0.9008
Right axis deviation	28	8%	12	7%	9	11%	7	9%	0.5293
BrS	70	21%	47	27%	NA	NA	17	21%	0.0091
Spontaneous type 1 Brugada ECG pattern	12	4%	3	2%	4	5%	5	6%	0.1444
SCN5A-E1784K	232	69%	127	74%	65	81%	40	50%	6.70E-05

Table 5. Clinical and ECG characteristics (categorical variables) and *SCN5A*-E1784K genotype of the total cohort and separated by ethnicity (n=336). Differences between ethnicities were analysed with the Fisher exact test and statistically significant values ($p<0.05$) are highlighted.

Variable	Total cohort n=336		Caucasian n=172 (51%)		Japanese n=80 (24%)		Other/mixed ethnicity n=80 (24%)		p-value
Parametric	Mean	SD	Mean	SD	Mean	SD	Mean	SD	
Age at baseline ECG (years)	29.9	18.4	32.7	19.6	24.8	17.1	29.0	15.7	0.0048
PR interval (ms)	160.9	28.3	157.9	30.0	164.2	27.6	164.0	24.5	0.0243
QRS duration (ms)	93.8	13.4	95.2	13.7	94.6	11.9	89.9	13.6	0.0040
QTc interval (ms)	468.5	41.9	461.6	34.9	497.1	41.2	454.1	43.5	8.15E-12
RR interval (s)	0.9	0.2	0.9	0.2	1.0	0.2	0.9	0.2	2.58E-05
Event free interval (years)	30.4	18.3	33.8	19.4	24.9	16.6	28.4	15.8	0.0005
Non-parametric	Median	IQR	Median	IQR	Median	IQR	Median	IQR	
QRS axis (degrees)	56.0	50.8	53.0	50.0	67.5	39.3	52.0	49.0	0.0125

Table 6. Clinical and ECG characteristics (continuous variables) of the total cohort separated by ethnicity (n=336). Differences between ethnicities were analysed with the Fisher exact test and statistically significant values ($p<0.05$) are highlighted. All continuous variables had a normal distribution apart from QRS axis that was positively skewed.

Cohort demographics

Data were submitted for 361 subjects: 232 *SCN5A*-E1784K carriers and 129 WT relatives. However, event data were incomplete for 25 WT individuals, who were all of other/mixed ethnicity and were excluded. Hence only 336 individuals (232 *SCN5A*-E1784K carriers and 104 WT relatives) have been included in the analyses described: 176 (52%) Caucasian (n=127 *SCN5A*-E1784K carriers, n=49 WT), 80 (22%) Japanese (n=65 *SCN5A*-E1784K carriers, n=15 WT) and 80 (22%) of other/mixed ethnicity (n=40 *SCN5A*-E1784K carriers, n=40 WT). The majority of subjects of other/mixed ethnicity originated from Ile de la Reunion and were recruited by the Nantes centre. Forty-four percent of those recruited were male. The mean age of the total cohort at recruitment was 30 years (SD 18). For *SCN5A*-E1784K carriers with no missing data only, the family sizes ranged from 1 to 25 *SCN5A*-E1784K carriers, with the median family size being 2 *SCN5A*-E1784K carriers. Four families had more then 10 *SCN5A*-E1784K carriers, 3 of which were Caucasian and 1 of other ethnicity.

Clinical evaluation

Demographic data, baseline ECG measurements (as made by the recruiting centres) and event data were obtained as a minimum from all recruited individuals. The baseline ECG was obtained for independent measurements in 330 individuals. Complete baseline ECG data were missing for 6 individuals, of whom 5 were *SCN5A*-E1784K carriers. Pedigree data were obtained from all recruited individuals. Whilst follow up data were requested from collaborating centres, follow up ECGs were not systematically collected due to the number of centres and magnitude of the data set. Further, ambulatory ECG data, exercise stress test data, imaging data were not systematically supplied and were available only from a subset of centres, again due to the number of centres and variable limitations of their resources to participate.

ECG characteristics

For each characteristic, I initially studied the total cohort (*SCN5A*-E1784K carriers and wild type [WT] relatives), followed by *SCN5A*-E1784K carriers and WT individuals only. There were differences in all the baseline ECG characteristics across ethnic groups for the total cohort (Figure 14). For *SCN5A*-E1784K carriers only, the mean PR interval and QRS duration were 165ms and 96ms respectively. When *SCN5A*-E1784K carriers from all three ethnic groups (Caucasians, Japanese and other/mixed ethnicity) were compared, there were no differences between ethnicities in age of baseline ECG, and of either QRS duration corrected for age or QRS axis. However, PR interval, QTc and RR interval were significantly different across ethnicities. This is illustrated in Figure 15. Japanese *SCN5A*-E1784K carriers had a longer resting RR interval and much longer QTc compared to Caucasians (mean RR interval 1.01s vs 0.88s, $p<0.001$; mean QTc 512ms vs 475ms, $p<0.001$).

Amongst WT relatives, there were no differences between ethnicities in age of baseline ECG, and of either QRS duration or RR interval corrected for age. However, PR interval, QTc corrected for age, and QRS axis were significantly different across ethnicities. This is illustrated in Figure 16. There were significant differences in the event free intervals between ethnicities amongst the overall cohort, *SCN5A*-E1784K carriers, and WT relatives (Figure 17).

Compared to WT relatives, *SCN5A*-E1784K carriers had longer PR interval, QRS duration, RR interval and QTc (mean PR interval 165ms vs 151ms, $p<0.0001$; mean QRS duration 97ms vs 88ms, $p<0.0001$; mean RR interval 0.92s vs 0.84s, $p=0.0005$; mean QTc 489ms vs 422ms; $p<0.0001$). There was no significant difference in the QRS axis (median 62ms vs 51ms, $p=0.0658$) between *SCN5A*-E1784K carriers and WT relatives.

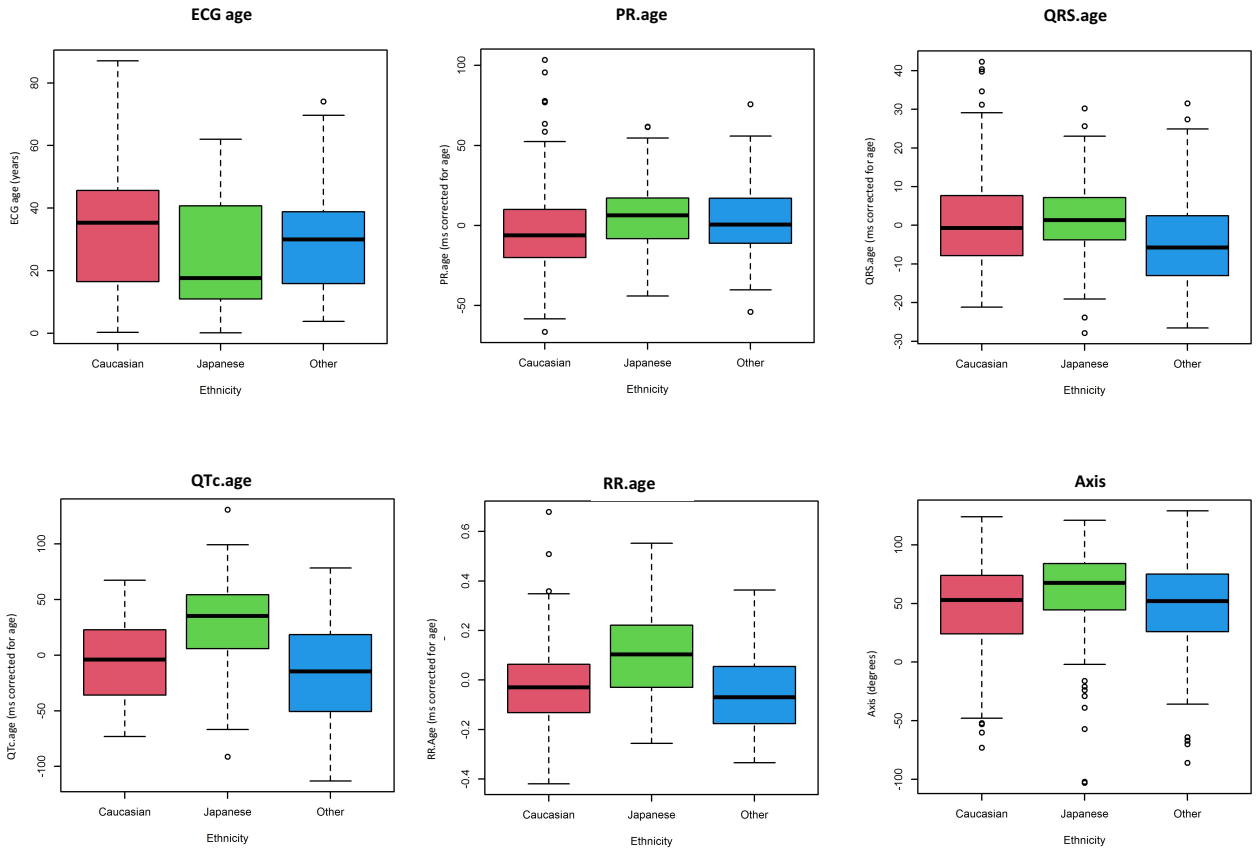


Figure 14. Box plots showing distribution of ECG age, PR interval, QRS duration, QTc, RR interval and QRS axis corrected for age in all individuals of *SCN5A*-E1784K pedigrees (carriers and WT individuals) according to ethnicity. The p-values were as follows: ECG age: p=0.005; PR.age: p<0.001; QRS.age: p=0.001; QTc.age: p<0.001; RR.age: p<0.001; QRS axis: p=0.013.

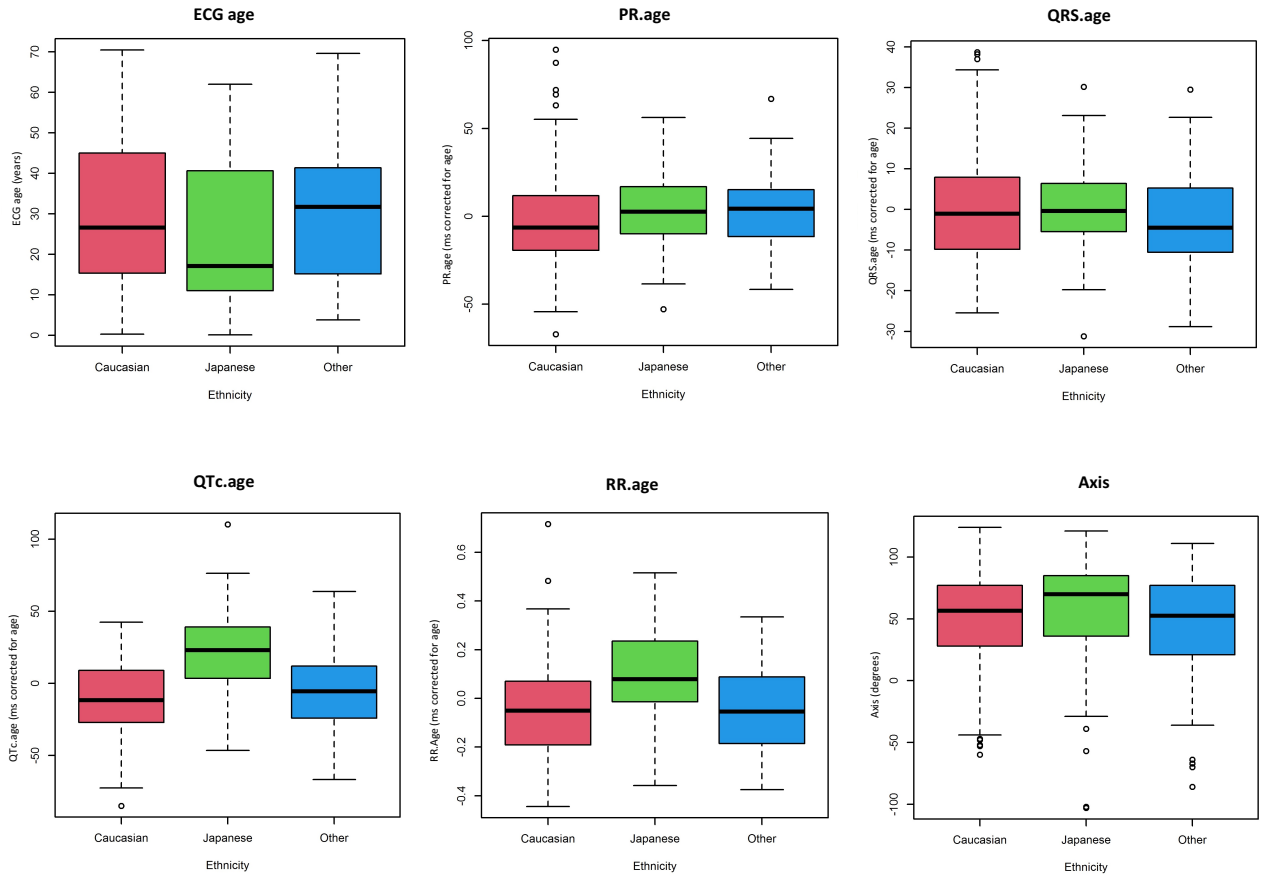


Figure 15. Box plots showing distribution of ECG age, PR interval, QRS duration, QTc, RR interval and QRS axis corrected for age in *SCN5A*-E1784K carriers according to ethnicity. The p-values were as follows: ECG age: p=0.086; PR.age: p=0.041; QRS.age: p=0.372; QTc.age: p<0.001; RR.age: p<0.001; QRS axis: p=0.072.

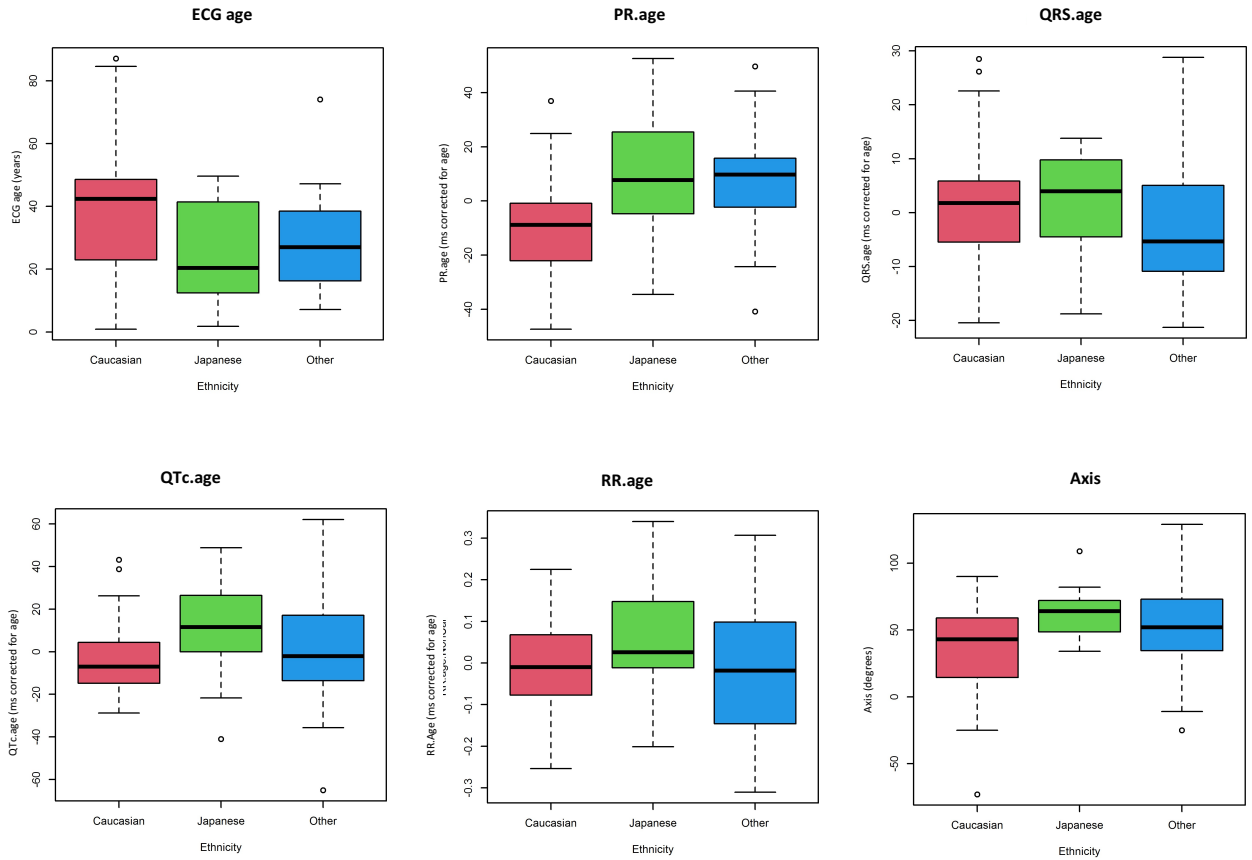


Figure 16. Box plots showing distribution of ECG age, PR interval, QRS duration, QTc, RR interval and QRS axis corrected for age in WT individuals of *SCN5A*-E1784K pedigrees according to ethnicity. The p-values were as follows: ECG age: p=0.004; PR.age: p<0.001; QRS.age: p=0.172; QTc.age: p=0.050; RR.age: p=0.425; QRS axis: p=0.016.

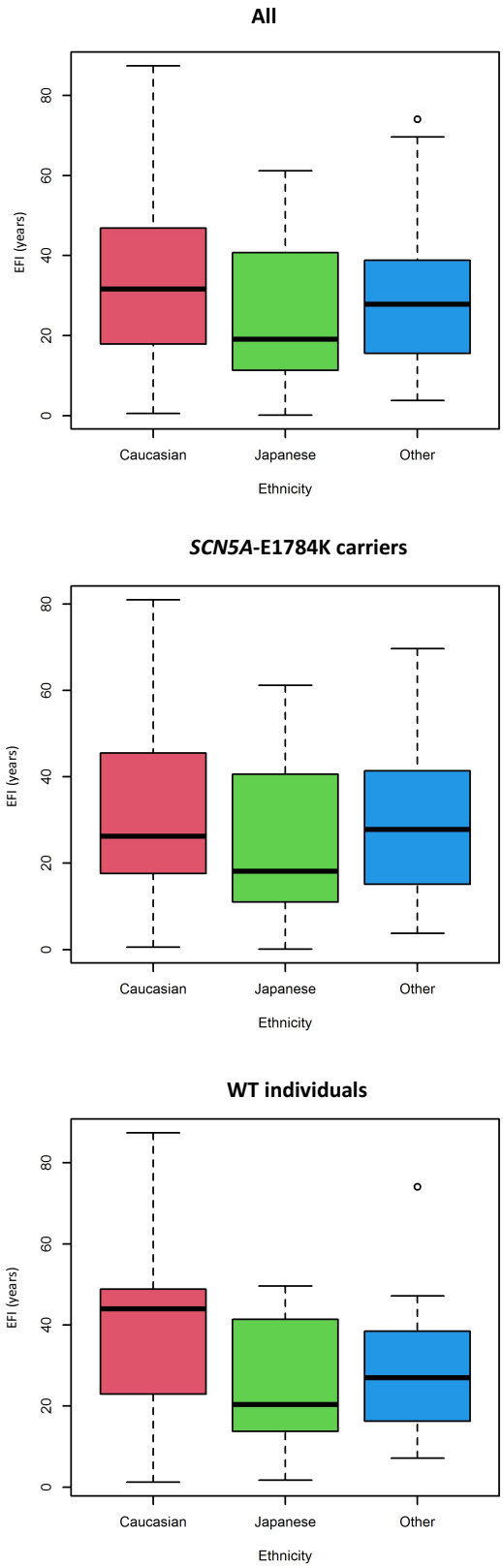
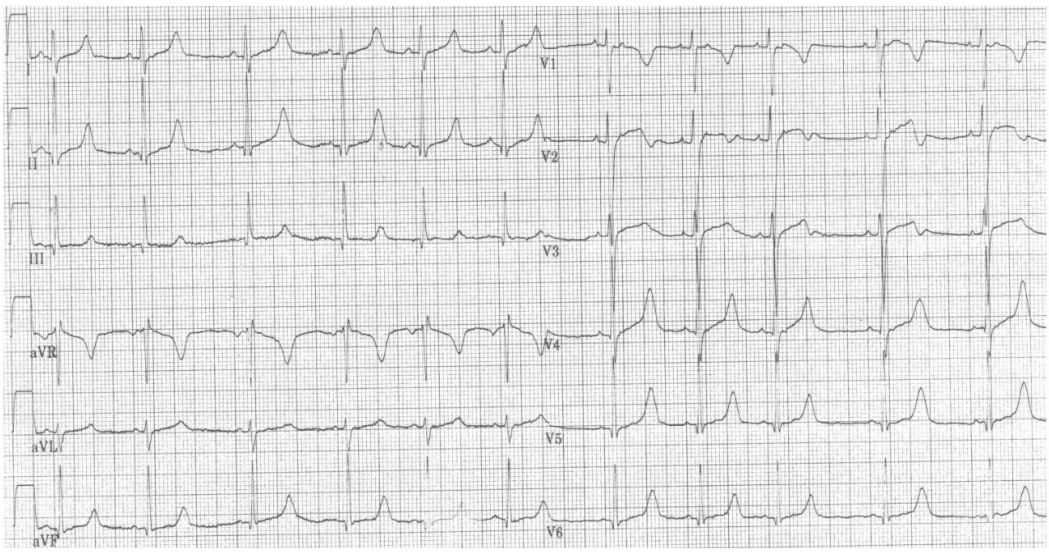
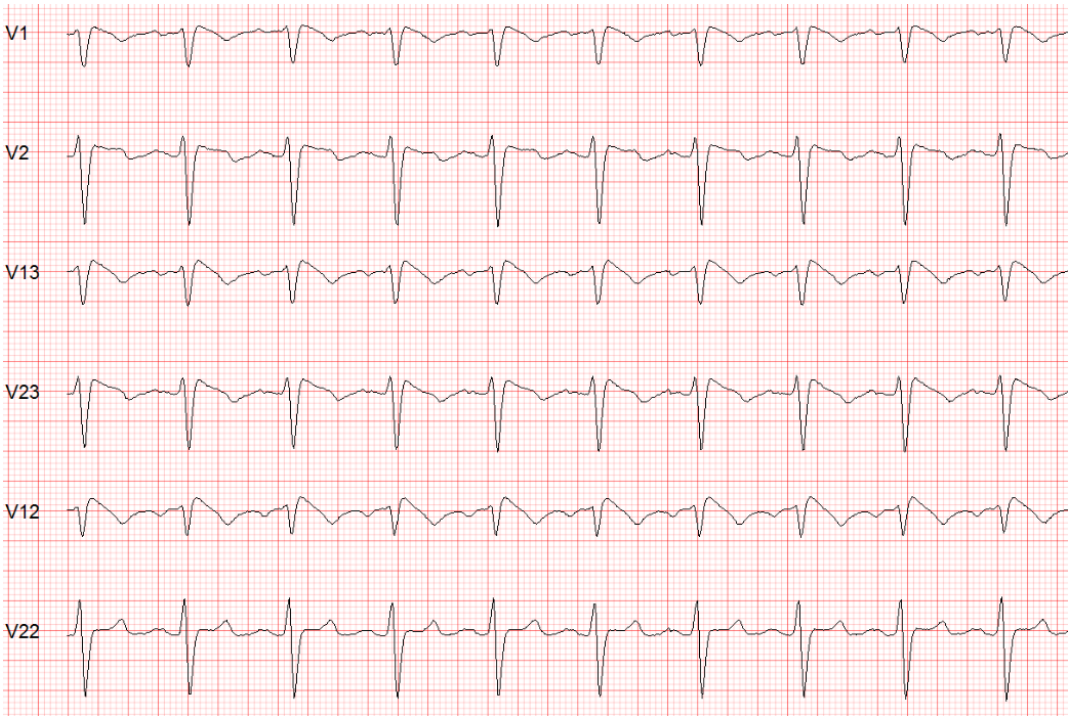


Figure 17. Box plots showing distribution of event-free interval (EFI) in all individuals of *SCN5A*-E1784K pedigrees (carriers and WT individuals), *SCN5A*-E1784K carriers, and WT individuals according to ethnicity. $p<0.001$; $p=0.021$; $p=0.002$ respectively.

Wide variation in T wave morphology including notched T waves and T wave alternans (beat-to-beat variation in the amplitude or morphology of the T wave) were observed. Example ECGs are shown in Figure 10. BrS phenotype status was only known in 120 subjects in total (i.e. where those subjects without a spontaneous type 1 Brugada ECG pattern had a systematic drug challenge to rule in or rule out the BrS phenotype). Sixty-six out of ninety-four (70%) *SCN5A*-E1784K carriers had the BrS phenotype (12 spontaneous; 54 drug-induced). Only 2% of Caucasians had a spontaneous type 1 Brugada ECG pattern compared to 6% Japanese. Drug-induced type 1 Brugada ECG pattern was unmasked in 64% of Caucasian *SCN5A*-E1784K carriers (43/67) who underwent a test. None of the Japanese individuals included in this study underwent sodium channel blocker challenge. Sixty-six out of ninety-four (70%) *SCN5A*-E1784K carriers had the BrS phenotype (12 spontaneous; 54 drug-induced). Interestingly, 4/26 (15%) WT subjects were found to have BrS phenotype, all drug induced. None of the WT subjects had a spontaneous type 1 Brugada ECG pattern on their baseline or follow up ECGs.



a)



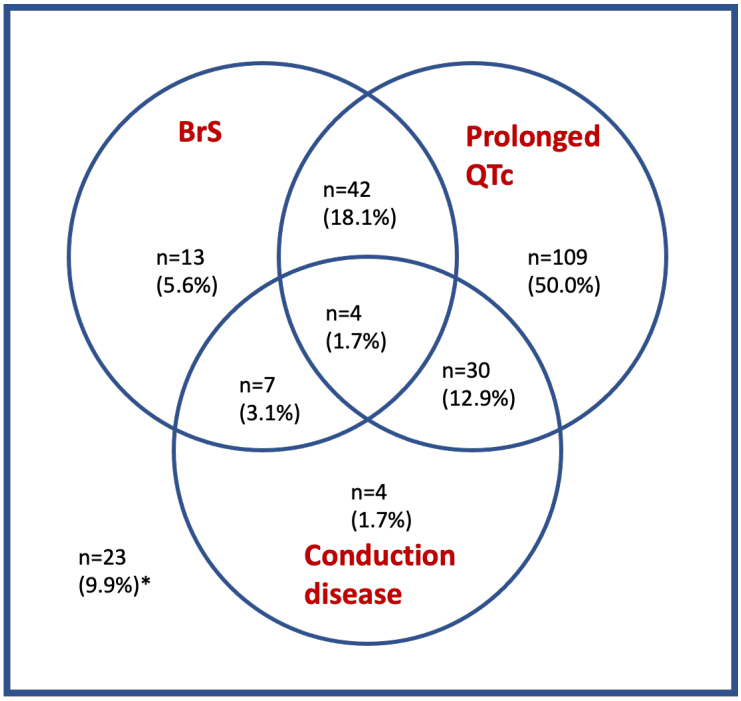
b)

Figure 10. ECG examples from *SCN5A*-E1784K carriers. a) 12 lead ECG showing prolonged QTc with abnormal T wave morphology; b) Right precordial leads of a 15-lead ECG showing the type 1 Brugada ECG pattern in leads V1,2 (V1 in the 2nd intercostal space) and V1,3 (V1 in the 3rd intercostal space).

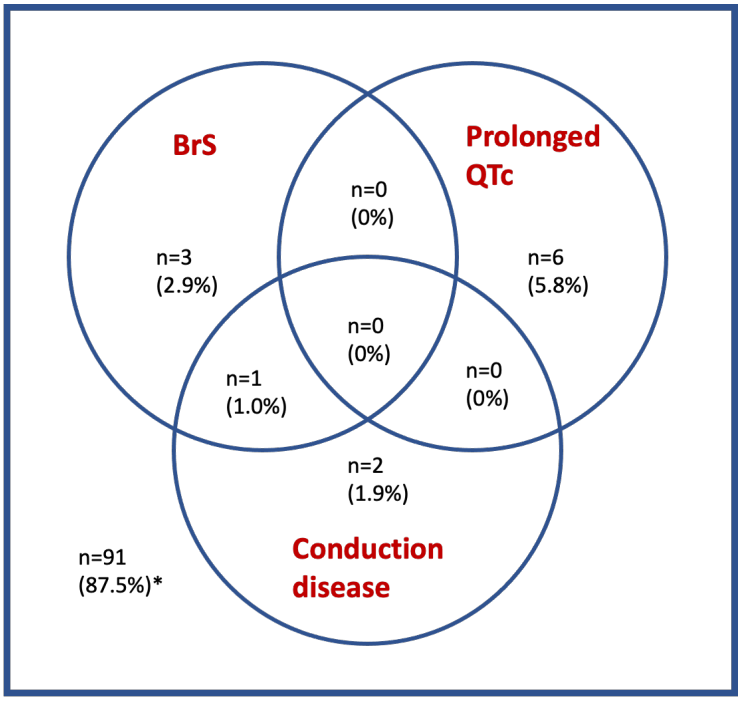
Disease phenotypes

The below Venn diagrams (Figure 18) represent the disease phenotypes in the genotype positive (n=232) and negative (n=104) cohorts. Complete ECG phenotype data were missing for 7 individuals (6 *SCN5A*-E1784K carriers and 1 WT relative). Four (1.7%) *SCN5A*-E1784K carriers had a mixed phenotype of BrS, LQT3 and cardiac conduction disease. A mixed phenotype of BrS and LQT3 without any evidence of conduction disease was seen in 20.7% and a mixed phenotype of BrS and conduction disease, and Long QT and conduction disease, were seen in 4.7% and 14.7% respectively. There was no phenotype in 9.9% (this includes the 6 individuals with missing data).

Amongst WT relatives, none had a mixed phenotype of BrS, Long QT and cardiac conduction disease. However, interestingly, four individuals had a drug-induced BrS phenotype, of which one individual had a mixed phenotype of drug-induced BrS and evidence of cardiac conduction disease. Amongst the WT relatives, all 4 with BrS had a drug-induced BrS pattern and no spontaneous BrS pattern was seen. A further 6 individuals had evidence of prolonged QTc without any overlap phenotype.



a)



b)

Figure 18. Venn diagrams showing disease phenotypes in a) n=232 *SCN5A*-E1784K carriers and b) n=104 genotype negative relatives. *n=23 and n=91 includes missing data from 6 individuals and 1 individual respectively.

Therapies

Twenty five percent of carriers were either on beta blockers and/or mexiletine (57/232 in total, with 47/232 being on beta blockers and 22/232 being on mexiletine, and 12/232 being on both). Amongst those on beta blockers, 37/47 were Caucasian and 3/47 were Japanese. Amongst those on mexiletine, 15/22 were Caucasian and 7/22 were Japanese.

Interestingly, of the 20.3% (47/232) of carriers who were on beta blockers, only 76.7% (36/47) had a Long QT phenotype on the baseline ECG. Amongst the 9.5% (22/232) of carriers who were on mexiletine, 81.8% (18/22) had a Long QT phenotype on the baseline ECG. Amongst the 5.2% (12/232) of carriers who were

on both beta blockers and mexiletine, only 75% (9/12) of these individuals had a Long QT phenotype on the baseline ECG. Amongst those on beta blockers, 23.4% (11/47) had events and 4.2% (2/47) had lethal events. Amongst those on mexiletine, 22.7% (5/22) have had events but none have had lethal events. Data were not collected on other antiarrhythmic drugs (see limitations). None of the WT relatives were on antiarrhythmic drugs.

An ICD was implanted in 15.9% (37/232) of carriers, of whom 48.6% (18/37) had a BrS phenotype (16 drug-induced, 2 spontaneous), and 70.3% (26/37) had a Long QT phenotype. Ten (27%) had a mixed Long QT/BrS phenotype. Amongst those with ICDs, 7/37 were dual chamber. A permanent pacemaker was implanted in a further 5.2% (12/232) of carriers. In total, 8.2% (19/232) were implanted with dual chamber devices, of whom 42.1% (8/19) had a conduction disease phenotype, 68.4% (13/19) had a Long QT phenotype, and a further 15.8% (3/19) had a mixed Long QT/BrS phenotype (both drug-induced Brugada ECG pattern). Amongst those with ICDs, 43.2% (16/37) had events, of whom 6 (16.2%) had lethal events; amongst those with a permanent pacemaker, only 8.3% (1/12) had an event. None of the WT relatives had device implantation.

Events and follow up

Event status was unavailable for 25 subjects of other/mixed ethnicity who were exclude as stated above. Event data included both events prior to the baseline ECG, and any follow up events, where follow up data were available. Follow up data since the baseline ECG were available for 130 (38.7%) of individuals. The mean duration of follow up was 51.9 months amongst the 90 carriers who had follow up data since the baseline ECG. Only 40 WT relatives had follow up data since the baseline ECG and the mean duration of follow up in these 40 WT individuals was

12.6 months. The lower rate and duration of follow up in WT relatives is expected, since most WT relatives are discharged following initial evaluation and negative genetic testing. Forty-five out of forty-seven subjects (96%) with events were carriers of the mutation. Only 2/104 (2%) of WT relatives had events that were recorded as arrhythmic syncope only. Lethal events, as defined previously, was observed in 10 (4%) of *SCN5A*-E1784K carriers and none in WT relatives. The presence of SCN5A-E1784K was strongly associated with events in the total cohort ($p<0.001$) and was driven by subjects of Caucasian ethnicity.

Since only 2/104 WT relatives had events, I focused all subsequent survival analyses on the *SCN5A*-E178K carriers only. Nineteen percent of *SCN5A*-E1784K carriers had experienced events at presentation or follow up, of which twenty-two percent were lethal events. The occurrence of lethal events was higher in Caucasian carriers compared to Japanese (4% compared to 2%), although the numbers were small (Table 7).

Cohort	No event	Event	Lethal event
E1784K	187	45 (19%)	10 (4%)
Caucasians	105	22 (17%)	7 (6%)
Japanese	50	15 (23%)	1 (2%)
Other / mixed	32	8 (20%)	2 (5%)

Table 7: Number of (and percentage of total) *SCN5A*-E1784K carriers with (lethal) events.

There was no association between gender and having an event in *SCN5A*-E1784K carriers (Tables 8 and 9). Furthermore, there was no association of a prolonged QTc or BrS phenotypes with events. However, left axis deviation was associated with events in the total cohort, 16% of those with events having left axis deviation compared to 5% of those with no events. This was driven by subjects of Caucasian ethnicity, where 29% of individuals with events had left axis deviation compared to

2% of individuals without events ($p<0.001$). Amongst Caucasian *SCN5A*-E1784K carriers with events, 5% had a spontaneous Brugada ECG pattern whereas only 2% without events had a spontaneous Brugada ECG pattern. Amongst Japanese *SCN5A*-E1784K carriers with events, 13% had a spontaneous type 1 Brugada ECG pattern compared to 4% without events. Of the continuous variables, mean age at ECG, mean PR interval and mean QRS duration were all higher in individuals with events.

This analysis compared the occurrence of events and did not take into account event-free interval. Hence, I then proceeded to study event-free interval in a multivariable analysis.

Variable	All *SCN5A* -E1784K carriers					Caucasian *SCN5A* -E1784K carriers					Japanese *SCN5A* -E1784K carriers					Other/mixed *SCN5A* -E1784K carriers				
	No events (n=187)		Events (n=45)		p-value	No events (n=105)		Events (n=22)		p-value	No events (n=50)		Events (n=15)		p-value	No events (n=32)		Events (n=8)		p-value
	n	%	n	%		n	%	n	%		n	%	n	%		n	%	n	%	
Male	89	48%	21	47%	1.0000	50	48%	9	41%	0.6423	25	50%	8	53%	1.0000	14	44%	4	50%	1.0000
Prolonged QTc	155	84%	34	79%	0.4955	81	79%	13	62%	0.0965	50	100%	14	93%	0.2308	24	75%	7	100%	0.3077
BrS	55	73%	11	58%	0.2607	40	70%	6	46%	0.1165	NA	NA	NA	NA	NA	13	81%	1	50%	0.4052
Spontaneous type 1 Brugada ECG pattern	8	4%	4	9%	0.2547	2	2%	1	5%	0.4377	2	4%	2	13%	0.2256	4	13%	1	13%	1.0000
Abnormal QRS axis	29	16%	11	26%	0.1806	13	13%	7	33%	0.0453	8	16%	4	27%	0.4492	8	25%	0	0%	0.3077
Left axis deviation	10	5%	7	16%	0.0242	2	2%	6	29%	<0.0001	3	6%	1	7%	1.0000	5	16%	0	0%	0.5628
Right axis deviation	18	10%	4	9%	1.0000	11	11%	1	5%	0.6892	5	10%	3	20%	0.3726	2	6%	0	0%	1.0000
Medication	43	23%	14	31%	0.2540	37	35%	4	18%	0.1396	5	10%	4	27%	0.1938	1	3%	6	75%	<0.0001

Table 8. Clinical and ECG characteristics (categorical variables) of *SCN5A*-E1784K carriers (n=232) separated by ethnicity and occurrence of events. [n] denotes the number of subjects with that characteristic, and [%] denotes the percentage of subjects with the said characteristic. The Fisher's exact test was used to compare the categorical variables between those with events and those without events. Statistically significant values ($p<0.05$) are highlighted.

Variable	All *SCN5A* -E1784K carriers					Caucasian *SCN5A* -E1784K carriers					Japanese *SCN5A* -E1784K carriers					Other/mixed SCN5A-E1784K carriers				
	No events		Events		p-value	No symptoms		Symptoms		p-value	No symptoms		Symptoms		p-value	No symptoms		Symptoms		p-value
Parametric	Mean	SD	Mean	SD		Mean	SD	Mean	SD		Mean	SD	Mean	SD		Mean	SD	Mean	SD	
Age at baseline ECG (years)	26.6	17.9	37.1	14.8	0.0003	27.8	18.1	41.4	13.6	0.0008	22.8	17.3	31.8	16.0	0.0377	29.0	17.7	35.6	13.8	0.2630
PR interval (ms)	161.6	27.9	180.4	31.4	0.0004	159.4	28.8	182.2	36.2	0.0075	161.4	25.8	180.0	28.2	0.0335	169.0	27.8	175.9	25.6	0.4980
QRS duration (ms)	94.5	12.2	105.1	14.2	<0.0001	94.8	12.1	107.8	17.2	0.0009	94.3	12.0	102.4	9.1	0.0070	93.8	13.3	103.1	13.6	0.0641
QTc interval (ms)	488.6	30.5	493.0	30.6	0.2463	478.9	24.8	474.9	26.1	0.5187	512.3	29.2	510.2	25.4	0.8274	482.4	29.7	510.3	23.5	0.0128
RR interval (s)	0.9	0.2	1.0	0.2	0.0595	0.9	0.2	0.9	0.2	0.2075	1.0	0.2	1.1	0.2	0.6128	0.9	0.2	1.0	0.2	0.1697
Non-parametric	Median	IQR	Median	IQR		Median	IQR	Median	IQR		Median	IQR	Median	IQR		Median	IQR	Median	IQR	
QRS axis (degrees)	61.5	51.0	55.0	66.0	0.3146	60.0	46.0	37.0	108.0	0.0129	69.5	54.3	76.0	40.0	0.3461	54.0	60.5	47.4	23.8	0.9400

Table 9. Clinical and ECG characteristics (continuous variables) of *SCN5A*-E1784K carriers (n=232) separated by occurrence of events. The Mann Whitney U test was used to compare the continuous variables between those with events and those without events. Statistically significant values ($p<0.05$) are highlighted.

Event-free Interval Analysis

Multivariable analyses were carried out to investigate the effect of all clinical and ECG variables (adjusted for age when continuous) on event-free interval. There were only two WT relatives with events, hence meaningful analyses for relative risk could only be done for *SCN5A*-E1784K carriers. Table 10 shows the effects of these variables on survival in *SCN5A*-E1784K carriers adjusted for ethnicity. QRS.age remained the only association with survival. Table 11 shows the effect of clinical variables on survival in *SCN5A*-E1784K carriers separated by ethnicity. Interestingly, the effect of left axis deviation and right axis deviation were reversed between Caucasian and Japanese *SCN5A*-E1784K carriers. However, the scarcity of events when the data were separated into ethnicities led to unstable estimates, especially in *SCN5A*-E1784K carriers of other/mixed ethnicity.

Variable	All *SCN5A* -E1784K carriers with adjustment for ethnicity		
	Relative risk	95% confidence interval	p-value
Male	1.22	0.65 - 2.28	0.5425
Spontaneous Brugada ECG pattern	1.61	0.50 - 5.17	0.4220
PR.age	1.01	1.00 - 1.02	0.2239
QRS.age	1.03	1.01 - 1.06	0.0008
QTc.age	1.00	0.99 - 1.02	0.5385
RR.age	0.90	0.14 - 5.86	0.9140
Long QT phenotype	0.86	0.36 - 2.01	0.7213
Abnormal axis	1.70	0.79 - 3.64	0.1752
Left axis deviation	1.57	0.62 - 4.00	0.3400
Right axis deviation	2.08	0.67 - 6.43	0.2034
Medication	1.91	0.92 - 3.98	0.0834

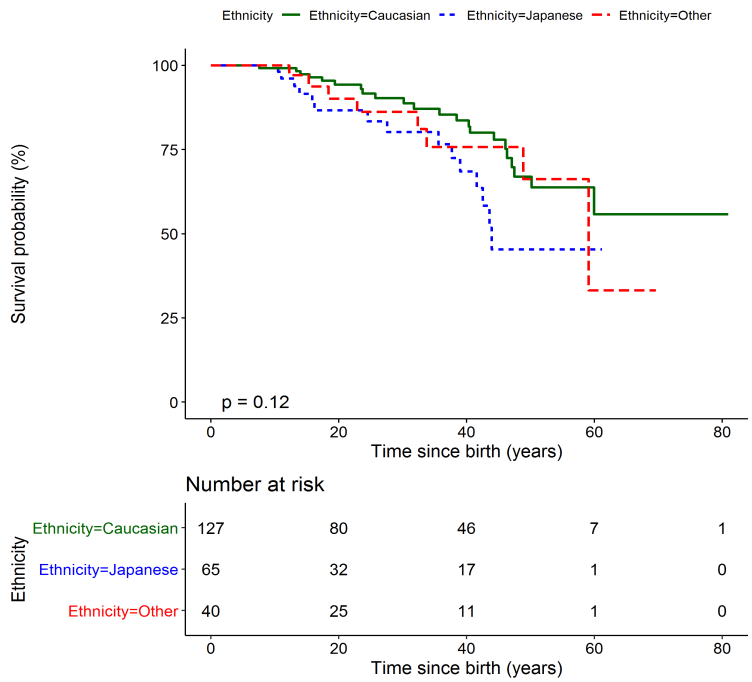
Table 10. Effect of clinical variables on survival in *SCN5A*-E1784K carriers, adjusted for ethnicity. PR.age, QRS.age, QTc.age and RR.age are age adjusted variables, p-values that reached nominal statistical significance ($p<0.05$) are highlighted in red; and where the results remained statistically significant after Bonferroni correction, these are highlighted in green.

Variable	Caucasian *SCN5A* -E1784K carriers			Japanese *SCN5A* -E1784K carriers			Other/mixed *SCN5A* -E1784K carriers		
	Relative risk	95% confidence interval	p-value	Relative risk	95% confidence interval	p-value	Relative risk	95% confidence interval	p-value
Male	0.80	0.31 - 2.05	0.6434	1.86	0.67 - 5.21	0.2344	1.18	0.29 - 4.81	0.8188
BrS	0.45	0.15 - 1.36	0.1560	1.61	0.36 - 7.22	0.5324	0.17	0.01 - 2.99	0.2279
Spontaneous Brugada ECG pattern	4.40	0.43 - 44.95	0.2111	1.61	0.36 - 7.22	0.5324	0.83	0.10 - 7.14	0.8661
PR.age	1.00	0.99 - 1.02	0.5125	1.01	0.99 - 1.03	0.2413	1.00	0.96 - 1.03	0.8594
QRS.age	1.03	1.00 - 1.06	0.0400	1.05	1.00 - 1.10	0.0459	1.02	0.97 - 1.08	0.3682
QTc.age	1.00	0.98 - 1.01	0.6456	1.00	0.98 - 1.02	0.8748	1.03	1.00 - 1.06	0.0326
RR.age	0.19	0.01 - 4.01	0.2849	3.24	0.20 - 51.96	0.4068	0.79	0.01 - 71.88	0.9178
Long QT phenotype	0.70	0.25 - 1.94	0.4923	0.19	0.02 - 1.59	0.1270	2199276147.89	2199276147.89 - 2199276147.89	<0.0001
Abnormal axis	2.13	0.75 - 6.00	0.1539	3.00	0.89 - 10.12	0.0760	0.00	0.00 - 0.00	<0.0001
Left axis deviation	3.83	1.10 - 13.38	0.0354	0.79	0.10 - 6.04	0.8200	0.00	0.00 - 0.00	<0.0001
Right axis deviation	0.58	0.07 - 4.96	0.6158	12.06	2.33 - 62.53	0.0030	0.00	0.00 - Infinity	0.9998
Medication	0.55	0.17 - 1.80	0.3201	2.55	0.81 - 8.05	0.1104	19.67	3.21 - 120.39	0.0013

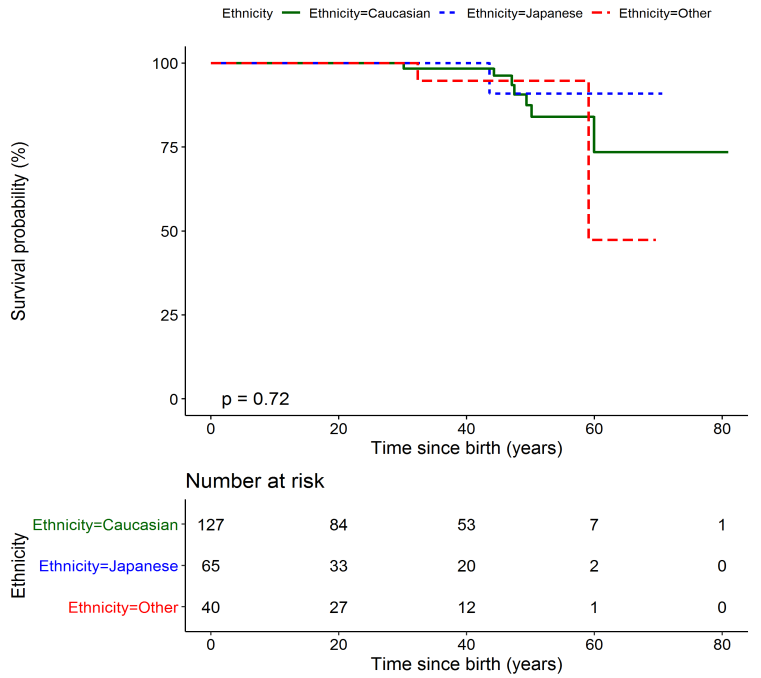
Table 11. Effect of clinical variables on survival in *SCN5A*-E1784K carriers separated by ethnicity. PR.age, QRS.age, QTc.age and RR.age are age adjusted variables, p-values that reached nominal statistical significance ($p<0.05$) are highlighted in red; and where the results remained statistically significant after Bonferroni correction, these are highlighted in green.

There were no significant differences in the event-free interval (Figure 19a) and then survival free of lethal events (Figure 19b) between ethnic groups. As shown in the Kaplan-Meier curve (Figure 20) those with QRS.age in the third tertile had the shortest event-free interval (p=0.029). None of the other variables studied were significantly associated with event-free interval. These Kaplan-Meier cures are therefore not shown.

In order to study the differences between ethnicities on the effect of QRS.age on event-free interval, we separated the results by ethnicity, and these are shown in Figure 21. As seen, the effect of QRS.age on event-free interval is driven by *SCN5A*-E1784K carriers of Japanese and Caucasian ethnicity, whilst QRS.age does not seem to have an impact on event-free interval in those of other ethnicity, probably due to lack of power.



(a)



(b)

Figure 19. Survival probability of *SCN5A*-E1784K carriers in terms of (a) events and (b) lethal events according to ethnicity.

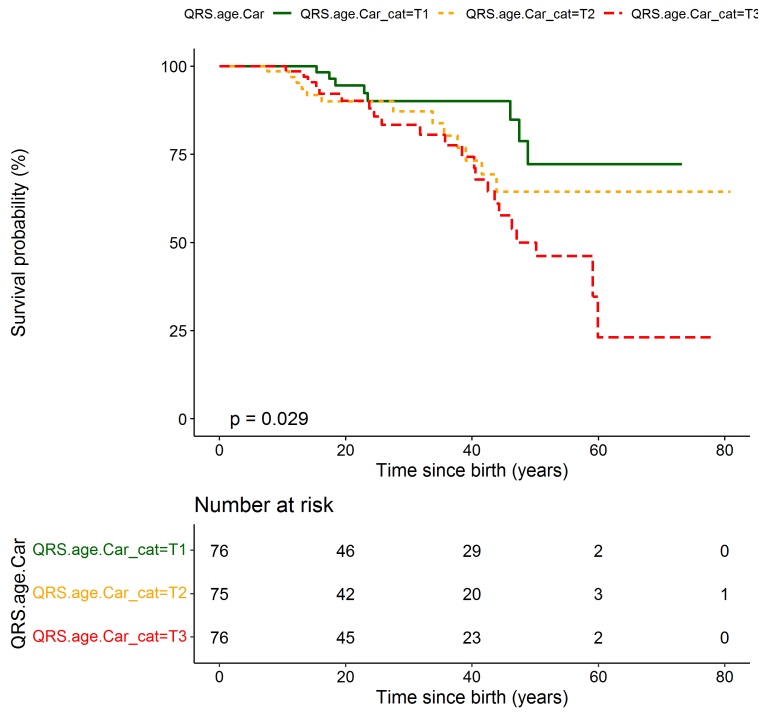
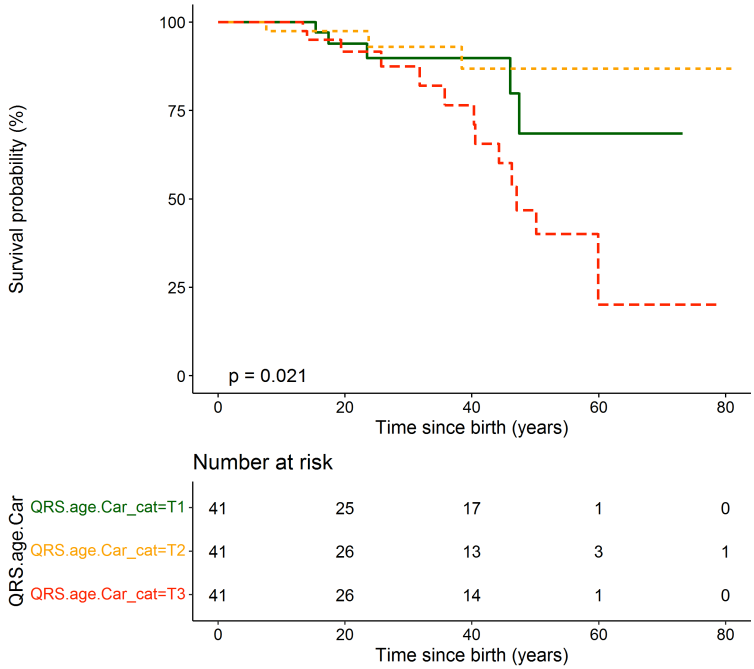
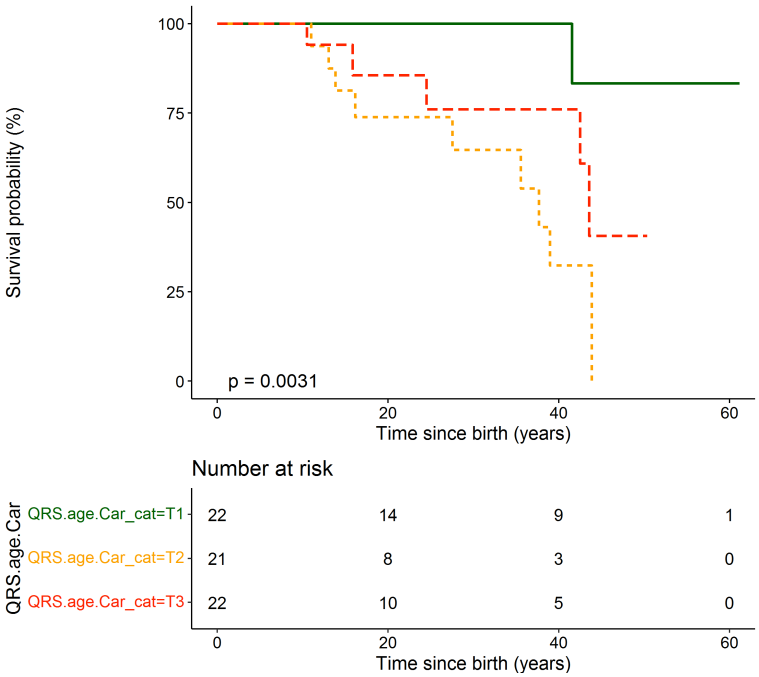


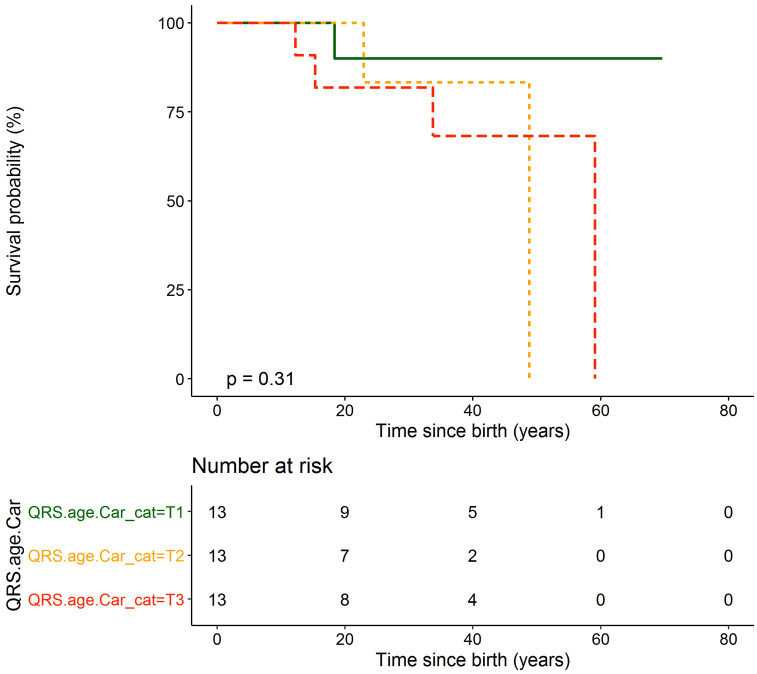
Figure 20. Survival probability of all *SCN5A*-E1784K carriers compared for QRS duration separated into tertiles and corrected for age with risk table.


Survival probability (%)
100
75
50
25
0
p = 0.021
0
20
40
60
80
Time since birth (years)
Number at risk
QRS.age.Car
QRS.age.Car_cat=T1
QRS.age.Car_cat=T2
QRS.age.Car_cat=T3
41
25
17
1
0
41
26
13
3
1
41
26
14
1
0
0
20
40
60
80
Time since birth (years)

a)


Survival probability (%)
100
75
50
25
0
p = 0.0031
0
20
40
60
Time since birth (years)
Number at risk
QRS.age.Car
QRS.age.Car_cat=T1
QRS.age.Car_cat=T2
QRS.age.Car_cat=T3
22
14
9
1
21
8
3
0
22
10
5
0
0
20
40
60
Time since birth (years)

b)



c)

Figure 21. Survival probability of *SCN5A*-E1784K carriers of a) Caucasian b) Japanese and c) other ethnicity separately compared for QRS duration separated into tertiles and corrected for age with risk table.

Data on BrS phenotype was only available in a subset of carriers due to selective use of sodium channel blocker challenge. However, in all *SCN5A*-E1784K carriers, the BrS phenotype confers a relative risk of 0.58 (95% confidence interval 0.23–1.47), p=0.2534. In Caucasian *SCN5A*-E1784K carriers, the relative risk was 0.45 (95% 0.0.15-1.36), p=0.1560. This is also reflected in the number with cardiac events. Amongst those who had cardiac events, 46% had a BrS phenotype, compared to 70% with a BrS phenotype amongst those with no cardiac events. However, the numbers are too small to be statistically significant.

Discussion

This analysis is the first opportunity for clinical characteristics and putative risk markers to be studied for associations with survival in a cohort of families of this magnitude with a single *SCN5A* mutation. The analyses were carried out initially in the total cohort (*SCN5A*-E1784K carriers and WT relatives), and then only followed up in the *SCN5A*-E1784K carriers only.

Cohort demographics

Approximately half of the cohort were Caucasian, and a significant proportion were Japanese or of other/mixed ethnicity. A large proportion of *SCN5A*-E1784K carriers globally are of Japanese origin and the patients recruited to this study are reflective of that. Ethnic differences are apparent throughout the results although some clinical and ECG features were consistent. In the total cohort (*SCN5A*-E1784K carriers and WT relatives), antiarrhythmic medication use, the prevalence of prolonged QTc and BrS were found to be significantly different between ethnicities. This is partly explained by differences between ethnicities in the proportion of *SCN5A*-E1784K positive subjects recruited to the study (Table 3).

ECG characteristics

As would be expected in an overlap syndrome, *SCN5A*-E1784K carriers had longer PR interval, QRS duration, RR interval and QTc compared to non-carriers. There was no significant difference in the QRS axis in *SCN5A*-E1784K carriers compared to WT relatives. There were differences in the ECG characteristics between Caucasian and Japanese *SCN5A*-E1784K carriers, with those of Japanese ethnicity having longer RR interval and QTc on average. This was also seen in WT relatives

suggesting consistent background ethnically specific differences regardless of carrier status, which could be genetic in basis.

Japanese *SCN5A*-E1784K carriers were more likely to have a spontaneous type 1 Brugada ECG pattern compared to Caucasians. However, a limitation of this study was that none of the Japanese individuals included in this study underwent sodium channel blocker challenge. This is due to variations in international practice for clinical investigation of these patients. Notably, 1 in 6 of WT individuals from *SCN5A*-E1784K pedigrees who underwent a sodium channel blocker challenge had a positive test for a diagnostic type 1 Brugada ECG pattern. None of the WT subjects had a spontaneous type 1 Brugada pattern. The clinical significance of the prevalence of drug-induced type 1 Brugada pattern in *SCN5A*-E1784K negative family members is uncertain in the absence of a gold standard test for BrS, particularly as none of these subjects had lethal events.

Therapies

There were discrepancies in the therapies, both drug therapy and device therapy, due to variability in clinical practice between centres, and the paucity of data available on the optimum management strategy for these patients with a known pathogenic variant causing a mixed / overlap phenotype.

Events and survival analysis – impact of cardiac conduction

Only patients with *SCN5A*-E1784K experienced lethal events. Indeed, a fifth of *SCN5A*-E1784K carriers had experienced an event prior to presentation or during follow-up. Whilst, the prevalence of lethal cardiac events was lower in Japanese, suggesting an ethnic difference in event severity among carriers of this mutation, there were no significant difference in the survival probability (both in terms of events and lethal events) between ethnicities in *SCN5A*-E1784K carriers.

On initial comparison of patients with and without events, mean age at the time of ECG acquisition was older in patients with events. This probably reflects that older patients were more likely to have suffered a symptom than younger individuals given their lifetime exposure to risk.

Left axis deviation was associated with events amongst *SCN5A*-E1784K carriers, particularly those of Caucasian ethnicity. Mean QRS and PR were significantly greater in patients with events. Further, in the survival to event analysis, QRS.age was the only clinical parameter associated with event-free interval. Indeed, *SCN5A*-E1784K carriers with QRS.age in the third tertile had the shortest survival to event time. These findings provide novel evidence that features of cardiac conduction disease are associated with risk in *SCN5A*-E1784K pedigrees, particularly in Caucasians.

These results bare similarity to the findings of Meregalli *et al*, who reported that BrS families with *SCN5A* variants had a more severe conduction phenotype with a greater likelihood of syncope.[201] Further, Shimizu *et al* found that BrS probands with *SCN5A* mutations, especially those with greater biophysical effects, exhibited more cardiac conduction abnormalities and had a higher risk of cardiac events.[92]

Japanese *SCN5A*-E1784K carriers with events were more likely to have a spontaneous BrS ECG pattern compared to those without events. Interestingly, a BrS diagnosis showed a tendency to be protective in *SCN5A*-E1784K carriers in the survival analysis. Although numbers were too small to deduce statistical significance this was an unexpected finding and warrants further investigation with larger cohorts with systemic provocation testing.

There was no association between the presence of a prolonged QTc or QTc.age with presence of events or survival to event in *SCN5A*-E1784K carriers. Thus, despite the presence of an LQT3 phenotype and prior evidence from other studies in LQT3 that QTc is an important marker of risk, measures of cardiac repolarisation did not appear to have any independent association with events or survival time.[202]

These are therefore important findings for risk stratification of these patients in clinic and requires further validation in an even larger cohort, and in other *SCN5A* overlap syndrome pedigrees.

The discrepancies between either the presence of Long QT or BrS phenotype and therapies reflect the lack of standard clinical practice or international guidelines for the appropriate management of carriers of this mutation, and that management strategies are likely based on practice at individual centres.

Limitations

This study was limited by retrospective data collection. Ethnicity data were based on patient-reported ethnicity and clinical records rather than primary component analysis. With regard to event data, arrhythmic syncope was included in the composite event status when calculating event-free interval (instead of focussing only on lethal events). This was so that there would be sufficient statistical power for the study. The diagnosis of likely arrhythmic syncope can be subjective, but we specified that this had to be likely to be reflective of primary arrhythmic syncope as diagnosed by a cardiologist in a tertiary inherited cardiac conditions clinic.

It should also be noted that the LQT3 phenotype is known to be maximal at night, however the surface ECG used to phenotype the patients in this cohort was always obtained during a clinic visit during the day (only the baseline ECG was used for measurements in this study). Due to the same reason, an accurate measurement of sinus node disease could not be made, as only RR interval from the single baseline 12 lead ECG was available. This was a limitation of the study and a more accurate measure of LQT3, diurnal variation in RR interval and dynamic BrS ECG pattern, could be obtained by collecting 24 hour 12 lead ECG data from all study participants. However, due to the resources available for the study and the large number of participating centres internationally, all participating centres did not have the capacity to supply ambulatory ECG data within the timeframe of the study. Due to this, we were not able to consider sinus node disease adequately to perform any analyses on sinus node dysfunction in this cohort. Further, follow up ECGs, exercise test data and imaging data were not systematically collected due to the same reason outlined above. As a result of the absence of follow up ECGs, I focussed all measurements on the baseline ECG to make the analyses most reproducible and robust with the data available.

There were also some limitations with the diagnosis of disease phenotypes. Prolonged QTc ('Long QT phenotype' as defined in this study) does not itself equate to LQTS, which has additional diagnostic criteria as discussed in Chapter 1. However, in the context of these families and the completeness of the dataset available, it was a reasonable surrogate to use. Secondly, the definition of conduction disease that was applied for the purposes of this chapter does not strictly equate to the clinical definition of premature cardiac conduction disease, but was used as a surrogate as it captures phenotype in these families within the constraints of the dataset available. Finally, drug provocation testing data for Brugada syndrome were only available for 120 (35.7%) of the individuals in the

complete dataset, hence Brugada syndrome status was unknown for nearly two-thirds of individuals in the complete data set (this includes WT individuals).

Data on events was strictly restricted to relevant arrhythmic events only. Lethal event data collection included mortality data from sudden cardiac deaths, however data on non-sudden cardiac deaths and hospitalisations that may or may not be relevant to arrhythmic events (data on which were already collected systematically) were not included in the data set. Furthermore, the follow up data available in the study were limited as many of the centres could not complete the follow up data collection within the resources available for the study. We therefore analysed event-free interval from birth and determined age-adjusted ECG variables since follow up ECGs were not routinely available.

A limitation with data collection on therapies was that the rationale for therapies was not collected systematically. For example, some patients on drug therapy may have had a Long QT phenotype detected on follow up ECGs that have not been captured on the data collection. Alternatively, the rationale for the drug therapy may have been simply the presence of the mutation. There was absence of systematic data collection on hydroquinidine use amongst this cohort although its QT prolonging effect is likely to have precluded its use.

The Kaplan Meier curves were limited by available numbers and the numbers of events were too small with insufficient power to differentiate risk according to ethnicity. Whilst trends were evident, I was unable to speculate further.

It was not feasible to complete all missing data from the large number of participating centres within the time-frame of this study, however, this will be an aim for future follow-on work.

Chapter 4: ECG Trait SNPs

Associations with Phenotype

Introduction

Large GWAS have identified SNPs modulating the PR interval, QRS duration and QTc in the general population,[19,21,22,168,170] Further, common genetic variation, including *SCN5A* promoter haplotype in chromosome 3, has been implicated in cardiac conduction disorders and drug-induced arrhythmia.[20,203] Common genetic variation has already been implicated in BrS.[77] I am also a co-author on an expanded BrS GWAS that has been accepted for publication by Nature Genetics. Further, in a large recent GWAS where I am a co-author, we have demonstrated the influence of common genetic variation amongst LQTS probands.[167] *SCN5A* overlap syndromes have wide variability in phenotype amongst affected individuals. In chapter 3 I have described the variation in phenotype and clinical markers of risk among *SCN5A*-E1784K carriers and WT relatives. It is the single most common *SCN5A* mutation implicated in LQTS and BrS, however, the impact of common genetic variation on phenotype in this mutation has not been described other than my recent first author publication, which was the subject of Chapter 6.[194]

In this chapter, I describe the associations of individual SNPs that reached genome-wide significance for their associations with ECG traits in large population GWASs, with ECG parameters and risk in *SCN5A*-E1784K carriers and their WT relatives.

Methods

Recruitment and case selection

Identical to Chapter 3, sixteen Inherited Cardiac Conditions (ICC) specialist centres from United Kingdom, Ireland, France, Germany, Italy, USA and Japan participated. Participants were recruited from *SCN5A*-E1784K families and required carrier status to be determined before inclusion in the study. Upon identification of the probands,

first- and second-degree relatives, whether hosting the mutation or not, were recruited. However, the population include here was different due to exclusion of cases with insufficient SNP data (see SNP genotyping).

Clinical evaluation

As in Chapter 3, comprehensive clinical data including initial presentation and follow-up data, presenting ECGs, and details of any drug provocation tests, were collected. BrS phenotype was defined as the presence of either a spontaneous or drug-induced type 1 Brugada ECG pattern in at least one right precordial lead (in the standard or higher intercostal spaces).[59] Intravenous drug provocation tests (either ajmaline 1mg/kg, flecainide 2mg/kg or pilsicainide 1mg/kg) were performed at a pre-determined rate as per local protocol. Other ECG data collected included baseline PR interval, QRS duration, heart rate and rhythm, QRS axis and QTc (Bazett's formula). A minimum of two observers made independent measurements on the baseline ECG, and where there was >5% discrepancy, the measurements were repeated and re-compared. If a discrepancy remained, a third observer made measurements and a mean was taken. Data were collected on the occurrence of events and lethal events at presentation or follow-up. Medications recorded were limited to antiarrhythmic drug use only.

SNP selection

SNPs that have previously been shown to be associated with different electrocardiographic (ECG) traits in the general population in large historical GWASs were genotyped. These SNPs are detailed in Table 12.[22,77,170,171,203–206]

ID	Sequence	Chr	Nearest gene	Position	Annotation required for project	Association	Association p-value	Source	LD (whole population)	LD (NW Eur - Utah residents from NW Eur)	LD (Japanese in Tokyo)	Comments
rs10850409	ATGGTGATGCCTGGTGGTTTCATTAGTAACCACTTGGCCATACTTAGGAACAGCATTRAACAGAAGACCAAAGGAACTG TCTTCCTGTTCCACCATCAAG[A/G]TGGGGGTGAGGGAGAAAATAGGAGGAAGAGATGGAAACAGAAAGTGTGACCA GTATCTCTCCYCAGCCTGAGCTGGGCTATGATASTCCGAGATTAATAT	12	*TBX3*	Intergenic	A/G	QRS duration	$3.06x10^{-10}$	Sotoodehnia *et al* , 2010	r20.808 with rs1896312		rs0.872 with rs1896312	
rs10865879	AGTGGTGTCTGTTCCCCCTCCTGTAGAATTACTATTTTCTCTTTCTAAGTAATAAGTAATTGTGGGGAGATAGTTTGAGACT ATATTCCTCATCAAACTT[A/C]TACCCACTAGTTTTTGCCCACTAATAATKTTTTACACCATCATTACTTCTAAACTTACTAG WTGGCCCAWTCATACTGGCTCCTGTGTCTTTTGACATTT	3	*SCN5A-EXOG*	Intergenic	A/C	QRS duration	$1.10x10^{-28}$	Sotoodehnia *et al* , 2010				
rs10919071	GGGAGAATGAAGAAGACTGTTTAAGTGACAGGTAGAATTTTAATAGAAGAAATAAGAAACATTGCTTTCAAGTATAAGTC TCAGTGAGATGAATTGTAGCT[A/G]TACTAGGTAAAACTTTTTAAAAGAACAGAAAGATGTAATCAGAATAAGACTGATG TCAGTTTCTCCACTGGCATAAGAAACTCAAATATCTGAATTTAATACATTGGGATATTTGCTTAT	1	*ATP1B1*	Intron 6	A/G	QT interval	$1.20x10^{-15}$	Pfeufer *et al* , 2009; Newton Cheh *et al* , 2009				
rs11047543	CAGCCTGAGTGTCAATTCCTGATCTCCATGTTGGGAGGTGAACTCAGAGCATTACTGACCATTTAAGGGACCGCTGAGG TGAACGAGCTAGAAAAATTTG[A/G]CCTCATATTCAACGAAGTGGAGACTTCTTGAAGGCAAAGATTTTGAATGATAATG AAATACCRTTATACCATTCATGTAAATGAATAAATGAAAGAACCA	12	*SOX5*	5KB 5' of *C12ORF67*	A/G	PR interval	$3.34x10^{-13}$	Pfeufer *et al* , 2010				
rs11153730	GGTATTAGAARGAAACAGAGCTGGGGCTAAATCTTAATTCTGTAACATACAGTTGTGTGGTGATATACAAACCATTTAAC CTCTATCACTCTTAATTTCA[C/T]CATCTGTAATGCAGGGAAAATTAAAGCACTTTAGTGTTGTGAGGATAAAATGAGATAA TGCAAGTAAAGCGTTTAGCATTGTCCTGGCACATAGAAAGCT	6	*C6orf204-SLC35F1-PLN-BRD7P3*	Intergenic	C/T	QRS duration	$1.26x10^{-18}$	Sotoodehnia *et al* , 2010	r2 0.79 with rs11970286	r2 0.884 with rs11970286	r2 0.891 with rs11970286	
rs11710077	CTGTGCTCCTGGCAGGCTTGCAAAGCCAGCTGAGTGGCTGGAAATAGGAGTGCAGCTGGTGGCCGTGTGTCTGTCTG GGAGAGCAATCATGAGTTAGAGG[A/T]AGTCTTAAAAGAGGACTTACAGGGTAAGGGTGTGGAATGTCTGGGRCCATG TTGGTGACTTGGTGTGCTACTGCCTCTTTTATTCTACCCAGATCCCCAC	3	*SCN5A*	Intron	A/T	QRS duration	$5.74x10^{-22}$	Sotoodehnia *et al* , 2010				
rs11848785	AATATTACTACATGATAGGTCCCATTCCAGAAGGCTTGTTGACGGAAACAATCTTGTCTCGTGACTAAACATCCATGTCTC ATTCCTACATATCTATAGC[A/G]TGGGTCTTGGAATCAATATGTATTGCATACCCTGATGTCATTTTTAAACATTTATCTTCT CAGAATAATTTTCTGAAGTTTATATTTTAGAAATTACATC	14	*SIPA1L1*	Intron	A/G	QRS duration	$1.04x10^{-10}$	Sotoodehnia *et al* , 2010				
rs11897119	AGATCACATGAAAAGTGACAGAGGAAAAAAAGGGTAGAACTTTCTAATTTTGTGATATTTAAATTATGAAATCAGAAACT ATATGATGTGAAGAAACAAC[C/T]GAAATTTGCACTGAAATTTTGAGAGCCATATTACTACCCTTTGAAGCTCCAGGTAGT GGTAATGATTCAAAGAGAATTTTTGTGACACCACTTGCATAAA	2	*MEIS1*	Intron 8	C/T	PR interval	$4.62x10^{-11}$	Pfeufer *et al* , 2010				
rs11970286	GGAATACSGGTGGTGTAATTCAGTCTTGAGTTTGAAAGCCTGAGAACCAGAGGAGCCCATGGTGTAACTCCCAGTCTGA GGCCAAAGGCATGAGAACTAG[C/T]GAATGGGAGGAGGAGTGAAGGTAGGTGAGGGTGTATGAGCCCCAGAGKGCA AAGGTCCAAGTACCAGGAGCTCCAACGTCCAAGGGCAGGAGAAGATGAT	6	*PLN*	-189KB	C/T	QT interval	$2.35x10^{-24}$	Pfeufer *et al* , 2009; Newton Cheh *et al* , 2009	r2 0.79 with rs11153730	r2 0.884 with rs11153730	r2 0.891 with rs11153730	
rs12053903	CTCATTCCTTAATCTTCAGTGTGTACCTACACAATAGAGCTGTCCTAGGCCCATCTTCTACATCTTGGGTTCTCAGGCCAG AGGGGATCTGCTTAGTATC[C/T]TGCCCACCCAGCTTGGGCCAGAACTCAGGTCTTTTAGCTCCTTGCTATTCAAAGTGT GGTTTGAGGACCAGCAGCCTTGGGATCTCCTAGGTRCTTATCA	3	*SCN5A*	Intron	C/T	QT interval	$1.00x10^{-14}$	Newton Cheh *et al* , 2009				
rs12143842	AGACATTTCTCAATTGTAGCTTAAATAAAAAAGTATTCATTTTTTGGTGGTAATGGGGAGGTAATCTTTCTGAATTAGCACC CAGGGTCACATCCCAGTT[C/T]AAAAATATCCCATGGAGTGCAGTCATCTCAGCCAGCTGTTGAAGGCCTCTCTAGCTGT CTCCTGACTCTGTTCCCAGCCTTATCACTAATGGCTCTCCAA	1	*NOS1AP*	-6KB	C/T	QT interval	$1.88x10^{-78}$	Pfeufer *et al* , 2009; Newton Cheh et al, 2009				
rs12296050	TTACCCCATCTGTAAAATAGGGATAACAGCAGCTTCTTAAAGGGCTGTTAGCCACGTGCTTAGACTGTGCCCGGAAAAT GCACTGTCTCTCCTGGGCTCC[C/T]AACCTTTCACAGGCCACAGGCCCATTCCCAGAAGTTTATTTTTTATTTTTCGAGACA GGGTCTCCCTCTGTCACTTAGGCTAAGAGTGCAGTGGTGTGAT	11	*KCNQ1*	Intron 1	C/T	QT interval	$2.80x10^{-17}$	Pfeufer *et al* , 2009; Newton Cheh et al, 2009				
rs13165478	ACCCTTCAGTTTCTCCTAAGGTCACCTTCTTACACAAAYAAGGTATGTTTATCGTAACTAAGACACTAACATTAATACATTAT TATTAAACTAAATTTTA[A/G]ACCTTATTCAGATGTCACCAGATTTTTCTTTTATGTCCCTTTTCTGTGCAAGGAAGCAATCC AGTAGACCATTTCACATTGAGCACAATTATGTTTGCCA	5	*HAND1-SAP3OL*	Intergenic	A/G	QRS duration	$7.36x10^{-14}$	Sotoodehnia *et al* , 2010				
rs1362212	AAAAAAATTTGGAGTCTTGTCCTTGCTTGCCTTCAAGGATTCAACTTCTGGTGGAGCTTCTTCTCATCTGGGTTGCACCAC AGTCATCTTTGTATTTTAA[A/G]TTTGACAGAACTCCACKMGGAATTCACTCTTTTGGAGGGGAGAAAATGGGGCAACAC TTACATATGATCAGATAAAATGTAAGTATTTGAAACAAAACTT	7	*TBX20*	Intergenic	A/G	QRS duration	$1.12x10^{-13}$	Sotoodehnia *et al* , 2010				
rs17020136	ATGATCAGTTGCAGCCATGAATGCCATGCGAATGAGGTCAGAGAGATGAAGTACCAAGAGGTCATCTAAMAATAAAAA TAGAATGCAAAAATGAAAACTT[C/T]TCCAAAAATAAGTGTAATAACATAAAAATATGAAATGAAATAAATTTTTGATAAAA AACACAATCCACATATTTCACAACTTTGAAAATAGCAAAGATAT	2	*HEATR5B-STRN*	Intron	C/T	QRS duration	$1.90x10^{-9}$	Sotoodehnia *et al* , 2010				
rs1733724	TGGAGTGGAAGTAGTAGAATGGTTCCATTGCATTCAAGAGCAGCTAGGAGTTGATGAGGTCTTTTAGAGGCAGCCCTG GCAAAGTACCTGTAGCCTCAGT[A/G]TGGAAGAGAAGTAGCAGAAAATCCTGCTATCAATGAAAGTAGCACTAAGTTCA ACAAGATAGCTGGTAGATGTGAATAGCCCTTTCTATTGGAAATATAA	10	*DKK1*	Intergenic	A/G	QRS duration	$3.05x10^{-8}$	Sotoodehnia *et al* , 2010				

Table 12. *Continued next page*

ID	Sequence	Chr	Nearest gene	Position	Annotation required for project	Association	Association p-value	Source	LD (whole population)	LD (NW Eur - Utah residents from NW Eur)	LD (Japanese in Tokyo)	Comments
rs17391905	TAGTGGAAAAGACAACCTCTTAGCTGTAAGAGGTCCTGCATTTCCTTAAAAAGGAGCTTAAGGAATGTGCATTCTCATTG GAAGTGAGAGTTAGGAGATT[G/T]GTCTTGAAATTGACAATAGCAAGCACACAATCTTTAAACTGTGTTTGGGATGGCTT GAGTAGAGACGTATTGAAATTAAGGGAGAACTAAAGTGACCAAA	1	*C1orf185-RNF11-CDKN2C-FAF1*	Intergenic	G/T	QRS duration	$3.26x10^{-10}$	Sotoodehnia *et al* , 2010				
rs17608766	ACACAGACTCTGATGTCAGTCATGATGTTTCAGCCTCTGCCCTTTTCCTGTATCAACCCTGATGGATRATAGGGCGTGGG TTCTGTCTGTTATCAGGGTG[C/T]GGTCCCCTGTGAATGAAGCACTCCCAGCCACTGAGCTGTGAGAAACAGTCACTCG GAAGTGTGAGCTTTATCTTAGTTTTTGTTGGATCATGTTGAGTCT	17	*GOSR2*	Intron, 3'UTR	C/T	QRS duration	$4.75x10^{-10}$	Sotoodehnia *et al* , 2010				
rs17779747	TGATCTTCACAAATAACCCTGTGAGCCCTATGAGTAAGGCAACACCAGCATTTTCATCCCCATTTTACAGATTCATAATCA GAAGTTGAGAGACAATAAC[C/T]ACCTTGCCTTGAGTCACCAAATTATTAAGTAGTAGAACTAGAAAGTAAAGCCAGGTT TTCTGACTCCACATTCAGGCCGTTCAAAGCCAAGCCTTGGCCA	17	*KCNJ2*	+319KB	C/T	QT interval	$6.02x10^{-12}$	Pfeufer *et al* , 2009; Newton Cheh *et al* , 2009				
rs1886512	CACATGGGGCAGGGATCTCAAATCCTAATGTGTCACTGGCTTCCGAGGTTGGCAGCAGCCAGCTTGGCTTACCACCATC CAGTCTCAGGAAAGCCTTCC[A/T]GCAGCCGGCCAGCCCTCGACTCTCCGGAGTCTGGCAGCAGCTCTAGGAATCCACC TTAACAAAGCACCCTGTAGGCTGTTTGGCTGGTAGACAATGAAGG	13	*KLF12*	Intron	A/T	QRS duration	$1.27x10^{-8}$	Sotoodehnia *et al* , 2010				
rs1896312	TTGAGCCAGCCAACTAACCTCTAAGTTTTCTTGCTCATAAAAGGACGATAATGACACCTTCTTTGGGAGCTGATGGTGTA GTGGATGKTGRGAAAATTAA[C/T]TGGGTGGTGGTAAATGACTCTGAGATCCCTAGATGAAAGGGGCCACAGAGATGA GCTGTTATTATGCTTGTTACTTCCCTCTCACCGCTTCTGCCTCCCT	12	*TBX5-TBX3*	226KB 5' of *TBX3*	C/T	PR interval	$3.13x10^{-17}$	Pfeufer *et al* , 2010	rs0.808 with rs10850409		rs0.872 with rs10850409	
rs2051211	TCTACCTAGGCAAGGTGAAGAGATGAGAAGCGATAGGATATATGCTGAGAAAACAGTTAAGTTAGAGCGTTCATGTAG GGAAGGAGACAAAAATAAAAGG[A/G]AAGTTTGGGGCCTGGTGGCAGAAACTTCAAATGACCAGCTAAAAAGTTTAGG CAAGAACTTCAAGATAATTTTCTAGCAAGCAGGGCCTTTGAAAAGTAG	3	*EXOG*	Intron	A/G	QRS duration	$1.57x10^{-8}$	Sotoodehnia *et al* , 2010				
rs2242285	ATTTCATAGACAATGTAGTCTTACTGCTTCYCGGGGGAAAAGCCATTAGCCTTAGGTACCATGCAGTGTTGGGTCTTTTCA ACAATTAGAAATAAGCCTC[A/G]AAATAGCCCTGGTRAAAAAGTGCTGACTGAAACTCTATACTTCGTTTGTGCCTTGCCC CTTATTTAAGTTGCTTATACATCTAGAAAATTCATGCTCAGG	3	*LRIG1-SLC25A26*	Intron	A/G	QRS duration	$1.09x10^{-8}$	Sotoodehnia *et al* , 2010				
rs251253	GGAAAGTTAGGACCTGTGCCAACCATTTTAATTCTTTCAGGATGTGCGCTCAGTGTTGAAGTTAAAAAGATCATAGAGAA TACCCAGTTTTACTTTTGAT[C/T]CCTTGTGGTGAAGAARCTGGAACTCAGAGAGGTCACCTTGGATCTTATAGTTAGTGG TAAAGCTCAAATAGGGGTCTTGGCTCCAAGAACAGTGTTCCAA	5	*ATP6VOE1-C5orf41-BNIP1-NKX2-5*	3KB 5' of *C5orf41*	C/T	PR interval	$9.45x10^{-13}$	Pfeufer *et al* , 2010				
rs3807989	ACTAATCACCCAGTATCCATGCTATCGCTGGCCCTTCTGTGGCCTATTTTTATACTGTTCACTGTTCAGTGTCACTTGTTTG GTAACACTCAACATCAAC[A/G]TGTGCTACCAAATTGACACCAGAGGACAAAAAAGAATCAAGATATGTACAGCCTGCTT TGTACTGAGCCAGCTGCCACTAGATGTTTTTTGTGATAATGA	7	*CAV1-CAV2*	Intron 2 of *CAV1*	A/G	PR interval	$3.66x10^{-28}$	Pfeufer *et al* , 2010				
rs4074536	CAAAGGCATTCCCTCGGCACCTCACTGAGGCAGYGCAGACAGCATGCCCTTTGGTTACTTACCTCAAGCAYGATTTCTTT CAGTTGGAACTGTTTTTGYG[C/T]GACCTTATCTGAAGACACCGGCTCATGGTAGTAGAGGCAAAGCAAGTCATATTTCTT TAAAACCTGCTTGAAGTTCTTCTCGGAAAGACTTACCACTCGG	1	*CASQ2*	Exon 1	C/T	QRS duration	$2.36x10^{-8}$	Sotoodehnia *et al* , 2010				
rs4687718	TTCGGAGGATGGGGCCACTAAGGTTCACAGAAAGTGACTTGCCTAAAGTCACACGGCCTGCCAGCAGCAGAGCTAGG ATAAGARCAAAATGCTAAGAAAA[A/G]CTGGTGAATGGATAAACAAAATGCACTATGTCCACACAACGGAATATTCAGCC GTAAAAAGAAATGAAGGGCTGGGCGTGGTGGCTCATGCCTGTTAATT	3	*TKT-PRKCD-CACNA1D*	Intron	A/G	QRS duration	$6.25x10^{-9}$	Sotoodehnia *et al* , 2010				
rs4725982	CTGAAAAGCAAGTTCAATCAGGTTTCAGTTTCCGGAAGACTGTCCRCCACCAGGGGAAAAGGTAGATCCCAYAGACCCG AATCTGGAACTGCAAAGCCCC[C/T]GGTGTAACCTCCCTCAGCCTTGACCATCGAAGGACAAATGAACAACCACCCAGA GGACGGTGAGCTGGAGCCCTCCACTCAGAGGCCACCTGGAAACTGG	7	*KCNH2*	Downstream *KCNH2*	C/T	QT interval	$5.00x10^{-16}$	Newton Cheh *et al* , 2009				
rs4944092	CAGGTTCTTGACTTCTCTGAAAGGAACTGTCTTGCCACCATGCCTTTGCCCAAGCTTTTCCTGATGCCAGGAATGCCTTTC CCCCTGCTTCTGGACATGA[A/G]TGAACTTGATCTGCTTGTGGAAGAAGTATTTACTAAGCACCAACTCTTCCCAGACTCA TTTGGTAATGAATATGACATAGATCCTTTCCTCAAGGATGCC	11	*WNT11*	Intron 1	A/G	PR interval	$3.22x10^{-8}$	Pfeufer *et al* , 2010				
rs6800541	AGGAGGCAAACTTTGAAGTTATATTGGCCTCCTTCAGGCATGGCAAAGTCACTTCTTGGAGTCCCACCTAGAGCTGTCTG GCTTGCATTAGGCTATGATA[C/T]GAGTGAGAAATAAACCTTTATTGGGGTCAGTTACTCAGTTTTAGAGATTGTCTGTAT AATAGGTAGCTTTATTTTTCAYTGATTAATAAAAATTTTTATA	3	*SCN10A*	Intron 14	C/T	PR interval	$2.10x10^{-74}$	Pfeufer *et al* , 2010				
rs6801957	GTAGGGAACTTGGCCACCTGGAGCTCYCTAAGAGCCCCAAAGTAACTGAAAATGCTTCTGAGTGGCAGACAGCTGTCA CAGAGTTCATGCTCTCTGCTGT[C/T]ACCTAGACAAAGGCATGTAAAATATGGCAGCTGATAACAGCAGCTGCTGGAACA CAAGTGACGACTGCAGGGAAGAAGGCTATGGGAGAGCTACAGACTC	3	*SCN10A*	Intron	C/T	QRS duration	$1.10x10^{-28}$	Sotoodehnia *et al* , 2010				
rs7342028	CGATTATGTGCTTCTATTGTTTTTTTAACAGCTTTATTGAGATATAATTTATATGTTATATAATGCGCCCATTTAAAATGTACA ATTCAGTAGCTGTTAG[G/T]ATATTCACTGCATCRTGCAACCATCACCACAAACAATTGTAGAACTTTTTTTTTTTTTTGAG GCAGAGATTTGCTCTTGTTGCCCAGGCTGCARTGCAA	10	*VTI1A*	Intron	G/T	QRS duration	$4.95x10^{-10}$	Sotoodehnia *et al* , 2010				

Table 12. *Continued next page*

ID	Sequence	Chr	Nearest gene	Position	Annotation required for project	Association	Association p-value	Source	LD (whole population)	LD (NW Eur - Utah residents from NW Eur)	LD (Japanese in Tokyo)	Comments
rs7562790	TTCTCTGGAATTGTATGTTTTCAGTTGATTCATTCATCTATTCATCAAACATGAATTGAGTTCTTAAGAGTGACAGACACTATTCTCCGGATGTTCTTAC[G/T]GTGCATGGGTTTCACTTTCCACTTCTATCCCTCACAAATACTGGTTTTCCCTTCTACCTGTGGCCTTTGTGAGTATAGGCTCTTCCTTATTTCCTTGCTG	2	*CRIM1*	Intron	G/T	QRS duration	$8.22x10^{-9}$	Sotoodehnia *et al* , 2010				
rs7692808	TAAAWTTGCCAGGGAAAGAATGTTGTCCTAAGGTAGATGGGAGCATGCTGCCATTTATAGAAGGGTAGTTGCTGGATGATAGAAAGCCATAGAAAGCAAA[A/G]AAGTGTAAGAGCAGAAACAAAAAAAMCAAACATCGCATGTTCTCACTCATAGCTGGGAATTGAACAGTGAGAACACTTGGACACAGGAAGGGGGACATCA	4	*ARHGAP24*	Intron 2	A/G	PR interval	$5.99x10^{-20}$	Pfeufer *et al* , 2010				
rs7784776	CCAAAATGGGTAGTACACAACTTGATAGTCCCCAAAGATGTGATGAAGACTTTTCTCAAAGTCAAAAGCCAGGACCAAAACTCAACGTCCTGCTTTCTTC[A/G]TTCAGCACTCTTCCTTCTCTTGAATCCCACCACTGCCCCACRAGCGTATACTGTAGTKATTGTTATGCCGGTGATCTCTTCCAGAGAAGATTAAAATTAA	7	*IGFBP3*	Intergenic	A/G	QRS duration	$1.28x10^{-9}$	Sotoodehnia *et al* , 2010				
rs8049607	TTTCCCCGCTCCAGCCCCGTCATTTTATAGCTGAGGCCCAGAAAGGGGTTGAGGAGCTAAAGGCCCCACAGCCAGGCTGGAAATGGGACAAAACCCAGCA[C/T]GCTTTTTTGCTTTCTTTTTTCTTTGTAGAGACAGGGTCTTGYGTAGTCACCCAGGCTGGAGTGCAGTGGCGCTATCATAGCTCACTGCAGCCTCTACCTC	16	*LITAF*	-11KB	C/T	QT interval	$5.78x10^{-15}$	Pfeufer *et al* , 2009; Newton Cheh *et al* , 2009				
rs846111	GGGCTTACATGAGGCTGTCCCTTTAGGAATAATCCAGGAAGTGTCCCGGAAAAGAGAGAGAAGACATCAGAGCCTAAAGGAAACAGCTGGGCTCCGAACG[C/G]CCTCTCAGAAGAGCCTCTACTGAAAAATATGGATCATCACAGATCCAAACAGAAAAATGGGGGCGATGTCCCCACATGGAGGGAACACCCGACTTAGCAA	1	*RNF207*	3'UTR	C/G	QT interval	$3.69x10^{-16}$	Pfeufer *et al* , 2009; Newton Cheh *et al* , 2009				
rs883079	AGTCACATTTTTAAAATTGTGGTTTCAAGCTACTGATTAGATCAGCATCCAGCGACCTTGAGTGCAGAMGTGAACATTGGGTGAAATGAAAAATCTTGTC[C/T]KKSRGGTTCTCTTGGCTACRGTCTCTCTCCTTCTCTCTCTTTCTCCTCTCTCTCTCYCTTTCTCTAGGAAATGTCTGTTGTGAAGCAGGCCTCACTTTAG	12	*TBX5*	3'UTR	C/T	QRS duration	$1.33x10^{-10}$	Sotoodehnia *et al* , 2010				
rs9436640	TTAAAATTATCCTTAGAATCTCTTTCTCCTTCCAGCCGCTGCTCAAATCCTACCCTCTTCCACCACCTCTTAAATCTTTTTCCTGCCTGCATTTTCTTAC[A/G]TAAAGCAATCTACTACTGCCATCGGTTCATTCACTCACCGGAACCTGTCTTGCCAGGACCTGACCTCAGCAGACTGAGTCATACCAGCATCATCCTTGTT	1	*NFIA*	Intron	C/T	QRS duration	$4.57x10^{-18}$	Sotoodehnia *et al* , 2010				
rs9470361	GACAACTGCATATAAAATGTAGCAGAAGATTAAGAGGCTGATAAAGCTGCTGCTGCAGARAGGAGACAGAACTCTAAAAAGGATGTGTGACACACAGAGC[A/G]CAGACACACTTAGTGCAGGTGCAAGCTGCCTAGCTGACCTCGGTAACGCCTGAAACTCTCACTATTCAACAGCAAAGAATGTTGAACCTGAGTCTTCTGT	6	*CKN1A*	Intergenic	A/G	QRS duration	$3.00x10^{-27}$	Sotoodehnia *et al* , 2010				
rs9851724	AAGTTTATAAAATGCCCAAGATATCATATATTACTCATTAAACAAATTTATGTAATATAAACACAAMACCTTTATTTATGTAATATAAAGATAAAAATCT[C/T]GCCAAAAAATACGTGCTCTAAATTCATCACAGTGGTTGTCTCTGGGATGGAAGGAAAGAGAATCAGAATGGGAAGGGATACAAGGGATACCTCAACTCTT	3	*SCN10A-SCN5A*	Intergenic	C/T	QRS duration	$1.91x10^{-20}$	Sotoodehnia *et al* , 2010				
rs991014	TGAATACCTGCAACTACAAGGTTCAGTTCATTGAGTTCTGCCTGGCTTTATCCCTTTCGGATGCCCAMCTGTAATCATGATYAATTGCTCCAGATTTGGC[C/T]GAGGGACCCAGATTCTCTGCCAAATTGGCTCCACTAAGCTGAGGAGCAGAGCTTTTGACTTCGGTGCTCAGATACTCTCTGAAACAAGCACCTTCTGACT	18	*SETBP1*	Intron	C/T	QRS duration	$6.20x10^{-10}$	Sotoodehnia *et al* , 2010				
rs9912468	GCATAGTTAATAGAAATGGAAGGCCAAAGATCTTATGTCATTGCCTGGTCTCTTAGGAGAGATGAAATAGGAATTCATGGAGCCTCAGAGATCTGGAAAA[C/G]CATCTTCCTGTAGACTAACACTGTCCTRTAGAATTTTGTGTGATCATGGAGTGTTCCCTAATCTGCACTGTRTAGTATGGTAGCCACTTGCACCATCTGG	17	*PRKCA*	Intron	C/G	QRS duration	$1.06x10^{-8}$	Sotoodehnia *et al* , 2010				

Table 12. List of SNPs studied.[19,21,22,170,171] Only SNPs with highly significant associations (p=<0.001) were included if qualifying data were from a GWAS. LD data were obtained from https://analysistools.nci.nih.gov/LDlink/[207]

SNP genotyping

SNP genotyping in *SCN5A*-E1784K families was carried out using the PCR-based Kompetitive Allele Specific PCR (KASP™) genotyping assay provided by LGC, UK. The KASP™ assays were designed using the Kraken™ software system and validated through LGC's assay validation pipeline.[208] Quality control post-genotyping included exclusion of samples and therefore cases where complete data were not available for all SNPs.

Statistical analyses

Categorical variables are described as count and percentage and numerical variables as mean ± standard deviation (SD) or median and interquartile range (Q1-Q3: IQR) where appropriate. Categorical variables were compared using the Fisher exact test. Numerical variables were compared using t-test or ANOVA for normally distributed variables with equal variances and Mann-Whitney or Kruskal-Wallis tests otherwise. Normality of the numerical variables was checked using histograms and the Shapiro-Wilk test. Equality of variances was tested using Levene's test.

As per Chapter 3, to correct for age-related differences in ECG traits (PR, QRS and QTc), a nonlinear relationship using restricted cubic splines (rcs() function) was fitted between age at the time of the ECG and the ECG parameters. The residuals from these models (i.e. PR.age, QRS.age and QTc.age) were used as ECG outcomes in the subsequent analyses. PR.age.Car, QRS.age.Car, QTc.age.Car and RR.age.Car denote PR interval, QRS duration, QTc and RR interval corrected for age and carrier status.

Effects of individual SNPs (assuming an additive genetic model) on these age-corrected ECG parameters were calculated using linear mixed models for numerical

outcomes with correction for *SCN5A*-E1784K status, ethnicity and related observations (lmekin() function). The kinship matrix used for relatedness correction was constructed using pedigree information (kinship() function). For the SNPs an additive genetic model was assumed.

Possible *SCN5A*-E1784K or ethnicity specific effects were investigated by comparing the fit of a model with the main predictor and ethnicity or *SCN5A*-E1784K status effects with that of a model with main and the interaction effect using a likelihood ratio test. In view of significant predictor * ethnicity interaction on the multivariable regression model, effects were estimated in the separate ethnicities.

These analyses were performed in all individuals irrespective of their *SCN5A*-E1784K status and in *SCN5A*-1784K carriers and WT individuals separately. All analyses were carried out using R (version 4.0.2) software and the rms, kinship2, and coxme packages.[196–199,209] For statistical significance, both nominal ($p<0.05$) and Bonferroni corrected p-value thresholds were considered. The Bonferroni correction was therefore made for comparing 43 SNPs with complete data i.e. $p<0.0012$.

Results

Population characteristics

Tables 13 and 14 show the clinical characteristics of the total cohort and separated by ethnicity in patients for whom SNP data were available (n=317). The sample is very similar to that employed in Chapter 3. There were no differences in gender, normal/abnormal QRS axis or the prevalence of the spontaneous type 1 Brugada pattern between Caucasian, Japanese and other/mixed ethnicities. Antiarrhythmic medication use, the prevalence of prolonged QTc and BrS remain significantly

different between ethnicities. Similarly, the continuous variables were significantly different between ethnicities: age at baseline ECG, PR interval, QRS duration, QTc, RR interval, event-free interval and QRS axis.

Variable	Total cohort (n=317)		Caucasian (n=158)		Japanese (n=80)		Other/mixed ethnicity (n=79)		p-value
	n	%	n	%	n	%	n	%	
Male	142	45%	66	42%	41	51%	35	44%	0.3836
Medication	55	17%	40	25%	9	11%	6	8%	0.0007
Long QT	181	58%	82	53%	66	83%	33	43%	2.5E-07
Left axis deviation	16	5%	7	5%	4	5%	5	6%	0.7538
Right axis deviation	26	8%	10	7%	9	11%	7	9%	0.4284
Abnormal QRS axis	44	14%	18	12%	13	16%	13	17%	0.4614
BrS	68	59%	45	64%	0	0%	17	43%	0.0080
Spontaneous type 1 Brugada ECG pattern	12	4%	3	2%	4	5%	5	6%	0.1623
SCN5A -E1784K	213	67%	109	69%	65	81%	39	49%	9.4E-05

Table 13. Clinical characteristics (categorical variables) and mutation status of the **total cohort** separated by ethnicity for those for whom SNP data were available (n=317). For each cohort, n denotes the number of subjects with that characteristic, and % denotes the percentage of subjects within that cohort with the said characteristic. Statistically significant values ($p<0.05$) are highlighted.

Variable	Total cohort (n=317)		Caucasian (n=158)		Japanese (n=80)		Other/mixed ethnicity (n=79)		
Parametric	Mean	SD	Mean	SD	Mean	SD	Mean	SD	p-value
Age at ECG (years)	30	19	32	20	25	17	29	16	0.0164
PR interval (ms)	160	29	157	31	164	28	164	25	0.0079
QRS duration (ms)	93	13	93	14	95	12	90	14	0.0063
QTc interval (ms)	468	42	468	35	497	41	453	42.1	2.4E-12
RR interval (s)	0.9	0.2	0.9	0.2	1.0	0.2	2.4	0.2	5.7E-06
PR.age	-0.1	25.8	-0.1	38.0	6.8	23.6	-4.3	21.4	0.0002
QRS.age	-0.3	12.9	-0.3	13.1	1.9	11.2	-15.2	13.4	0.0011
QTc.age	-1.0	41.8	-1.0	34.9	27.0	41.4	-15.2	41.9	2.2E-11
RR.age	0.0	0.2	0.0	0.2	0.1	0.2	0.0	0.2	1.5E-08
Event free interval (years)	30	18	34	20	25	17	29	16	0.0014
Non-parametric	Median	IQR	Median	IQR	Median	IQR	Median	IQR	p-value
QRS axis (degrees)	56	50	52	50	68	39	52	49	0.0079

Table 14. Clinical characteristics (continuous variables) of the **total cohort** separated by ethnicity for whom SNP data were available, in the total cohort and separated by ethnicity. PR.age.Car, QRS.age.Car, QTc.age.Car and RR.age.Car denote PR interval, QRS duration, QTc and RR interval corrected for age and carrier status.

Among *SCN5A*-E1784K carriers (Tables 15 and 16), antiarrhythmic medication, and the prevalence of prolonged QTc remained significantly different between ethnic groups. When continuous variables were compared, QTc, deviation of QTc from that predicted at a specified age, RR interval, deviation of RR interval from that predicted at a specified age, and event-free interval were significantly different between ethnicities.

Variable	All *SCN5A* -E1784K (n=213)		Caucasian (n=109)		Japanese (n=65)		Other/mixed ethnicity (n=39)		p-value
	n	%	n	%	n	%	n	%	
Male	104	49%	53	49%	33	51%	18	46%	0.9004
Medication	52	24%	37	34%	9	14%	6	15%	0.0046
Long QT	176	84%	82	77%	64	98%	30	79%	0.0001
Left axis deviation	15	7%	6	6%	4	6%	5	13%	0.3019
Right axis deviation	20	10%	10	10%	8	12%	2	5%	0.5451
Abnormal QRS axis	36	17%	16	15%	12	18%	8	21%	0.6475
BrS	64	71%	44	67%	0	0%	14	78%	0.2178
Spontaneous type 1 Brugada ECG pattern	12	6%	3	3%	4	6%	5	13%	0.0581

Table 15. Clinical characteristics (continuous variables) and mutation status of the ***SCN5A*-E1784K carriers** separated by ethnicity for those for whom SNP data were available (n=213). For each cohort, n denotes the number of subjects with that characteristic, and % denotes the percentage of subjects within that cohort with the said characteristic. Statistically significant values ($p<0.05$) are highlighted.

Variable	All *SCN5A* -E1784K (n=213)		Caucasian (n=109)		Japanese (n=65)		Other/mixed ethnicity (n=39)		
Parametric	Mean	SD	Mean	SD	Mean	SD	Mean	SD	P-value
Age at ECG (years)	28	18	29	18	25	17	31	17	0.1459
PR interval (ms)	165	30	163	32	166	27	170	28	0.1651
QRS duration (ms)	96	13	96	14	96	12	95	14	0.5947
QTc interval (ms)	490	30	478	24	512	28	486	29	9.5E-12
RR interval (s)	0.9	0.2	0.9	0.2	1.0	0.2	0.9	0.2	3.2E-05
PR.age	0.3	25.7	-2.5	27.8	3.8	24.0	2.4	21.8	0.0804
QRS.age	-0.2	12.7	-0.1	13.6	0.6	10.9	-1.9	13.4	0.2700
QTc.age	0.4	30.1	-11.2	24.5	21.8	27.9	-3.6	28.7	2.7E-11
RR.age	0.0	0.2	-0.1	0.2	0.1	0.2	0.0	0.2	4.7E-07
Event free interval (years)	29	18	31	18	25	17	30	17	0.0463
Non-parametric	Median	IQR	Median	IQR	Median	IQR	Median	IQR	P-value
QRS axis (degrees)	61	54	55	49	70	49	54	54	0.0799

Table 16. Clinical characteristics (continuous variables) of ***SCN5A*-E1784K carriers** separated by ethnicity for whom SNP data were available, in the total cohort and separated by ethnicity. PR.age, QRS.age, QTc.age and RR.age denote the deviation from the predicted PR interval, QRS duration, QTc and RR interval respectively at age X considering the carriers only. Statistically significant values ($p<0.05$) are highlighted.

SNP interactions and frequencies

Eight SNPs previously associated with PR interval, twenty-six SNPs previously associated with QRS duration, and nine SNPs previously associated with QTc, were studied. Similar to the basic assumption of a GWAS (the allele dosage effect), it was assumed that the SNPs are additive (0,1,2). None of the SNPs were in LD with other SNPs associated with the same ECG trait. There was little evidence of different SNP interactions across ethnicities or between *SCN5A*-E1784K carriers and WT relatives. One SNP, rs4073797, had evidence of an interaction with the PR interval in the total cohort (*SCN5A*-E1784K carriers and WT relatives) showing a larger effect (9.2 ± 3.4 ms) in the Caucasians compared to the Japanese (6.7 ± 5.1 ms) and the other/mixed ethnicities (2.9 ± 4.7 ms).

When assessing SNP genotype frequencies across ethnicities, some of the SNPs were monomorphic across the cohort whilst others were polymorphic. There were differences in frequencies between ethnicities amongst both the total cohort and amongst *SCN5A*-E1784K carriers as expected, with only some of the differences remaining significant upon Bonferroni correction (Tables 17 and 18).

SNP	A1	A2	Caucasian				Japanese				Other/mixed ethnicity				p-value
			A1A1	A1A2	A2A2	MAF	A1A1	A1A2	A2A2	MAF	A1A1	A1A2	A2A2	MAF	
rs10850409	G	A	70	54	8	0.265	3	8	7	0.611	24	38	13	0.427	0.0001
rs10865879	A	C	70	53	8	0.263	15	2	0	0.059	45	26	2	0.205	0.0790
rs10919071	A	G	95	28	8	0.168	15	2	0	0.059	46	20	9	0.253	0.1854
rs11047543	G	A	105	45	6	0.183	68	12	0	0.075	64	14	1	0.101	0.0155
rs11153730	T	C	83	18	15	0.207	16	0	0	0.000	47	22	3	0.194	0.0030
rs11710077	A	T	114	15	3	0.080	16	1	0	0.029	53	20	0	0.137	0.0180
rs11848785	A	G	75	53	4	0.231	13	5	0	0.139	56	18	2	0.145	0.1291
rs11897119	T	C	53	65	15	0.357	12	4	1	0.176	27	44	4	0.347	0.0488
rs11970286	C	T	46	59	26	0.424	11	7	0	0.194	25	45	6	0.375	0.0105
rs12053903	T	C	68	74	15	0.331	44	34	2	0.238	11	51	17	0.538	0.0000
rs12143842	C	T	63	56	11	0.300	7	6	3	0.375	52	19	0	0.134	0.0005
rs12296050	C	T	71	49	8	0.254	5	4	7	0.563	34	30	11	0.347	0.0022
rs13165478	G	A	48	64	18	0.385	7	8	1	0.313	32	33	11	0.362	0.8660
rs1362212	G	A	97	31	3	0.141	16	2	0	0.056	53	23	0	0.151	0.3186
rs17020136	T	C	92	54	8	0.227	16	37	27	0.569	35	30	13	0.359	0.0000
rs1733724	G	A	61	60	10	0.305	10	8	0	0.222	48	21	5	0.209	0.0928
rs17391905	T	T	128	0	0	0.000	16	0	0	0.000	74	0	0	0.000	NA
rs17608766	T	C	90	36	5	0.176	16	0	0	0.000	70	6	0	0.039	0.0002
rs17779747	C	T	42	62	27	0.443	5	9	2	0.406	36	29	11	0.336	0.2299
rs1886512	T	A	64	70	20	0.357	47	27	5	0.234	40	33	6	0.285	0.0980
rs1896312	T	C	66	55	10	0.286	4	8	4	0.500	24	39	10	0.404	0.0256
rs2051211	A	G	108	22	0	0.085	13	4	1	0.167	62	9	0	0.063	0.1037
rs2242285	G	A	40	72	17	0.411	8	9	1	0.306	33	34	8	0.333	0.3731
rs251253	C	T	26	75	52	0.585	59	19	1	0.133	28	41	10	0.386	0.0000
rs3807989	G	A	51	61	20	0.383	11	5	2	0.250	30	37	9	0.362	0.4533
rs4074536	T	C	64	66	25	0.374	21	43	16	0.469	50	24	5	0.215	0.0001
rs4687718	G	A	86	44	0	0.169	15	3	0	0.083	52	22	2	0.171	0.1960
rs4725982	C	T	94	52	9	0.226	7	37	35	0.677	39	37	2	0.263	0.0000
rs4944092	A	G	57	62	14	0.338	12	5	0	0.147	29	35	11	0.380	0.1585
rs6800541	T	C	65	58	34	0.401	62	18	0	0.113	40	37	2	0.259	0.0000
rs6801957	C	T	58	48	25	0.374	13	4	0	0.118	35	39	2	0.283	0.0003
rs7342028	G	T	85	67	4	0.240	25	34	19	0.462	41	30	8	0.291	0.0000
rs7562790	T	G	52	49	19	0.363	5	8	4	0.471	13	35	18	0.538	0.0170
rs7692808	A	G	13	80	62	0.658	53	23	4	0.194	25	37	16	0.442	0.0000
rs7784776	A	G	37	67	24	0.449	5	7	5	0.500	17	47	10	0.453	0.3316
rs8049607	C	T	33	78	42	0.529	24	34	22	0.488	24	44	11	0.418	0.0711
rs846111	G	C	87	40	4	0.183	6	11	1	0.361	61	13	2	0.112	0.0020
rs883079	T	C	68	52	12	0.288	2	10	6	0.611	29	30	16	0.413	0.0012
rs9436640	G	A	59	55	17	0.340	4	7	5	0.531	14	41	20	0.540	0.0008
rs9470361	G	A	102	50	4	0.186	63	15	2	0.119	26	36	16	0.436	0.0000
rs9851724	T	C	103	49	4	0.183	23	33	24	0.506	24	39	16	0.449	0.0000
rs991014	C	T	60	71	22	0.376	43	30	6	0.266	41	28	9	0.295	0.1305
rs9912468	C	G	29	72	28	0.496	5	10	2	0.412	28	31	16	0.420	0.1611

Table 17. Genotype frequencies of the SNPs of interest per population in *SCN5A*-E1784K carriers and WT relatives (n=317). The Fisher test was used to compare across ethnic groups. Values with $p<0.05$ are highlighted in red. The p-value for significance following Bonferroni correction was $p<0.000833$ are highlighted in green. A1 and A2 denote major and minor alleles in this population.

SNP	A1	A2	Caucasian				Japanese				Other/mixed ethnicity				p-value
			A1A1	A1A2	A2A2	MAF	A1A1	A1A2	A2A2	MAF	A1A1	A1A2	A2A2	MAF	
rs10919071	A	G	52	27	8	0.247	12	2	0	0.071	12	16	9	0.459	0.0037
rs846111	G	C	51	33	3	0.224	4	10	1	0.400	31	7	0	0.092	0.0022
rs17391905	T	T	85	0	0	0.000	13	0	0	0.000	36	0	0	0.000	NA
rs9436640	G	A	41	35	11	0.328	4	6	3	0.462	6	22	10	0.553	0.0093
rs4074536	T	C	51	37	18	0.344	17	34	14	0.477	20	14	5	0.308	0.0367
rs12143842	C	T	45	37	6	0.278	5	6	3	0.429	29	9	0	0.118	0.0073
rs7562790	T	G	30	34	13	0.390	4	7	3	0.464	4	12	13	0.655	0.0252
rs17020136	T	C	62	39	6	0.238	14	30	21	0.554	13	18	8	0.436	0.0000
rs11897119	T	C	32	47	9	0.369	9	4	1	0.214	12	23	2	0.365	0.2209
rs2051211	A	G	73	14	0	0.080	10	4	1	0.200	33	4	0	0.054	0.0951
rs10865879	A	C	52	31	5	0.233	12	2	0	0.071	30	7	0	0.095	0.0769
rs12053903	T	C	51	48	9	0.306	35	30	0	0.231	1	27	11	0.628	0.0000
rs11710077	A	T	76	11	1	0.074	13	1	0	0.036	29	7	0	0.097	0.6926
rs9851724	T	C	72	35	0	0.164	15	28	22	0.554	0	27	12	0.654	0.0000
rs6801957	C	T	42	34	12	0.330	10	4	0	0.143	22	16	0	0.211	0.0559
rs6800541	T	C	47	41	20	0.375	51	14	0	0.108	25	14	0	0.179	0.0000
rs4687718	G	A	57	29	0	0.169	12	3	0	0.100	29	8	1	0.132	0.2706
rs2242285	G	A	23	51	11	0.429	6	8	1	0.333	18	16	3	0.297	0.2174
rs7692808	A	G	11	56	39	0.632	43	19	3	0.192	13	20	5	0.395	0.0000
rs13165478	G	A	38	37	11	0.343	6	6	1	0.308	19	16	3	0.289	0.9524
rs251253	C	T	18	54	32	0.567	47	17	0	0.133	12	23	4	0.397	0.0000
rs9470361	G	A	75	28	4	0.168	51	12	2	0.123	9	18	11	0.526	0.0000
rs11153730	T	C	45	18	15	0.308	13	0	0	0.000	13	22	3	0.368	0.0000
rs11970286	C	T	33	34	20	0.425	8	7	0	0.233	10	25	3	0.408	0.0127
rs1362212	G	A	61	23	3	0.167	13	2	0	0.067	31	7	0	0.092	0.5703
rs7784776	A	G	25	42	17	0.452	4	5	5	0.536	6	26	6	0.500	0.1554
rs3807989	G	A	35	39	14	0.381	10	3	2	0.233	15	17	6	0.382	0.3882
rs4725982	C	T	62	38	8	0.250	6	30	28	0.672	23	14	2	0.231	0.0000
rs1733724	G	A	40	40	7	0.310	8	7	0	0.233	21	12	4	0.270	0.5251
rs7342028	G	T	55	48	4	0.262	20	26	17	0.476	17	14	8	0.385	0.0002
rs12296050	C	T	46	33	7	0.273	5	3	6	0.536	14	18	5	0.378	0.0145
rs4944092	A	G	38	40	11	0.348	9	5	0	0.179	19	15	3	0.284	0.5468
rs11047543	G	A	76	31	1	0.153	57	8	0	0.062	32	7	0	0.090	0.0477
rs883079	T	C	49	33	6	0.256	2	9	4	0.567	14	17	7	0.408	0.0048
rs1896312	T	C	45	36	6	0.276	4	8	1	0.385	12	20	5	0.405	0.1975
rs10850409	G	A	46	36	6	0.273	3	8	4	0.533	11	20	6	0.432	0.0151
rs1886512	T	A	43	47	15	0.367	37	23	4	0.242	26	12	1	0.179	0.0254
rs11848785	A	G	52	32	4	0.227	10	5	0	0.167	29	8	1	0.132	0.4294
rs8049607	C	T	26	48	32	0.528	19	27	19	0.500	19	16	4	0.308	0.0326
rs17608766	T	C	67	19	1	0.121	13	0	0	0.000	37	1	0	0.013	0.0082
rs17779747	C	T	27	42	17	0.442	3	8	2	0.462	17	18	3	0.316	0.3366
rs9912468	C	G	15	49	22	0.541	5	8	1	0.357	17	13	7	0.365	0.0115
rs991014	C	T	40	50	17	0.393	34	25	5	0.273	20	12	6	0.316	0.1463

Table 18. Genotype frequencies of the SNPs of interest per population in *SCN5A*-E1784K carriers (n=213). The Fisher test was used to compare across ethnic groups. Values with p<0.05 are highlighted in red. The p-value for significance following Bonferroni correction was p<0.000833 are highlighted in green. A1 and A2 denote major and minor alleles, respectively, in this population.

Associations with ECG traits

PR interval

No SNPs showed a significant association with PR.age, nominal or otherwise, in the total cohort or all *SCN5A*-E1784K carriers. One SNP (rs1896312) remained significantly associated with PR interval in the overall Japanese cohort and in

Japanese *SCN5A*-E1784K carriers after Bonferroni correction. No other SNPs remained significantly associated with PR interval in other ethnic groups in both the overall cohort and SCN5A-E1784K carriers after Bonferroni correction (see Tables 19 and 20 for all nominally significant results).

SNP	A1	A2	B	SE	p	Cohort
rs11047543	G	A	-17.7	5.4	0.0011	Other/mixed ethnicity
rs11897119	T	C	-15.6	5.1	0.0021	Japanese
rs1896312	T	C	16.4	3.7	0.0000	Japanese
rs4944092	A	G	-7.7	3.8	0.0399	Other/mixed ethnicity

Table 19. Effects per A2 allele of SNPs on PR.age in the entire cohort (*SCN5A*-E1784K carriers and WT relatives) adjusted for gender (and ethnicity for the total cohort). B is the effect per A2 allele on the predicted mean PR interval for the age of the individual (an individual homozygous for the A2 allele would have an effect size that is 2xB), and SE is the standard error. Only statistically significant results are shown. Two significance thresholds are shown ($p<0.05$ highlighted in red and p-values that remained statistically significant after Bonferroni correction are highlighted in green).

SNP	A1	A2	B	SE	p	Cohort
rs1896312	T	C	19.3	3.1	0.0000	Japanese
rs6800541	T	C	10.9	3.5	0.0019	Caucasian
rs11897119	T	C	-16.1	5.8	0.0056	Japanese
rs1896312	T	C	-10.8	5.2	0.0372	Caucasian

Table 20. Effects per A2 allele of SNPs on PR.age in *SCN5A*-E1784K carriers adjusted for gender (and ethnicity for the total cohort). The previous associations of the SNPs are shown. Only nominally statistically significant results are shown ($p<0.05$ highlighted in red); none of the p-values remained statistically significant after Bonferroni correction.

QRS duration

None of the SNPs previously associated with QRS duration remained significantly associated with QRS.age after Bonferroni correction in either the total cohort or SCN5A-E1784K carriers only, in separate ethnic groups (Tables 21 and 22).

SNP	A1	A2	B	SE	p	Cohort
rs10850409	G	A	-6.5	2.7	0.0185	Japanese
rs10850409	G	A	-2.7	1.4	0.0470	Total cohort
rs10865879	A	C	-6.3	2.4	0.0091	Other/mixed ethnicity
rs11153730	T	C	5.7	2.8	0.0400	Other/mixed ethnicity
rs13165478	G	A	-5.5	1.8	0.0028	Caucasian
rs13165478	G	A	-3.2	1.3	0.0156	Total cohort
rs1362212	G	A	6.5	2.4	0.0079	Caucasian
rs1362212	G	A	4.0	1.9	0.0348	Total cohort
rs2051211	A	G	-7.5	3.0	0.0140	Caucasian
rs2051211	A	G	-4.9	2.2	0.0286	Total cohort
rs4074536	T	C	5.4	2.3	0.0195	Other/mixed ethnicity
rs4687718	G	A	-5.4	2.7	0.0489	Other/mixed ethnicity
rs7342028	G	T	3.4	1.5	0.0299	Japanese
rs7784776	A	G	3.7	1.3	0.0055	Total cohort
rs7784776	A	G	4.2	1.8	0.0155	Caucasian
rs7784776	A	G	4.8	2.4	0.0458	Other/mixed ethnicity
rs9436640	G	A	-6.1	2.9	0.0337	Japanese
rs9470361	G	A	2.9	1.2	0.0149	Total cohort
rs9470361	G	A	3.9	1.9	0.0375	Total cohort
rs9912468	C	G	3.2	1.3	0.0141	Total cohort
rs9912468	C	G	4.4	1.9	0.0198	Caucasian

Table 21. Effects per A2 allele of SNPs on QRS.age in the different ethnicities (*SCN5A*-E1784K carriers and WT relatives) adjusted for *SCN5A*-E1784K carrier status, male gender (and ethnicity for the total cohort). Only the statistically significant results are shown (p<0.05 highlighted in red; none of the p-values remained statistically significant after Bonferroni correction).

SNP	A1	A2	B	SE	P	Cohort
rs13165478	G	A	-4.1	1.8	0.0218	All *SCN5A* -E1784K
rs13165478	G	A	-5.2	2.4	0.0317	Caucasian
rs1362212	G	A	6.8	2.8	0.0153	Caucasian
rs1362212	G	A	5.5	2.4	0.0249	All *SCN5A* -E1784K
rs1733724	G	A	9.2	4.6	0.0427	Japanese
rs2051211	A	G	-15.8	7.1	0.0274	Other/mixed ethnicity
rs2051211	A	G	-6.0	3.0	0.0466	All *SCN5A* -E1784K
rs6801957	C	T	8.5	4.0	0.0329	Other/mixed ethnicity
rs7342028	G	T	4.3	1.6	0.0082	Japanese
rs7342028	G	T	3.4	1.3	0.0104	All *SCN5A* -E1784K
rs7562790	T	G	-8.4	2.8	0.0029	Other/mixed ethnicity
rs7562790	T	G	7.3	3.2	0.0221	Japanese
rs9851724	T	C	-11.0	4.4	0.0137	Other/mixed ethnicity
rs9912468	C	G	3.6	1.8	0.0488	All *SCN5A* -E1784K

Table 22. Effects per A2 allele of SNPs on the QRS.age in *SCN5A*-E1784K carriers adjusted for male gender and ethnicity. The previous associations of the SNPs are shown. Only statistically significant results are shown (p<0.05 highlighted in red; none of the p-values remained statistically significant after Bonferroni correction).

QT interval

Of the SNPs previously associated with QT interval, only rs10919071 remained significantly associated with QTc.age after Bonferroni correction in the total cohort for the other/mixed ethnicity group only (Table 23). However, none of the SNPs remained significantly associated with QTc.age after Bonferroni correction when *SCN5A*-E1784K carriers only were studied (Table 24).

SNP	A1	A2	B	SE	p	Cohort
rs10919071	A	G	22.0	6.5	0.0007	Other/mixed ethnicity
rs10919071	A	G	-7.1	3.1	0.0234	Total cohort
rs11970286	C	T	36.3	16.8	0.0303	Japanese
rs12053903	T	C	24.1	7.8	0.0020	Other/mixed ethnicity
rs12053903	T	C	-8.8	4.4	0.0469	Caucasian
rs4725982	C	T	12.5	4.8	0.0095	Caucasian
rs4725982	C	T	5.0	2.5	0.0483	Total cohort
rs8049607	C	T	-18.8	7.6	0.0134	Other/mixed ethnicity

Table 23. Effects per A2 allele of SNPs on QTc.age interval in the different ethnicities (*SCN5A*-E1784K carriers and WT relatives) adjusted for *SCN5A*-E1784K carrier status, male gender and ethnicity. The previous associations of the SNPs are shown. Only the statistically significant results are shown ($p<0.05$ highlighted in red and p-values that remained statistically significant after Bonferroni correction, $p<0.000833$, are highlighted in green).

SNP	A1	A2	B	SE	P	Cohort
rs4725982	C	T	5.9	3.0	0.0486	All *SCN5A* -E1784K

Table 24. Effects per A2 allele of SNPs on the QTc.age interval in the different ethnicities in *SCN5A*-E1784K carriers adjusted for male gender (and ethnicity). The previous associations of the SNPs are shown. Due to the number of comparisons made, only the statistically significant results are shown ($p<0.05$ highlighted in red; none of the p-values remained statistically significant after Bonferroni correction).

Discussion

This chapter is the first attempt to identify associations of common genetic variation with phenotype in *SCN5A*-E1784K carriers and WT relatives. A combined approach was taken to analyse both carriers and WT individuals, followed by carriers only, in each ethnicity subgroup. This approach took into account evidence of genotype-phenotype mismatch in pedigrees with this mutation and the ethnic diversity of common genetic variation. There were differences in allele frequencies and disease phenotype frequencies across ethnicities, therefore combining results across ethnicities can show associations that may be false. As such, results were analysed separately by ethnicity. The SNP effects were not consistent across ethnicities.

The Bonferroni correction employed was strict, with the same significance threshold used consistently, although it may have been overly restrictive. An alternative option to correct for multiple testing includes the Benjamini-Hochberg correction. This is where the threshold for the first p-value (lowest p value) is the same as in the Bonferroni correction but each subsequent p-value have progressively less stringent thresholds.

There were a number of significant associations of the SNPs with phenotype, but most were nominal, and only one association, rs1896312 and PR.age, remained consistent in the total cohort and then in *SCN5A*-E1784K carriers when corrected for multiple testing. Of all three phenotypes, QRS.age seemed to show the greatest number of SNP associations.

The SNP rs1896312 is an intergenic variant at the *TBX3*-*TBX5* locus and was previously associated with PR interval in two studies, one in Europeans and the other in African Americans.[21,210] It remained significantly associated with the PR

interval in Japanese *SCN5A*-E1784K carriers and WT relatives, after correcting for multiple testing. This suggests significant ethnic transferability of the variant. This SNP is 230KB downstream of the paralog *TBX5* and *TBX3* genes. Both contain T-box containing transcription factors important for cardiac conduction system formation in the developing heart. *TBX5* plays a role in the patterning and maturation of the murine atrioventricular and bundle branch conduction system. Deletion of *TBX5* results in longer PR intervals in mice.[21,211–213] Direct functional data on the SNP are, however, not available.

The haplotype analyses for chromosome 3 SNPs were considered and attempted but were uninformative due to the relative lack of linkage disequilibrium and the absence of some key haplotypes.

Limitations

This was a candidate SNP study, where a limited number of SNPs that were previously associated with ECG traits at a genome-wide level, were investigated within the *SCN5A*-E1784K cohort. ECG trait studies can be limited by the resolution for measurement of ECG intervals on paper ECGs available for this work. This was mitigated by use of a minimum of two observers to make independent manual measurements on the baseline ECG using electronic callipers (Cardio Calipers)[149]. As described previously, where there was >5% discrepancy, the measurements were repeated and re-compared. If a discrepancy remained, a third observer made measurements and a mean was taken.

The study was limited by the sample size despite this being, to our knowledge, the largest identified cohort of *SCN5A*-E1784K families to date, and hence the limited size of each separate ethnic group. Recruitment of more individuals from more centres worldwide would improve the reliability of estimates. It was further limited by

the number of SNPs studied. I therefore proceeded to study the impact of genetic risk scores derived using these SNPs, on phenotype. This is the subject of Chapter 5.

Chapter 5: Genetic Risk Scores for PR interval, QRS duration and QTc

Introduction

Following the lack of significant single SNP associations with ECG traits in *SCN5A*-E1784K as described in the previous chapter, we investigated GRSs for PR interval, QRS duration and QTc in this cohort. GRSs calculated for PR interval and QRS duration in patients who have undergone ajmaline infusion for suspected BrS have been shown to predict ajmaline dose-related PR change (slope) and QRS slope.[96] GRS calculation for ECG parameters have not been undertaken for PR interval, QRS duration or QTc in individuals from families with a single *SCN5A* mutation.

Weighted GRSs are defined as weighted sums of risk alleles of SNPs and are statistically powerful for identification of gene-environment interactions. In order to assign appropriate weighting, the gold standard is the use external weights from an independent study. However appropriate external weights may not be available, where internal weights can be a powerful and reliable alternative.[214] In this study, both weighted and unweighted GRSs were calculated.

Methods

Recruitment and case selection; clinical evaluation; SNP selection; SNP genotyping were as described in Chapter 4. SNPs selected for the GRSs were identical to those selected in Chapter 3. SNPs associated with a specific ECG trait were only applied in the GRS generated for that trait and were only studied for association with that phenotype i.e. PR SNPs were used in the PRS GRSs and studied for the PR interval adjusted for age (PR.age).

Statistical analyses

Categorical variables are described as count and percentage and numerical variables as mean ± standard deviation (SD) or median and interquartile range (Q1-Q3: IQR). where appropriate. Categorical variables were compared using Fisher exact tests. Numerical variables were compared using t-test or ANOVA for normally distributed variables with equal variances and Mann-Whitney or Kruskal-Wallis tests otherwise. Normality of the numerical variables was checked using histograms and the Shapiro-Wilk test. Equality of variances was tested using Levene's test.

Effects of calculated (weighted) genetic risk scores (GRS) on the age-corrected ECG parameters (PR.age, QRS.age and QTc.age) were calculated using linear mixed models with correction for *SCN5A*-E1784K status, ethnicity and related observations (lmekin() function. This is a linear mixed effect model, i.e. a linear regression model with mixed effect corrected for relatedness based on the kinship coefficient.

The kinship matrix used for relatedness correction was constructed using pedigree information (kinship() function). For the SNPs an additive genetic model was assumed. For the (weighted) GRSs, linearity was checked using x-y scatter plots and by comparing the fit of models assuming a linear or nonlinear relationship using a likelihood ratio test.

Possible ethnicity specific risk factors were investigated by comparing the fit of a model with the main predictor and ethnicity effects with that of a model with main and the interaction effect using a likelihood ratio test. In case of a significant interaction, risks were estimated in the separate ethnicities.

In addition, GRS effects were also estimated by meta-analysis of the ethnicity specific effects (metagen() and forest() function). The metagen is a function that calculates the overall estimate (i.e. meta-analysis) across the ethnicities (i.e. the weighted average of the three estimates). It is a weighted analysis based on the sample size of the ethnicities. It uses the standard errors of inaccuracies that are being measured. All analyses were carried out using R (version 4.0.2) software and the rms, kinship2, coxme, and meta packages.[196–199,209,215] GRS and wGRS are the unweighted and weighted GRSs respectively. For statistical significance, we considered both Bonferroni corrected for 3 phenotypes ($p<0.017$) and nominal ($p<0.05$) p-value thresholds.

Power statement

With the present sample size of 317 and the (Bonferroni corrected) two sided significance level of 0.0012, ECG trait effect sizes (i.e. effect divided by (observed) standard deviation) ranging from 0.32 to 0.74 can be found with 80% power for SNPs with minor allele frequencies ranging from 0.5 to 0.05 assuming an additive genetic model. For PR interval with an observed standard deviation of 25.8 ms this would translate into detectable allele effects of 8.3 to 19.0 ms; for QRS with an observed standard deviation of 12.9 ms would translate into detectable allele effects of 4.1 to 9.5 ms; and for QTc with an observed standard deviation of 30.0 ms would translate into detectable allele effects of 9.6 to 22 ms.

For the *SCN5A*-E1784K only analysis with a sample size of 213, the corresponding minimal detectable effect sizes are higher, ranging from 0.39 to 0.90. In the Caucasian *SCN5A*-E1784K (n = 158) these effect sizes range from 0.45 to 1.1 and in the Japanese *SCN5A*-E1784K (n = 80) or Other *SCN5A*-E1784K (n= 79) from 0.62 to 1.42, respectively.

Results

Descriptive characteristics for unweighted and weighted genetic risk scores (GRS and wGRS respectively) in the total cohort of *SCN5A*-E1784K carriers and WT relatives combined, and in *SCN5A*-E1784K carriers only (both the total cohort and separated by ethnicity) are shown in Tables 25 and 26. These indicate marked heterogeneity across ethnic groups except for QRS.GRS and QRS.wGRS where allele associated effects were very similar other than for Japanese *SCN5A*-E1784K carriers in the weighted GRS. There seemed to be greatest differences between Caucasian and Japanese subjects, with the other/mixed ethnicity group appearing more similar to the Caucasian group. Meta-analyses (Appendix 2) confirmed the presence of heterogeneity between ethnicities, hence why the results are presented by ethnicity.

Variable	Total cohort (n=317)		Caucasian (n=158)		Japanese (n=80)		Other/mixed ethnicity (n=79)		p-value
	Mean	SD	Mean	SD	Mean	SD	Mean	SD	
PR.GRS	4.55	2.10	5.10	2.07	1.60	0.99	4.19	1.72	5.5E-09
QRS.GRS	3.41	3.69	3.67	3.89	2.40	2.87	3.29	3.55	0.2648
QTc.GRS	3.35	2.14	3.67	1.78	6.00	1.47	2.28	2.21	5.5E-10
PR.wGRS	10.72	4.73	12.07	4.66	3.30	1.93	9.95	3.51	5.2E-10
QRS.wGRS	1.58	2.06	1.77	2.14	0.68	1.45	1.53	2.02	0.0737
QTc.wGRS	5.57	3.79	6.15	3.24	10.04	2.61	3.68	3.83	1.1E-09

Table 25. Descriptive characteristics for unweighted and weighted genetic risk scores (GRS and wGRS respectively) in *SCN5A*-E1784K carriers and WT relatives (total cohort and separated by ethnicity showing significant heterogeneity except for QRS GRSs).

Variable	All *SCN5A* - E1784K (n=213)		Caucasian (n=109)		Japanese (n=65)		Other/mixed ethnicity (n=39)		p-value
	Mean	SD	Mean	SD	Mean	SD	Mean	SD	
PR.GRS	4.57	2.11	5.04	2.05	1.33	0.89	4.58	1.52	5.1E-07
QRS.GRS	4.25	3.64	4.35	3.97	2.75	3.14	4.70	3.07	0.1508
QTc.GRS	3.27	2.31	3.66	1.91	6.25	1.42	1.46	1.94	3.1E-10
PR.wGRS	10.69	4.77	11.88	4.63	2.76	1.70	10.61	2.89	1.2E-07
QRS.wGRS	2.07	2.01	2.18	2.17	0.89	1.56	2.38	1.69	0.0429
QTc.wGRS	5.38	4.12	6.04	3.46	10.53	2.49	2.27	3.50	8.7E-10

Table 26. Descriptive characteristics for unweighted and weighted genetic risk scores (GRS and wGRS respectively) in *SCN5A*-E1784K carriers (all *SCN5A*-E1784K and separated by ethnicity showing significant heterogeneity except for QRS.GRS).

Descriptive statistics for the WT individuals, and unweighted and weighted GRSs for PR, QRS and QTc for WT individuals are shown in Appendix 1. These are presented in the Appendix due to the limited clinical relevance of these GRSs. It was not possible to calculate meaningful GRS results for Japanese WT individuals as only 15 Japanese WT individuals underwent SNP genotyping.

PR interval

The unweighted PR GRS calculated from 8 SNPs previously associated with PR interval (see Chapter 4) had a significant association with PR.age after Bonferroni correction in subjects of other/mixed ethnicity but not when *SCN5A*-E1784K carriers only were analysed (Tables 27 and 28). In *SCN5A*-E1784K carriers, the weighted GRS had a significant association with PR.age (nominal significance only) in Japanese, and no other associations. These indicate inconsistent findings.

GRS	B	SE	p-value	Cohort
PR.GRS	0.9	0.9	0.3242	Total cohort
PR.GRS	0.1	1.2	0.9045	Caucasian
PR.GRS	4.2	3.4	0.2095	Japanese
PR.GRS	3.5	1.3	0.0093	Other/mixed ethnicity
PR.wGRS	0.4	0.4	0.3686	Total cohort
PR.wGRS	0.1	0.5	0.8118	Caucasian
PR.wGRS	2.9	1.8	0.1061	Japanese
PR.wGRS	1.5	0.7	0.0241	Other/mixed ethnicity

Table 27. Effects of unweighted and weighted genetic risk scores (GRS) on PR.age in *SCN5A*-E1784K carriers and WT relatives adjusted for *SCN5A*-E1784K carrier status, male gender (and ethnicity for the total cohort). $p<0.05$ are highlighted in red and p-values that remained statistically significant after Bonferroni correction are highlighted in green.

GRS	B	SE	p-value	Cohort
PR.GRS	1.7	1.2	0.1656	All *SCN5A* -E1784K carriers
PR.GRS	1.0	1.5	0.5238	Caucasian *SCN5A* -E1784K carriers
PR.GRS	7.0	4.0	0.0779	Japanese *SCN5A* -E1784K carriers
PR.GRS	3.8	2.3	0.0937	Other *SCN5A* -E1784K carriers
PR.wGRS	0.9	0.6	0.0942	All *SCN5A* -E1784K carriers
PR.wGRS	0.7	0.7	0.3263	Caucasian *SCN5A* -E1784K carriers
PR.wGRS	4.3	2.1	0.0388	Japanese *SCN5A* -E1784K carriers
PR.wGRS	2.0	1.2	0.0997	Other *SCN5A* -E1784K carriers

Table 28. Effects of unweighted and weighted genetic risk scores (GRS) on PR.age in *SCN5A*-E1784K carriers adjusted for male gender (and ethnicity for the total cohort). p<0.05 are highlighted in red; none remained statistically significant after Bonferroni correction.

QRS duration

When analysing GRSs for QRS duration in the total cohort (calculated from 26 SNPs previously associated with QRS duration), apart from the unweighted GRS in subjects of other/mixed ethnicity, both the unweighted and the weighted GRSs for QRS duration had a significant association with QRS.age after Bonferroni correction across all ethnicities. Among *SCN5A*-E1784K carriers only, the weighted GRSs had a significant association after Bonferroni correction with QRS.age across all ethnicities, apart from those of other/mixed ethnicity (Tables 29 and 30). In Japanese *SCN5A*-E1784K carriers, the unweighted GRS also reached significance after Bonferroni correction. Amongst *SCN5A*-E1784K carriers of the other/mixed ethnicities, the unweighted GRS only achieved nominal significance, and the weighted GRS did not achieve nominal significance. Further the unweighted GRS had a negative effect (Beta) instead of an additive effect, which did not achieve significance with Bonferroni correction.

GRS	B	SE	p-value	Cohort
QRS.GRS	1.0	0.3	0.0007	Total cohort
QRS.GRS	1.2	0.4	0.0050	Caucasian
QRS.GRS	2.7	0.5	0.0000	Japanese
QRS.GRS	1.1	0.5	0.0232	Other/mixed ethnicity
QRS.wGRS	2.0	0.5	0.0002	Total cohort
QRS.wGRS	2.1	0.8	0.0051	Caucasian
QRS.wGRS	5.5	0.9	0.0000	Japanese
QRS.wGRS	2.4	0.8	0.0030	Other/mixed ethnicity

Table 29. Effects of unweighted and weighted genetic risk scores (GRS) on QRS.age in the different ethnicities (*SCN5A*-E1784K carriers and WT relatives) adjusted for *SCN5A*-E1784K carrier status, male gender and (ethnicity for the total cohort). p<0.05 are highlighted in red and p-values that remained statistically significant after Bonferroni correction are highlighted in green.

GRS	B	SE	p-value	Cohort
QRS.GRS	1.0	0.4	0.0217	All *SCN5A* -E1784K carriers
QRS.GRS	1.3	0.6	0.0199	Caucasian *SCN5A* -E1784K carriers
QRS.GRS	2.6	0.4	0.0000	Japanese *SCN5A* -E1784K carriers
QRS.GRS	-1.5	0.7	0.0426	Other *SCN5A* -E1784K carriers
QRS.wGRS	2.1	0.8	0.0065	All *SCN5A* -E1784K carriers
QRS.wGRS	2.5	1.0	0.0136	Caucasian *SCN5A* -E1784K carriers
QRS.wGRS	5.2	0.9	0.0000	Japanese *SCN5A* -E1784K carriers
QRS.wGRS	5.2	0.9	0.0000	Other *SCN5A* -E1784K carriers

Table 30. Effects of unweighted and weighted genetic risk scores (GRS) on QRS.age in *SCN5A*-E1784K carriers. p<0.05 are highlighted in red and p-values that remained statistically significant after Bonferroni correction are highlighted in green.

QT interval

The unweighted QTc GRS (calculated from 9 SNPs previously associated with QTc) had a significant association with QTc.age both before and after Bonferroni correction in *SCN5A*-E1784K carriers of other/mixed ethnicity and their WT relatives combined (Tables 31 and 32). However, when solely *SCN5A*-E1784K carriers were analysed for GRS associations with QTc, there were no statistically significant

findings. There were no significant associations at all in either Caucasians or Japanese.

GRS	B	SE	p-value	Cohort
QTc.GRS	1.4	1.0	0.1721	Total cohort
QTc.GRS	0.2	1.9	0.9079	Caucasian
QTc.GRS	11.2	6.2	0.0684	Japanese
QTc.GRS	-6.0	2.5	0.0157	Other/mixed ethnicity
QTc.wGRS	1.0	0.6	0.0750	Total cohort
QTc.wGRS	0.2	1.0	0.8200	Caucasian
QTc.wGRS	0.2	1.0	0.8200	Japanese
QTc.wGRS	-3.1	1.4	0.0281	Other/mixed ethnicity

Table 31. Effects of unweighted and weighted genetic risk scores (GRS) on QTc.age in the different ethnicities (*SCN5A*-E1784K carriers and WT relatives). p<0.05 are highlighted in red and p-values that remained statistically significant after Bonferroni correction are highlighted in green.

SNP	B	SE	p-value	Cohort
QTc.GRS	0.8	1.3	0.5498	All *SCN5A* -E1784K carriers
QTc.GRS	1.6	1.5	0.3039	Caucasian *SCN5A* -E1784K carriers
QTc.GRS	3.5	5.0	0.4797	Japanese *SCN5A* -E1784K carriers
QTc.GRS	-1.0	2.8	0.7183	Other *SCN5A* -E1784K carriers
QTc.wGRS	0.7	0.7	0.3027	All *SCN5A* -E1784K carriers
QTc.wGRS	1.4	0.8	0.0865	Caucasian *SCN5A* -E1784K carriers
QTc.wGRS	-0.2	2.9	0.9572	Japanese *SCN5A* -E1784K carriers
QTc.wGRS	-0.3	1.6	0.8282	Other *SCN5A* -E1784K carriers

Table 32. Effects of unweighted and weighted genetic risk scores (GRS) on QRS.age in *SCN5A*-E1784K carriers. None of the results were statistically significant.

Figures 22-25 are graphical representations of the correlation between GRSs and the corresponding ECG traits in the total cohort (*SCN5A*-E1784K carriers and WT relatives), and then in *SCN5A*-E1784K carriers and WT relatives separated by ethnicity (Caucasian – Figure 23; Japanese – Figure 24; Other/mixed ethnicity – Figure 25). Figures 26-29 are graphical representations of the correlation between GRSs and the corresponding ECG traits in *SCN5A*-E1784K carriers of all

ethnicities, and then in *SCN5A*-E1784K carriers separated by ethnicity (Caucasian – Figure 27; Japanese – Figure 28; Other/mixed ethnicity – Figure 29). The positive slope in the QRS figures illustrate, in particular, the positive association of the QRS GRS with QRS duration. This association is strongest (R^2 = 11%) in the overall cohort of *SCN5A*-E1784K carriers and WT relatives, and weaker (R^2 = 3.5- 4%) when only *SCN5A*-E1784K carriers were studied. The correlation lines were relatively flat for the PR and QTc GRSs, particularly in the overall population (with correlation coefficient values ≤ 0.1%). The associations were unstable for Japanese because there were only 15 Japanese participants in the total cohort and 12 Japanese *SCN5A*-E1784K carriers for whom there was no missing genotype data.

Amongst *SCN5A*-E1784K carriers, the correlation coefficients for the PR and QTc GRSs improved to 1.3% and 2.4% for the unweighted and weighted PR GRSs respectively, and to 0.8% and 1.2% for the unweighted and weighted QTc GRSs respectively.

Interestingly, when divided by ethnicity, the direction of association between the QTc GRS and QTc in *SCN5A*-E1784K carriers and WT relatives of other/mixed ethnicity was negative and opposite to the association in the other ethnicities. Amongst *SCN5A*-E1784K carriers, the direction of association between the QRS GRS and QRS in *SCN5A*-E1784K carriers of other/mixed ethnicity was negative and opposite to the association in the other ethnicities.

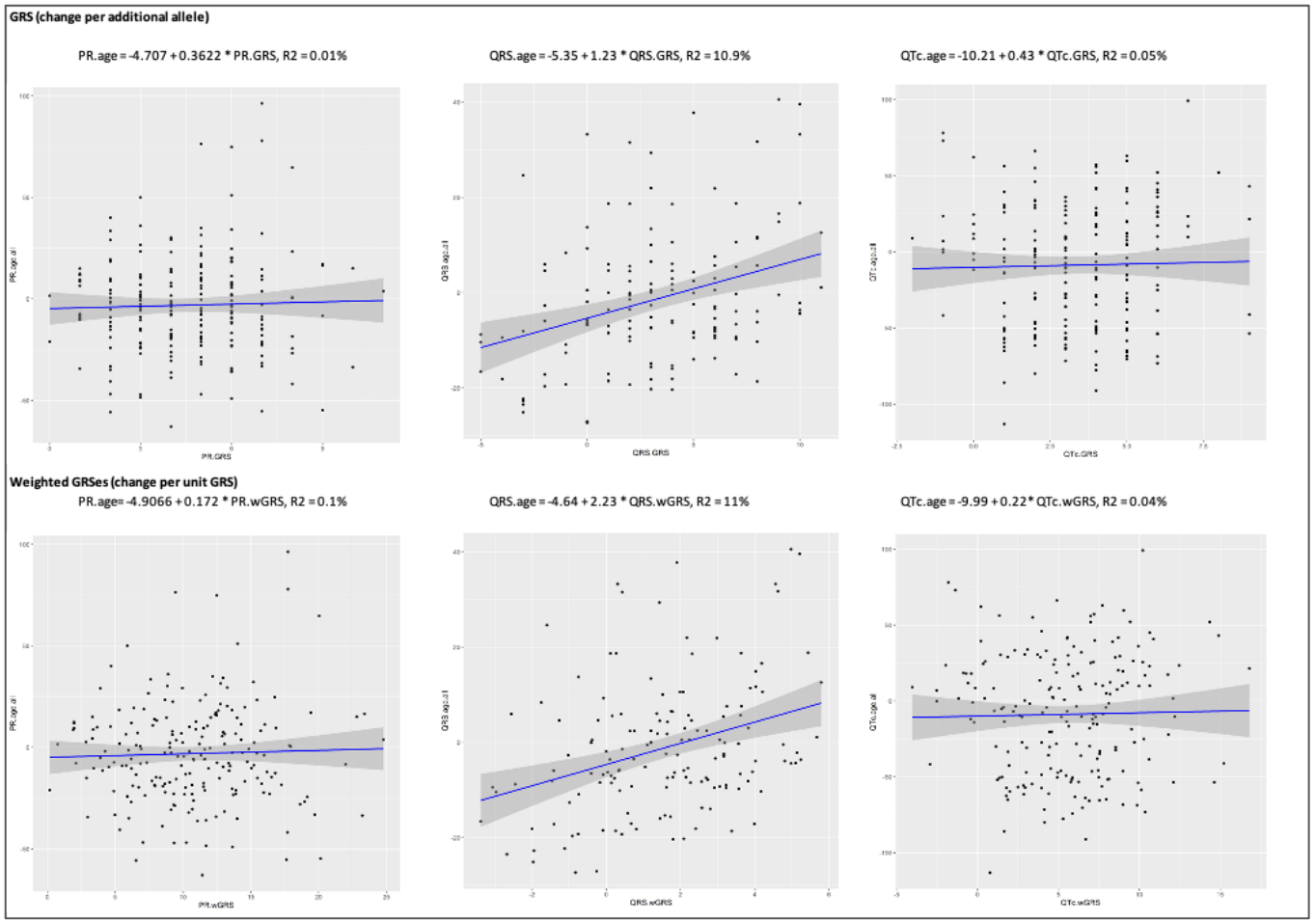


Figure 22. Relationship between unweighted and weighted GRSs and corresponding ECG traits in the total cohort (*SCN5A*-E1784K carriers and WT relatives).

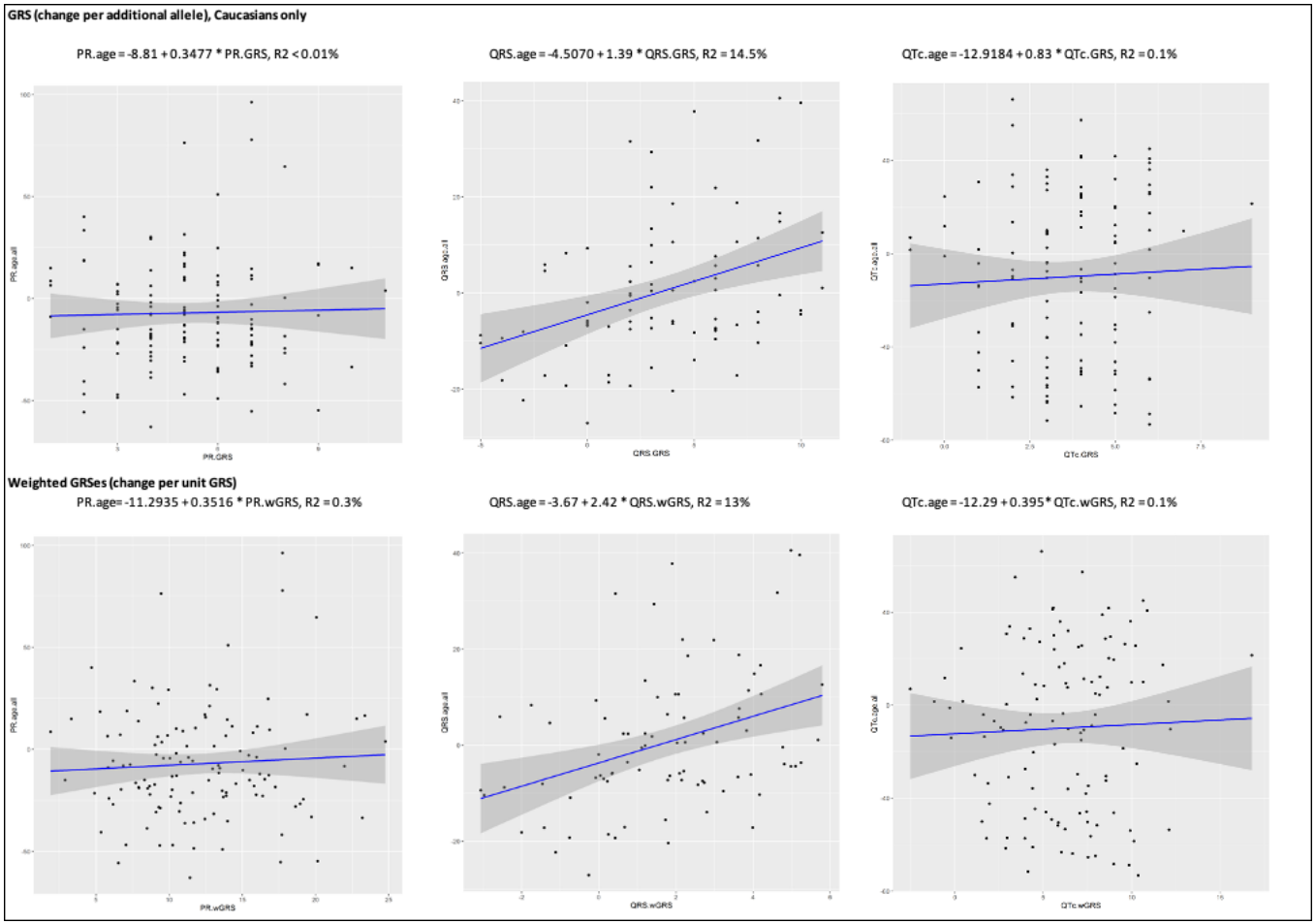


Figure 23. Relationship between unweighted and weighted GRSs and corresponding ECG traits amongst Caucasians in the total cohort (*SCN5A*-E1784K carriers and WT relatives).

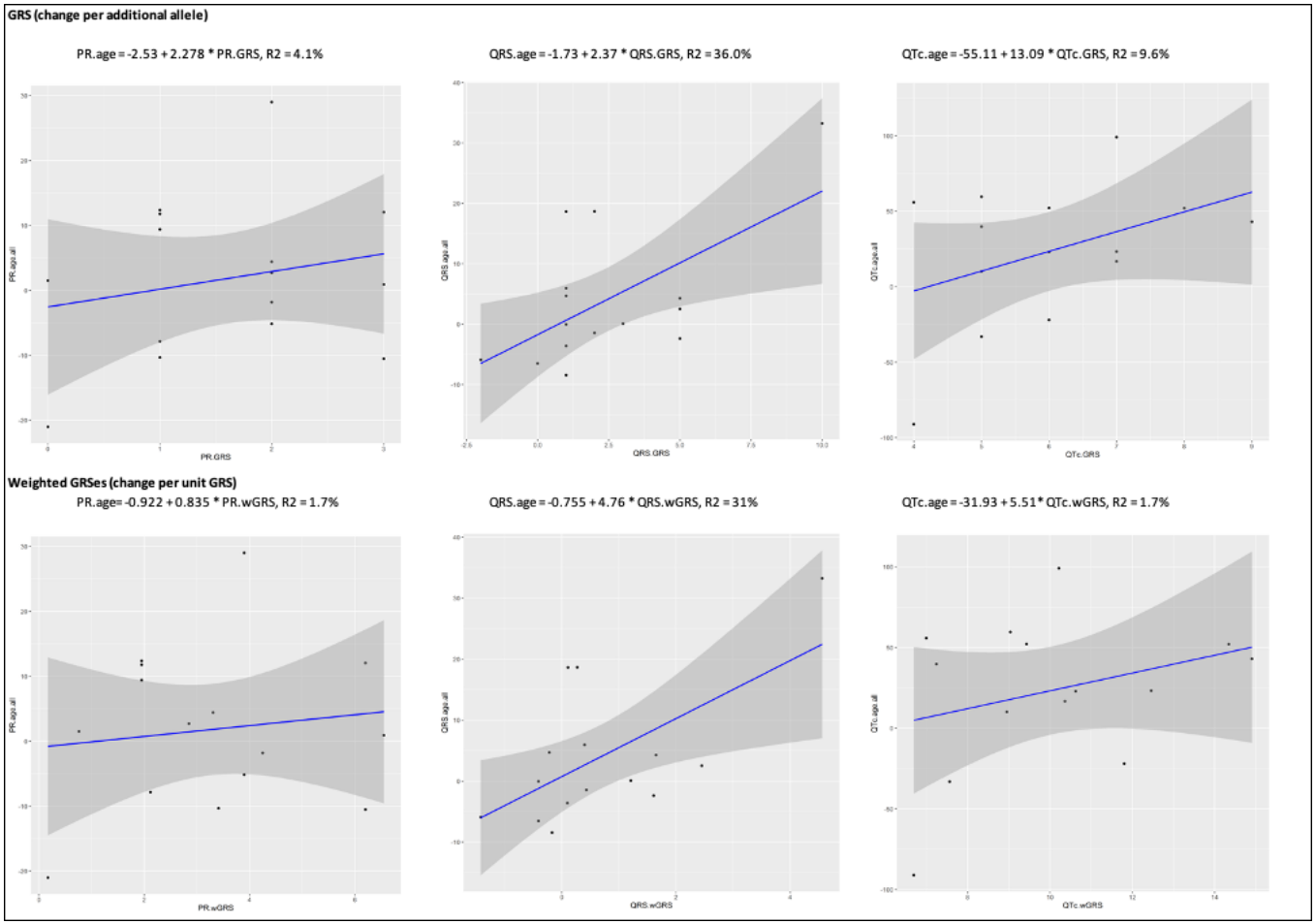


Figure 24. Relationship between unweighted and weighted GRSs and corresponding ECG traits amongst Japanese in the total cohort (*SCN5A*-E1784K carriers and WT relatives).

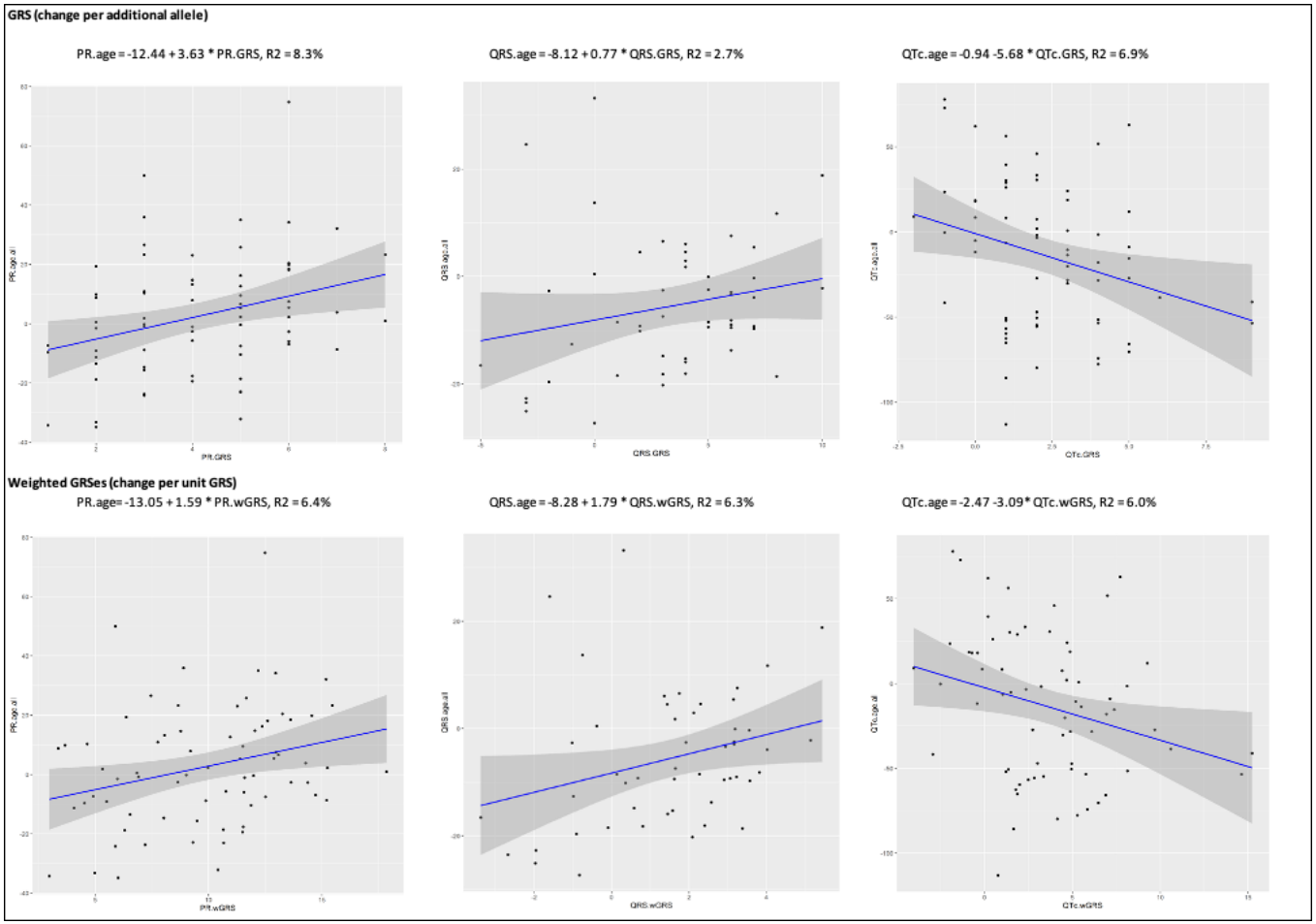


Figure 25. Relationship between unweighted and weighted GRSs and corresponding ECG traits amongst those of other ethnicity in the total cohort (*SCN5A*-E1784K carriers and WT relatives).

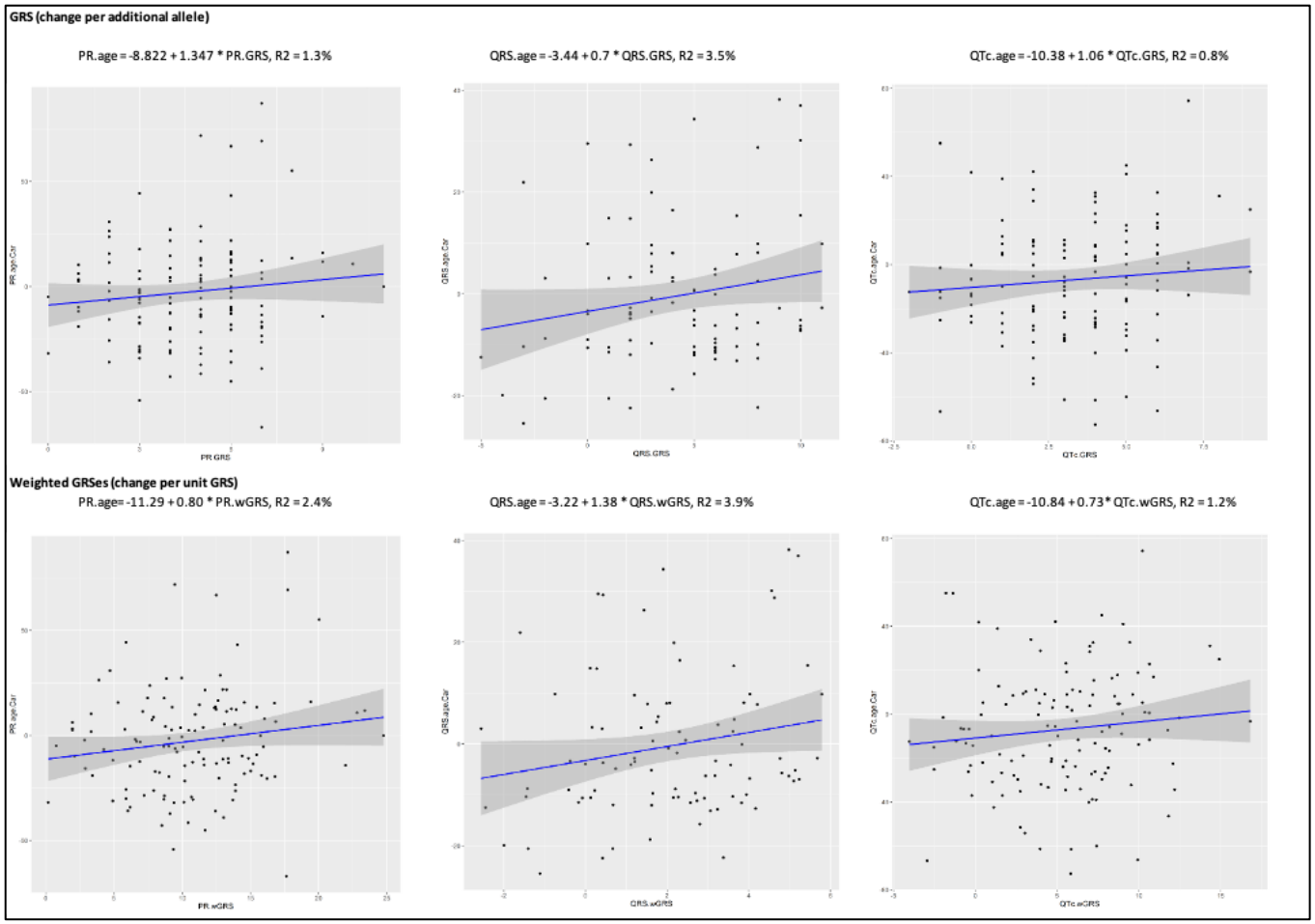


Figure 26. Relationship between unweighted and weighted GRSs and corresponding ECG traits in *SCN5A*-E1784K carriers.

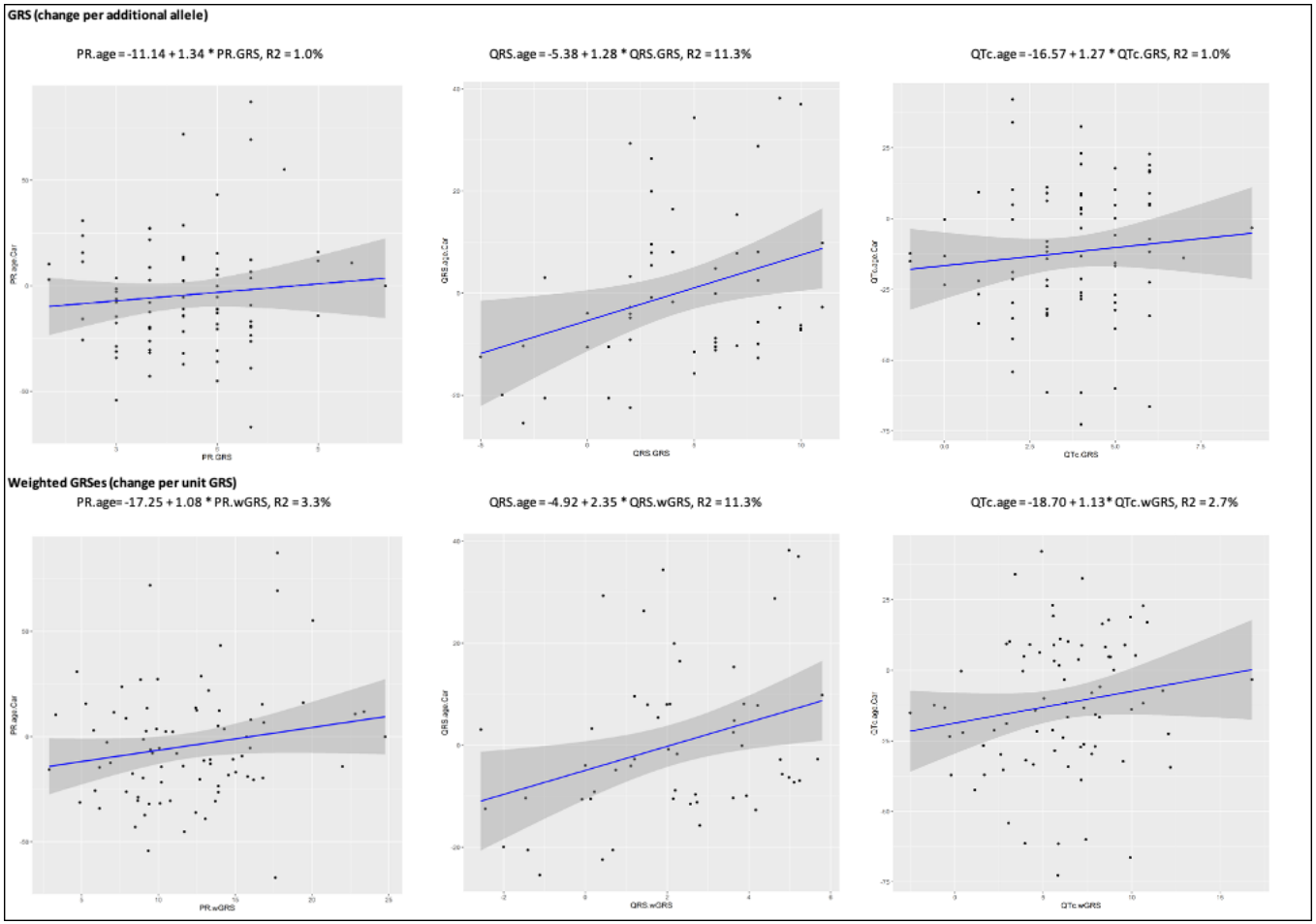


Figure 27. Relationship between unweighted and weighted GRSs and corresponding ECG traits amongst Caucasian *SCN5A*-E1784K carriers.

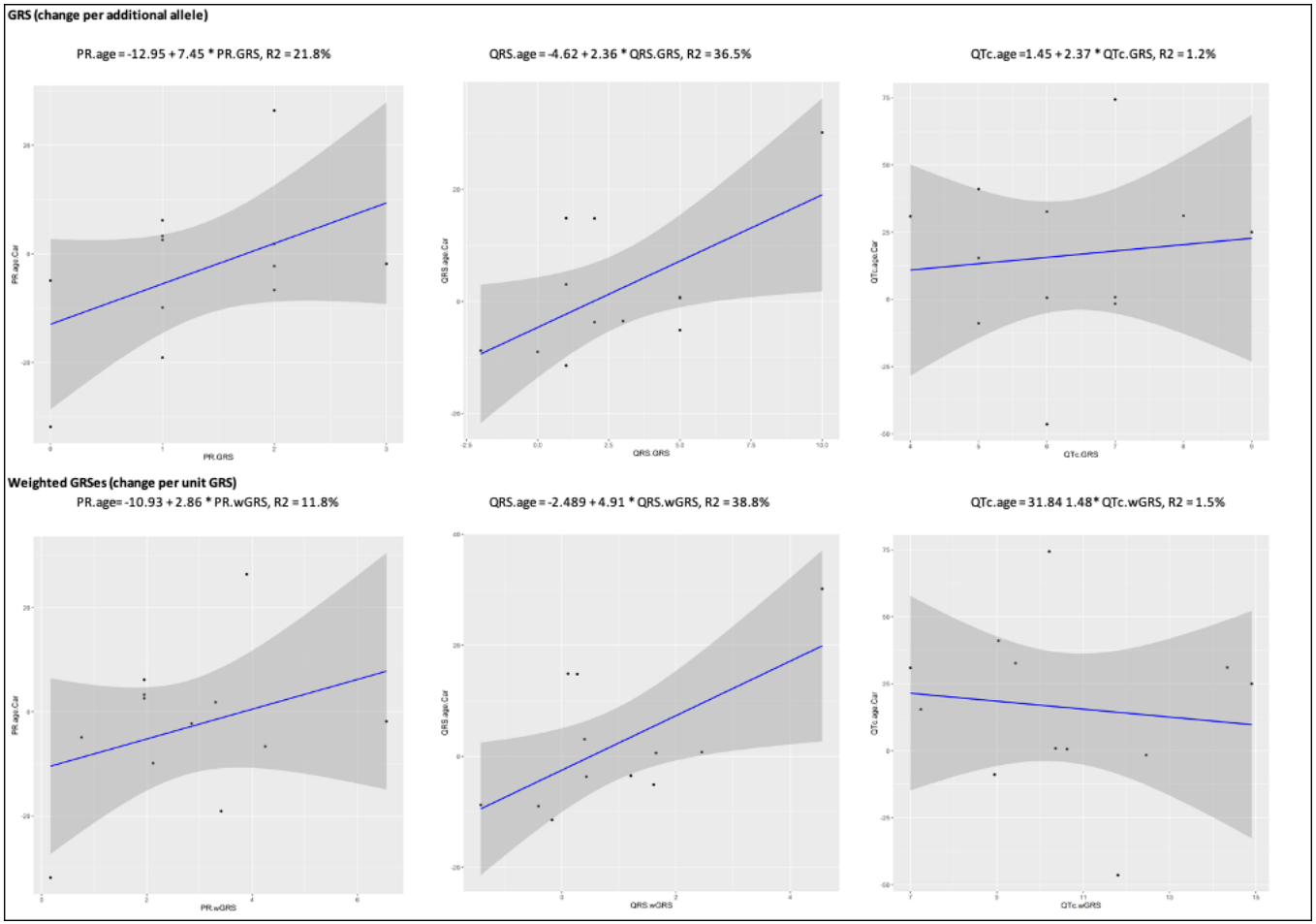


Figure 28. Relationship between unweighted and weighted GRSs and corresponding ECG traits amongst Japanese *SCN5A*-E1784K carriers.

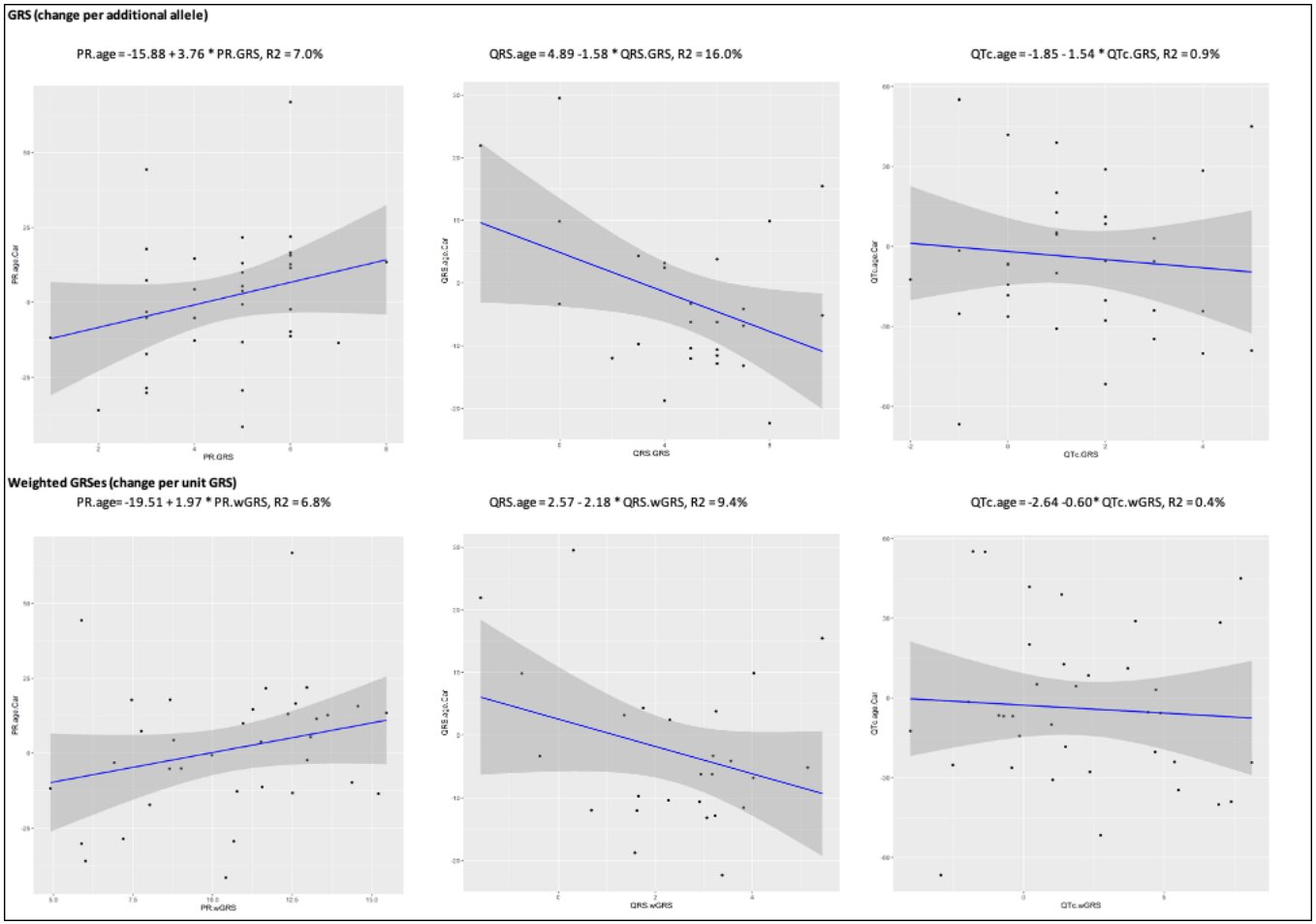


Figure 29. Relationship between unweighted and weighted GRSs and corresponding ECG traits amongst *SCN5A*-E1784K carriers of other ethnicity.

Discussion

In this chapter, GRSs for PR interval, QRS duration and QTc were calculated in *SCN5A*-E1784K carriers and their WT relatives combined, in *SCN5A*-E1784K carriers separately, as well as across different ethnic groups. As described in the power statement, the study was better powered for QRS variability seen in our cohort than PR and QTc, which might explain the more impressive QRS GRS results.

The GRS was studied in the complete cohort, separated by ethnicity and then meta-analysed. An alternative would have been a multiple regression model, however due to the number of SNPs, that would have resulted in a loss of power. The SNPs of interest were therefore summed and added as a single predictor, the GRS. The unweighted GRS involves summing up the number of risk increasing alleles an individual carries, while the weighted GRS (wGRS) takes into account the size of effect of each SNP within the cohort.

The linearity assumption between the outcomes (ECG trait) and predictor (GRS) was tested by comparing the fit of a linear and a non-linear (i.e. restricted cubic splines with three knots) model. In all cases, the linear model did not fit the data significantly worse than the linear model. Hence the linear assumption was not violated for any of the outcomes tested.

The PR GRS and wGRS showed inconsistent associations between ethnicities, both in the total cohort (*SCN5A*-E1784K carriers and WT relatives), and in *SCN5A*-E1784K carriers only, with no overall effect in the total cohort. This probably reflects heterogeneity of the SNPs making up the GRS, with different allele frequencies in

different ethnic groups, including some SNPs being monomorphic. This indicates little utility of the PR GRS from the currently available evidence in *SCN5A*-E1784K. The QTc GRS was only associated with phenotype when *SCN5A*-E1784K carriers and WT relatives of other/mixed ethnicity were studied. Further, the Beta value was consistently negative in this cohort, indicating that this is likely to be an idiosyncratic population-specific result. There were no other significant findings in the other ethnicities, and the association was lost when *SCN5A*-E1784K carriers only were studied. In summary, the QTc GRS does not show any clinically relevant associations with phenotype at all.

When analysing the QRS GRSs, there appears to be significant associations across ethnic groups with less heterogeneity in the unweighted and weighted GRSs. This is probably in part reflective of the larger number of SNPs used in the GRS for this ECG trait. The associated effect of increasing GRS was particularly strong when *SCN5A*-E1784K carriers and WT relatives are combined (accounting for approximately 11% of variability of the QRS.age), but also to a lesser extent in *SCN5A*-E1784K carriers alone (accounting for 3.5-3.9% of variability of the QRS.age). This indicates potential greater generalisability of the QRS GRS across ethnic groups in this study. An exception may apply for subjects of other/mixed ethnicity where the negative Beta value in the unweighted GRS in *SCN5A*-E1784K carriers of other/mixed ethnicity indicated a likely idiosyncratic population result. Nonetheless, both the unweighted and weighted GRS appear to have a degree of consistency in associating with the QRS duration and therefore may offer utility for future transethnic clinical application.

Thus the direction of associations between the QTc GRS and QTc in *SCN5A*-E1784K carriers and WT relatives of other/mixed ethnicity, and the QRS GRS and

QRS in *SCN5A*-E1784K carriers of other/mixed ethnicity, were both negative and opposite to the associations seen in Caucasian and Japanese ethnicities. This does not fit the assumption of a positive association between QRS and QTc and their respective GRSs and indicates an interaction between ethnicities. However, the significance of these results is likely to be limited by the numbers available.

The correlation coefficient (R^2) of the QRS GRSs of approximately 11% is an impressive finding, given the relatively small number of SNPs studied. However, the flat correlation lines and small correlation coefficients for the PR and QTc GRSs in the overall population further illustrate the lack of potential utility of these GRSs for predicting PR interval and QTc and suggest that >99% of the variation in PR and QTc in *SCN5A*-E1784K carriers and WT relatives remains unexplained by the respective GRSs.

When only *SCN5A*-E1784K carriers are studied, the correlation coefficients for the QRS GRSs reduce by over half, while the PR and QTc GRSs show a slightly greater (albeit still very weak compared to the QRS GRS) correlation with their respective ECG traits. This suggests an interaction between the GRSs and their constituent SNPs with *SCN5A*-E1784K. As described in Chapter 3, the PR interval, QRS duration and QTc were longer in *SCN5A*-E1784K carriers. The results of the GRSs suggest, however, that the rare variant (*SCN5A*-E1784K) has a much larger impact on PR interval and QTc than common genetic variants. Conversely the QRS duration is relatively less strongly affected by the presence of *SCN5A*-E1784K, but when it is present, it still reduces the amount of variation in QRS duration explained by the QRS GRSs.

Of note, the GRS standard deviations were similar between the total cohort and *SCN5A*-E1784K carriers, indicating that the distribution of the GRSs are independent *SCN5A*-E1784K status.

Limitations

This is a pilot GRS association study, and it is likely that the numbers of patients and numbers of included SNPs were too small to have sufficient statistical power to detect associations with PR and QTc ECG traits. As a targeted single SNP study, this analysis would have been far less powerful than a GWAS for detecting GRS associations. The QRS GRS findings showed less inconsistencies but need to be validated in an expanded cohort and in other *SCN5A* mutations.

When separated by ethnicity, the associations were unstable for the Japanese due to the limited number of individuals of Japanese ethnicity for whom complete genotyping data were available.

The power calculations on page 142 indicate that the effect sizes have to be large to be detected in the current experiment. Furthermore, according to GWAS sample-size calculations (see pages 239-241) the numbers would also have to be larger. Indeed if analysed in ethnic groups separately, this would result in the same numbers needed per ethnicity. This may not be feasible given that the size of the cohort is limited by the worldwide prevalence of the SCN5A-E1784K mutation, despite it being the most prevalent *SCN5A* mutation causing LQT3 and BrS. Much effort will be required, however, to include all available, well phenotyped *SCN5A*-E1784K individuals and their mutation negative family members worldwide. The power would otherwise be absent to detect variants with (very) low minor allele frequencies, unless these have a very large effect size per allele.

Chapter 6: *SCN5A* Mutation Type and a Genetic Risk Score Associate Variably with Brugada Syndrome Phenotype in *SCN5A* Families

This chapter has been reproduced and adapted for the thesis from my recent first author publication, Wijeyeratne Y. D. *et al*. *SCN5A* Mutation Type and a Genetic Risk Score Associate Variably With Brugada Syndrome Phenotype in *SCN5A* Families. Circ Genom Precis Med 13, e002911 (2020).[194]

Introduction

BrS, as previously described in this thesis, is characterised by the type 1 Brugada ECG pattern, present either spontaneously or after provocation with a sodium channel blocking agent.[59] Pathogenic rare variants (mutations) in the *SCN5A* gene, encoding the Nav1.5 sodium channel, are identified in 20% of cases.[75,216] Incomplete penetrance and variable expression is common in BrS pedigrees with *SCN5A* mutations, suggesting a complex inheritance wherein other genetic variants may affect the phenotype.[75] Genotype-negative individuals from *SCN5A*-positive pedigrees have shown the type 1 Brugada ECG pattern.[75] Furthermore, common genetic variation has been associated with BrS in probands, independent of *SCN5A* status.[77]

I hypothesised that common genetic variation previously associated with BrS[77], and a genetic risk score derived thereof (BrS-GRS), is associated with a type 1 Brugada ECG pattern in genotype-positive individuals from BrS families hosting *SCN5A*-E1784K as well as in genotype-negative relatives. I then applied these findings in other families with other *SCN5A* variants in order to further validate if common genetic variation predicts BrS phenotype. Further, I explored the effects of *SCN5A* mutation type on the likelihood of a type 1 Brugada ECG pattern.

This chapter describes a broader population, including families with other *SCN5A* mutations, compared to Chapters 3-5.

Methods

Recruitment and case selection

Seventeen Inherited Cardiac Conditions (ICC) specialist centres from France, Germany, Ireland, Italy, Japan, Netherlands, United Kingdom and USA participated. Probands positive for pathogenic or likely pathogenic *SCN5A* variants were recruited. First- and second-degree relatives, whether hosting the familial *SCN5A* variant or not, were then recruited. We only included subjects (n=312) in whom the presence or absence of the type 1 Brugada ECG pattern had been ascertained as: spontaneous; provoked following drug challenge; or confirmed negative following drug challenge according to the 2013 HRS/EHRA/APHRS guidelines.[59] Three individuals in this cohort had been included in a large BrS GWAS by Bezzina *et al* from which the SNPs studied here were identified (see below), hence these three individuals were excluded from the analyses in this chapter.[77]

Clinical evaluation

Presenting 12 lead ECGs and details of drug provocation were collected. BrS phenotype was defined as the presence of either a spontaneous or drug-induced type 1 Brugada ECG pattern in at least one right precordial lead as determined by at least 2 observers (in the standard or higher intercostal spaces).[59] Intravenous drug provocation tests (either ajmaline 1mg/kg, flecainide 2mg/kg or pilsicainide 1mg/kg) were performed at a pre-determined rate as per local protocol.

Classification of variant pathogenicity and subsets

All variants were curated using CardioClassifier (including paralogue annotation).[217] Variants were annotated further by including published functional data to determine variant class using ACMG criteria.[218] Only pathogenic and likely pathogenic variants were included as mutations for this study (Table 33). Frameshift or splice site variants were defined as 'loss-of-function' causing haploinsufficiency. Missense variants were divided into *SCN5A*-E1784K and 'other missense' mutations.

Variant (cDNA)	Variant (protein)	gnomAD allele frequency	No BrS	BrS	Total
c.1036G>T	p.E346*	0	0	1	1
c.1100G>A	p.R367H	0	0	3	3
c.1100G>T	p.R367L	0	0	1	1
c.1106T>A	p.M369K	0	1	2	3
c.1127G>A	p.R376H	3.20E-05	0	2	2
c.1540G>T	p.G514C	0	0	2	2
c.1603C>T	p.R535*	4.10E-06	11	6	17
c.1657G>T	p.E553*	0	0	1	1
c.1672delC	p.H558Tfs*65	0	0	1	1
c.1890G>A	Splice	5.80E-06	1	2	3
c.1936delC	p.Q646Rfs*5	0	0	1	1
c.1983_1993dup	p.A665Gfs*16	0	5	1	6
c.217C>T	p.Q73*	0	0	1	1
c.2254G>A	p.G752R	4.10E-06	4	6	10
c.2320delT	p.Y774Tfs*28	0	0	2	2
c.2335C>T	p.Q779*	0	0	1	1
c.2373_2374insA	p.S792Kfs*160	0	0	1	1
c.2423G>C	p.R808P	0	0	2	2
c.2516T>C	p.L839P	0	3	5	8
c.2559delT	p.F853Lfs*16	0	0	1	1
c.2582_2583delTT	p.F861Wfs*90	0	0	12	12
c.2632C>T	p.R878C	0	0	2	2
c.2674T>A	p.F892I	0	0	2	2
c.2678G>A	p.R893H	4.10E-06	0	2	2
c.2729C>T	p.S910L	4.10E-06	0	1	1
c.2863G>T	p.E955*	0	0	1	1
c.2894G>A	p.R965H	8.20E-06	0	1	1
c.2943C>A	p.C981*	0	0	2	2
c.3005_3012delCCAGCTGC	p.P1002Hfs*25	0	0	1	1
c.3142_3143insTG	p.P1048Lfs*98	0	0	2	2
c.3175C>T	p.Q1059*	0	1	2	3
c.3352C>T	p.Q1118*	0	0	3	3
c.3491dup	p.E1165Rfs*6	0	0	1	1
c.361C>T	p.R121W	0	0	1	1
c.3622G>T	p.E1208*	0	0	1	1
c.3667delG	p.A1223Pfs*7	0	1	3	4
c.3673G>A	p.E1225K	4.10E-06	0	2	2
c.3676G>T	p.D1226Y	0	0	1	1
c.3694C>T	p.R1232W	0	2	7	9
c.3823G>A	p.D1275N	8.10E-06	0	1	1

Table 33. Continued next page.

Variant (cDNA)	Variant (protein)	gnomAD allele frequency	No BrS	BrS	Total
c.3956G>T	p.G1319V	4.20E-05	0	5	5
c.3988G>A	p.A1330T	0	0	1	1
c.3G>C	p.M1I	0	0	1	1
c.4030T>C	p.F1344L	0	0	1	1
c.4079T>G	p.F1360C	0	0	1	1
c.4140C>G	p.N1380K	0	0	1	1
c.4213G>A	p.V1405M	0	0	3	3
c.4213G>C	p.V1405L	0	2	3	5
c.4216G>C	p.G1406R	0	2	2	4
c.4222G>A	p.G1408R	0	3	7	10
c.4226A>G	p.Y1409C	0	0	1	1
c.4346A>G	p.Y1449C	0	0	1	1
c.4385T>A	p.L1462Q	0	0	1	1
c.4387A>T	p.N1463Y	0	1	0	1
c.4642G>A	p.E1548K	3.20E-05	0	2	2
c.4719C>T	p.G1573G	3.20E-05	1	1	2
c.4747C>T	p.R1583C	8.10E-06	0	1	1
c.481G>A	p.E161K	8.40E-06	1	9	10
c.4886G>A	p.R1629Q	1.20E-05	0	1	1
c.4894C>T	p.R1632C	4.10E-06	0	2	2
c.4912C>T	p.R1638*	1.20E-05	0	2	2
c.4930C>T	p.R1644C	4.10E-06	0	2	2
c.4952_4953insT	p.M1651Ifs*138	0	0	1	1
c.4958C>T	p.S1653F	0	0	1	1
c.4978A>G	p.I1660V	3.20E-05	1	1	2
c.4981G>A	p.G1661R	0	0	1	1
c.5083C>T	p.Q1695*	0	0	1	1
c.5102T>C	p.M1701T	0	0	1	1
c.511G>A	p.E171K	0	0	1	1
c.5126C>T	p.T1709M	4.10E-06	0	1	1
c.5155C>A	p.P1719T	0	0	2	2
c.5182T>C	p.C1728R	0	1	1	2
c.5228G>A	p.G1743E	0	2	8	10
c.5265C>A	p.Y1755*	0	0	1	1
c.5324delT	p.F1775Sfs*12	0	0	2	2
c.5356_5357delCT	p.L1786Efs*2	0	0	1	1
c.535C>T	p.R179*	4.10E-06	0	1	1
c.5417_5420del CTCA	p.T1806Sfs*27	0	0	1	1
c.5433T>G	p.Y1811*	0	0	1	1
c.617delC	p.T206Kfs*22	0	0	1	1
c.812_813insAGCT	p.F272Afs*40	0	0	1	1

Table 33 continued. List of *SCN5A* mutations in the secondary cohort with GnomAD allele frequencies (AF) and breakdown by BrS phenotype.

SNP selection

Three single nucleotide polymorphisms (SNPs) have been associated previously with BrS phenotype in Caucasian, Japanese, Taiwanese and Thai cohorts at a genome-wide level of significance: rs11708996 (*SCN5A*), rs10428132 (*SCN10A*), and rs9388451 (*HEY2*) (see Table 34 for general population frequencies).[77,94,219,220] The genes tagged by rs10428132 and rs9388451 have undergone functional evaluation previously.[25,77,221,222] rs11708996 and rs9388451 were genotyped in all individuals. In families harbouring *SCN5A* mutations other than *SCN5A*-E1784K, rs6800541 formed part of a multi-SNP assay previously carried out in this cohort and was found to be in complete linkage disequilibrium (LD) with rs10428132 (r^2 = 1). It was therefore used as a proxy SNP.

SNP	Chr	Position	Gene/ nearest gene	Alleles	Risk allele	Reported odds ratio	Frequency of the risk allele in the general population (1000 Genomes)[1]
rs11708996[2]	3	intron	*SCN5A*	G/C	C	1.73	0.0901
rs10428132[2]	3	intron	*SCN10A*	G/T	T	2.66	0.2815
rs9388451[2,3]	6	intergenic	*HEY2-NCOA7*	C/T	C	1.58	0.4133
rs6800541	3	intron	*SCN10A*	C/T	C	NA	0.242

Table 34. List of SNPs evaluated.[25,77,219] The proxy SNP rs6800541 (highlighted) was in complete linkage disequilibrium (r^2=1.000) with rs10428132. NA= not applicable. Chr = chromosome

SNP genotyping

SNP genotyping in *SCN5A*-E1784K families was carried out using the PCR-based Kompetitive Allele Specific PCR (KASP™) genotyping assay provided by LGC, UK.[208] The KASP assay uses simple non-modified oligonucleotide probes that act as the reaction primers to amplify directly from genomic DNA. KASP assays have a small oligonucleotide tail sequence at the 5' end of the allele specific primers. In the

master mix there are complimentary fluorophore cassettes with either FAM or HEX attached that are complimentary to this tail sequence. As the reaction progresses the 3' end of the primer will bind to the allele. A PCR uses the 3' end specificity to amplify and bind only the corresponding allele within the sample and delivers high assay specificity, robustness and accuracy. Each SNP of interest and 100 base pairs of the surrounding sequence were annotated with known variants using 1000 genomes browser. Interspaced repeats and low complexity DNA were screened using RepeatMasker. The KASP™ assays were designed using the Kraken™ software system and validated through LGC's assay validation pipeline.[208] Quality control post-genotyping included exclusion of samples where complete data were not available for all SNPs.

Genotyping of the three SNPs in the rest of the cases was performed as part of a multi-SNP assay on the MassARRAY system using matrix-assisted laser desorption ionization time-of-flight mass spectrometry with iPLEX™ Gold chemistry (Sequenom Inc, San Diego, CA, USA). Primers were designed using Assay Designer 4.0.0.2 with iPLEX Gold default parameters. Automated genotype calling was done with MassArrayTyper (version 4.0.22.67). An experienced evaluator checked genotype clustering visually. We excluded samples where the overall SNP call rate was <95% or where the genotype for any of the three SNPs was missing.

Statistical analyses

Categorical variables are described as count and percentage and numerical variables as mean ± standard deviation (SD) or median and interquartile range (Q1-Q3: IQR). Categorical variables were compared using Chi-squared and Fisher exact tests where appropriate and numerical variables were compared using ANOVA. For SNP effects, an additive genetic model was assumed. The BrS-GRS was calculated

by summing the number of risk alleles for the three included SNPs that each person carried (range 0-6 alleles). The weighted BrS-GRS was calculated by multiplying the individual risk allele counts with their respective associated effects size (β). The risk alleles and associated effect sizes were assigned based on literature.[77] The weighted BrS-GRS was also tested, but this did not outperform the non-weighted BrS-GRS. We did not separate the analysis by ethnicity as the SNPs included had been validated in multiple ethnic groups.

The assumption of a linear relationship between the BrS-GRS and the natural logarithm of the odds ratio was tested by comparing the fit of the linear model with that of a more flexible model with restricted cubic splines. No significant deviation from linearity was found. Next to a model with the BrS-GRS as a numerical predictor, we also tested the association with a dichotomised predictor (BrS-GRS $\geq$ 4 yes/no) based on the distribution of risk alleles seen in the overall cohort. All comparisons between BrS phenotype-negative and -positive individuals were carried out using generalised linear models and corrected for sex and age. Generalised estimation equations (GEE), with an independence correlation structure and robust sandwich variance estimations were used to correct for relatedness (geepack, version 1.2-1).[223] The BrS-GRS thus developed was then examined in the total population and subsets of family members harbouring *SCN5A* mutations: loss-of-function causing haploinsufficiency; *SCN5A*-E1784K; and other missense mutations. *SCN5A* negative relatives were then studied separately. Interaction terms were added to the models to check for differences in mutation/GRS effects in genotype negative vs. positive and among genotype positive subgroups. Based on GWAS data, the size of effect of these SNPs in the GWAS population was known, so that unweighted and weighted BrS-GRS could be created. For the unweighted GRS, alleles that increased risk and alleles that

decreased risk were taken into account, such that these were summed appropriately.

All analyses were carried out using R (version 4.0.2)[196] software and the rms, kinship2 and meta packages.[196–200,209] For statistical significance, we considered both Bonferroni-corrected and nominal ($p<0.05$) p-value thresholds.

Results

Clinical characteristics

The total cohort comprised of 312 individuals from families harbouring *SCN5A* mutations. The individuals that fulfilled inclusion criteria had the presence or absence of the BrS phenotype definitively established, and had undergone complete SNP genotyping (Figure 30). These 312 individuals were recruited from 137 families. The median family size was 1 (Q1-Q3: 1-2); four families had between 10 and 20 individuals and a single family contributed 31 individuals. Figure 16 illustrates the breakdown of included cases according to *SCN5A* genotype and mutation type.

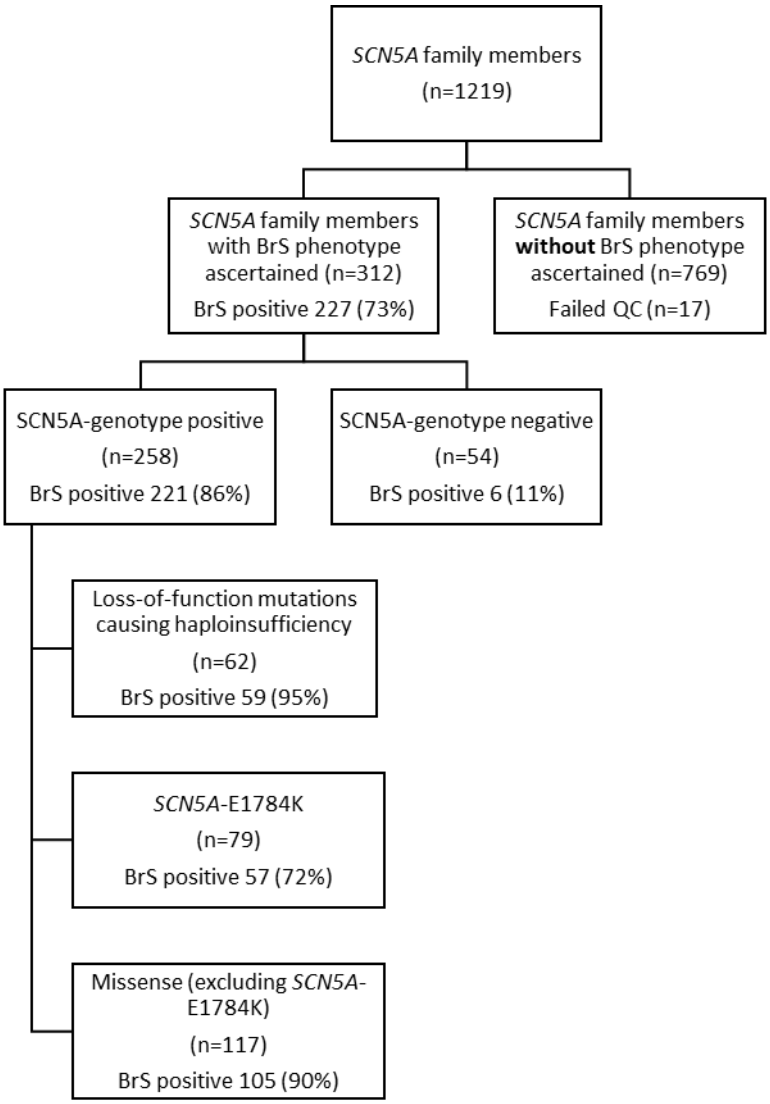


Figure 30. Flow diagram summarizing inclusion and numbers of individuals separated by genotype and BrS phenotype in each cohort.

Clinical characteristics are described and compared in Table 35. Subjects hosting *SCN5A*-E1784K, when compared to individuals harbouring loss-of-function mutations causing haploinsufficiency and other missense *SCN5A* mutations, were younger and more likely to be female. As would be expected when comparing individuals with an overlap syndromes, they exhibited longer QTc but shorter PR intervals and QRS durations on their presenting ECGs compared to those with conduction disease.

	Total population, n=312		*SCN5A* genotype positive, n=258		*SCN5A* genotype negative, n=54		p-value
	n	%	n	%	N	%	
Male	169	54	143	55	26	48	0.3603
Caucasian	270	87	237	92	33	61	**0.0015**
BrS	227	73	221	86	6	11	**<0.0001**
Spontaneous BrS ECG pattern *	88/201	44	88/196	45	0/5	0	**<0.0001**
Mutation type:							
E1784K	103	33	79	31	24	44	0.2700**
LOF	79	25	62	24	17	31	
Missense	130	42	117	45	13	24	
Quantitative variables							
	mean	**SD**	**mean**	**SD**	**mean**	**SD**	
Age at ECG	38	17	39	17	35	16	0.39
PR interval	186	38	192	38	159	42	**<0.0001**
QRS duration	101	21	104	20	84	20	**<0.0001**
QTc	425	43	429	45	410	31	**0.0064**

a)

	Mutation type						
	Loss-of-function causing haploinsufficiency n=62		Missense (excluding *SCN5A*-E1784K) n=117		*SCN5A*-E1784K n=79		p-value
	n	%	n	%	n	%	
Male	44	71	68	58	31	39	**0.0001**
Caucasian	62	100	117	100	58	73	**<0.0001**
BrS	59	95	105	90	57	72	**0.0007**
Spontaneous BrS ECG pattern *	31/50	62	47/89	53	Oct-57	18	**0.0011**
Quantitative variables							
	mean	**SD**	**mean**	**SD**	**mean**	**SD**	
Age at ECG	36	16	44	15	33	17	**0.0002**
PR interval	206	42	202	35	167	27	**<0.0001**
QRS duration	112	20	104	21	98	14	**0.0003**
QTc	402	31	408	33	479	22	**<0.0001**

b)

Table 35. Clinical characteristics of: a) the total cohort broken down by genotype status; b) comparing families harbouring loss-of-function causing haploinsufficiency, other missense mutations and *SCN5A*-E1784K. BrS = Brugada syndrome; QTc = QT interval corrected by Bazett's formula. *In 26 cases (25 genotype positive) specific data on the spontaneity of the type 1 pattern were missing. **Overall p-value (chi-square test) testing the distribution of the three mutation types among *SCN5A* genotype positive vs. *SCN5A* genotype negative individuals.

Seventy-nine individuals were *SCN5A*-E1784K positive. Fifty-seven (72%) with *SCN5A*-E1784K had BrS phenotype (10 spontaneous; 47 drug-induced). Amongst the 179 individuals harbouring loss-of-function mutations causing haploinsufficiency and other missense *SCN5A* mutations, 164 (92%) had BrS phenotype (78 spontaneous; 61 drug-induced; 25 unspecified). Importantly, 6/54 (17%) *SCN5A* negative subjects displayed a drug-induced BrS phenotype. The associations of *SCN5A* mutation and/or BrS-GRS with the spontaneous BrS phenotype are similar to those described in both spontaneous and drug induced BrS combined, but were less accurate with higher p-values (data not shown).

SCN5A mutation associations

SCN5A mutation associations are shown in Figure 31. Amongst *SCN5A* families the presence of an *SCN5A* mutation was associated with an odds ratio (OR) of 51.98 (95%CI:20.02-134.93, p<0.0001) for BrS phenotype. In all three *SCN5A* mutation type subgroups, i.e. *SCN5A*-E1784K*,* loss-of-function mutations causing haploinsufficiency and missense mutations other than *SCN5A*-E1784K, genotype positive patients were at an increased risk of BrS compared to genotype negative patients, but the odds ratios differed significantly ($p_{interaction}$=0.004) between the mutation types.

Amongst *SCN5A* genotype positive individuals only, both loss-of-function mutations causing haploinsufficiency and other missense mutations had an increased risk of BrS compared to *SCN5A*-E1784K with OR = 6.11 (95%CI:1.78-20.97, p=0.0040) and OR = 3.44 (95%CI:1.35- 8.75, p=0.0095), respectively.

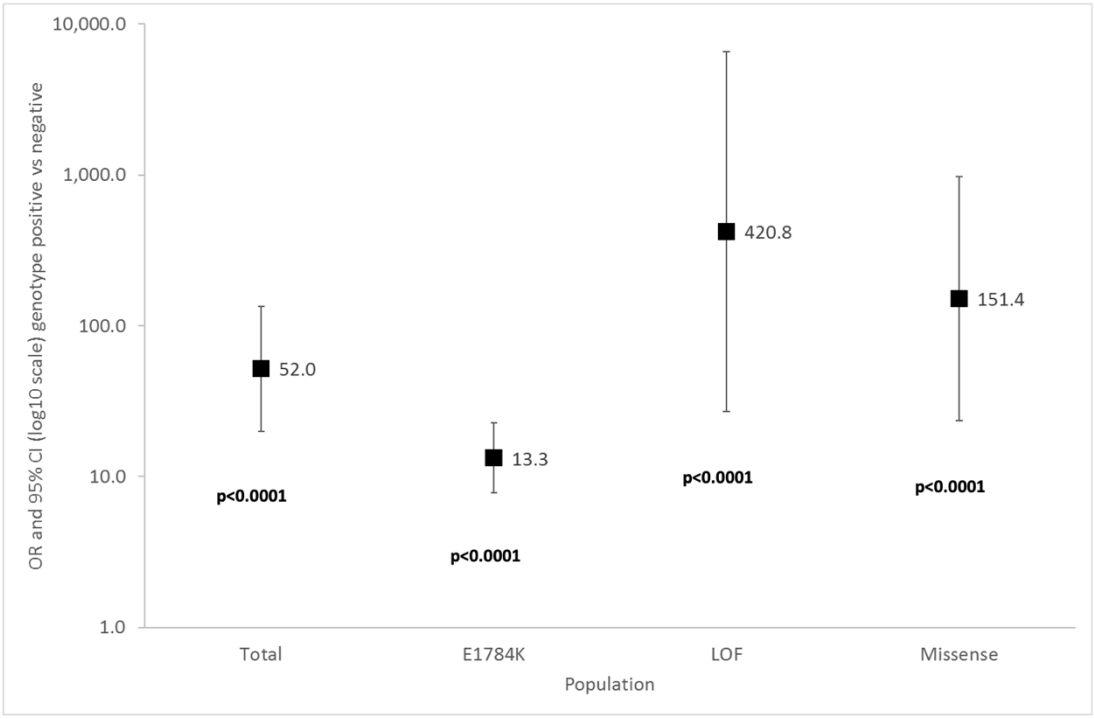


Figure 31. Risk of Brugada Syndrome in patients carrying an *SCN5A* mutation, Loss-of-function mutations causing haploinsufficiency, missense mutations other than *SCN5A*, and *SCN5A*-E1784K. The odds ratio (OR) and 95% confidence interval for each mutation type are shown (adjusted for sex and age). The p-values denote the levels of significance of the odds ratios for Brugada Syndrome comparing each cohort to negative genotype using GEE.

Brugada Syndrome Genetic Risk Score

The BrS-GRS was calculated for each subject in the total cohort as described. A weighted BrS-GRS was also tested, but this did not outperform the non-weighted BrS-GRS (data not shown). Figure 32 shows the distribution of proportion of subjects according to numbers of risk alleles (range 0-6) for the total cohort and subsets of *SCN5A* mutations. In the total population, the odds ratio per allele was 1.46 (95%CI 1.11-1.94, p=0.0076) and individuals with a BrS-GRS ≥4 risk alleles had an OR=4.15 (95%CI 1.45-11.85, p=0.0078) for BrS phenotype compared to individuals with a GRS <4 risk alleles.

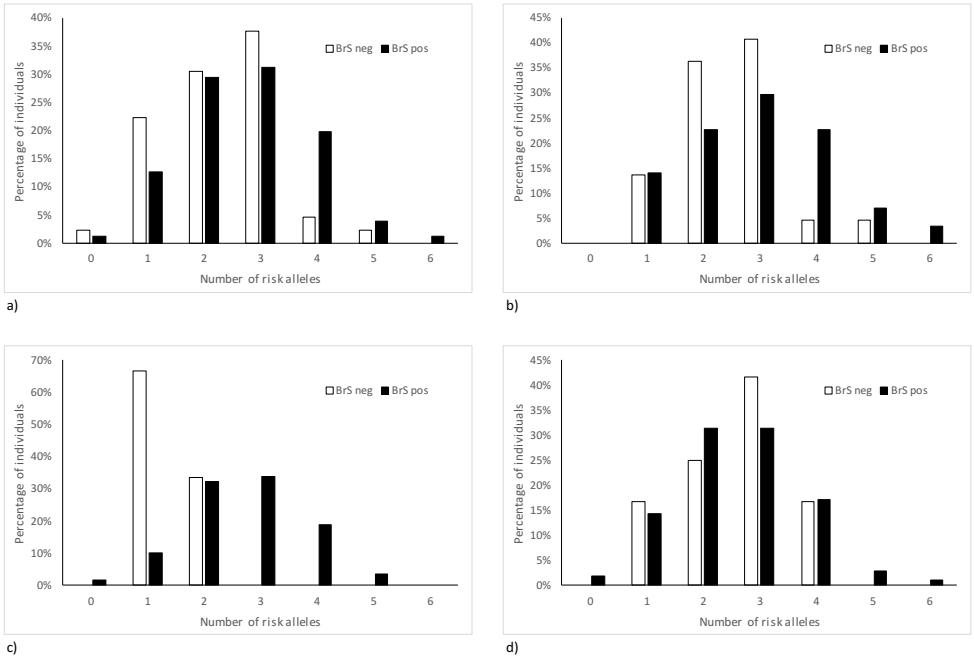


Figure 32. Cumulative number of risk alleles at the three loci and the associated likelihood of BrS phenotype showing performance of the BrS-GRS for prediction of BrS phenotype in mutation positive individuals in the (a) total cohort; (b) individuals from families harbouring *SCN5A*-E1784K); (c) individuals from families harbouring loss-of-function *SCN5A* mutations causing haploinsufficiency; (d) other missense *SCN5A* mutations. Distribution of numbers of risk alleles hosted by individuals with BrS phenotype (black bars) in each cohort are shown vs family members ascertained to be BrS phenotype-

negative (white bars). Each bar represents the proportion of individuals carrying the corresponding number of risk alleles as a percentage of the total number of individuals with the corresponding phenotype, i.e. denominator for the white bars being the total number of individuals with no BrS within the cohort, and the denominator for the black bars being the total number of individuals with BrS within the cohort.

Figure 33 shows the risk per additional risk allele in a linear model in the total cohort; genotype negative individuals; genotype positive individuals from families harbouring loss-of-function mutations causing haploinsufficiency; genotype positive individuals from families harbouring *SCN5A*-E1784K; genotype positive individuals from families harbouring other missense *SCN5A* mutations. The BrS-GRS effects per allele and ≥4 risk alleles appeared smaller in *SCN5A* genotype positives, but this was not significant ($p_{interaction}$ = 0.090 and 0.076, respectively). Within *SCN5A* genotype positives only, the BrS-GRS effects per allele and ≥4 risk alleles were significantly different between mutation types ($p_{interaction}$ = 0.0096 and <0.0001, respectively).

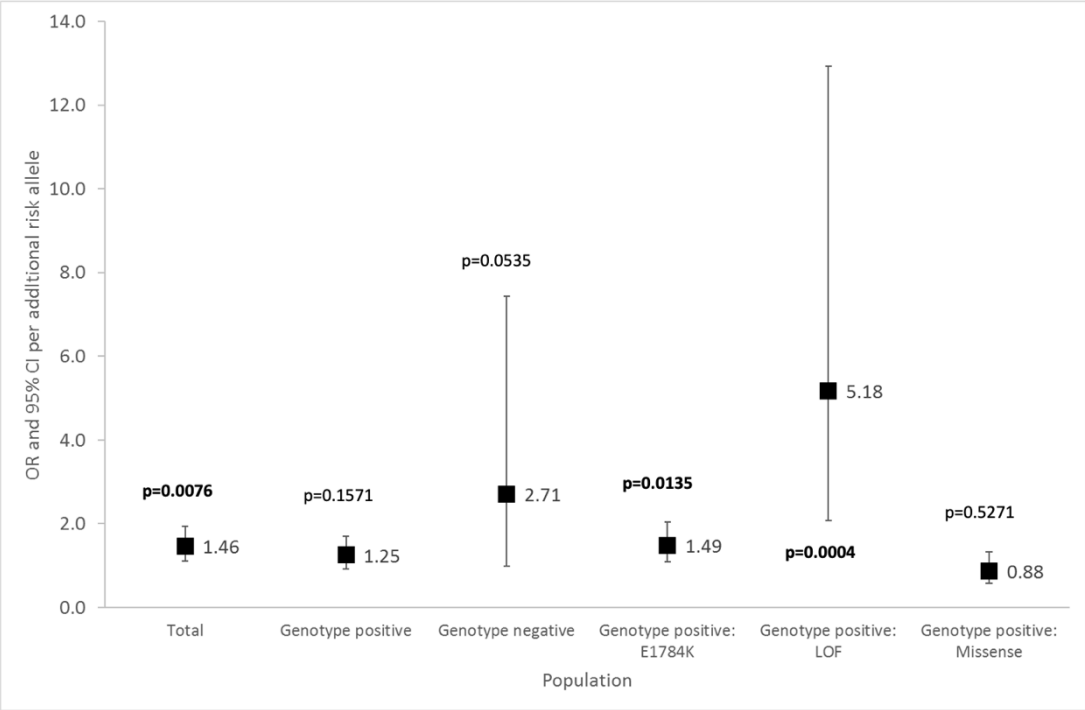


Figure 33. Risk per additional risk allele in a linear model in the total cohort; genotype negative individuals; genotype positive individuals from families harbouring loss-of-function mutations causing haploinsufficiency; genotype positive individuals from families harbouring *SCN5A*-E1784K; genotype positive individuals from families harbouring other missense *SCN5A* mutations. The odds ratio (OR) per additional risk allele and 95% confidence interval are shown (adjusted for sex and age). The p-values denote the levels of significance of the odds ratios per additional risk allele for BrS in each cohort using GEE. The OR and 95%CI for Genotype positive: Loss-of-function causing haploinsufficiency cohort are not shown as these are off the scale of this figure.

Figure 34 shows the risk of BrS in patients carrying ≥4 risk alleles in the total cohort; genotype negative individuals; genotype positive individuals from families harbouring loss-of-function mutations causing haploinsufficiency; genotype positive individuals from families harbouring *SCN5A*-E1784K; genotype positive individuals from families harbouring other missense *SCN5A* mutations. *SCN5A* genotype-positive relatives (n=258) yielded an OR=1.25 (95%CI 0.92-1.71, p=0.1571) for BrS phenotype per risk allele. Individuals with a BrS-GRS ≥4 risk alleles had an OR=2.35 (95%CI:0.89-6.22, p=0.0846) for BrS phenotype compared to individuals

with a GRS <4 risk alleles. *SCN5A* genotype-negative relatives (n=54) yielded an OR for BrS phenotype of 2.71 per risk allele (95%CI 0.98-7.43, p=0.0535). *SCN5A* genotype-negative individuals with a BrS-GRS ≥4 risk alleles had an OR=22.29 (95%CI 1.84-269.30, p=0.0146) for BrS phenotype compared to individuals with a BrS-GRS <4 risk alleles (Figures 20 and 21).

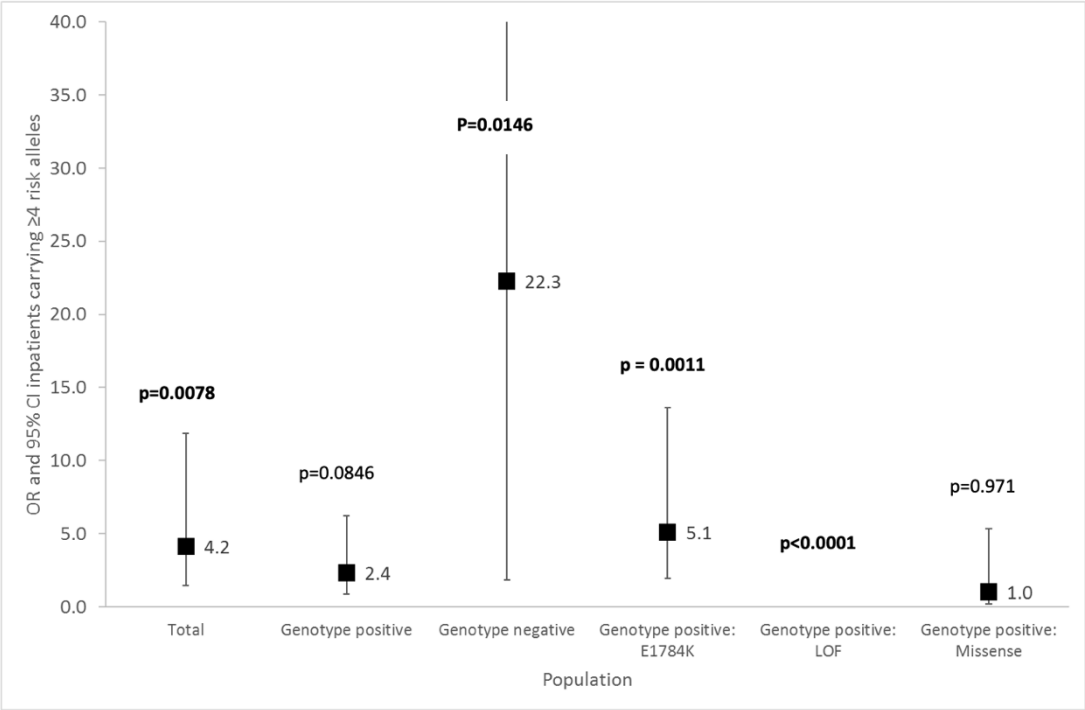


Figure 34. Risk of BrS in patients carrying ≥4 risk alleles in the total cohort; genotype negative individuals; genotype positive individuals from families harbouring loss-of-function mutations causing haploinsufficiency; genotype positive individuals from families harbouring *SCN5A*-E1784K; genotype positive individuals from families harbouring other missense *SCN5A* mutations. The odds ratio (OR) and 95% confidence interval for a cut off of ≥4 risk alleles are shown (adjusted for age and sex). The p-values denote the level of significance of the odds ratios for this cut-off for Brugada Syndrome for each cohort using GEE.

SCN5A-E1784K

When examining *SCN5A*-E1784K positive family members alone, a weaker BrS-GRS performance was found: OR=1.49 (95%CI 1.09-2.04, p=0.0135) per risk allele. Individuals with a BrS-GRS ≥4 risk alleles had an OR=5.12 (95%CI:1.93-13.62, p=0.0011) for BrS phenotype compared to individuals with a GRS <4 risk alleles (Figures 32-34).

SCN5A loss-of-function mutations causing haploinsufficiency

For subjects hosting loss-of-function *SCN5A* mutations causing haploinsufficiency the association between the BrS-GRS and BrS phenotype appeared the strongest (OR per risk allele of 5.18; 95%CI:2.07-12.93, p=0.0004). Since there were no BrS negative cases that had more than 2 risk alleles, the OR of subjects with ≥4 risk alleles was infinite compared to subjects with <4 risk alleles (Figures 32-34).

Other missense *SCN5A* mutations

For individuals hosting other *SCN5A* mutations there was no statistically significant association between the BrS-GRS and BrS phenotype (OR per risk allele=0.88, 95%CI 0.58-1.32, p=0.5271). Subjects with ≥4 risk alleles had an OR=1.03 (95%CI:0.20-5.35, p=0.9705) for BrS phenotype compared to those with less than 4 risk alleles (Figures 32-34).

Discussion

Historically, BrS was considered an autosomal dominant monogenic disorder. In 2013, a common variant GWAS comparing index cases of BrS to healthy controls indicated association with common genetic variation, regardless of presence of an *SCN5A* mutation.[77] While that work identified susceptibility loci, up to now, the variable expression of the BrS phenotype in members of families with *SCN5A* mutations has remained unexplained. Here, for the first time we report that common genetic variation, in the form of a BrS-GRS, correlates with the BrS phenotype in individuals from families with *SCN5A* loss-of-function mutations causing haploinsufficiency and the recurrent mutation *SCN5A*-E1784K. Furthermore, our study extends beyond the findings of the original GWAS by emphasizing the role of common variation in expression of the BrS phenotype independent of the presence of an *SCN5A* mutation. The BrS-GRS explained in part the variable expression of BrS phenotype in both *SCN5A*-positive and *SCN5A*-negative relatives. There was significant heterogeneity of the strength of association of different types of *SCN5A* mutation (loss-of-function causing haploinsufficiency, *SCN5A*-E1784K and other missense) and their associated BrS-GRS with BrS phenotype indicating a variable biological effect of common and rare variants on disease susceptibility. Given the size of the *SCN5A* gene, the effect of *SCN5A* mutation–SNP interaction may be different depending on whether the mutation is in a pore-forming region or outside. In families, there are multiple individuals with the same genetic background (same haplotype), making it difficult to find the specific combination of mutation and variant that influences the phenotype. These findings support a complex polygenic architecture for BrS and are an important proof of principle in cardiac genetics.

A BrS-GRS and variability in BrS phenotype within affected families

We sought to investigate whether a BrS-GRS is associated with BrS phenotype. The SNPs studied have been previously shown to be transethnically relevant.[77,94,220] As a result, we have analysed these SNPs in the total cohort, instead of separating by ethnicity, especially as number would be very limited for analyses when dividing by ethnicity.

The BrS-GRS demonstrated association with BrS phenotype in pedigrees carrying pathogenic or likely pathogenic *SCN5A* variants, reflecting the cumulative effect of the three SNPs (six risk alleles) on BrS phenotype. The BrS-GRS was then tested separately in the subset of families harbouring loss-of-function *SCN5A* mutations causing haploinsufficiency, detecting a strong effect size and a near infinite OR when harbouring four or more risk alleles. This may reflect the small numbers of Brugada negative cases with loss-of-function mutations causing haploinsufficiency and that chromosome 3 risk alleles in *trans* with the mutant allele are more likely to have a more potent effect by further altering the expression of already haplo-insufficient wild-type *SCN5A*. The dichotomised risk score makes the model simpler in that there is no linearity assumption. Based on the results seen, the most appropriate threshold for dichotomising was chosen.

Families with missense *SCN5A* mutations other than *SCN5A*-E1784K showed no significant associations with the BrS-GRS whilst the *SCN5A*-E1784K subset exhibited a significant association, albeit weaker than for loss-of-function mutations causing haploinsufficiency. The reasons for this difference are likely to be complex. Firstly, *SCN5A*-E1784K is considered a relatively mild missense mutation in its biophysical and clinical consequences and showed lower penetrance in our study

compared to other missense mutations (72% vs 90% expression of BrS phenotype respectively, Table 8).[224] The association of the BrS-GRS may therefore reflect a greater impact of common variation in this setting. Secondly, the diversity of the other included missense *SCN5A* mutations may have led to a weaker power for evaluating the BrS-GRS compared to *SCN5A*-E1784K families. Each mutation is expected to have different severity of biophysical defects with the potential for variable effects of SNPs on the lesion. Furthermore, due to the small size and heterogeneity of the total cohort, there was insufficient power to analyse chromosomal phasing between *SCN5A* mutations and the SNPs of interest. The other missense *SCN5A* mutation group was therefore a less homogeneous group to test for associations than a large group of families with a single mutation such as *SCN5A*-E1784K. More homogeneous samples, particularly founder populations, may be more appropriate for future studies of how common variants modify phenotype. Interestingly in *SCN5A* genotype-negative relatives, the association of BrS-GRS ≥4 risk alleles with BrS phenotype was even more apparent. In fact, the OR was greater than that of *SCN5A*-E1784K in isolation. This supports a greater strength of association of common variation with the likelihood of BrS phenotype in the absence of a *SCN5A* mutation.

These results therefore reveal the potential for clinical utility of incorporating common genetic variation in the form of a genetic risk score in genetic diagnostics for rare disease. It is expected, however, that additional SNPs underlie the complex genetic nature of BrS and a larger GWAS is needed to identify other common variants that could be incorporated to improve the power of an optimised BrS-GRS for diagnostic purposes. This will also require further investigation of greater numbers of relatives with integration of haplotype structure and detailed knowledge of *SCN5A* variants' biophysical properties.

The analyses in this chapter were different to the previous two chapters as this chapter focuses on a combination of both SNPs and GRS on a dichotomous outcome (presence or absence of BrS). Since any model that is created will perform better in the data set it was created in than in reality (statistical ‘optimism'), we sought to validate the model in another cohort. Given that this cohort (*SCN5A*-E1784K) was the largest available worldwide, we validated the GRS in pedigrees with other *SCN5A* mutations. Although this approach increased the heterogeneity, it also made the validation more generalisable.

Association of rare SCN5A variation with BrS phenotype and common variants

While common variation in the form of a BrS-GRS has clear independent association with BrS phenotype, the strongest contribution comes from the presence of an *SCN5A* mutation. However, not all *SCN5A* BrS susceptibility mutations have comparable functional effects. The OR for the BrS phenotype associated with *SCN5A*-E1784K is significantly lower than for other missense *SCN5A* mutations but is greatest in loss-of-function mutations causing haploinsufficiency. Furthermore, the OR of the BrS-GRS for BrS phenotype varied according to *SCN5A* mutation and was strongest in genotype negative relatives. This suggests that there may be an interaction and synergy of common and rare variation affecting sodium channel function whereby a certain level of impairment is necessary to achieve a threshold where BrS phenotype can manifest. This further supports a polygenic genetic architecture underlying the condition.[225]

Genotype-phenotype mismatch in BrS and its implications

The proposed polygenic model of heritability in BrS may explain the paradox of clinically affected mutation-negative individuals in *SCN5A* families, first demonstrated by Probst et al.[75] Indeed, 12% of *SCN5A*-negative relatives showed a

drug-induced BrS phenotype. Importantly, cascade genetic screening in *SCN5A* pedigrees can result in *SCN5A* genotype-negative relatives being discharged from further follow-up. A small proportion of these individuals may still be at risk of developing a BrS phenotype. Conversely, these findings also raise further questions about the specificity of drug provocation tests for BrS in the absence of a gold standard test for the condition. The prevalence of the type 1 Brugada ECG pattern after drug provocation testing has already been shown to be much higher than expected (4%) in healthy controls.[84] Indeed recent data have associated a similar BrS polygenic risk score with the ajmaline induced type 1 Brugada ECG pattern.[96] The Shanghai consensus document downgraded the diagnostic certainty offered by such a result when found in isolation.[85] The likelihood of a drug-induced type 1 Brugada ECG pattern indicating a diagnosis of BrS is considered greater, however, if an individual had a family history of premature autopsy negative SCD and/or BrS. The significance of a drug-induced type 1 Brugada ECG pattern in *SCN5A* genotype-negative relatives is therefore uncertain in *SCN5A* BrS families. Other, as yet unknown, polygenic and acquired contributions to the risk of developing BrS phenotype may be present in these *SCN5A* genotype-negative relatives.

BrS phenotype-positive *SCN5A* genotype-negative individuals may be identified due to clinical evaluation taking place either prior to genetic studies being available, or prior to determination of the pathogenicity of a detected rare *SCN5A* variant. There is insufficient follow-up data available, however, in the literature to determine if these individuals subsequently develop arrhythmic events. In the meantime, these patients may be offered monitoring for evidence of evolving risk and lifestyle advice such as avoidance of prescription sodium channel blocking drugs, cocaine and alcohol intoxication, and treatment of fever.[226] Asymptomatic *SCN5A*-negative relatives of autopsy-negative SCD victims, who go on to have a positive ajmaline

test, have been managed with this strategy. During follow-up, a spontaneous type 1 Brugada ECG pattern and/or clinically significant arrhythmic events developed in 17% of these individuals.[54] This may be a worthwhile approach in BrS *SCN5A* family members, regardless of genotype status, although further prospective research will be required.

Future perspective: an optimised BrS-GRS

There is already strong association of a BrS-GRS ≥4 risk alleles utilizing only three SNPs with BrS phenotype. We propose that an optimised BrS-GRS employing additional SNPs emerging from a larger GWAS could act as a complementary approach to quantifying the probability of developing BrS phenotype. Furthermore, incorporating phasing of SNPs could further refine the predictive accuracy of a BrS-GRS, especially in *SCN5A* families where SNPs in *trans* to the *SCN5A* mutant allele would be expected to have more pronounced effects than SNPs in *cis*. An optimised and validated GRS may therefore aid decision-making over follow-up in *SCN5A* families and determining whether preventative and monitoring strategies for BrS should be instituted.[59,85] A GRS-based approach may even replace the unnecessary use of drug challenge and form part of clinical genetic testing in BrS.

Limitations

The completeness of clinical evaluation was subject to variations in practice between specialist centres internationally, thus reducing the cohort size of those who underwent complete clinical evaluation for the presence or absence of a BrS phenotype. BrS phenotype was defined in accordance with the 2013 HRS/EHRA/APHRS guidelines. Other guidelines have been proposed due to concerns over the specificity of the sodium channel blocker-induced BrS phenotype.[54,59,85] These guidelines maintain the same definition of the type 1

Brugada ECG pattern and give extra weight to a family history of BrS. We therefore used the same ECG definition for BrS phenotype in this study. We also treated spontaneous and drug-induced BrS phenotype as one group for analysis purposes. This was due to low numbers, the similarity of findings in spontaneous BrS (data not shown) as well as the consistency of the association demonstrated by the BrS GWAS regardless of whether the phenotype was drug-induced or spontaneous.[77]

A smaller proportion of the *SCN5A* genotype-negative cases underwent sodium channel blocker challenge, probably reflecting variation in local clinical practice. Furthermore, only a relatively small proportion of *SCN5A* genotype-positive relatives were found to be BrS phenotype-negative after drug challenge. Both factors likely weakened the power to detect associations. Due to the heterogeneity of the total cohort, there was insufficient power to analyse chromosomal phasing between the *SCN5A* mutations and the SNPs of interest at this chromosomal locus - rs11708996 (*SCN5A*) and rs10428132 (*SCN10A*) - and therefore SNP interactions. These potential interactions may explain why the weighted model for the BrS-GRS did not show additional significance over the additive model. Furthermore, families of Japanese and other non-Caucasian ancestry were included but due to small numbers could not be analysed separately. This was offset, however, by the three SNPs used to create the BrS-GRS having been replicated in Japanese BrS cases.[219]

Conclusions

Common genetic variation explains in part, the variable expression of BrS phenotype in families with sodium channel disease. Association of common variants was cumulative leading to a BrS-GRS associated with BrS phenotype in both

genotype positive **and** negative subjects i.e. independent of the presence of an *SCN5A* mutation. *SCN5A* mutations and the BrS-GRS also show differing effect sizes on BrS phenotype according to variant type, further confirming a complex polygenic architecture underlying BrS. These findings have important implications in BrS *SCN5A* families where a *SCN5A*-negative relative may still develop a BrS phenotype. Further work is required to elucidate other genetic factors to develop an optimized BrS-GRS that may become a surrogate marker for BrS phenotype in *SCN5A* families, form part of clinical genetic testing, obviate drug provocation testing and guide follow-up.

Chapter 7: Functional characterisation

Introduction

Human induced pluripotent stem cell derived cardiomyocytes (hiPSC-CMs) are a novel and powerful platform for *in vitro* disease modelling. hiPSC-CMs enable study patient-specific disease pathophysiology and drug responses under controlled conditions *in vitro* without resorting to invasive biopsies. Further, these models can obviate the need for animal studies and associated ethical concerns. Further, animal models fall short in predicting pathophysiology of human diseases as a result of differences in physiology, embryology, metabolism and crucially, different genetic backgrounds. This makes animal models challenging to use in personalised medicine, particularly to investigate common genetic variation that can affect phenotype amongst individuals from families harbouring a certain mutation of interest, as is the subject of this study. *In silico* (computational) models are an alternative option, and are widely used as drug discovery platforms, however, biological entities are non-linear systems and 'algorithmically incompressible' that make it challenging to replicate via in silico models, as no computer programme can fully model the complexity of biological systems.[227] Despite limitations with hiPSC-CM models (as discussed in Chapter 1), these provide a unique patient-specific yet minimally invasive model of disease *in vitro*.

The aim of this arm of the thesis was to produce hiPSC-CMs from *SCN5A*-E1784K carriers with extremes of phenotype: one with severely prolonged QTc but no BrS and one with a spontaneous type 1 Brugada ECG pattern but no LQTS phenotype. Differentiation of a cell line from an *SCN5A*-E1784K carrier with a mixed phenotype of LQTS and BrS was also attempted. The control cell line was a healthy cell line that had been produced in-house at University of Nottingham.[228] The number of lines and the phenotypes to be studied were selected carefully in order to manage risk and feasibility effectively within the timeframe available.

Justification of the proposed functional work in the context of Chapters 3-6

As described in Chapter 1, one of the main challenges with managing patients with *SCN5A*-E1784K, is determining appropriate therapy, where a mixed phenotype increases the propensity for drug interaction and adverse effects. In Chapter 3, I characterised the range of phenotypes observed amongst *SCN5A*-E1784K carriers and non-carriers. Challenges in clinical management of these patients were evident from the data available, including the lack of consistency in management whether BrS and/or Long QT phenotype were present, and/or prior events had occurred. This was present despite all the patients being recruited from expert tertiary centres. The main aim of this chapter was to undertake functional modelling of this mutation using hiPSC-CMs from two *SCN5A*-E1784K carriers with extremes of phenotype (BrS phenotype and Long QT phenotype) in order to demonstrate the potential for recapitulation of the clinical phenotype *in vitro* in a cellular model. This would enable the study of drug responses *in vitro* and would provide proof-of-concept to predict which patients would benefit from proposed therapies. Thus, recapitulating the clinical phenotype *in vitro* would help guide which patients would be most likely to benefit from different drug therapies currently in clinical use in this cohort (thus contributing to personalised medicine).[188] Future work could include extending this to novel therapies for pre-clinical studies.

It is envisaged that genetic modifiers of the BrS/Long QT phenotype would be faithfully maintained during reprogramming.[229] Whilst exploring the potential genetic modifiers identified in Chapters 4-6 would be beyond the scope of this project, this could be a focus of future work. Although no single obvious modifier signal was identified in Chapter 4, this would be the aim of future work involving GWAS. If a clear modifying SNP signal is identified in GWAS, this could be studied in patient specific and control line hiPSC-CM models, with target-specific genome editing

using CRISPR-Cas9 technology. Studying the effect of polygenic risk scores identified for QRS and BrS in Chapters 5 and 6 *in vitro* is challenging at present due to the need to target multiple SNPs whilst avoiding off-target effects. Whilst CRISPR multiplex gene editing is an emerging technology and commercial systems that can be used on hiPSC models are available, the utility of such multiplex gene editing systems have not yet been published in hiPSC models by independent researchers.[230,231] Targeting of multiple SNPs using genome editing could lead to off-target effects that amplify during tissue morphogenesis. It has been shown recently in a hiPSC model that two distinct mutant alleles can be corrected with a high degree of precision.[232] However, further work is needed to assess the reliability and applicability of polygenic gene editing.

Justification of the proposed functional work in the context of existing literature

It has been shown that LQT3 hiPSC-CMs have markedly prolonged action potential duration and inward Ca^{2+} transients, with reduced I_{Na} density, increased late I_{Na}, a positive shift of steady state inactivation (not seen in heterologous models) and faster recovery from inactivation.[27,193,233,234] In fact, the positive shift of steady state inactivation in mutated LQT3 hiPSC-CMs noted by de la Roche *et al* with a different *SCN5A* mutation was opposite to that seen by Makita *et al* in a heterologous model of *SCN5A*-E1784K, where a negative shift in steady state inactivation was noted.[32,193] Interestingly, one study found that hiPSC-CMs from patients with BrS and no identified mutations revealed no differences in sodium current (I_{Na}) compared to unrelated controls.[29] LQT3 iPSC-CMs have been shown to display a greater response to I_{Na} blockade, which was normalised by gene correction.[235] Further, propranolol has been shown to inhibit the late I_{Na} in LQT3 hiPSC-CMs that was independent of β-adrenergic receptor signalling pathway.[236] Further, early

afterdepolarisation development with marked arrhythmogenicity have been observed in LQT3 hiPSC-CM *in vitro*.[237]

As described in Chapter 1, there has been one publication in the literature where *SCN5A*-E1784K was studied in patient-derived hiPSC-CMs, where Okata *et al* studied hiPSC-cardiomyocytes from a single *SCN5A*-E1784K patient with BrS/LQTS overlap.[195] Whilst they were able to recapitulate the LQT3 phenotype, the investigators were unable, initially, to recapitulate the BrS phenotype in hiPSC-cardiomyocytes derived from that patient, although they were able to do so after knockdown of *SCN3B*. This was because there is differential expression of β-subunits of the sodium channel in embryonic and adult hearts. Expression of the beta-subunits of sodium channels is similar between embryonic hearts and iPSC-cardiomyocytes, but lower in adult hearts.[195] However, in a different study, hiPSC-CMs from a BrS patient carrying a different, non-overlap *SCN5A* mutation exhibited reduced action potential upstroke velocity and conduction slowing. They further showed that I_{to} in the mutated hiPSC-CMs was significantly augmented, and the I_{CaL} window current probability was increased.[238]

Okata *et al* demonstrated through a heterologous expression system that *SCN3B* can augment the otherwise reduced inward sodium current (I_{Na}) in cells transfected with *SCN5A*-E1784K. They propose that high *SCN3B* expression in the embryonic heart and iPSC-derived cardiomyocytes may explain why the BrS phenotype is masked in young children and only manifests itself in adulthood. They demonstrate that knockdown of *SCN3B* in control hiPSC-CMs had no significant effect on I_{Na} density, whereas knockdown of *SCN3B* in LQT3/BrS hiPSC-CMs showed decreased I_{Na} density and a negative shift in the voltage dependence of steady state inactivation. The authors conclude that the decrease of *SCN3B* is therefore

necessary to successfully unmask the BrS phenotype in LQTS3/BrS iPSC-CMs. The knockdown of *SCN3B* in both control and LQT3/BrS hiPSC-CMs, however, had no effect on the voltage dependence of steady state activation. Further, the authors demonstrated that isogenic control of the LQT3/BrS mutant line exhibited a shorter action potential duration and smaller late current compared to the mutant cells.[195]

Compared to the study reported by Okata *et al*, the novelty of this chapter lies within the attempt to derive hiPSC-CMs from patients with differing phenotypic extremes despite carrying the same mutation. Particularly, the strength of phenotypic data as detailed in Chapter 3 is a unique feature of this study, given that I have detailed phenotype and pedigree data on the largest international cohort of carriers of this mutation and WT relatives. Multiple affected family members were recruited, so that the patients at the extremes of the phenotypic spectrum of this mutation could be taken forward for functional characterisation using hiPSC-CMs. *In silico* simulations have demonstrated the ability to recapitulate variability in LQT3 and control hiPSC-CM phenotypes, and drug testing.[239] However, there have been no studies published to date of hiPSC-CMs derived from *SCN5A*-E1784K carriers with phenotypic extremes.

Methods

General lab procedures

All cells were maintained and differentiated in a 37°C and 5% CO_2 humidified incubator. Cell reprogramming, initial hiPSC expansion and cardiac differentiation were carried out in an antibiotic-free environment at University of Nottingham. Initial fibroblast harvesting and culture, subsequent hiPSC expansion and cardiac differentiation were carried out in tissue culture facilities at St George's, University of

London in media containing 1% penicillin-streptomycin. Cell phenotyping was carried out at St George's, University of London, University of Nottingham and Queen Mary, University of London.

The reagents, and where appropriate, preparation of reagents, are listed in the Appendix 3.

hiPSC reprogramming and characterisation

Harvesting dermal fibroblasts: Following patient consent, the inner aspect of the forearm was prepared with a Chloraprep™ applicator and 1ml 1% lignocaine was administered. A 4mm punch biopsy was taken using aseptic technique and placed in sterile transport media (Dulbecco's phosphate buffered saline, DPBS). The skin was closed with a single dissolvable suture and a sterile dressing was applied to the site. The skin biopsy was transported in phosphate-buffered saline (transport medium) to the lab at ambient temperature (if transit time was <2 hours) or on ice (if transit time was >2 hours). In a class II safety cabinet, the samples were washed in fresh transport media, and placed in 90mm Petri dishes. Subcutaneous fat and loose connective tissue (hypodermis) were removed using fine tweezers and a scalpel, until only the dermis and epidermis remained. This was cut into $1mm^3$ pieces using a scalpel. The pieces of dermis/epidermis were digested overnight in an incubator (37°C, 5% CO_2) in fibroblast medium (78% DMEM + 20% FBS + 1% GlutaMAX + 1% NEAA + 100 μM β-mercaptoethanol) containing 2mg/ml Collagenase I and 0.1mg/ml DNase I. 8-10ml phosphate buffered saline was added after 8-12 hours' digestion, and the suspension was centrifuged at 300g for 4 minutes. The supernatant was removed, and the pellet was resuspended in fibroblast medium. This was plated in a T25 pre-coated with 0.1% gelatin. The

human dermal fibroblasts (HDFs) were allowed to adhere and outgrow for 2-3 days before the first change of medium.

Fibroblast expansion and cryopreservation: The medium was changed every 3 days with fibroblast medium until the cells were 80-90% confluent (passage 0). The HDFs were enzymatically passaged using Trypsin-EDTA 0.05% and split at a 1:3 ratio onto 0.1% gelatin pre-coated culture vessels. Following the first passage, the HDFs were cryopreserved in liquid nitrogen following enzymatic dissociation and reconstitution in foetal bovine serum (FBS) containing 10% dimethyl sulfoxide (DMSO) at a density of $5x10^5$ HDFs per vial. The cryovials were frozen in a controlled environment overnight in isopropanol, such that the temperature drops by a maximum of 1°C per minute, before transfer to liquid nitrogen. When the cells were thawed, these were rapidly but gently thawed in warmed fibroblast medium and centrifuged to remove DMSO, before resuspending the cells in fresh fibroblast culture medium prior to plating.

hiPSC reprogramming (feeder-free): Thawed HDFs were passaged twice to optimise cell health prior to transfection. On the day prior to transfection, 2×10^5 HDFs were plated in 1 well of a 6 well plate in fibroblast medium and allowed to adhere to the plate overnight. The following day, the HDFs (now 50-80% confluent) were transfected with fresh fibroblast medium containing CytoTune® 2.0 Sendai reprogramming vectors (combination of plasmids encoding polycistronic Klf4–Oct3/4–Sox2 (KOS), L-Myc, Lin28 and shRNA for TP53 to produce integration-free hiPSC)[174] at the appropriate multiplicity of infection (MOI): KOS MOI=5; hc-Myc MOI=5; hKlf4 MOI=3. The volume of virus to add was calculated as follows:

$$\text{Volume of virus (µL)} = \frac{\text{MOI (CIU/cell)* } \times \text{ number of cells (i.e. 200,000)}}{\text{titre of virus** (CIU/mL)} \times 10^{-3} \text{ (µL/ (mL)}}$$

*CIU=cell infectious units; **as per Life Technologies™ for the relevant lot number

The cells were incubated overnight in the medium containing transfection vectors. After 18 hours' incubation, the medium was replaced with fresh fibroblast medium in order to remove the CytoTune® 2.0 Sendai Reprogramming vectors. The fibroblast medium was replaced daily until the cells were 100% confluent. When cells were 100% confluent, the cells were passaged enzymatically using 0.05% trypsin/EDTA (incubated in trypsin-EDTA for no more than 2 minutes), diluted with fibroblast medium and centrifuged at 200g for 4 minutes. The cells were resuspended in E6 medium containing 1ng/ml fibroblast growth factor (FGF) and plated in 35mm tissue culture treated dishes pre-coated with vitronectin. When sizeable colonies were forming (approximately day 8-14), the medium was changed to E8 medium. Between weeks 3 and 6 after transfection, colonies were isolated by manually cutting under the microscope and transferring to Matrigel-coated 48 well tissue culture plates.[240]

Expansion of hiPSC clones: The hiPSC clones were passaged (split) every 3-7 days from 48 well plates to increasingly larger culture surface areas using EDTA (0.5μM EDTA in DPBS). Some clones were slow-growing initially, therefore up to a week was allowed between passages during early expansion, instead of splitting the cells prematurely. Once the clones had been expanded in a T25 and reached 70-80% confluence, the cells were split 1:3 using TryplE. Following this, $8x10^5$ - $1.2x10^6$ cells were seeded per T25 (the appropriate number was dependent on cell line) and passaged once cells reached 80% confluence (i.e. every 3 days) using TryplE (incubated for 2-3 minutes in TryplE depending on cell line, and centrifuged at 160g for 4 minutes after dilution with either E8 or B-GK medium, see Appendix 3). Following each passage, the cells were cultured in E8 medium containing 10μM ROCK inhibitor for the first 24 hours following the split. ROCK Inhibitor (Y-27632) is

a cell-permeable, highly potent and selective ATP-competitive inhibitor of Rho-associated protein kinase (ROCK) including p160Rock (Ki=140nM) and Rock-II. It also acts as a potent inhibitor of agonist-induced Ca2+ sensitization of myosin phosphorylation and smooth muscle contraction.[240]

hiPSC cryopreservation: The cells were dissociated using TryplE as above, then resuspended in an appropriate volume of FBS following centrifugation, depending on the number of cells to be frozen per vial (either $7x10^5$ cells/vial if thawing onto a single well of a 6 well plate, or $1.5x10^6$ cells/vial if thawing into a T25; a higher density than when the cells are routinely passaged). 500µl of the cell suspension was then added in a dropwise manner (to minimise osmotic shock) to 500µl FBS containing 20% DMSO in appropriately labelled cryovials, to make a final concentration of 10% DMSO, and mixed thoroughly. The cryovials were frozen overnight in isopropanol in a controlled manner, such that the temperature drops by a maximum of 1°C per minute, before transfer to liquid nitrogen. When the cells were thawed, these were rapidly but gently thawed in warmed B-GK medium and centrifuged to remove DMSO, before resuspending the cells in fresh E8 medium containing 10µM ROCK inhibitor for the first 24 hours following cell thawing.

hiPSC karyotyping: Frequent gains of chromosomes 12, 17, 20 and X have been reported on repeated passaging of hiPSCs, suggesting a mutational advantage of such karyotype abnormalities (eg. from NANOG on chromosome 12). Each clone was karyotyped to check for karyotype abnormalities prior to differentiation. When the cells were approximately 70% confluent (so that the maximal number of cells will be in metaphase), Karyomax was added to the medium to achieve a final concentration of 0.1ug/ml and incubated for 2 hours (this arrests the cells in metaphase). Meanwhile, the following were prepared -

- Hypotonic solution - 0.6% sodium citrate in distilled water (0.12g in 20ml)
- Fix - Methanol: Acetic acid at a 5:1 ratio

The cells were then dissociated using TryplE, which was discarded and the cells were resuspended in DPBS. The cell suspension was then centrifuged at 300g for 7 minutes and the supernatant was discarded. The cell pellet was then resuspended and incubated for 10 minutes in 10ml hypotonic solution at room temperature (to swell the cells). Following this, the cells were centrifuged at 700g for 5 minutes (but at a slower rate of deceleration, as the swollen cells are less likely to form a tight pellet). The supernatant was aspirated, and the cell pellet was fixed in methanol: acetic acid and centrifuged again at 700g for 5 minutes. The supernatant was discarded and the fixing process was repeated twice more, but the cells were left in 1ml supernatant after the final spin. The cells were resuspended in the residual supernatant and stored at -20°C until further processing in a clinical genetics laboratory.

In the clinical genetics laboratory, ethanol-soaked slides were dried and polished, then cells were dropped in a humid environment from a height of approximately 30cm onto the slides so that these burst and the metaphase chromosomes spread out. The slides were dried for a minimum of 2 minutes and checked for metaphase spreads. These were matured at 75°C overnight prior to G-banding. The aged slide was then inserted into a Coplin jar containing Trypsin and left for 2min and gently rinsed with water, flooded with diluted (1:5) Leishman's stain and left for 10 minutes. The slides were again rinsed with water and left to dry on a hot plate for a few minutes. One drop of VECTASHIELD Antifade Mounting Medium was applied to a glass cover slip and the slide was lowered onto the coverslip, applying pressure to spread the mounting media to fill the gap between the coverslip and the slide. The

above were left for at least 1 hour to set and the metaphase spreads were analysed under 100x oil objective.

Differentiation into hiPSC-CMs and characterisation

hiPSC differentiation (monolayer cardiac differentiation): It has been shown that the small molecules KY02111 and XAV-939 are Wnt/β-catenin inhibitors that promote efficient differentiation of hiPSCs to cardiomyocytes, and that combined use of these with stage-specific optimisation of activin/nodal and BMP signalling enables robust cardiac differentiation in a xeno-free, defined medium.[241–243] The following protocol, that has been developed in Prof Denning's lab, was thus used for this study.[228]

hiPSCs were seeded at the optimum density for differentiation once a stable growth curve was established, such that the cells will be 80-90% confluent 2 days after seeding. For every new cell line, the optimal seeding density was determined using a density gradient screen in a 24 well plate). On day -1 of differentiation, the cells were preconditioned by changing the medium to StemPro 34 medium supplemented with L-glutamine + 1ng/ml BMP4 + Matrigel (1:100 dilution). Preconditioning is a critical step that enriches the culture before differentiation, which also increases the mesodermal formation process. On day 0 of differentiation (12 hours after the preconditioning medium was added), the medium was changed to StemPro 34 supplemented with L-glutamine + Activin A 8ng/ml + BMP4 10ng/ml. Activin A and BMP4 modulate cell type specification and efficient induction of mesoderm. By day 2, the cells would begin to form a monolayer and the medium was changed to RPMI supplemented with B27 (minus insulin) + 10μM [KY0211 + XAV939]. At day 4, the medium was changed to RPMI supplemented B27 + 10uM of [KY0211 + XAV939]. This is a custom-designed protocol developed in Professor Denning's lab based on systematic modulation of BMP and WNT signalling to

enhance mesodermal induction followed by efficient cardiac differentiation.[228] From day 6 onwards, the cells were maintained in culture on RPMI supplemented with B27. From day 8 onwards, spontaneously contracting hiPSC-cardiomyocytes (hiPSC-CMs) are visible in the culture, and by day 9-13, a beating monolayer would have formed.

Lactate enrichment of hiPSC-CM: hiPSC-CMs were treated with lactate enrichment for a 6 day period at day 9-13 to improve purity of the differentiated cultures, once a beating monolayer had been formed. Lactate enrichment with 2x3 day treatments with lactate enrichment medium. The lactate enrichment medium comprised of RPMI 1640 (no glucose) supplemented with sodium-L-Lactate (4mM final concentration). The cells were washed with RPMI-1640 (no glucose) before the first lactate enrichment treatment to remove any traces of glucose. The cells were washed with RPMI-1640 (no glucose) at day 3, to remove dead cells, before the second treatment. After 6 days of lactate enrichment, cells were cultured in RB27 for 1.5 days to recover, prior to dissociation.

hiPSC-CM dissociation: This hiPSC-CM dissociation protocol was adapted from the protocol published by Mosqueira et al, 2018.[228] hiPSC-CM were dissociated at day 16-20. Collagenase solution was prepared as follows:

Collagenase II solution with the following additives**:**

+ 1mM HEPES pH 7.4, sterile filtered

+ 10 μM Y-27632 ROCK inhibitor

+ 30 μM BTS

Cell culture medium was aspirated and the cells were washed twice with pre-warmed Ca^{2+}-free HBSS. Either 300μl or 2.5ml collagenase solution (in Ca^{2+}-free HBSS) were added per well of a 24 well plate or T25 flask respectively. The hiPSC-

CMs in collagenase solution were incubated for 3.5 - 4 hours at 37°C until the cells were detached into single cells and small clumps. The cell suspension was gently collected into a centrifuge tube and the same volume of pre-warmed blocking buffer (RPMI + DNase 1:500) was added was added. The final cell suspension was checked under the microscope to check the size of the cell clumps. If there were multiple large clumps, the cells were gently pipetted up and down 3-6 times with a 10ml pipette to gently break up the clumps. The cells were centrifuged for 15 minutes at 100g and the supernatant was aspirated carefully. The cells were resuspended in RB27 + 10% FBS+ 10 μM ROCK inhibitor and very gently mixed using 10ml pipette to create a uniform suspension. The cell suspension was passed through a 100μm mesh into a centrifuge to remove any remaining large clumps and the cells were centrifuged for 15 minutes at 100g. The supernatant was carefully aspirated to remove any traces of DNase and collagenase, and the cells were resuspended in RB27 + 10% FBS+ 10 μM ROCK inhibitor. The cells were plated on Matrigel-coated vessels as follows: 3.5 million hiPSC-CMs / T25 or an equivalent number of cells per cm^2 surface area of a cell culture plate. Collagenase was made up in Ca^{2+}-free HBSS. The medium was changed to RB27 approximately 16 hours afterwards.

hiPSC-CM maturation using T3 + dexamethasone: Two days following hiPSC-CM dissociation at day 16-20, the medium was changed to RB27 + 1:10,000 T3 + 1:10,000 Dexamethasone. The hiPSC-CMs were maintained in this medium with medium changes every 2-3 days until phenotyping.[244]

Accutase dissociation and preparation of hiPSC-CMs for single cell electrophysiology: hiPSC-CMs were dissociated using accutase 3-4 days prior to study of single cell electrophysiology at day 40+/-3 days. Accutase was used neat.

Medium was removed, the cells were washed with DPBS, after which 3ml accutase was added per T25 (or an equivalent volume per well of a cell culture plate). The cells in accutase was placed in the incubator at 37ºC for 16-20 minutes and once detached, the cell suspension was diluted and gently mixed with RB27 + 10% FBS + 10 μM ROCK inhibitor and centrifuged for 4 minutes at 200g. The cells were resuspended in the appropriate volume of RB27 + 10% FBS + 10 μM ROCK inhibitor + T3 + Dexamethasone to make up 2 million cells/ml. The cell suspension was further diluted to make up a cell suspension of 40,000 cells per ml. The diluted cell suspension was plated on 0.1% gelatin-coated coverslips on a 24-well plate. The remaining cells were re-plated on Matrigel-coated wells of a 6 well plate to be used for further characterisation (immunostaining or FACS). The medium was changed 12-16 hours later to RB27 + 1:10,000 T3 + 1:10,000 dexamethasone.

All phenotyping was carried out at day 40+/-3 (day 37-43) after initiation of the differentiation protocol.[228]

FACS assessment of differentiation purity: hiPSC-CMs were dissociated as already described, the cell suspension was transferred to a universal tube, centrifuged at 300g for 4 minutes, resuspended in 0.5-1ml DPBS and transferred to an eppendorf. This was centrifuged at 5000-6000 rpm in a microcentrifuge for 3 minutes. The supernatant was discarded, and the cells were fixed by resuspending in 200μL of 4% PFA and left for 15-20 minutes at room temperature. This was centrifuged again at 5000-6000rpm, the PFA was discarded and the cell pellet was washed twice in DPBS before resuspending in 20% FBS in DPBS. The resuspended pellet was stored at 4°C for up to 2 weeks. On the day of flow cytometry (or 1-2 days prior to this), the pellet was centrifuged again and washed with DPBS, then permeabilised with 0.1% Triton X-100 at room temperature for 15

mins. This was then washed with Tween and then incubated with 5% FBS for 30 minutes before further centrifugation. The pellet was then incubated with fluorochrome-conjugated primary antibody at the appropriate dilution in 5% FBS according to the manufacturer's instructions for 1 hour/overnight at 4°C on a shaker. The pellet was then washed twice with 0.5% Tween for 10-20 minutes before incubation with secondary antibody for 1 hour/overnight on a shaker at 4°C. The pellet was washed twice more with Tween, followed by DPBS before performing flow cytometry. Flow cytometry of each batch of differentiated cells had the following three controls: an untreated control, a secondary antibody control (no primary antibody), and an undifferentiated control (HDFs). Stained cells were run on an LSRII flow cytometer (BD Biosciences), and data were analysed using FlowJo (FlowJo LLC, Ashland, OR) software. For each batch of analyses, the gating was set consistent between the differentiated cells and all three controls.

Immunostaining: The appropriate density of cells for immunostaining were seeded (220,000 hiPSC-CMs per well of a 24 well plate with cover slips coated with gelatin) and cultured until ready for fixing (approximately 3 days). The blocking buffer was prepared as follows: 1.5ml Normal Goat Serum, 0.5g Bovine Serum Albumin and 75µl Triton-X were added to 48.5ml DPBS and stirred thoroughly. Medium was aspirated from the cultures and washed carefully with DPBS on a rocking platform for 5 minutes at room temperature. DPBS was aspirated and ice-cold acetone was added and rested for 10 min at room temperature on the bench. Acetone was aspirated and the cultures on cover slips were left to air-dry for 10 minutes at room temperature. The cover slips were transferred to a separate 24-well plate (as plastic in the 24-well plates was found to react with acetone resulting in opacity). The cells were washed three times with DPBS and blocking buffer was added. The cells were left in blocking buffer for 45 minutes to 1 hour at room temperature on a rocking

platform. The primary antibody was made up in the aforementioned blocking buffer at the appropriate dilution factor (see Appendix 3) two minutes before use. This was then added to the cells and left overnight (or up to 24 hours) at +4°C.

The plates containing the primary antibody were equilibrated at room temperature for 30 minutes on a rocking platform the following day. Cells were washed with DPBS+0.5% Triton-X three times at room temperature on a rocking platform, five minutes each time. The secondary antibody was diluted at the appropriate ratio (see Appendix 3) in blocking buffer containing 1% milk and added to the cells. The plate was covered from light and left overnight (or up to 24 hours) at 4°C. The plate was equilibrated at room temperature for 30 minutes covered from light. Cells were washed with DPBS+0.5% Triton-X three times, covered from light, at room temperature on a rocking platform, five minutes each time. The cells were then washed once with DPBS for 5 minutes on a rocking platform at room temperature. The cover slips were mounted in

The cells were fixed with PFA and the plate was stored at 4°C. Within 2 weeks of fixing, the cells were washed with DPBS and permeabilised by incubating in 0.1% Triton X-100 in DPBS for 10 minutes (hiPSC-CM) at room temperature (or incubate for 30 minutes if staining hiPSC due to higher levels of cell compaction). Permeabilisation is only required if staining for intracellular markers. The cells were then washed 3x in 0.1% DPBS-Tween before blocking for 1 hour at room temperature (on a shaker set to approximately 65 rpm) in 10% species-block (i.e. 10% FBS in DPBS). This was then washed twice with DPBS-Tween before treating with primary antibody made up in 1% Species-Block (in DPBS) and incubating overnight at 4°C. The following the day, the plate was washed three times in 0.1% DPBS-Tween, with 5 minutes on shaker at 65rpm for each wash. The fixed and

stained cells were treated with the appropriate secondary antibody (made up in 5% species block) for 1 hour at room temp on the shaker at low speed whilst protecting from light. The cells were washed once again 3x times in 0.1% DPBS-Tween with 5 minutes wash on the shaker each time. Finally, the cells were stained with non-specific DAPI stain for a minimum of 15 minutes, before 2 further washes in DPBS-Tween, followed by suspension in DPBS at 4°C until imaging. The controls included a secondary antibody control (1x well with secondary antibody only, where the primary antibody was replaced with 1% FBS in DPBS); and a labelling control (1x well with no primary or secondary antibody, where each antibody was replaced with the relevant dilution of species block).

The cells were imaged using a Nikon A1R Confocal microscope. Images were acquired at random points on the coverslip at (x) magnification using an image size of a*b pixels, acquiring 3 channels (DAPI/green/red) using a 405/488/561nm laser respectively. A fixed laser power and gain was used for the red channel to eliminate discrepancies in signal that would influence the image analysis.

Image analysis was carried out in NIS-Elements AR. To avoid skewing the data by analysing empty space, a binary mask was applied to the intercellular space by thresholding pixels below the intensity of emitted fluorescence and then inverting the mask, resulting in a complete selection of the cellular space. Once applied, the binary mask was converted into a Region of Interest (ROI). Area data were collected from these ROIs. To count the red marker, a binary mask was applied using a selected intensity range that was deemed to pick up all red signal without artefacts, and this mask was applied to space within the ROIs. Area and object count was collected from this binary mask. This approach counts only the red marker seen inside the cells and allows comparison of the ratio of green: red area

across all images, eliminating any skew that would occur in images with a greater abundance of cells. Nuclei were counted and noted per image so that cell count could be considered alongside the green: red ratio.

Action potential recordings: Action potential (AP) recordings were performed on single CMs, at day 40+/-3 of differentiation. Action potential (AP) measurements were attempted from both quiescent cardiomyocytes that contracted upon field stimulation, and spontaneously contracting cardiomyocytes using whole cell patch clamp technique using an Axopatch 200B amplifier (Molecular Devices). Temperature control apparatus was used to maintain the bath temperature at 37°C. Voltage control, data acquisition, and analysis of I_{Na} and APs were performed with pClamp10.7/Clampfit (Axon Instruments). Adequate voltage control was achieved with low-resistance pipettes (2-2.5 MΩ), series resistance (Rs) and cell membrane capacitance (Cm) compensation, and at a holding potential of -40mV. The protocols used were similar to those previously used by Professor Tinker's group and by other groups[27]. Extracellular and pipette solutions as used by El-Battrawy et al[245] were used. MatLab® was used to make 16-bit integer digitised electrophysiological recordings.

Sodium current recordings: Sodium current recordings were performed on single CMs, at day 40+/-3 of differentiation. Whole cell patch clamp technique using an Axopatch 200B amplifier (Molecular Devices) was used. Temperature control apparatus was used to maintain the bath temperature at 25°C, and the recordings were digitised at 20 kHz and filtered at 4 kHz, with series resistance compensation at 85%. Extracellular fluid was composed as follows: NaCl 20mM, CsCl 120mM, $CaCl_2$ 1mM, $MgCl_2$ 1mM, D-glucose 10mM, HEPES 5mM, and CsOH was added to make the pH 7.4, and 0.01mM Nifedipine +/- either 100μM Ajmaline or 300nmol/L

GS-967. The intracellular fluid concentrations were as follows: NaCl 3mM, CsCl 133mM, $MgCl_2$ 2mM, Na_2ATP 2mM, TEACL 2mM, EGTA 10mM and HEPES 5mM. CsOH was added to make the pH 7.4. The protocol illustrated in Figure 35 was carried out to study the sodium current characteristics.



Figure 35. Protocol for studying INa activation, fast inactivation, characterising voltage dependency of peak INa and late INa.[25]

Results

Recruitment for hiPSC studies and harvesting of dermal fibroblasts

I harvested, isolated, expanded and cryopreserved HDFs from 12 *SCN5A*-E1784K carriers and 2 WT individuals of Caucasian *SCN5A*-E1784K pedigrees (including one WT individual demonstrating genotype-phenotype mismatch). The clinical characteristics of the recruited individuals are depicted in Table 36.

Cell line ID	Age (years)	Sex (M=male; F=female)	Family ID	Spontaneous type 1 Brugada ECG pattern (0=No; 1=Intermittent; 2=Persistent)	Drug-induced type 1 Brugada ECG	QTcB on baseline ECG (ms)	Events (0=None; 1=Pre-syncope; 2=Syncope)	Device (0=None; 1=Single lead ICD; 2=S-ICD;	Medical therapy (0=None; 1=Beta blocker;	E1784K (HET= heterozygous; WT= wild-type)
EC0466	55	F	1	0	1	433	2	1	0	HET
EC1234	49	F	1	0	1	447	1	1	0	WT
EC1425	26	F	1	1	1	482	0	3	0	HET
EC0455	64	F	1	0	1	460	0	1	0	HET
EC0454	46	F	1	0	1	457	0	1	0	HET
EC1055	25	M	2	0	1	498	0	1	0	HET
EC1131	54	F	3	1	1	458	2	1	0	HET
EC1403	16	F	3	0	1	503	0	0	2	HET
EC1630	56	M	4	0	1	469	0	0	2	HET
EC1631	32	F	4	0	0	497	0	0	2	HET
EC1632	55	F	4	0	0	500	2	3	2	HET
EC1633	28	M	4	0	0	485	0	0	1	HET
EC1634	27	M	4	0	0	447	0	0	1	HET
EC1635	48	F	4	0	0	488	1	2	2	HET
EC1636	26	F	4	0	2	440	0	0	0	WT

Table 36. Clinical characteristics of *SCN5A*-E1784K family members who have been recruited for hiPSC studies and from whom fibroblasts have been harvested and cryopreserved (n=14). QTcB: Corrected QT interval using the Bazett's formula.

Figure 36 shows a representative image of harvested HDFs during cell culture.

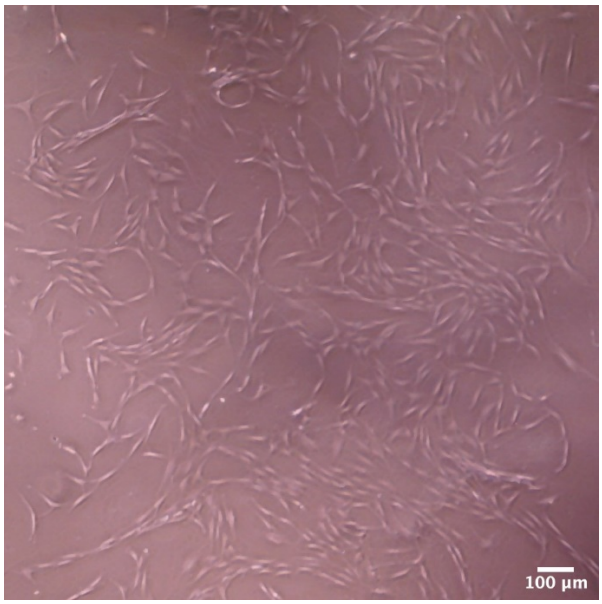


Figure 36. Representative image of HDFs during culture.

Cellular reprogramming and clonal isolation

Three patient cell lines, EC1131 (BrS phenotype); EC1635 (Long QT phenotype); EC1425 (mixed BrS/Long QT phenotype), were initially selected for hiPSC reprogramming and differentiation.

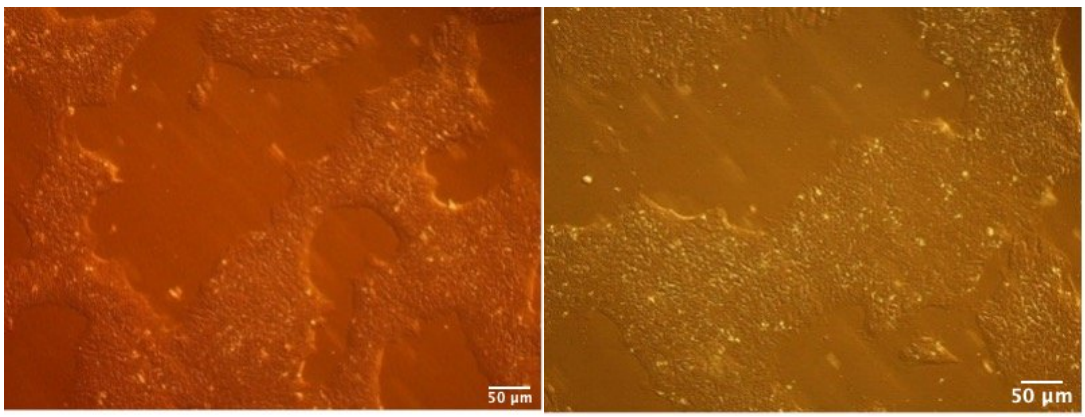
EC1131 (BrS): On reprogramming with Sendai virus, this cell line did not form distinct colonies, but instead formed uneven colonies that merged. In the first attempt at reprogramming this line, all the reprogrammed clones were lost to bacterial contamination between days 25-30. In the second attempt at reprogramming this line, none of the manually cut colonies survived passaging and clonal expansion. The third attempt at reprogramming was successful and two monoclonal lines were cryopreserved. However, both clones did not survive beyond passages 6-9, and could not be thawed successfully. Two polyclonal lines were

expanded (polyclonal line 1 was obtained by peeling off fibroblasts from a 35mm dish, allowing the clones to expand, then harvesting all the clones using EDTA, and polyclonal line 2 was obtained by cutting 2-3 colonies into 1 well of a 48 well plate). At P8, polyclonal line 1 was seeded at low densities onto 35mm dishes (100 cells, 1000 cells, 5000 cells, 10,000 cells and 20,000 cells per 35mm dish). The cells in the dish with just 100 cells did not survive, but the others survived, although 20,000 cells became confluent very quickly. Best densities to isolate single clones were found to be 1000 and 5000 cells per 35mm dish, and single clones were isolated from all the four higher densities between 6 and 12 days of seeding. These clones were expanded 4-5 passages after isolation and cryopreserved. However, none of the cryopreserved clones survived thawing. Both polyclonal lines thawed successfully, and these were expanded and further polyclonal cell stocks cryopreserved. Further attempts at isolating monoclonal lines were made by seeding the polyclonal cells at low densities in 96 well plates followed by clonal expansion from wells that only formed single colonies of monoclonal morphology. Such colonies were passaged and expanded until monoclonal lines were successfully isolated and clonally expanded.

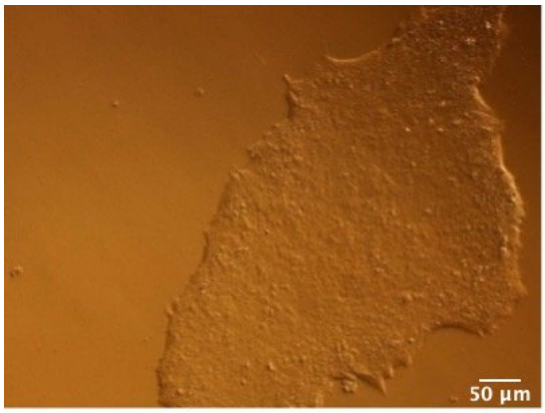
EC1425 (BrS and LQT3): Reprogramming efficiency of this line was very low. The first attempt at reprogramming was successful but only very few colonies formed. Two colonies grew to sufficient size to be manually cut in the fifth week after transfection and these survived clonal expansion. Given the low efficiency of reprogramming, another attempt at reprogramming was made using 2xMOI of klf4, however no colonies formed at all. By this time, the clones isolated from the first attempt were becoming established, therefore the second attempt was abandoned. The clonal lines were expanded and cryopreserved.

EC1635 (LQT3): Only one clone survived following the first reprogramming attempt, but cell survival dropped by passage 5-6. An attempt was made to expand and cryopreserve these cells, but this line could not be expanded, and as expected, none of the cells survived thawing. The second attempt at reprogramming was successful, although clumping of HDFs was observed on passaging the cells from the 6 well plate to 3x 35mm dishes. The colonies didn't expand well and appeared to be growing in 3D structures. Manual colony cutting that was attempted at day 18-24 failed. The fibroblasts were then peeled off from all 3 dishes by washing with media carefully from one edge to lift the HDF layer using a 200uL pipette. Only few colonies remained on the dish and whilst these initially appeared unhealthy, on maintained culture for a further week, multiple sizeable colonies appeared and grew well. These colonies were cut manually between days 28-32 and the clonal lines were expanded.

Representative images of the hiPSC cultures are shown in Figure 37.



a) b)



c)

Figure 37: Representative images of hiPSC clones being expanded from (a) EC1131, (b) EC1425, and (c) EC1635.

Cell banks of monoclonal lines were cryopreserved from all three patient lines, however hiPSCs from EC1425 had poor survival on thawing and slow growth. Due to limited time available and previous failure to reprogram EC1425 on the second attempt, the decision was made not take this cell line forward, and to focus the study on EC1131 (BrS phenotype only) and EC1635 (Long QT phenotype only). The monoclonal lines from EC1131 and EC1635 had stable growth curves, therefore these were taken forward for further characterisation, along with the healthy control (REBL-PAT) cell line from University of Nottingham.[228]

Karyotyping

Karyotyping was carried out every 10-15 passages. The below hiPSC clones had normal karyotypes (n=30 cells analysed from each batch):

EC1131 clone 2: 46,XX[22]; 45,XX,-19[1]; 45,XX,-21[1]; 24 metaphase cells only present.

EC1131 clone 3: 46,XX[30]

EC1425 clone 3: 46,XX[29]; 45,XX,-5[1]

EC1635 clone 3: 46,XX[30]

EC1635 clone 5: 46,XX[30]

The below karyotype was equivocal and will need to be repeated if further work is to be done using this clone: EC1425 clone 1: 46,XX[26]; 45,XX,-20[1]; 45,XX,-21[1]; 45,XX,-22[1]; 44,XX,-17,-18[1]

The karyotyping results for EC1635 clone 4 were abnormal:

46,XX,t(7;15)(q32;q22),t(11;16)(p11.2;p11.2)[15]

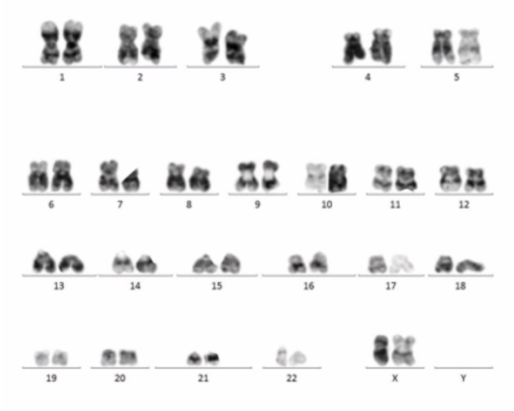
47,XX,t(7;15)(q32;q22),t(11;16)(p11.2;p11.2),+mar[15]

EC1635 clone 5 and EC1425 clone 3 were expanded and cell banks were cryopreserved (P10-15).

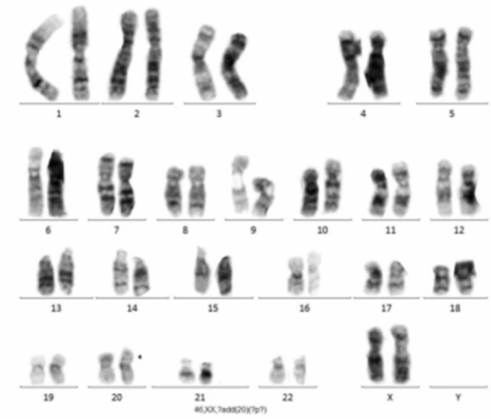
The clones of the three hiPSC lines that were taken forward for differentiation and phenotyping during the study were all karyotyped at passage 10-15 and again at passage 25-35. All were found to have a normal karyotype (46,XY for REBL-PAT, and 46,XX for EC1131 and EC1635). The karyograms of the three clones from the three cell lines that were taken forward for phenotyping are shown in Figure 38.



a)



b)



c)

Figure 38. Karyograms for (a) REBL-PAT (passage 34) EC1131 (passage 27) and (b) EC1635 (passage 29). All three clones had normal karyotype.

Growth curves

Growth curves were recorded for REBL-PAT, EC1131 and EC1635 over 15 passages demonstrating steady growth curves. Figure 39 shows the results of the growth curves recorded. One data point is missing due to a manual cell count error.

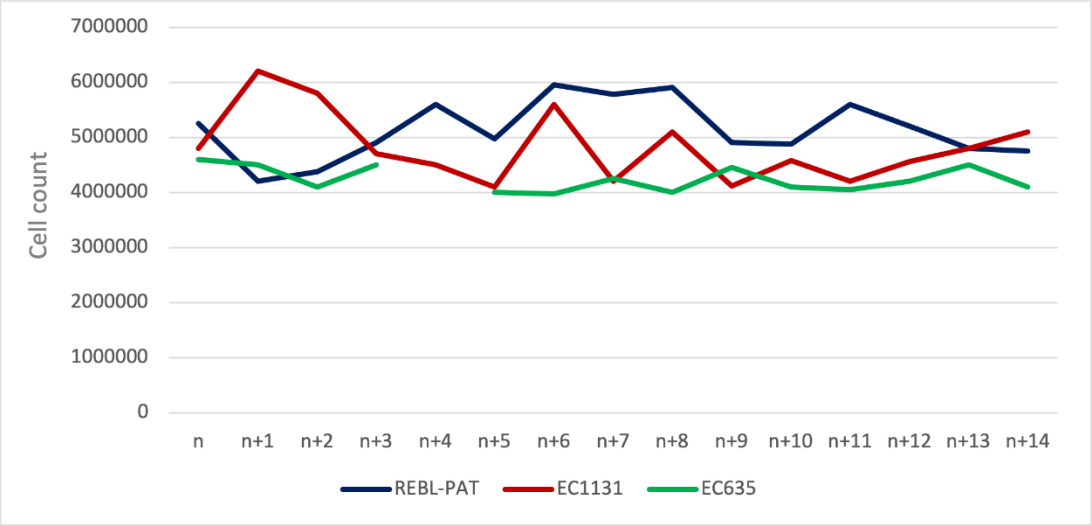


Figure 39. Growth curves of REBL-PAT (seeding density 800,000 cells / T25), EC1131 (seeding density 900,000 cells / T25) and EC1635 (1,000,000 cells / T25) hiPSC lines across 15 passages. One data point is missing (EC1635) due to a cell count error.

Immunostaining of hiPSC

Figure 40 shows immunostaining of REBL-PAT, EC1131 and EC1635 hiPSCs for the pluripotency markers Oct4, Sox2, Tra-1-60 and SSEA4 respectively.

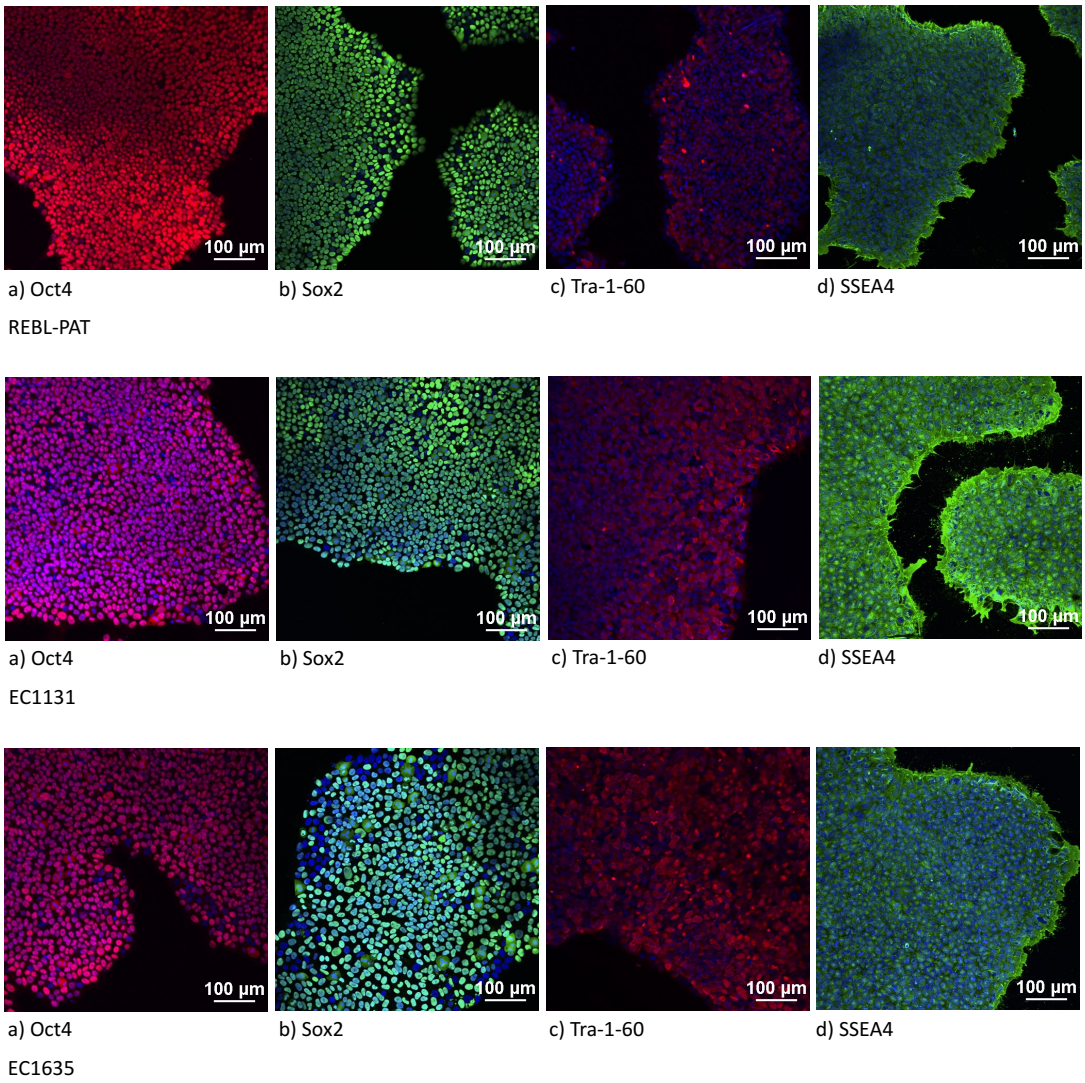


Figure 40. Immunostaining of REBL-PAT, EC1131 and EC1635 hiPSCs for pluripotency markers a) Oct4, b) Sox2, c) Tra-1-60 and d) SSEA4. Non-specific DAPI (nuclear) staining is shown in blue.

hiPSC differentiation to cardiomyocytes

The hiPSC-CMs from initial differentiation attempts were cryopreserved for use as initial practice lines for electrophysiological characterisation. Of these, only one line were thawed successfully and survived at a sufficiently high purity for initial attempts at electrophysiological phenotyping. Further differentiation attempts were made at St George's, University of London by applying the same protocols and the seeding densities that were optimised for these lines by myself at University of Nottingham. However, initial success at differentiation were variable. Whilst some batches of

cells differentiated very well into uniform monolayers, appearing visually close to 100% purity (particularly EC1635-CM), other attempts failed, with no cells surviving beyond day 2 of differentiation. The seeding densities for differentiation were re-optimised for each line to attempt to achieve consistency in differentiation between attempts and to maintain a constant supply of cells for electrophysiological characterisation.

From each batch of cardiac differentiation, I have (a) extracted RNA, reverse transcribed this and stored cDNA; and (b) extracted protein for future work on: qPCR and Western blotting respectively.

FACS assessment of purity of hiPSC-CM differentiation

The purity of differentiated hiPSC-CMs were assessed with flow cytometry. Purity assessment was done for each line from at least 2 separate differentiations. Results are shown on Figure 41. The mean purities were as follows: REBL-PAT: 89% (n=3); EC1131: 92% (n=2); EC1635: 96% (n=2). Troponin-T2 (TNNT2) positivity for the undifferentiated controls (HDFs) was 0.37% (n=6). The TNNT2 positivity for the untreated controls and the secondary antibody controls were 0.03 and 0.17 respectively (n=13).

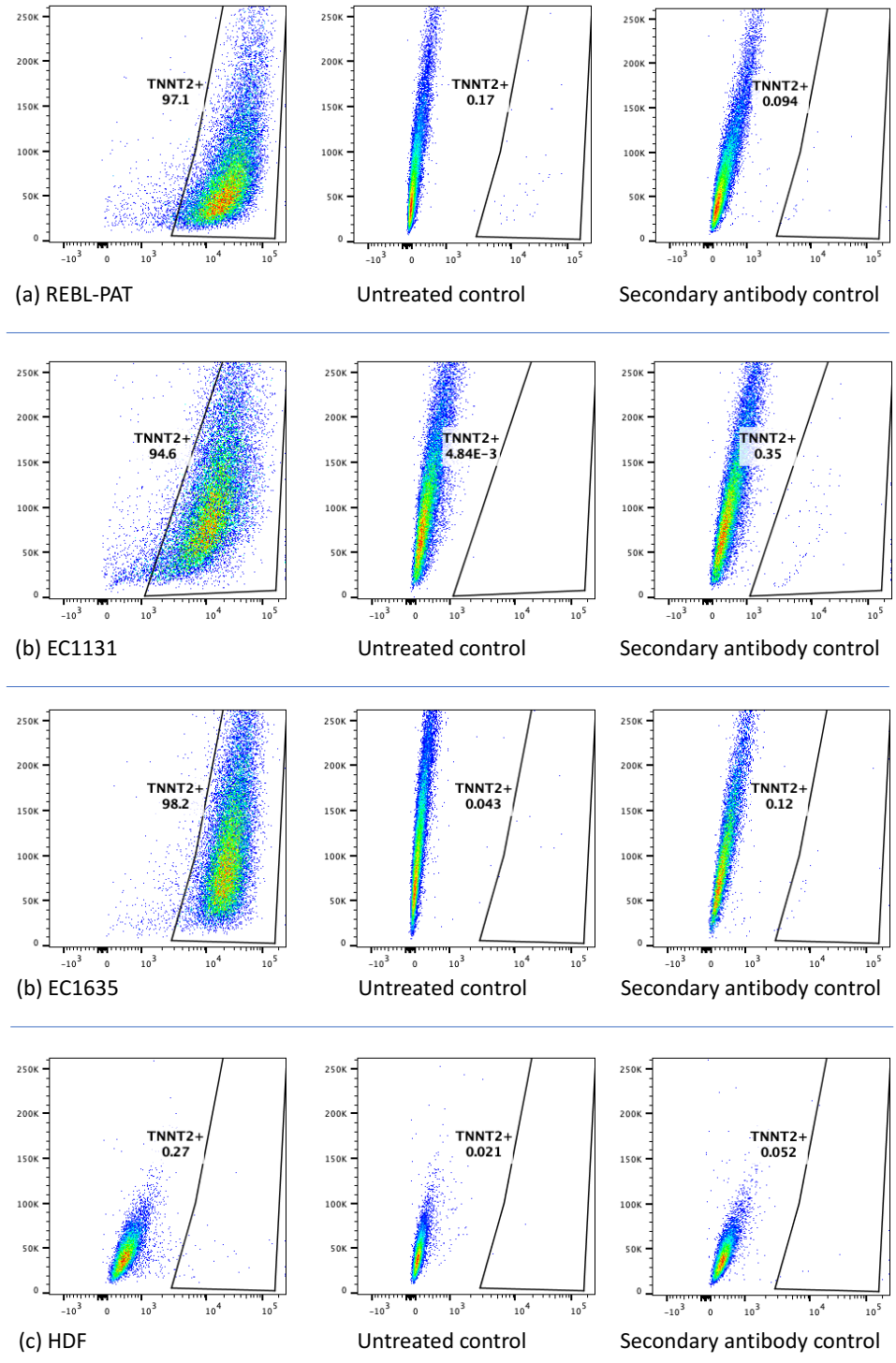


Figure 41. FACS assessment of purity. Representative differentiations are shown. (a) REBL-PAT; (b) EC1131; (c) EC1635; (d) HDFs (undifferentiated control). The first panel are the cells of interest; the second panel shows the respective untreated controls, and the third panel shows the respective secondary antibody controls (no primary antibody).

Immunostaining of hiPSC-CM

Figure 42 shows the myofilament architecture of the differentiated cells in a monolayer (REBL-PAT). Figure 43 shows randomly selected images at high magnification of dissociated hiPSC-CMs from one line (EC1131) to demonstrate the structure of the differentiated cells and variability in morphology.

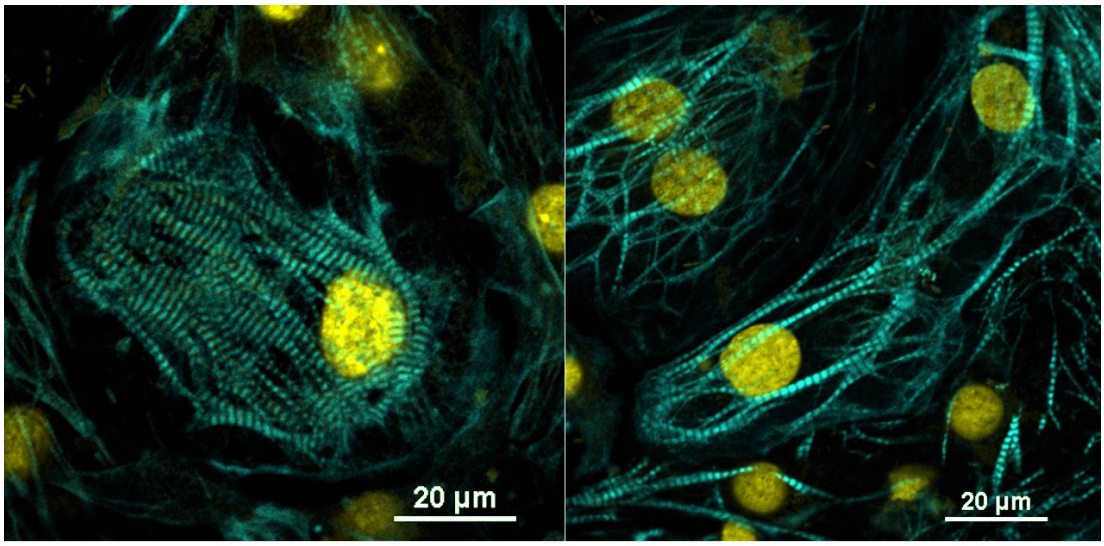


Figure 42. Myofilament architecture in differentiated cardiomyocytes in a monolayer (REBL-PAT). Troponin-T staining is in cyan, Non-specific DAPI staining is shown in yellow.

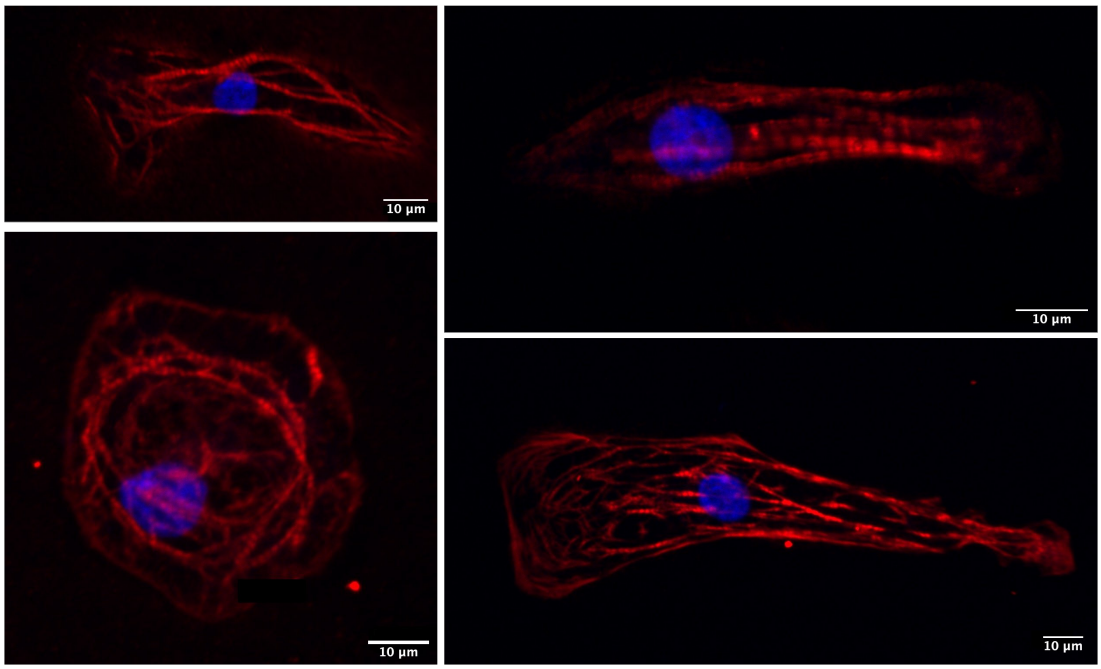
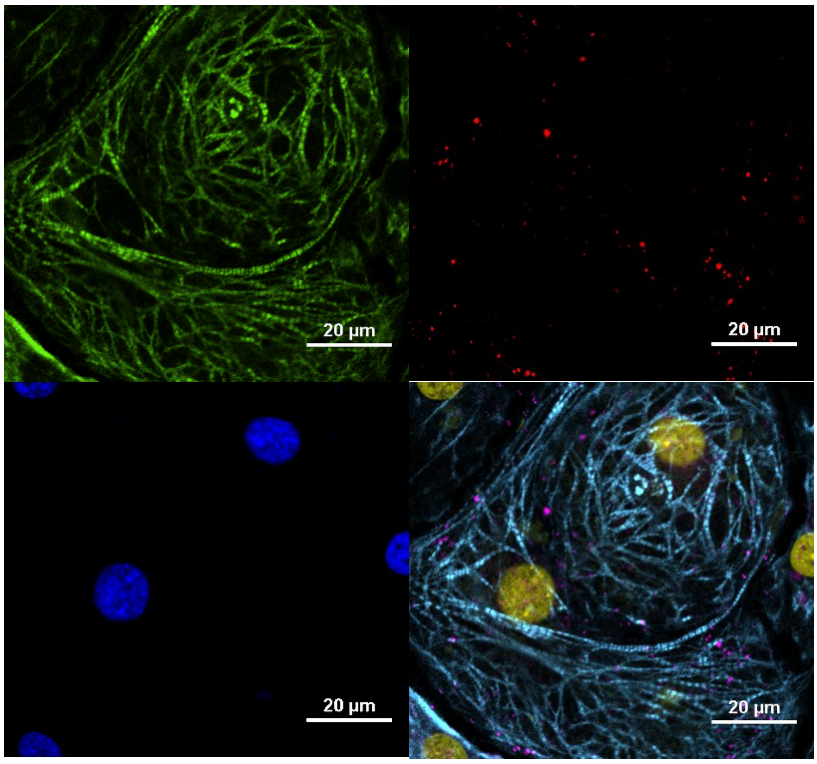


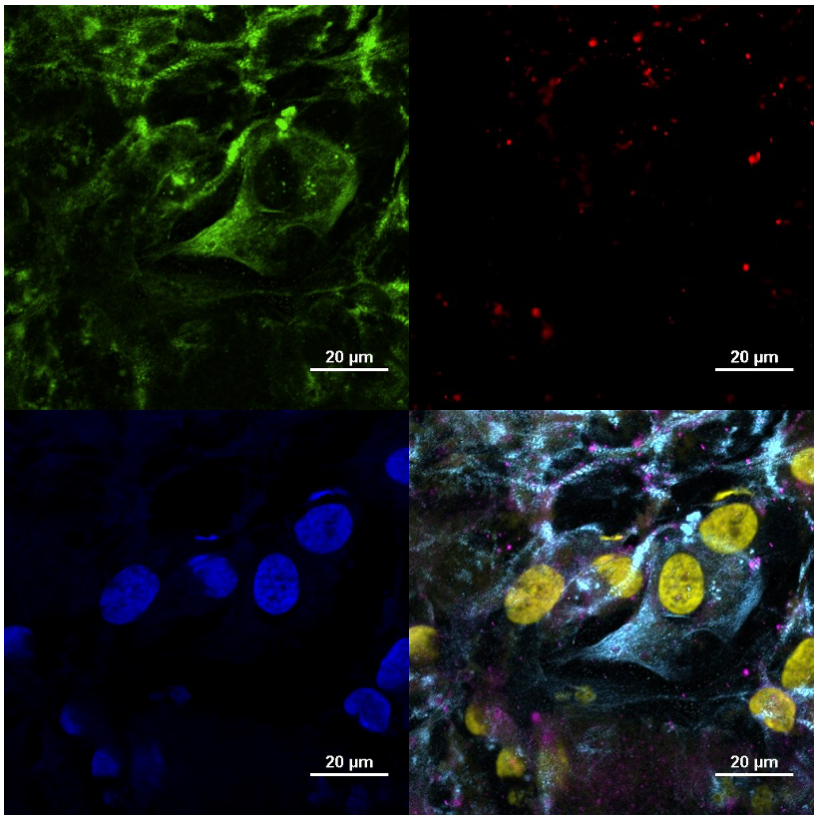
Figure 43. Dissociated hiPSC-CMs from one line (EC1131) to demonstrate the structure of the differentiated cells and variability in morphology. Troponin T2 is stained red. Non-specific DAPI (nuclear) staining is shown in blue.

Figure 44 shows representative examples of dual staining images of hiPSC-CMs from the three cell lines of interest: a) REBL-PAT (control); b) EC-1131 (BrS) and c) EC1635 (Long QT phenotype) with DAPI, Troponin T2 and $Na_v1.5$. In each case, the three stains are depicted separately, followed by the combined image in a different colour palette to improve visibility of the co-staining. A limitation is that a membrane marker was not used as a primary antibody co-stain with $Na_v1.5$. The quality of immunostaining in the REBL-PAT line was better compared to the staining quality achieved in the EC1131 and EC1635 lines when co-staining with Troponin T2 and $Na_v1.5$. The image quality of the EC1131 and EC1635 lines were affected by uneven monolayer formation on the coverslips used for imaging. Overall, the quality of the $Na_v1.5$ staining was weak. Due to difficulty in interpretation of the qualitative data from $Na_v1.5$ staining, I sought to undertake quantitative analysis.

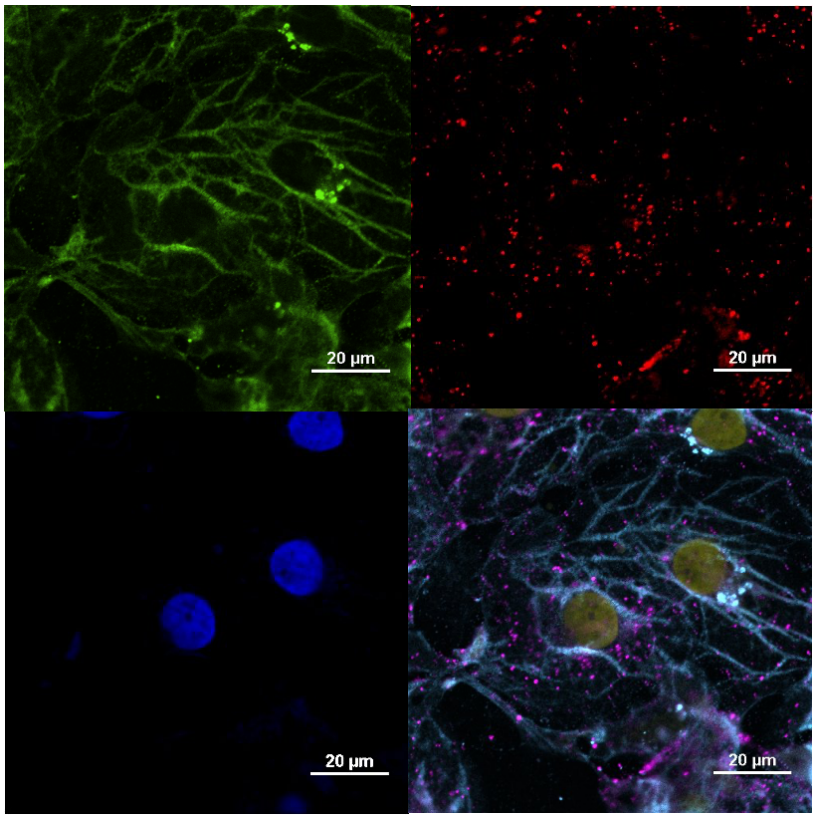
Results of quantitative analyses of $Na_v1.5$ expression between the three cell lines are shown in Table 37. The number, area and intensity of $Na_v1.5$ signals per cell in the control line, BrS line and Long QT line were compared. The BrS line had a trend towards less $Na_v1.5$ signals per cell, less total area of $Na_v1.5$ signals per cell, and less [area x mean intensity] of $Na_v1.5$ signal per cell compared to both the control line and the Long QT line, however the results failed to reach statistical significance ($p=0.298$, $p=0.314$, $p=0.133$ when comparing control vs BrS, control vs Long QT phenotype and BrS vs Long QT phenotype respectively).



a)



b)



c)

Figure 44. Example images of immunostaining of REBL-PAT-CM (healthy control), EC1131-CM (BrS phenotype) and EC1635-CM (Long QT phenotype) with Troponin-T (green), $Na_v1.5$ (red) and nuclear (blue) staining as individual channels. The contrast of the red channel only has been increased by an equal extent in all three images for comparability. The colour palette was changed for the combined imagith Troponin-T (cyan), $Na_v1.5$ (magenta) and nuclear staining (yellow).

	Cell line	Number of Nav1.5 signals	Total area covered by Nav1.5 signal (μm^2)	Sum of the mean intensity of Nav1.5 signal within the field of view (M)	[Area (A) x Mean intensity] of Nav1.5 signal (M)	Sum of the total intensity of Nav1.5 signal within the field of view (T)	Total area covered by cells (μm^2)	Number of complete nuclei (n)	Number of partial nuclei (pn)	Representative number of nuclei (n+0.5pn)	Number of Nav1.5 signals / area covered by cells	Total area of Nav1.5 signal / area covered by cells	[Area (A) x Mean intensity (M)] of Nav1.5 signal / area covered by cells	Number of Nav1.5 signals / representative number of nuclei	Total area of Nav1.5 signal / representative number of nuclei	[Area (A) x Mean intensity (M)] of Nav1.5 signal / representative number of nuclei
	Control	234	80.6	406423	32737373	3817157	9280.6	5	2	6	0.0252	0.0087	3528	39.00	13.43	5456229
	Control	201	50.7	364660	18480969	2726866	10368.8	4	1	4.5	0.0194	0.0049	1782	44.67	11.26	4106882
	Control	378	140.4	714966	100409825	7718598	10709.9	7	3	8.5	0.0353	0.0131	9375	44.47	16.52	11812921
	Control	303	74.1	567341	42056988	3965581	9538.5	2	2	3	0.0318	0.0078	4409	101.00	24.71	14018996
	Control	386	112.7	687976	77534895	5675350	10201.6	9	2	10	0.0378	0.0110	7600	38.60	11.27	7753490
	Control	450	133.3	788541	105096744	6494540	10118.5	7	5	9.5	0.0445	0.0132	10387	47.37	14.03	11062815
	Control	463	220.2	809992	178376438	10963630	9674.0	8	6	11	0.0479	0.0228	18439	42.09	20.02	16216040
	Control	374	156.9	711988	111689558	8482856	10252.2	5	8	9	0.0365	0.0153	10894	41.56	17.43	12409951
	Control	275	67.9	504286	34235977	3533040	10474.8	5	6	8	0.0263	0.0065	3268	34.38	8.49	4279497
	Control	290	68.7	521169	35793887	3468858	10220.7	10	2	11	0.0284	0.0067	3502	26.36	6.24	3253990
	Control	372	104.2	709045	73903760	5706883	10524.9	5	5	7.5	0.0353	0.0099	7022	49.60	13.90	9853835
Mean	**Control**	**339**	**110.0**	**616944**	**73665129**	**5686669**	**10124.0**	**6.1**	**3.8**	**8.0**	**0.03**	**0.01**	**7292**	**46.28**	**14.30**	**9111331**
SD	**Control**	**85**	**50.0**	**152044**	**47787979**	**2553847**	**444.5**	**2.3**	**2.3**	**2.6**	**0.01**	**0.01**	**4845**	**19.24**	**5.23**	**4415928**
SEM	**Control**	**26**	**15.1**	**45843**	**14408618**	**770014**	**134.0**	**0.7**	**0.7**	**0.8**	**0.00**	**0.00**	**1461**	**5.80**	**1.58**	**1331452**
	BrS	508	206.4	853424	176138113	10161638	8071.8	7	6	10	0.0629	0.0256	21821	50.80	20.64	17613811
	BrS	545	121.3	863483	104714536	5253237	8738.5	13	3	14.5	0.0624	0.0139	11983	37.59	8.36	7221692
	BrS	524	159.9	8300280	1327214793	6724347	9606.6	10	12	16	0.0545	0.0166	138157	32.75	9.99	82950925
	BrS	455	108.1	717089	77488588	4764009	9174.6	16	10	21	0.0496	0.0118	8446	21.67	5.15	3689933
	BrS	308	85.5	506623	43336490	3976354	9617.3	18	3	19.5	0.0320	0.0089	4506	15.79	4.39	2222384
	BrS	474	178.6	789225	140963452	8651104	8173.5	15	2	16	0.0580	0.0219	17246	29.63	11.16	8810216
	BrS	335	184.2	638899	117653291	10151190	8886.1	5	4	7	0.0377	0.0207	13240	47.86	26.31	16807613
	BrS	265	88.0	472888	41604692	4445169	8829.0	8	2	9	0.0300	0.0100	4712	29.44	9.78	4622744
	BrS	415	107.8	672067	72435386	4824674	10415.0	17	5	19.5	0.0398	0.0103	6955	21.28	5.53	3714635
Mean	**BrS**	**425**	**137.7**	**1534886**	**233505482**	**6550191**	**9056.9**	**12.1**	**5.2**	**14.7**	**0.05**	**0.02**	**25230**	**31.87**	**11.26**	**16405995**
SD	**BrS**	**101**	**45.1**	**2540742**	**412513476**	**2483939**	**742.3**	**4.8**	**3.6**	**5.0**	**0.01**	**0.01**	**42739**	**11.90**	**7.45**	**25579982**
SEM	**BrS**	**34**	**15.0**	**846914**	**137504492**	**827980**	**247.4**	**1.6**	**1.2**	**1.7**	**0.00**	**0.00**	**14246**	**3.97**	**2.48**	**8526661**
	LQTS	317	107.2	568567	60956014	5282521	10360.4	9	5	11.5	0.0306	0.0103	5884	27.57	9.32	5300523
	LQTS	274	106.8	439836	46956891	4915309	9256.2	9	3	10.5	0.0296	0.0115	5073	26.10	10.17	4472085
	LQTS	603	294.0	1052395	309351510	14393435	10367.9	9	3	10.5	0.0582	0.0284	29837	57.43	28.00	29462049
	LQTS	160	55.7	289147	16114173	2864198	10619.6	6	4	8	0.0151	0.0052	1517	20.00	6.97	2014272
	LQTS	708	321.4	1240845	398807583	16082293	9524.1	8	2	9	0.0743	0.0337	41873	78.67	35.71	44311954
	LQTS	700	276.3	1239252	342392935	13928674	10258.2	12	7	15.5	0.0682	0.0269	33378	45.16	17.83	22089867
	LQTS	671	233.9	1169865	273678218	11437122	9857.8	9	3	10.5	0.0681	0.0237	27763	63.90	22.28	26064592
	LQTS	490	170.7	934851	159607077	9294037	10012.8	3	1	3.5	0.0489	0.0171	15940	140.00	48.78	45602022
	LQTS	214	62.9	398481	25044525	3486693	10318.4	9	6	12	0.0207	0.0061	2427	17.83	5.24	2087044
	LQTS	420	152.0	752988	114446646	7858346	9588.3	9	4	11	0.0438	0.0159	11936	38.18	13.82	10404241
	LQTS	362	134.2	637799	85618071	6843700	9767.2	6	6	9	0.0371	0.0137	8766	40.22	14.92	9513119
	LQTS	572	167.6	1025668	171891700	8405513	9081.7	7	2	8	0.0630	0.0185	18927	71.50	20.95	21486463
	LQTS	350	133.8	613212	82066095	6753757	10298.1	15	7	18.5	0.0340	0.0130	7969	18.92	7.23	4436005
	LQTS	585	258.5	1044530	269969224	13207492	10528.6	13	6	16	0.0556	0.0245	25641	36.56	16.15	16873076
Mean	**LQTS**	**459**	**176.8**	**814817**	**168350047**	**8910935**	**9988.5**	**8.9**	**4.2**	**11.0**	**0.05**	**0.02**	**16924**	**41.86**	**16.12**	**17436951**
SD	**LQTS**	**184**	**86.0**	**326108**	**127692409**	**4270280**	**484.4**	**3.0**	**2.0**	**3.8**	**0.02**	**0.01**	**12830**	**32.84**	**12.26**	**14788437**
SEM	**LQTS**	**49**	**23.0**	**87156**	**34127232**	**1423427**	**161.5**	**1.0**	**0.7**	**1.3**	**0.31**	**0.14**	**3429**	**39.11**	**18.25**	**3952376**

Table 37. Quantitative analyses of hiPSC-CM from EC1131 (BrS), EC1635 (Long QT phenotype), REBL-PAT (control line) to compare $Na_v1.5$ expression.

Preliminary electrophysiological characterisation

Figure 45 shows example action potential recordings from the three differentiated hiPSC-CM lines. Both spontaneous and triggered action potentials are shown. As is evident in the figure, wide variability in the resting membrane potentials (-20 to -90mV) was observed in all three cell lines. Further, spontaneity of the cell contractions was also widely variable between cells, both within a single cell line and between cell lines. Some cells were quiescent. The morphologies of the action potentials from different cells also resembled atrial-like action potentials, ventricular-like action potentials or pacemaker-like action potentials. Due to time constraints, the recordings made were insufficient for quantitative analyses of the action potential characteristics between cell lines.

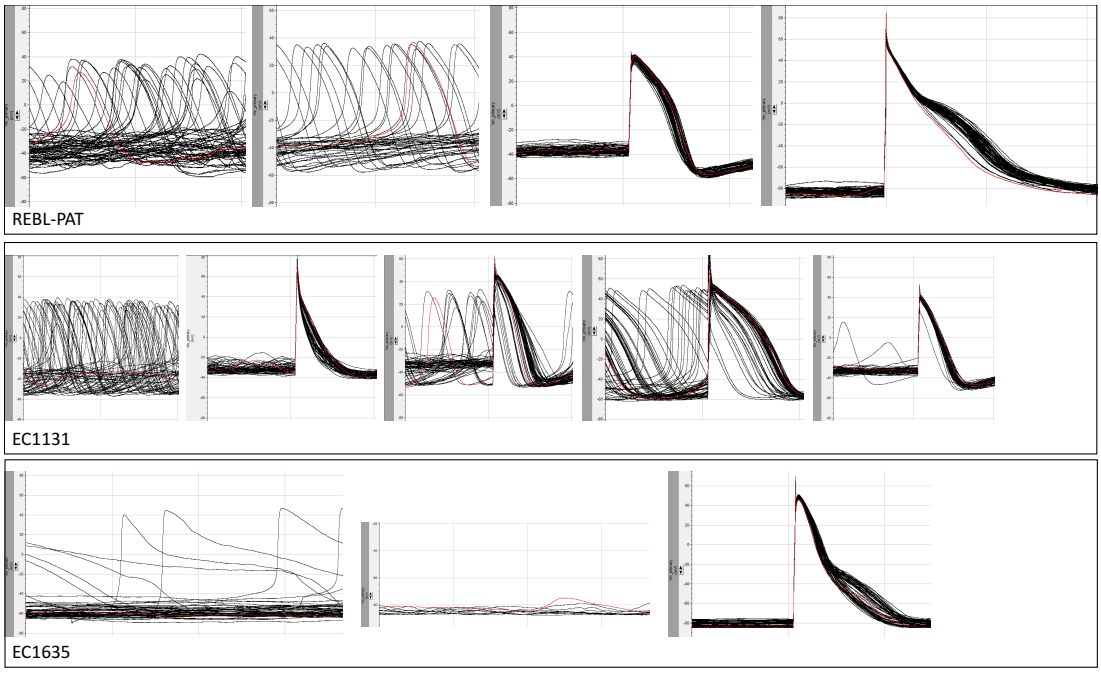


Figure 45. Example action potential recordings from REBL-PAT (Control line), EC1131 (BrS line), EC1635 (Long QT line).

INa characterisation was also attempted, however this was only possible for two cell lines (REBL-PAT and EC1635). Again, variability in the measurements was observed, with some cells having a large INa, while other cells had comparably minute INa. Further, some cells, including in the control line (as shown in the recording on the top right of the panel in Figure 46) had a marked late inward sodium current, but this was observed inconsistently in the cells. The recordings made were limited by time constraints, meaning quantitative analyses were not possible, and no reliable pharmacological studies could be done on these cells.

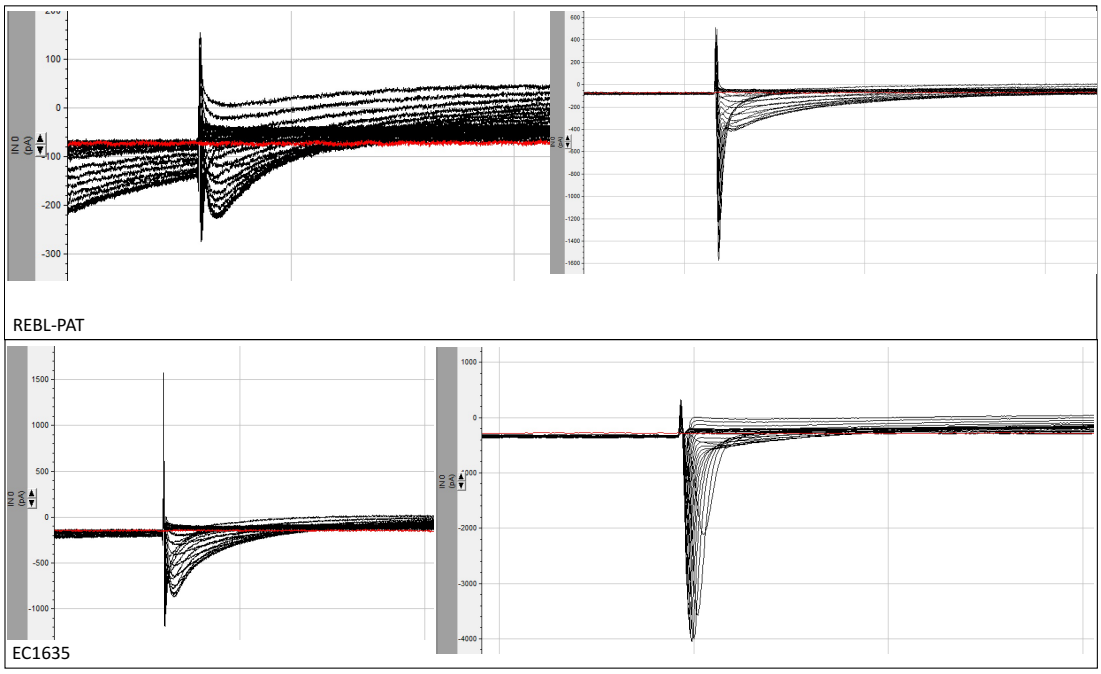


Figure 46. Example INa recordings from REBL-PAT (Control line) and the EC1635 (Long QT line).

Discussion

The aim of this arm of the study was to produce hiPSC-CMs from *SCN5A*-E1784K carriers with extremes of phenotype. hiPSC-CM lines were successfully produced and characterised from a patient with severely prolonged QTc but no BrS (EC1635) and one with a spontaneous type 1 Brugada ECG pattern but no Long QT

phenotype (EC1131). The control cell line was a healthy cell line that had been produced in-house at University of Nottingham (REBL-PAT)[228].

hiPSC reprogramming and validation

hiPSC validation was carried out through demonstration of cell morphology, immunostaining for pluripotency markers, demonstration of steady growth curves, and ability to differentiate to cardiomyocytes. The variability in the counts on the growth curves is likely to be accounted for by limitations in manual counting. The cells were stained for pluripotency markers Oct4, Sox2, Tra-1-60 and SSEA4 with strong demonstrability of pluripotency. Sox2 and Oct4 were among reprogramming factors that the HDFs were transfected with, however positivity for Tra-1-60 and SSEA4 demonstrate that the cells have been successfully reprogrammed and have produced the latter. Oct4 and Sox2 are intracellular markers, whereas Tra-1-60 and SSEA4 are surface markers, which accounts for the differences between these markers in the morphological appearances of the stained cells. Cells are known to accumulate karyotype abnormalities on repeated passaging.[246] All cell lines had normal karyotype at passages used for differentiation. Differentiation of the reprogrammed cells to three germ layers was not carried out due to time constraints. The decision was made not to carry out a further test for pluripotency, teratoma formation, in mouse models, for ethical reasons.

Cardiomyocyte differentiation and validation

The reprogrammed hiPSCs were successfully differentiated to hiPSC-CMs from the three cell lines REBL-PAT, EC1131 and EC1635 once optimal seeding densities were determined for each cell line. It has been shown that cryopreservation of hiPSC-CMs is not detrimental to the *in vitro* molecular and functional properties of the cells.[247] However, in order to avoid bias, I only subjected fibroblasts and hiPSCs

through the freeze-thaw process. All hiPSC-CMs were freshly differentiated and used for phenotyping between day 37 and 43. None of the differentiated cells were cryopreserved. Culture of the differentiated cells to day 40 has been shown to improve the maturation properties of the cells. Specifically, prolonged culture has been shown to result in more efficient intercellular calcium handling, a statistically significant increase in *CX43*, a better developed contractile apparatus, and expression of many genes similar to human ventricular cardiomyocytes.[248] The increase in *CX43* expression is relevant to functional studies on the BrS phenotype, as BrS has been shown to reduce *CX43* expression. The hiPSC-CM cultures were validated with Troponin T2 staining, assessed for purity using flow cytometry, and electrophysiological features studied (albeit incompletely) with whole cell patch clamp techniques. The quality of immunostaining was variable, with better quality images obtained from the control lines. The electrophysiological characterisation is discussed further below.

Electrophysiological characterisation

Action potential and sodium current recordings made on the cells demonstrated wide inter- and intra-line variability in the electrophysiological phenotype. Whole cell patch clamp recordings on both quiescent and spontaneously beating cells revealed heterogeneity in the electrophysiological characteristics of the cells. Action potential morphologies were heterogeneous and resembled ventricular-like, atrial-like and pacemaker-like morphologies. When inadequate patch champ recordings were eliminated, there were limited numbers of cells for reliable quantitative analyses.

Larger numbers of cells, and from at least three separate differentiations, are required to effectively study quantitative associations with phenotype, due to limitations with intra-line and inter-line variability as has been described before.

[228,249,250] The highly negative resting membrane potential (-80 to -90mV) observed in some cells was close to the human ventricular action potential, and is a reflection of better maturation of the cells. However, these findings were variable between cells and no clear association with phenotype was seen on qualitative data. While the findings are preliminary, the study gave me a strong foundation in practical skills required to perform whole cell patch clamp, and the skills acquired can be taken forward for future work.

Limitations

I derived and characterised two hiPSC-CM lines from extremes of phenotype in *SCN5A*-E1784K. To our knowledge, this is the first time that this has been done and the two hiPSC cell lines that were created and validated provide an invaluable resource for future work.

The quality of immunostaining in the patient lines was compromised due to unevenness of the cell monolayers that formed on the coverslips used for imaging, and staining for $Na_v1.5$ was weak. Change in the colour palette did not improve interpretability of the images. The quantitative data were limited by the number of cells analysed and further work is required with larger numbers of cells.

The electrophysiological phenotyping that was achieved during this study was severely limited by cellular heterogeneity and feasibility within the time resources available. The electrophysiological phenotype was assessed using single cell electrophysiology, which requires a high level of skill and is low throughput. The chemically defined, monolayer differentiation method was chosen as it has been shown to be more efficient and reliable with high cardiac specification compared to the embryoid body method used by Okata *et al*, for example.[177,195,242] Metabolic

selection by use of a gluocose-depleted medium with lactate enrichment was used to improve purity of the differentiated cultures.[251] A maturation technique involving the addition of T3 and dexamethasone to the hiPSC-CM culture medium was then employed to improve the maturity of the cells in accordance with available data at the time.[244,252] However, issues with the inter-line and intra-line variability in the differentiated cells could not be sufficiently overcome within the time constraints of the study to derive reliable electrophysiological data through whole cell single cell patch clamp technique. The reasons for this are multiple, including contamination of cells during reprogramming and failed differentiation attempts that required repetition and re-optimisation of differentiation attempts, all of which led to loss of valuable time that could have been used to obtain a higher volume of electrophysiological data to enable quantitative analyses of action potentials and sodium current characteristics.

Future work involving deep single cell electrophysiological phenotyping (as described below) is planned with optimised differentiation techniques and better cell selection into mature ventricular-like hiPSC-CMs. Techniques for achieving this would involve, for example, use exogeneous fatty acids as an energy source, and recapitulating the key events that regulate ventricular development and maturation in vivo, as has been described by Funakoshi *et al* this year.[253] Cardiac tissue engineering using engineered heart tissue combining scaffolding polymers and electromechanical stimulation are other techniques that can be explored to achieve a more mature, ventricular-like hiPSC-CM model.[254,255]

Future work: Planned electrophysiological characterisation

Action potential analyses

Quantitative analyses of the action potential recordings are planned once more recordings have been made from these cells. The resting membrane potential (RMP), maximal upstroke velocity (Vmax), AP amplitude (APA), and AP duration (APD) at 20, 50 and 90% repolarisation (APD20, APD50, and APD90, respectively) will be analysed. APD90/50 and APD30-40/APD70-80 ratios will be calculated for a minimum of 30 cells from each batch of differentiation (both quiescent and spontaneously contracting cells), and separated into atrial-like, ventricular-like and pacemaker-like cells based on their APD ratios.

Sodium current characteristics and pharmacological studies

Sodium current recordings will be performed on single CMs, at day 40+/-3 of differentiation. Whole cell patch clamp technique using an Axopatch 200B amplifier (Molecular Devices) will be used. Temperature control apparatus will be used to maintain the bath temperature at 25°C, and the recordings will be digitised at 20 kHz and filtered at 4 kHz, with series resistance compensation at 85%. Extracellular fluid will be composed as follows: NaCl 20mM, CsCl 120mM, $CaCl_2$ 1mM, $MgCl_2$ 1mM, D-glucose 10mM, HEPES 5mM, and CsOH will be added to make the pH 7.4, and 0.01mM Nifedipine +/- either 100μM Ajmaline or 300nmol/L GS-967. The intracellular fluid concentrations will be as follows: NaCl 3mM, CsCl 133mM, $MgCl_2$ 2mM, Na_2ATP 2mM, TEACL 2mM, EGTA 10mM and HEPES 5mM. CsOH will be added to make the pH 7.4.

Preliminary studies on pharmacological responses will be carried out using ajmaline and GS967, a novel sodium channel inhibitor that had exhibited antiarrhythmic effects in various *in vitro* and *in vivo* models. All the protocols described in Chapter

1 (Figures 3-7) would be carried out with extracellular fluid and nifedipine, followed by repeat of all protocols after addition of GS967, after which protocol 1 and 5 would be done after washout of the drug. A similar process will be carried out in the case of ajmaline, but with protocol 1 only after washout of the drug (protocols described in Figures 3-7, Chapter 1).

Chapter 8: Summary and Future Work

Summary

SCN5A-E1784K is the single most common mutation identified in BrS but predicting phenotype and genotype-phenotype correlation is difficult due to variable expression and mixed phenotype. Genotype-negative individuals from affected pedigrees can exhibit a type 1 Brugada ECG pattern after drug challenge. The aims of this translational study were to study genotype-phenotype correlation in *SCN5A*-E1784K pedigrees using a large, international cohort of mutation carriers and family members, and subsequent characterisation *in vitro* using hiPSC-CMs from *SCN5A*-E1784K carriers with extremes of phenotype (Long QT and BrS phenotype).

Ethnic differences in phenotype were studied (Caucasian, mixed ethnicity and Japanese *SCN5A*-E1784K carriers and their relatives). I showed that events and event-free interval in *SCN5A*-E1784K carriers across ethnic groups were associated with QRS duration, and therefore the degree of associated conduction disease. This was backed up by the association of events with left axis and PR interval. Surprisingly, there was no association with gender, the presence of Long QT or BrS phenotypes or QTc with event-free interval. This indicated a novel marker for risk in channelopathic disease and LQT3.

There were several limitations in the quality of the clinical data available for the study as have been described in Chapter 3. Follow on work would focus on more complete data collection of follow up data and ECGs from participating centres, and enriched phenotyping of a subset with ambulatory ECGs, exercise stress test data and imaging data.

I explored candidate SNPs previously associated with ECG traits (PR, QRS and QTc) in the general population and BrS, derive weighted and unweighted GRSs, and then study their associations with ECG phenotype in this cohort. Indeed, this was the first time that these SNPs have been specifically studied in LQT3, probably owing to the difficulty of obtaining large groups of well phenotyped cases with a single *SCN5A* mutation.

Whilst most SNP associations were insufficiently strong to infer robust conclusions, the QRS GRSs showed transethnic consistency and transferability when correlated to QRS duration. Given the importance of QRS duration and its association with risk for events, this offers an intriguing opportunity to study the utility of a QRS duration and GRS score in risk stratification in *SCN5A* associated syndromes.

In BrS, the association of common variants was cumulative leading to a novel GRS that associated with BrS phenotype in both genotype positive and negative subjects i.e. independent of *SCN5A*-E1784K status, explaining why some WT individuals in *SCN5A* families with BrS phenotype. This finding was replicated in families with other *SCN5A* mutations. *SCN5A* mutations and the BrS-GRS also showed differing effect sizes on BrS phenotype according to variant type (haploinsufficiency or other missense mutations), further confirming a complex polygenic architecture underlying BrS. This has important implications in families where the BrS phenotype is already present. However, further work is required to elucidate other genetic factors to develop an optimised BrS-GRS that may become a surrogate marker for BrS phenotype in *SCN5A* families, form part of clinical genetic testing, obviate drug provocation testing and guide follow-up.

In the functional arm of the study, I recruited patients to the study; harvested fibroblasts; reprogrammed these to hiPSCs; characterised the hiPSCs to demonstrate pluripotency; differentiated these to cardiomyocytes; characterised the cardiomyocytes; and carried out preliminary cellular electrophysiology studies using single cell electrophysiology, albeit limited by low throughput of the technique and time constraints. All hiPSC lines were validated using standard criteria to accepted international standards: morphology characterisation (showing high nuclear to cytoplasmic ratio), demonstration of growth kinetics across at least 15 passages, karyotype, expression of pluripotency markers and *in vitro* differentiation capacity. The differentiated hiPSC-CMs were validated as per internationally agreed standards including demonstration of beating monolayers of cells; Troponin T2 and α-actinin staining to show sarcomeric striations; flow cytometry for purity using Troponin T2; and preliminary electrophysiological characterisation. Despite the limited results of the functional work, the wide array of practical skills in basic translational research that I learned in this arm of the study will be invaluable for my future development as a clinician scientist. Indeed, further work to compare differences in phenotype *in vitro* is required, and ongoing.

Planned future work

My aim following completion of my PhD is to attain an Academic Clinical Lectureship to further develop the skills I have learned whilst studying for this doctorate and to take this forward. Specifically, planned future work will be: 1) Detailed phenotyping of the existing cohort and additional participants including comprehensive follow up data and ambulatory ECG data from each of the existing centres, as well as new centres; 2) a GWAS on an even expanded cohort of families with SCN5A-E1784K and families with other *SCN5A* mutations; 3) Haplotype analyses for SNPs on chromosome 3; 4) sodium current characterisation

of hiPSC-CMs from carriers of extremes of phenotype and study of responses to pharmacological agents. Preliminary work in these areas have already been done as follows.

Detailed clinical characterisation

Detailed phenotyping data will be obtained from existing centres with application of funding for local data collection to overcome issues with resource limitation that limited the follow up data collection during the reported study (as detailed in Chapter 3). Further, each of the other limitations described in Chapter 3 will be addressed, including ambulatory data collection. Where possible, digital ECG and ambulatory ECG data will be collected to improve the accuracy of ECG measurements from participants recruited at sites where another multi-centre study led by our group is already in progress. As such, resources are already available for digital ECG and digital ambulatory ECG data collection (data digitised at 500-1000 Hz) from a subset of participants. For other participants, digital calipers on scanned analogue ECGs and ambulatory ECGs will be used, similarly to the current study, to make as accurate measurements as feasible within the context of clinically available data. These measures, together with increasing the cohort size through a further recruitment drive, will enable a large data set to be built on a richly characterised cohort for a high impact study on the clinical characterisation of an even larger global cohort of *SCN5A*-E1784K pedigrees.

GWAS and whole genome sequencing

In this study, variability in phenotype in *SCN5A*-E1784K, and also in other sodium channel disease in the case of BrS, are associated with common genetic variants previously linked to ECG traits in the general population and disease groups. Further, this study has revealed that the ECG trait phenotypes can be associated

with GRSs. Further work is needed to identify other common variants that could be incorporated to optimise the risk scores. This, a GWAS is planned on an expanded international cohort of patients harbouring *SCN5A*-E1784K, planned to extend to a large cohort of patients carrying other pathogenic *SCN5A* variants. The aim will be to more robustly identify common genetic variants that associate with the risk of:

- BrS phenotype
- Long QT phenotype
- Conduction disease
- Arrhythmic syncope, VT / VF, aborted cardiac arrest or sudden death

Identifying such common variants would enable us to derive optimised GRS for each of the above characteristics, thereby potentially aiding in risk stratification in clinic. Follow on work could involve testing the applicability of the derived GRS in other inherited cardiac conditions, and then potentially the wider population. The inclusion criteria would be patients carrying pathogenic or likely pathogenic *SCN5A* variants and their first-degree relatives. Clinical data, including patient demographics, pedigrees, and clinical characteristics including ECG data and arrhythmic events, will be collected, much as for this project.

The GWAS methodology would involve an Illumina global screening array (GSA) with standard QC, principal component analysis for ethnicity and adjustment for relatedness. The analyses would comprise of a primary analysis of the overall cohort, followed by secondary subgroup analyses by ethnicity. Testing of expanded ECG trait GWAS-derived genetic risk scores will be based upon the most recent data form large-scale GWAS studies that were not available when this project was first conceived: BrS, PR interval, QRS duration, QTc and RR interval.[256] We will also investigate GRS and SNP associations, integrated with QRS duration, with arrhythmia outcomes i.e. time to first events or lethal events. Replication with or

without meta-analyses would be carried out with additional *SCN5A*-E1784K cases and WT relatives as data becomes available, and other *SCN5A* family cohorts.

Whilst GWAS would involve further investigation of common variants, a whole genome sequencing study (WGS) would enable investigation of the effects of lower frequency and rare variants that may not be captured by a standard GWAS.

Despite *SCN5A*-E1784K being the most common *SCN5A* mutation implicated in LQT3 and BrS, due to the limited number of cases worldwide, replication efforts would be dependent on wider collaboration and inclusion of newly diagnosed patients and families. GWAS sample sizes needed for PR, QRS and QTc in *SCN5A*-E1784K individuals are estimated assuming an additive genetic model, 80% power and a two-sided significance threshold of $5x10^{-8}$ for all. For each trait, minimal relevant differences of 2, 5 and 10 milliseconds (ms) are assumed and converted to effect sizes (ES) using the observed standard deviation (SD) in the *SCN5A*-E1784K population.

When considering PR interval and QRS duration, the observed SDs are similar for *SCN5A*-E1784K carriers with their WT relatives and *SCN5A*-E1784K only. For QTc, the SD in the *SCN5A*-E1784K individuals only was 10 ms smaller.

For PR interval with an observed SD of 25.8 ms, the clinically relevant ES are 0.08, 0.19 and 0.39, respectively. For a 2 ms difference, the estimated required sample sizes for a SNP with a minor allele frequency of 0.01, 0.05 or 0.5 are 312488, 65113 and 12355 respectively. For a 5 ms difference, these would be 55383, 11527 and 2174 respectively, and for a 10 ms difference, 13130, 2721 and 501 respectively.

For QRS with an observed SD of 12.9 ms, the clinically relevant ES are 0.16, 0.39 and 0.78, respectively. For a 2 ms difference, the estimated required sample sizes for a SNP with a minor allele frequency of 0.01, 0.05 or 0.5 are 78107, 16263 and 3074 respectively. For a 5 ms difference, these would be 13130, 2721 and 501 respectively, and for a 10 ms difference 3268, 665 and 109 respectively.
For QTc with an observed SD of 41.8 ms, the clinically relevant ES are 0.05, 0.12 and 0.24, respectively. For a 2 ms difference, the estimated required sample sizes for a SNP with a minor allele frequency of 0.01, 0.05 or 0.5 are 800000, 166721 and 31664 respectively. For a 5 ms difference, these would be 138863, 28928 and 5580 respectively, and for a 10 ms difference 34703, 7217 and 1355 respectively. The observed SD in *SCN5A*-E1784K individuals only is smaller, i.e. 30.1, resulting in somewhat larger ES of 0.07, 0.17 and 0.33 and, subsequently, smaller required minimal sample sizes. For a 2 ms difference, the required sample sizes for a SNP with a minor allele frequency of 0.01, 0.05 and 0.5 are 408154, 85052 and 16144 respectively. For a 5 or 10 ms difference the samples sizes were 69186, 14404 and 2721 and 18346, 3808 and 707 respectively.

Table 38 shows the required minimal sample sizes (N) for PR, QRS and QTc at different detectable differences (in ms) and SNP minor allele frequencies. For all estimations, an additive genetic model with 80% power and a two-sided significance level of $5x10^{-8}$ was assumed.

	Total cohort									***SCN5A*-E1784K carriers**		
	For PR and QRS, the variation among carriers/non-carriers is similar									(SD smaller in E1784K)		
	PR	SD	25.8	QRS	SD	12.9	QTc	SD	41.8	QTc	SD	30.1
Difference (ms)	2	5	10	2	5	10	2	5	10	2	5	10
Effect size (ES)	0.08	0.19	0.39	0.16	0.39	0.78	0.05	0.12	0.24	0.07	0.17	0.33
Minor allele frequency	N	N	N	N	N	N	N	N	N	N	N	N
0.01	312488	55383	13130	78107	13130	3268	800000	138873	34703	408154	69186	18346
0.05	65113	11527	2721	16263	2721	665	166721	28928	7217	85052	14404	3808
0.5	12355	2174	501	3074	501	109	31661	5480	1355	16144	2721	707

Table 38. The required minimal sample sizes (N) for PR, QRS and QTc at different detectable differences (in ms) and SNP minor allele frequencies.

With regard to a dichotomous outcome, e.g. BrS yes/no, the minimal required case sample size to find an odds ratio of 2 with 80% power assuming an additive genetic model, a 1:1 case-control ratio and a two-sided significance level of $5x10^{-8}$ are 5945, 1288 and 350 for SNPs with a minor allele frequency of 0.01, 0.05 and 0.5 respectively. The corresponding total minimal sample sizes are 11890, 2576 and 700 individuals. All calculations were performed using Quanto software (Morrison & Gauderman, version 1.2.4, 2009).[257]

Overall, these calculations support the need to increase cohort size and indicate that there will only be the power to detect individual SNPs with large effect sizes. I will therefore focus efforts on generating more substantial and powerful GRSs to find associations.

Haplotype analyses

In addition to individual SNP effects and GRSs arising from the GWAS, as future work, haplotype effects of SNPs in high linkage disequilibrium with the *SCN5A*-E1784K variant will be estimated using a linear mixed model. Per individual, compatible haplotype pairs and their probabilities will be estimated using an Expectation-Maximization (EM) algorithm (haplo.glm() function). Next, the haplotype pair with a probability greater or equal to 0.50 will be assigned as the (most likely) haplotype pair for that individual. The haplotype effects would then be estimated using a linear mixed model with correction for ethnicity and relatedness. Furthermore, given the global prevalence of *SCN5A*-E1784K ancestry analyses of haplotypes will then be undertaken, to understand the evolutionary development of this overlap syndrome. The sample size required for haplotype analyses would be dependent on the degree of linkage disequilibrium. A formal sample calculation is

not possible at this stage as this is dependent on the strength of linkage disequilibrium of two variants within an individual family.

Functional characterisation using hiPSC-CM models

Studying SNP associations with phenotypic extremes of severe QT prolongation or Brugada phenotype will give us further insight into genetic modification. It is plausible that these SNPs may tag haplotype blocks of interest that alter gene expression and affect the late sodium current and the inward sodium current. Deriving patient-derived iPSC-CMs from patients with known SNP associations and attempting to recapitulate their clinical phenotype, will permit further investigation of the molecular mechanisms underlying variable disease expression in this mutation. I therefore aim to generate isogenic controls as part of future functional work to assess the physiological association of patient-specific genomic background on cellular phenotype. Gene editing will be carried out using an oligo-based approach with *in vitro* transcribed gRNA and recombinant Cas9 protein, as described by Kim et al.[258] Amaxa 4D nucleofection has been used in Professor Denning's laboratory to alter polymorphisms at the β2 adrenoceptor locus in hiPSCs with efficiencies of 33%, of which 25% of these colonies had undergone bi-allelic targeting.[187] Whilst the potential to use gene editing to study genetic modifiers and polygenic risk scores would be limited as described on page 191 above, isogenic controls of the *SCN5A*-E1784K cell lines from patients with extremes of phenotype will enable the study of the residual phenotype in the absence of the mutation. The optimised differentiation techniques into more adult ventricular-like cells as described on page 230 would be crucial for the success of this work.

Studying patient-specific responses to provocative (e.g. ajmaline) and therapeutic agents (e.g. mexiletine) *in vitro* could also help risk stratification and guide clinical

management. These clinical data are available for all the patients who have had cells harvested. As I have experienced, relative immaturity of hiPSC-CMs is, however, a limitation with currently available technology. Sudden death associated with Long QT and BrS phenotype rarely, if ever, occurs in the perinatal stage, however the phenotype, particularly Long QT phenotype, is detectable from birth. Thus, even relatively immature hiPSC-CMs would be appropriate as patient-specific *in vitro* models for disease modelling and drug testing. There is good precedence for the use of this model to study the pathophysiology of this mutation using further optimised differentiation and maturation protocols to reduce cellular heterogeneity and improve the robustness of electrophysiological characterisation. Further, the BrS phenotype might be more evident in clusters of cells, and multi-electrode array is more likely to show differences in the BrS phenotype between the lines. This would complement single cell electrophysiology assessment of the cellular phenotype.

cDNA and protein have already been extracted and stored from each batch of differentiation I have carried out. I plan to carry out relative quantification of the WT and mutant *SCN5A* allele expression, and SCN3B expression, using allele-specific TaqMan PCR for unbiased quantification of transcript. I will identify a heterozygotic SNP that is in cis with *SCN5A*-E1784K, and then design one primer that will recognise the mutant strand and the other WT. An alternative approach would be to explore non-sense mediated RNA decay with Western blots using a monoclonal antibody against the WT protein. Healthy adult cardiomyocyte RNA will be used as a positive control and fibroblast RNA as a negative control. The electrophysiological characterisation of these cells will involve evaluation of action potential characteristics, and isolation of the sodium current to compare peak current density, persistent inward current density; and activation and deactivation steady-state and

current dynamics, and pharmacological responses. I will learn principles and techniques of in vitro drug testing, evaluating responses to selective sodium channel blockers that provoke phenotype, as well as responses to therapeutic agents such as beta blockers and mexiletine. Multi-electrode array will be used to generate field potential duration data.

In this way I hope to take forward the work I am already invested in and develop approaches to patient risk stratification and therapy that will be personalised according to clinical and genomic features.

References

References

1. Grant, A. O. Cardiac ion channels. *Circ. Arrhythm. Electrophysiol.* **2**, 185–94 (2009).
2. Nijak, A. *et al.* iPSC-Cardiomyocyte Models of Brugada Syndrome-Achievements, Challenges and Future Perspectives. *Int. J. Mol. Sci.* **22**, (2021).
3. Amin, A. S., Tan, H. L. & Wilde, A. A. M. Cardiac ion channels in health and disease. *Hear. Rhythm* **7**, 117–26 (2010).
4. Tamargo, J., Caballero, R., Gómez, R., Valenzuela, C. & Delpón, E. Pharmacology of cardiac potassium channels. *Cardiovasc. Res.* **62**, 9–33 (2004).
5. Guo, J. *et al.* Interaction between the cardiac rapidly (IKr) and slowly (IKs) activating delayed rectifier potassium channels revealed by low K+-induced hERG endocytic degradation. *J. Biol. Chem.* **286**, 34664–74 (2011).
6. Brandenburg, S., Arakel, E. C., Schwappach, B. & Lehnart, S. E. The molecular and functional identities of atrial cardiomyocytes in health and disease. *Biochim. Biophys. Acta* **1863**, 1882–93 (2016).
7. Boyett, M. R., Honjo, H. & Kodama, I. The sinoatrial node, a heterogeneous pacemaker structure. *Cardiovasc. Res.* **47**, 658–87 (2000).
8. Knol, W. G. *et al.* The Bachmann bundle and interatrial conduction: comparing atrial morphology to electrical activity. *Hear. Rhythm* **16**, 606–614 (2019).
9. Bakker, M. L., Moorman, A. F. M. & Christoffels, V. M. The atrioventricular node: origin, development, and genetic program. *Trends Cardiovasc. Med.* **20**, 164–71 (2010).
10. Temple, I. P., Inada, S., Dobrzynski, H. & Boyett, M. R. Connexins and the

atrioventricular node. *Hear. Rhythm* **10**, 297–304 (2013).

11. Gellens, M. E. *et al.* Primary structure and functional expression of the human cardiac tetrodotoxin-insensitive voltage-dependent sodium channel. *Proc. Natl. Acad. Sci. U. S. A.* **89**, 554–8 (1992).
12. Nerbonne, J. M. & Kass, R. S. Molecular physiology of cardiac repolarization. *Physiol. Rev.* **85**, 1205–53 (2005).
13. Wilde, A. A. M. & Amin, A. S. Clinical Spectrum of SCN5A Mutations: Long QT Syndrome, Brugada Syndrome, and Cardiomyopathy. *JACC. Clin. Electrophysiol.* **4**, 569–579 (2018).
14. Abriel, H. Roles and regulation of the cardiac sodium channel Na v 1.5: recent insights from experimental studies. *Cardiovasc. Res.* **76**, 381–9 (2007).
15. Balser, J. R. The cardiac sodium channel: gating function and molecular pharmacology. *J. Mol. Cell. Cardiol.* **33**, 599–613 (2001).
16. Detta, N., Frisso, G. & Salvatore, F. The multi-faceted aspects of the complex cardiac Nav1.5 protein in membrane function and pathophysiology. *Biochim. Biophys. Acta* **1854**, 1502–9 (2015).
17. Noble, D. & Noble, P. J. Late sodium current in the pathophysiology of cardiovascular disease: consequences of sodium-calcium overload. *Heart* **92 Suppl 4**, iv1–iv5 (2006).
18. Makielski, J. C. Late sodium current: A mechanism for angina, heart failure, and arrhythmia. *Trends Cardiovasc. Med.* **26**, 115–22 (2016).
19. Holm, H. *et al.* Several common variants modulate heart rate, PR interval and QRS duration. *Nat. Genet.* **42**, 117–22 (2010).
20. Chambers, J. C. *et al.* Genetic variation in SCN10A influences cardiac conduction. *Nat. Genet.* **42**, 149–52 (2010).
21. Pfeufer, A. *et al.* Genome-wide association study of PR interval. *Nat. Genet.*

42, 153–9 (2010).

22. Sotoodehnia, N. *et al.* Common variants in 22 loci are associated with QRS duration and cardiac ventricular conduction. *Nat. Genet.* **42**, 1068–76 (2010).
23. Yang, T. *et al.* Blocking Scn10a channels in heart reduces late sodium current and is antiarrhythmic. *Circ. Res.* **111**, 322–32 (2012).
24. Wang, Q. *et al.* SCN5A mutations associated with an inherited cardiac arrhythmia, long QT syndrome. *Cell* **80**, 805–11 (1995).
25. Veerman, C. C. *et al.* The Brugada Syndrome Susceptibility Gene HEY2 Modulates Cardiac Transmural Ion Channel Patterning and Electrical Heterogeneity. *Circ. Res.* **121**, 537–548 (2017).
26. Portero, V. *et al.* Anti-arrhythmic potential of the late sodium current inhibitor GS-458967 in murine Scn5a-1798insD+/- and human SCN5A-1795insD+/- iPSC-derived cardiomyocytes. *Cardiovasc. Res.* **113**, 829–838 (2017).
27. Davis, R. P. *et al.* Cardiomyocytes derived from pluripotent stem cells recapitulate electrophysiological characteristics of an overlap syndrome of cardiac sodium channel disease. *Circulation* **125**, 3079–91 (2012).
28. El-Bizri, N. *et al.* Eleclazine exhibits enhanced selectivity for long QT syndrome type 3-associated late Na+ current. *Hear. Rhythm* **15**, 277–286 (2018).
29. Veerman, C. C. *et al.* hiPSC-derived cardiomyocytes from Brugada Syndrome patients without identified mutations do not exhibit clear cellular electrophysiological abnormalities. *Sci. Rep.* **6**, 30967 (2016).
30. Kapplinger, J. D. *et al.* An international compendium of mutations in the SCN5A-encoded cardiac sodium channel in patients referred for Brugada syndrome genetic testing. *Heart Rhythm* **7**, 33–46 (2010).
31. Tester, D. J., Will, M. L., Haglund, C. M. & Ackerman, M. J. Compendium of cardiac channel mutations in 541 consecutive unrelated patients referred for

long QT syndrome genetic testing. *Heart Rhythm* **2**, 507–17 (2005).

32. Makita, N. *et al.* The E1784K mutation in SCN5A is associated with mixed clinical phenotype of type 3 long QT syndrome. *J. Clin. Invest.* **118**, 2219–29 (2008).
33. Funasako, M. *et al.* Pronounced Shortening of QT Interval With Mexiletine Infusion Test in Patients With Type 3 Congenital Long QT Syndrome. *Circ. J.* **80**, 340–5 (2016).
34. Heather N Anderson, M. D. *et al.* Lidocaine Attenuation Testing: An In Vivo Investigation of Putative LQT3-Associated Variants in the SCN5A-Encoded Sodium Channel. *Hear. Rhythm* (2017) doi:10.1016/j.hrthm.2017.04.020.
35. Hohmann, S. *et al.* Systematic ajmaline challenge in patients with long QT 3 syndrome caused by the most common mutation: a multicentre study. *Europace* (2016) doi:10.1093/europace/euw214.
36. Mazzanti, A. *et al.* Gene-Specific Therapy With Mexiletine Reduces Arrhythmic Events in Patients With Long QT Syndrome Type 3. *J. Am. Coll. Cardiol.* **67**, 1053–8 (2016).
37. Schwartz, P. J., Crotti, L. & George, A. L. Modifier genes for sudden cardiac death. *Eur. Heart J.* **39**, 3925–3931 (2018).
38. Veltmann, C. *et al.* Further Insights in the Most Common SCN5A Mutation Causing Overlapping Phenotype of Long QT Syndrome, Brugada Syndrome, and Conduction Defect. *J. Am. Heart Assoc.* **5**, pii: e003379 (2016).
39. Burashnikov, E. *et al.* Mutations in the cardiac L-type calcium channel associated with inherited J-wave syndromes and sudden cardiac death. *Heart Rhythm* **7**, 1872–82 (2010).
40. Zhang, Q., Chen, J., Qin, Y., Wang, J. & Zhou, L. Mutations in voltage-gated L-type calcium channel: implications in cardiac arrhythmia. *Channels (Austin).* **12**, 201–218 (2018).

41. Cordeiro, J. M. *et al.* Accelerated inactivation of the L-type calcium current due to a mutation in CACNB2b underlies Brugada syndrome. *J. Mol. Cell. Cardiol.* **46**, 695–703 (2009).

42. Antzelevitch, C. *et al.* Loss-of-function mutations in the cardiac calcium channel underlie a new clinical entity characterized by ST-segment elevation, short QT intervals, and sudden cardiac death. *Circulation* **115**, 442–9 (2007).

43. Wong, C. X. *et al.* Epidemiology of Sudden Cardiac Death: Global and Regional Perspectives. *Heart. Lung Circ.* **28**, 6–14 (2019).

44. Perkins, G. D., Brace-McDonnell, S. J. & OHCAO Project Group. The UK Out of Hospital Cardiac Arrest Outcome (OHCAO) project. *BMJ Open* **5**, e008736 (2015).

45. Perkins, G. D. & Cooke, M. W. Variability in cardiac arrest survival: the NHS Ambulance Service Quality Indicators. *Emerg. Med. J.* **29**, 3–5 (2012).

46. London Ambulance Service NHS Trust. *Cardiac arrest annual report : 2016/17*. https://www.londonambulance.nhs.uk/wp-content/uploads/2020/01/Cardiac-Arrest-Annual-Report-2018-2019.pdf (2017).

47. NHS England. *2013/14 NHS Standard Contract for Cardiology: Inherited Cardiac Conditions (All Ages)*. https://www.england.nhs.uk/wp-content/uploads/2017/11/cardiology-inherited-cardiac-conditions.pdf (2013).

48. Papadakis, M. *et al.* Sudden cardiac death with autopsy findings of uncertain significance: potential for erroneous interpretation. *Circ. Arrhythm. Electrophysiol.* **6**, 588–96 (2013).

49. de Noronha, S. V *et al.* The importance of specialist cardiac histopathological examination in the investigation of young sudden cardiac deaths. *Europace* **16**, 899–907 (2014).

50. Behr, E. R. *et al.* Sudden arrhythmic death syndrome: a national survey of

sudden unexplained cardiac death. *Heart* **93**, 601–5 (2007).

51. Mellor, G. *et al.* Clinical characteristics and circumstances of death in the sudden arrhythmic death syndrome. *Circ. Arrhythm. Electrophysiol.* **7**, 1078–83 (2014).
52. Tan, H. L., Hofman, N., van Langen, I. M., van der Wal, A. C. & Wilde, A. A. M. Sudden unexplained death: heritability and diagnostic yield of cardiological and genetic examination in surviving relatives. *Circulation* **112**, 207–13 (2005).
53. Behr, E. R. *et al.* Sudden arrhythmic death syndrome: familial evaluation identifies inheritable heart disease in the majority of families. *Eur. Heart J.* **29**, 1670–80 (2008).
54. Papadakis, M. *et al.* The Diagnostic Yield of Brugada Syndrome After Sudden Death With Normal Autopsy. *J. Am. Coll. Cardiol.* **71**, 1204–1214 (2018).
55. Bastiaenen, R. *et al.* Late gadolinium enhancement in Brugada syndrome: A marker for subtle underlying cardiomyopathy? *Hear. Rhythm* **14**, (2017).
56. Nademanee, K. *et al.* Fibrosis, Connexin-43, and Conduction Abnormalities in the Brugada Syndrome. *J. Am. Coll. Cardiol.* **66**, 1976–86 (2015).
57. Raju, H. & Behr, E. R. Unexplained sudden death, focussing on genetics and family phenotyping. *Curr. Opin. Cardiol.* **28**, 19–25 (2013).
58. Wijeyeratne, Yanushi Dullewe; Behr, E. R. Long QT Syndrome. in *Clinical Cardiogenetics, 2nd edition* (ed. Baars, H.F.; Doevendans, P.A.F.M; Houweling, A.C.; van Tintelen, J. P.) 155–173 (Springer, 2016).
59. Priori, S. G. *et al.* HRS/EHRA/APHRS expert consensus statement on the diagnosis and management of patients with inherited primary arrhythmia syndromes: document endorsed by HRS, EHRA, and APHRS in May 2013 and by ACCF, AHA, PACES, and AEPC in June 2013. *Heart Rhythm* **10**,

1932–63 (2013).

60. Wijeyeratne, Y. D. & Behr, E. R. Sudden death and cardiac arrest without phenotype: the utility of genetic testing. *Trends Cardiovasc. Med.* **27**, (2017).
61. Ackerman, M. J. *et al.* HRS/EHRA expert consensus statement on the state of genetic testing for the channelopathies and cardiomyopathies this document was developed as a partnership between the Heart Rhythm Society (HRS) and the European Heart Rhythm Association (EHRA). *Heart Rhythm* **8**, 1308–39 (2011).
62. Miles, C. J. & Behr, E. R. The role of genetic testing in unexplained sudden death. *Transl. Res.* **168**, 59–73 (2016).
63. Bagnall, R. D., Das K, J., Duflou, J. & Semsarian, C. Exome analysis-based molecular autopsy in cases of sudden unexplained death in the young. *Heart Rhythm* **11**, 655–62 (2014).
64. Richards, S. *et al.* Standards and guidelines for the interpretation of sequence variants: a joint consensus recommendation of the American College of Medical Genetics and Genomics and the Association for Molecular Pathology. *Genet. Med.* **17**, 405–24 (2015).
65. Ackerman, M. J. Genetic purgatory and the cardiac channelopathies: Exposing the variants of uncertain/unknown significance issue. *Hear. Rhythm* **12**, 2325–31 (2015).
66. Refsgaard, L. *et al.* High prevalence of genetic variants previously associated with LQT syndrome in new exome data. *Eur. J. Hum. Genet.* **20**, 905–8 (2012).
67. Risgaard, B. *et al.* High prevalence of genetic variants previously associated with Brugada syndrome in new exome data. *Clin. Genet.* **84**, 489–95 (2013).
68. Jabbari, J. *et al.* New exome data question the pathogenicity of genetic variants previously associated with catecholaminergic polymorphic ventricular

tachycardia. *Circ. Cardiovasc. Genet.* **6**, 481–9 (2013).

69. Kapa, S. *et al.* Genetic testing for long-QT syndrome: distinguishing pathogenic mutations from benign variants. *Circulation* **120**, 1752–60 (2009).
70. MacRae, C. A. Closer look at genetic testing in long-QT syndrome: will DNA diagnostics ever be enough? *Circulation* **120**, 1745–8 (2009).
71. Ackerman, M. J. *et al.* Spectrum and prevalence of cardiac sodium channel variants among black, white, Asian, and Hispanic individuals: implications for arrhythmogenic susceptibility and Brugada/long QT syndrome genetic testing. *Heart Rhythm* **1**, 600–7 (2004).
72. Clinical Genome Resource. ClinGen and ClinVar Partnership. https://www.clinicalgenome.org/data-sharing/clinvar/.
73. Consortium, T. E. A. ExAC Browser (Beta) | Exome Aggregation Consortium. http://exac.broadinstitute.org.
74. Abreu, M. and gnomAD I. gnomAD - Genome Aggregation Database. https://gnomad.broadinstitute.org.
75. Probst, V. *et al.* SCN5A mutations and the role of genetic background in the pathophysiology of Brugada syndrome. *Circ. Cardiovasc. Genet.* **2**, 552–7 (2009).
76. Hedley, P. L. *et al.* The genetic basis of long QT and short QT syndromes: A mutation update. *Human Mutation* vol. 30 1486–1511 (2009).
77. Bezzina, C. R. *et al.* Common variants at SCN5A-SCN10A and HEY2 are associated with Brugada syndrome, a rare disease with high risk of sudden cardiac death. *Nat. Genet.* **45**, 1044–9 (2013).
78. Brugada, P. & Brugada, J. Right bundle branch block, persistent ST segment elevation and sudden cardiac death: a distinct clinical and electrocardiographic syndrome. A multicenter report. *J. Am. Coll. Cardiol.* **20**, 1391–6 (1992).

79. Postema, P. G. About Brugada syndrome and its prevalence. *Europace* **14**, 925–8 (2012).

80. Brugada, P., Brugada, J. & Roy, D. Brugada syndrome 1992-2012: 20 years of scientific excitement, and more. *Eur. Heart J.* **34**, 3610–5 (2013).

81. Wilde, A. A. M. *et al.* Proposed diagnostic criteria for the Brugada syndrome: consensus report. *Circulation* **106**, 2514–9 (2002).

82. Brugada, P. Brugada syndrome: More than 20 years of scientific excitement. *J. Cardiol.* **67**, 215–20 (2016).

83. Wolpert, C. *et al.* Intravenous drug challenge using flecainide and ajmaline in patients with Brugada syndrome. *Hear. Rhythm* **2**, 254–60 (2005).

84. Hasdemir, C. *et al.* High prevalence of concealed Brugada syndrome in patients with atrioventricular nodal reentrant tachycardia. *Hear. Rhythm* **12**, 1584–94 (2015).

85. Antzelevitch, C. *et al.* J-Wave syndromes expert consensus conference report: Emerging concepts and gaps in knowledge. *Hear. Rhythm* **13**, e295-324 (2016).

86. Kawada, S. *et al.* Shanghai Score System for Diagnosis of Brugada Syndrome: Validation of the Score System and System and Reclassification of the Patients. *JACC. Clin. Electrophysiol.* **4**, 724–730 (2018).

87. Wilde, A. A. M. The Shanghai Score System in Brugada Syndrome: Using it Beyond a Diagnostic Score. *JACC. Clin. Electrophysiol.* **4**, 731–732 (2018).

88. Juang, J.-M. J. & Horie, M. Genetics of Brugada syndrome. *J. arrhythmia* **32**, 418–425 (2016).

89. Chen, Q. *et al.* Genetic basis and molecular mechanism for idiopathic ventricular fibrillation. *Nature* **392**, 293–6 (1998).

90. Hosseini, S. M. *et al.* Reappraisal of Reported Genes for Sudden Arrhythmic Death. *Circulation* **138**, 1195–1205 (2018).

91. Priori, S. G., Napolitano, C. & Grillo, M. Concealed arrhythmogenic syndromes: the hidden substrate of idiopathic ventricular fibrillation? *Cardiovasc. Res.* **50**, 218–23 (2001).

92. Yamagata, K. *et al.* Genotype-Phenotype Correlation of SCN5A Mutation for the Clinical and Electrocardiographic Characteristics of Probands With Brugada Syndrome: A Japanese Multicenter Registry. *Circulation* **135**, 2255–2270 (2017).

93. Smits, J. P. P. *et al.* Genotype-phenotype relationship in Brugada syndrome: electrocardiographic features differentiate SCN5A-related patients from non-SCN5A-related patients. *J. Am. Coll. Cardiol.* **40**, 350–6 (2002).

94. Jimmy Juang, J.-M. *et al.* Validation and Disease Risk Assessment of Previously Reported Genome-Wide Genetic Variants Associated With Brugada Syndrome: SADS-TW BrS Registry. *Circ. Genomic Precis. Med.* **13**, e002797 (2020).

95. Choi, S. W., Mak, T. S.-H. & O'Reilly, P. F. Tutorial: a guide to performing polygenic risk score analyses. *Nat. Protoc.* **15**, 2759–2772 (2020).

96. Tadros, R. *et al.* Predicting cardiac electrical response to sodium-channel blockade and Brugada syndrome using polygenic risk scores. *Eur. Heart J.* **40**, 3097–3107 (2019).

97. Catalano, O. *et al.* Magnetic resonance investigations in Brugada syndrome reveal unexpectedly high rate of structural abnormalities. *Eur. Heart J.* **30**, 2241–8 (2009).

98. Tessa, C. *et al.* Evaluation of Brugada syndrome by cardiac magnetic resonance. *Int. J. Cardiovasc. Imaging* **28**, 1961–70 (2012).

99. Papavassiliu, T. *et al.* Spontaneous type 1 electrocardiographic pattern is associated with cardiovascular magnetic resonance imaging changes in Brugada syndrome. *Hear. Rhythm* **7**, 1790–6 (2010).

100. Rouzet, F. *et al.* Contraction delay of the RV outflow tract in patients with Brugada syndrome is dependent on the spontaneous ST-segment elevation pattern. *Hear. Rhythm* **8**, 1905–12 (2011).

101. Antzelevitch, C. *et al.* Brugada syndrome: report of the second consensus conference: endorsed by the Heart Rhythm Society and the European Heart Rhythm Association. *Circulation* **111**, 659–70 (2005).

102. Corrado, D. *et al.* Relationship Between Arrhythmogenic Right Ventricular Cardiomyopathy and Brugada Syndrome: New Insights From Molecular Biology and Clinical Implications. *Circ. Arrhythm. Electrophysiol.* **9**, e003631 (2016).

103. Meregalli, P. G., Wilde, A. A. M. & Tan, H. L. Pathophysiological mechanisms of Brugada syndrome: depolarization disorder, repolarization disorder, or more? *Cardiovasc. Res.* **67**, 367–78 (2005).

104. Hoogendijk, M. G. *et al.* The Brugada ECG pattern: a marker of channelopathy, structural heart disease, or neither? Toward a unifying mechanism of the Brugada syndrome. *Circ. Arrhythm. Electrophysiol.* **3**, 283–90 (2010).

105. Brugada, P. Commentary on the Brugada ECG pattern: a marker of channelopathy, structural heart disease, or neither? Toward a unifying mechanism of the Brugada syndrome. *Circ. Arrhythm. Electrophysiol.* **3**, 280–2 (2010).

106. Postema, P. G. *et al.* Slow and discontinuous conduction conspire in Brugada syndrome: a right ventricular mapping and stimulation study. *Circ. Arrhythm. Electrophysiol.* **1**, 379–86 (2008).

107. Lambiase, P. D. *et al.* High-density substrate mapping in Brugada syndrome: combined role of conduction and repolarization heterogeneities in arrhythmogenesis. *Circulation* **120**, 106–17, 1–4 (2009).

108. Nademanee, K. *et al.* Prevention of ventricular fibrillation episodes in Brugada syndrome by catheter ablation over the anterior right ventricular outflow tract epicardium. *Circulation* **123**, 1270–9 (2011).

109. Coronel, R. *et al.* Right ventricular fibrosis and conduction delay in a patient with clinical signs of Brugada syndrome: a combined electrophysiological, genetic, histopathologic, and computational study. *Circulation* **112**, 2769–77 (2005).

110. Probst, V. *et al.* Long-Term Prognosis of Patients Diagnosed With Brugada Syndrome. *Circulation* **121**, 635–643 (2010).

111. Rodríguez-Mañero, M. *et al.* Long-term prognosis of women with Brugada syndrome and electrophysiological study. *Hear. Rhythm* **18**, 664–671 (2021).

112. Milman, A. *et al.* Time-To-first appropriate shock in patients implanted prophylactically with an implantable cardioverter-defibrillator: Data from the Survey on Arrhythmic Events in BRUgada Syndrome (SABRUS). *Europace* **21**, (2019).

113. Milman, A. *et al.* Profile of Brugada syndrome patients presenting with their first documented arrhythmic event. Data from the Survey on Arrhythmic Events in BRUgada Syndrome (SABRUS). *Heart Rhythm* (2018).

114. Milman, A. *et al.* Age of First Arrhythmic Event in Brugada Syndrome: Data from the SABRUS (Survey on Arrhythmic Events in Brugada Syndrome) in 678 Patients. *Circ. Arrhythmia Electrophysiol.* **10**, (2017).

115. Yan, G. X. & Antzelevitch, C. Cellular basis for the Brugada syndrome and other mechanisms of arrhythmogenesis associated with ST-segment elevation. *Circulation* **100**, 1660–6 (1999).

116. George, A. L. Molecular and genetic basis of sudden cardiac death. *J. Clin. Invest.* **123**, 75–83 (2013).

117. Yuan, M. *et al.* Gender Differences in Prognosis and Risk Stratification of

Brugada Syndrome: A Pooled Analysis of 4,140 Patients From 24 Clinical Trials. *Front. Physiol.* **9**, 1127 (2018).

118. Tadros, R., Ton, A.-T., Fiset, C. & Nattel, S. Sex differences in cardiac electrophysiology and clinical arrhythmias: epidemiology, therapeutics, and mechanisms. *Can. J. Cardiol.* **30**, 783–92 (2014).
119. Liu, S., Yuan, S., Kongstad, O. & Olsson, S. B. Gender differences in the electrophysiological characteristics of atrioventricular conduction system and their clinical implications. *Scand. Cardiovasc. J.* **35**, 313–7 (2001).
120. Antzelevitch, C. Brugada syndrome. *Pacing Clin. Electrophysiol.* **29**, 1130–59 (2006).
121. Macedo, P. G. *et al.* Sleep-disordered breathing in patients with the Brugada syndrome. *Am. J. Cardiol.* **107**, 709–13 (2011).
122. Wu, Q. *et al.* Genetic variants of alcohol-metabolizing enzymes in Brugada syndrome: Insights into syncope after drinking alcohol. *J. arrhythmia* **35**, 752–759 (2019).
123. Dumaine, R. *et al.* Ionic mechanisms responsible for the electrocardiographic phenotype of the Brugada syndrome are temperature dependent. *Circ. Res.* **85**, 803–9 (1999).
124. Keller, D. I. *et al.* Brugada syndrome and fever: genetic and molecular characterization of patients carrying SCN5A mutations. *Cardiovasc. Res.* **67**, 510–9 (2005).
125. Adler, A. *et al.* Fever-induced Brugada pattern: how common is it and what does it mean? *Hear. Rhythm* **10**, 1375–82 (2013).
126. Belhassen, B., Glick, A. & Viskin, S. Efficacy of quinidine in high-risk patients with Brugada syndrome. *Circulation* **110**, 1731–7 (2004).
127. Maury, P., Hocini, M. & Haïssaguerre, M. Electrical storms in Brugada syndrome: review of pharmacologic and ablative therapeutic options. *Indian*

Pacing Electrophysiol. J. **5**, 25–34 (2005).

128. Jervell, A. & Lange-Nielsen, F. Congenital deaf-mutism, functional heart disease with prolongation of the Q-T interval and sudden death. *Am. Heart J.* **54**, 59–68 (1957).

129. Romano, C., Gemme, G. & Pongiglione, R. Rare cardiac arrythmias of the pediatric age. II. Syncopal attacks due to paroxysmal ventricular fibrillation (presentation of 1st case in Italian Pediatric literature). *Clin. Pediatr. (Bologna).* **45**, 656–83 (1963).

130. Ward, O. C. A new familial cardiac syndrome in children. *J. Ir. Med. Assoc.* **54**, 103–6 (1964).

131. Keating, M. *et al.* Linkage of a cardiac arrhythmia, the long QT syndrome, and the Harvey ras-1 gene. *Science* **252**, 704–6 (1991).

132. Jiang, C. *et al.* Two long QT syndrome loci map to chromosomes 3 and 7 with evidence for further heterogeneity. *Nat. Genet.* **8**, 141–7 (1994).

133. Curran, M. E. *et al.* A molecular basis for cardiac arrhythmia: HERG mutations cause long QT syndrome. *Cell* **80**, 795–803 (1995).

134. Wang, Q. *et al.* Positional cloning of a novel potassium channel gene: KVLQT1 mutations cause cardiac arrhythmias. *Nat. Genet.* **12**, 17–23 (1996).

135. Schwartz, P. J. *et al.* Prevalence of the congenital long-QT syndrome. *Circulation* **120**, 1761–7 (2009).

136. Tester, D. J. & Ackerman, M. J. Postmortem long QT syndrome genetic testing for sudden unexplained death in the young. *J. Am. Coll. Cardiol.* **49**, 240–6 (2007).

137. Zareba, W. *et al.* Influence of genotype on the clinical course of the long-QT syndrome. International Long-QT Syndrome Registry Research Group. *N. Engl. J. Med.* **339**, 960–5 (1998).

138. Schwartz, P. J. *et al.* Genotype-phenotype correlation in the long-QT

syndrome: gene-specific triggers for life-threatening arrhythmias. *Circulation* **103**, 89–95 (2001).

139. Priori, S. G. *et al.* Risk stratification in the long-QT syndrome. *N. Engl. J. Med.* **348**, 1866–74 (2003).
140. Sauer, A. J. *et al.* Long QT syndrome in adults. *J. Am. Coll. Cardiol.* **49**, 329–37 (2007).
141. Migdalovich, D. *et al.* Mutation and gender-specific risk in type 2 long QT syndrome: implications for risk stratification for life-threatening cardiac events in patients with long QT syndrome. *Heart Rhythm* **8**, 1537–43 (2011).
142. Chiang, C. E. & Roden, D. M. The long QT syndromes: genetic basis and clinical implications. *J. Am. Coll. Cardiol.* **36**, 1–12 (2000).
143. Priori, S. G. *et al.* 2015 ESC Guidelines for the management of patients with ventricular arrhythmias and the prevention of sudden cardiac death: The Task Force for the Management of Patients with Ventricular Arrhythmias and the Prevention of Sudden Cardiac Death of the Europe. *Eur. Heart J.* **36**, 2793–867 (2015).
144. Schwartz, P. J. & Crotti, L. QTc behavior during exercise and genetic testing for the long-QT syndrome. *Circulation* **124**, 2181–4 (2011).
145. Schwartz, P. J. & Ackerman, M. J. The long QT syndrome: a transatlantic clinical approach to diagnosis and therapy. *Eur. Heart J.* **34**, 3109–16 (2013).
146. Lepeschkin, E. & Surawicz, B. The measurement of the Q-T interval of the electrocardiogram. *Circulation* **6**, 378–88 (1952).
147. Taggart, N. W., Haglund, C. M., Tester, D. J. & Ackerman, M. J. Diagnostic miscues in congenital long-QT syndrome. *Circulation* **115**, 2613–20 (2007).
148. Kukla, P., Biernacka, E. K., Baranchuk, A., Jastrzebski, M. & Jagodzinska, M. Electrocardiogram in Andersen-Tawil syndrome. New electrocardiographic criteria for diagnosis of type-1 Andersen-Tawil syndrome. *Curr. Cardiol. Rev.*

10, 222–8 (2014).

149. ICONICO. Cardio Calipers.

150. Bogossian, H. *et al.* New formula for evaluation of the QT interval in patients with left bundle branch block. *Heart Rhythm* **11**, 2273–7 (2014).

151. Viskin, S. *et al.* Inaccurate electrocardiographic interpretation of long QT: the majority of physicians cannot recognize a long QT when they see one. *Heart Rhythm* **2**, 569–74 (2005).

152. Postema, P. G., De Jong, J. S. S. G., Van der Bilt, I. A. C. & Wilde, A. A. M. Accurate electrocardiographic assessment of the QT interval: teach the tangent. *Heart Rhythm* **5**, 1015–8 (2008).

153. Hibino, S. *et al.* Detection of QT prolongation through approximation of the T wave on Gaussian mixture modeling. *Circ. J.* **77**, 2728–35 (2013).

154. Goldenberg, I., Moss, A. J. & Zareba, W. QT interval: how to measure it and what is 'normal'. *J. Cardiovasc. Electrophysiol.* **17**, 333–6 (2006).

155. Moss, A. J. *et al.* ECG T-wave patterns in genetically distinct forms of the hereditary long QT syndrome. *Circulation* **92**, 2929–34 (1995).

156. Kop, W. J. *et al.* Effects of acute mental stress and exercise on T-wave alternans in patients with implantable cardioverter defibrillators and controls. *Circulation* **109**, 1864–9 (2004).

157. Zareba, W., Moss, A. J., le Cessie, S. & Hall, W. J. T wave alternans in idiopathic long QT syndrome. *J. Am. Coll. Cardiol.* **23**, 1541–6 (1994).

158. Takasugi, N. *et al.* Prevalence of Microvolt T-Wave Alternans in Patients With Long QT Syndrome and Its Association With Torsade de Pointes. *Circ. Arrhythm. Electrophysiol.* **9**, e003206 (2016).

159. Reiffel, A. J. & Reiffel, J. A. QT Prolongation Following Ectopic Beats: Initial Data Regarding The Upper Limit Of Normal With Possible Implications For Antiarrhythmic Therapy And Concealed (Unexpressed) Long QT. *J. Atr.*

Fibrillation **1**, 113 (2009).

160. Veldkamp, M. W. *et al.* Contribution of sodium channel mutations to bradycardia and sinus node dysfunction in LQT3 families. *Circ. Res.* **92**, 976–83 (2003).

161. Wilde, A. A. M. & Behr, E. R. Genetic testing for inherited cardiac disease. *Nat. Rev. Cardiol.* **10**, 571–83 (2013).

162. Splawski, I. *et al.* Spectrum of mutations in long-QT syndrome genes. KVLQT1, HERG, SCN5A, KCNE1, and KCNE2. *Circulation* **102**, 1178–85 (2000).

163. Moss, A. J. *et al.* Clinical aspects of type-1 long-QT syndrome by location, coding type, and biophysical function of mutations involving the KCNQ1 gene. *Circulation* **115**, 2481–9 (2007).

164. Tester, D. J. *et al.* Prevalence and spectrum of large deletions or duplications in the major long QT syndrome-susceptibility genes and implications for long QT syndrome genetic testing. *Am. J. Cardiol.* **106**, 1124–8 (2010).

165. Ghouse, J. *et al.* Rare genetic variants previously associated with congenital forms of long QT syndrome have little or no effect on the QT interval. *Eur. Heart J.* **36**, 2523–9 (2015).

166. Mogensen, J. *et al.* The current role of next-generation DNA sequencing in routine care of patients with hereditary cardiovascular conditions: a viewpoint paper of the European Society of Cardiology working group on myocardial and pericardial diseases and members of the Europ. *Eur. Heart J.* **36**, 1367–70 (2015).

167. Lahrouchi, N. *et al.* Transethnic Genome-Wide Association Study Provides Insights in the Genetic Architecture and Heritability of Long QT Syndrome. *Circulation* **142**, 324–338 (2020).

168. Nolte, I. M. *et al.* Common genetic variation near the phospholamban gene is

associated with cardiac repolarisation: meta-analysis of three genome-wide association studies. *PLoS One* **4**, e6138 (2009).

169. Arking, D. E. *et al.* A common genetic variant in the NOS1 regulator NOS1AP modulates cardiac repolarization. *Nat. Genet.* **38**, 644–51 (2006).
170. Pfeufer, A. *et al.* Common variants at ten loci modulate the QT interval duration in the QTSCD Study. *Nat. Genet.* **41**, 407–14 (2009).
171. Newton-Cheh, C. *et al.* Common variants at ten loci influence QT interval duration in the QTGEN Study. *Nat. Genet.* **41**, 399–406 (2009).
172. Crotti, L. *et al.* NOS1AP is a genetic modifier of the long-QT syndrome. *Circulation* **120**, 1657–63 (2009).
173. Kolder, I. C. R. M. *et al.* Analysis for Genetic Modifiers of Disease Severity in Patients With Long-QT Syndrome Type 2. *Circ. Cardiovasc. Genet.* **8**, 447–56 (2015).
174. Takahashi, K. & Yamanaka, S. Induction of pluripotent stem cells from mouse embryonic and adult fibroblast cultures by defined factors. *Cell* **126**, 663–76 (2006).
175. Takahashi, K. *et al.* Induction of pluripotent stem cells from adult human fibroblasts by defined factors. *Cell* **131**, 861–72 (2007).
176. Zhang, J. *et al.* Functional cardiomyocytes derived from human induced pluripotent stem cells. *Circ. Res.* **104**, e30-41 (2009).
177. Burridge, P. W. *et al.* A universal system for highly efficient cardiac differentiation of human induced pluripotent stem cells that eliminates interline variability. *PLoS One* **6**, e18293 (2011).
178. Zhao, M., Tang, Y., Zhou, Y. & Zhang, J. Deciphering Role of Wnt Signalling in Cardiac Mesoderm and Cardiomyocyte Differentiation from Human iPSCs: Four-dimensional control of Wnt pathway for hiPSC-CMs differentiation. *Sci. Rep.* **9**, 19389 (2019).

179. Mehta, A. *et al.* Phasic modulation of Wnt signaling enhances cardiac differentiation in human pluripotent stem cells by recapitulating developmental ontogeny. *Biochim. Biophys. Acta* **1843**, 2394–402 (2014).

180. Patel, A. K. *et al.* A defined synthetic substrate for serum-free culture of human stem cell derived cardiomyocytes with improved functional maturity identified using combinatorial materials microarrays. *Biomaterials* **61**, 257–65 (2015).

181. Ribeiro, M. C. *et al.* Functional maturation of human pluripotent stem cell derived cardiomyocytes in vitro--correlation between contraction force and electrophysiology. *Biomaterials* **51**, 138–50 (2015).

182. Kang, X. *et al.* Effects of Integrating and Non-Integrating Reprogramming Methods on Copy Number Variation and Genomic Stability of Human Induced Pluripotent Stem Cells. *PLoS One* **10**, e0131128 (2015).

183. Perin, E. C., Miller, L. W., Taylor, D. A. & Willerson, J. T. *Stem Cell and Gene Therapy for Cardiovascular Disease*. (Elsevier, 2016). doi:10.1016/C2014-0-00701-0.

184. Schlaeger, T. M. *et al.* A comparison of non-integrating reprogramming methods. *Nat. Biotechnol.* **33**, 58–63 (2015).

185. Bellin, M. & Mummery, C. L. Inherited heart disease - what can we expect from the second decade of human iPS cell research? *FEBS Lett.* **590**, 2482–93 (2016).

186. Hoekstra, M., Mummery, C. L., Wilde, A. A. M., Bezzina, C. R. & Verkerk, A. O. Induced pluripotent stem cell derived cardiomyocytes as models for cardiac arrhythmias. *Front. Physiol.* **3**, 346 (2012).

187. Denning, C. *et al.* Cardiomyocytes from human pluripotent stem cells: From laboratory curiosity to industrial biomedical platform. *Biochim. Biophys. Acta* **1863**, 1728–48 (2016).

188. Wang, Y. *et al.* Genome editing of isogenic human induced pluripotent stem cells recapitulates long QT phenotype for drug testing. *J. Am. Coll. Cardiol.* **64**, 451–9 (2014).

189. Sala, L., Gnecchi, M. & Schwartz, P. J. Long QT Syndrome Modelling with Cardiomyocytes Derived from Human-induced Pluripotent Stem Cells. *Arrhythmia Electrophysiol. Rev.* **8**, 105–110 (2019).

190. Kasai-Brunswick, T. H. *et al.* Generation of patient-specific induced pluripotent stem cell lines from one patient with Jervell and Lange-Nielsen syndrome, one with type 1 long QT syndrome and two healthy relatives. *Stem Cell Res.* **31**, 174–180 (2018).

191. Zhang, M. *et al.* Recessive cardiac phenotypes in induced pluripotent stem cell models of Jervell and Lange-Nielsen syndrome: disease mechanisms and pharmacological rescue. *Proc. Natl. Acad. Sci. U. S. A.* **111**, E5383-92 (2014).

192. Schwartz, P. J. *et al.* From patient-specific induced pluripotent stem cells to clinical translation in long QT syndrome Type 2. *Eur. Heart J.* **40**, 1832–1836 (2019).

193. de la Roche, J. *et al.* Comparing human iPSC-cardiomyocytes versus HEK293T cells unveils disease-causing effects of Brugada mutation A735V of NaV1.5 sodium channels. *Sci. Rep.* **9**, 11173 (2019).

194. Wijeyeratne, Y. D. *et al.* SCN5A Mutation Type and a Genetic Risk Score Associate Variably With Brugada Syndrome Phenotype in SCN5A Families. *Circ. Genomic Precis. Med.* **13**, e002911 (2020).

195. Okata, S. *et al.* Embryonic type Na(+) channel β-subunit, SCN3B masks the disease phenotype of Brugada syndrome. *Sci. Rep.* **6**, 34198 (2016).

196. R Core Team. R: A language and environment for statistical computing. (2020).

197. Harrell, F. E. J. rms: Regression Modeling Strategies. R package version 6.0-1. (2020).

198. Jason Sinnwell and Terry Therneau. kinship2: Pedigree Functions. R package version 1.8.5. (2020).

199. Therneau, T. M. coxme: Mixed Effects Cox Models. R package version 2.2-16. (2020).

200. Alboukadel Kassambara, M. K. and P. B. survminer: Drawing Survival Curves using 'ggplot2'. R package version 0.4.8. (2020).

201. Meregalli, P. G. *et al.* Type of SCN5A mutation determines clinical severity and degree of conduction slowing in loss-of-function sodium channelopathies. *Hear. Rhythm* **6**, 341–8 (2009).

202. Wilde, A. A. M. *et al.* Clinical Aspects of Type 3 Long-QT Syndrome. *Circulation* **134**, 872–882 (2016).

203. Jamshidi, Y. *et al.* Common variation in the NOS1AP gene is associated with drug-induced QT prolongation and ventricular arrhythmia. *J. Am. Coll. Cardiol.* **60**, 841–850 (2012).

204. Park, J. K., Martin, L. J., Zhang, X., Jegga, A. G. & Benson, D. W. Genetic variants in SCN5A promoter are associated with arrhythmia phenotype severity in patients with heterozygous loss-of-function mutation. *Hear. Rhythm* **9**, 1090–6 (2012).

205. Uziębło-Życzkowska, B., Gielerak, G., Siedlecki, P. & Pająk, B. Genetic diversity of SCN5A gene and its possible association with the concealed form of Brugada syndrome development in Polish group of patients. *Biomed Res. Int.* **2014**, 462609 (2014).

206. Sudandiradoss, C. & Sethumadhavan, R. In silico investigations on functional and haplotype tag SNPs associated with congenital long QT syndromes (LQTSs). *Genomic Med.* **2**, 55–67 (2008).

207. Machiela, M. J. & Chanock, S. J. LDlink: a web-based application for exploring population-specific haplotype structure and linking correlated alleles of possible functional variants. *Bioinformatics* **31**, 3555–7 (2015).

208. LGC. Genotyping manuals: KASP Genotyping. (2018).

209. Balduzzi, S., Rücker, G. & Schwarzer, G. How to perform a meta-analysis with R: a practical tutorial. *Evid. Based. Ment. Health* **22**, 153–160 (2019).

210. Smith, J. G. *et al.* Genome-Wide Association Studies of the PR Interval in African Americans. *PLoS Genet.* **7**, e1001304 (2011).

211. Moskowitz, I. P. G. *et al.* A Molecular Pathway Including Id2, Tbx5, and Nkx2-5 Required for Cardiac Conduction System Development. *Cell* **129**, 1365–1376 (2007).

212. Mesbah, K., Harrelson, Z., Théveniau-Ruissy, M., Papaioannou, V. E. & Kelly, R. G. Tbx3 Is Required for Outflow Tract Development. *Circ. Res.* **103**, 743–750 (2008).

213. Mori, A. D. *et al.* Tbx5-dependent rheostatic control of cardiac gene expression and morphogenesis. *Dev. Biol.* **297**, 566–586 (2006).

214. Hüls, A. *et al.* Comparison of weighting approaches for genetic risk scores in gene-environment interaction studies. *BMC Genet.* **18**, 115 (2017).

215. Kassambara, A., Kosinski, M. & Biecek, P. survminer: Drawing Survival Curves using 'ggplot2'. R package version 0.4.8. (2020).

216. Kapplinger, J. D. *et al.* An international compendium of mutations in the SCN5A-encoded cardiac sodium channel in patients referred for Brugada syndrome genetic testing. *Heart Rhythm* **7**, 33–46 (2010).

217. Whiffin, N. *et al.* CardioClassifier: disease- and gene-specific computational decision support for clinical genome interpretation. *Genet. Med.* **20**, 1246–1254 (2018).

218. Denham, N. C. *et al.* Systematic re-evaluation of SCN5A variants associated

with Brugada syndrome. *J. Cardiovasc. Electrophysiol.* **30**, 118–127 (2019).

219. Bethesda (MD): National Center for Biotechnology Information, N. L. of M. Database of Single Nucleotide Polymorphisms (dbSNP). *dbSNP Build ID: 151* https://www.ncbi.nlm.nih.gov/snp.
220. Makarawate, P. *et al.* Common and rare susceptibility genetic variants predisposing to Brugada syndrome in Thailand. *Hear. Rhythm* **17**, 2145–2153 (2020).
221. van den Boogaard, M. *et al.* A common genetic variant within SCN10A modulates cardiac SCN5A expression. *J. Clin. Invest.* **124**, 1844–52 (2014).
222. van den Boogaard, M. *et al.* Genetic variation in T-box binding element functionally affects SCN5A/SCN10A enhancer. *J. Clin. Invest.* **122**, 2519–30 (2012).
223. Halekoh, U., Hojsgaard, S. & Jun, Y. The R Package geepack for Generalized Estimating Equations. *J. Stat. Softw.* **15**, 1–11 (2006).
224. Baruteau, A.-E. *et al.* SCN5A mutations in 442 neonates and children: genotype-phenotype correlation and identification of higher-risk subgroups. *Eur. Heart J.* **39**, 2879–2887 (2018).
225. Schwartz, P. J. & Gentilini, D. Can genetics predict risk for sudden cardiac death? The relentless search for the Holy Grail. *Eur. Heart J.* **39**, 3970–72 (2018).
226. Priori, S. G. *et al.* A novel form of short QT syndrome (SQT3) is caused by a mutation in the KCNJ2 gene. *Circ. Res.* **96**, 800–7 (2005).
227. Ekins, S., Mestres, J. & Testa, B. In silico pharmacology for drug discovery: applications to targets and beyond. *Br. J. Pharmacol.* **152**, 21–37 (2007).
228. Mosqueira, D. *et al.* CRISPR/Cas9 editing in human pluripotent stem cell-cardiomyocytes highlights arrhythmias, hypocontractility, and energy depletion as potential therapeutic targets for hypertrophic cardiomyopathy.

Eur. Heart J. **39**, 3879–3892 (2018).

229. Wu, J. C. *et al.* Towards Precision Medicine With Human iPSCs for Cardiac Channelopathies. *Circ. Res.* **125**, 653–658 (2019).

230. Liu, X. *et al.* CRISPR-Cas9-mediated multiplex gene editing in CAR-T cells. *Cell Res.* **27**, 154–157 (2017).

231. REPROCELL. Increase detection of positive clones 30X with CRISPR-SNIPER. https://www.reprocell.com/blog/5-ways-to-enhance-your-gene-editing (2020).

232. Carlson-Stevermer, J. *et al.* Design of efficacious somatic cell genome editing strategies for recessive and polygenic diseases. *Nat. Commun.* **11**, 6277 (2020).

233. Spencer, C. I. *et al.* Calcium transients closely reflect prolonged action potentials in iPSC models of inherited cardiac arrhythmia. *Stem cell reports* **3**, 269–81 (2014).

234. Ma, D. *et al.* Modeling type 3 long QT syndrome with cardiomyocytes derived from patient-specific induced pluripotent stem cells. *Int. J. Cardiol.* **168**, 5277–86 (2013).

235. Yoshinaga, D. *et al.* Phenotype-Based High-Throughput Classification of Long QT Syndrome Subtypes Using Human Induced Pluripotent Stem Cells. *Stem cell reports* **13**, 394–404 (2019).

236. Hirose, S. *et al.* Propranolol Attenuates Late Sodium Current in a Long QT Syndrome Type 3-Human Induced Pluripotent Stem Cell Model. *Front. cell Dev. Biol.* **8**, 761 (2020).

237. Furutani, Y. *et al.* Establishment of an In Vitro LQT3 model Using Induced Pluripotent Stem Cells from LQT3 Patient-Derived Cardiomyocytes. in *Molecular Mechanism of Congenital Heart Disease and Pulmonary Hypertension* 393–394 (2020).

238. Li, W. *et al.* Disease Phenotypes and Mechanisms of iPSC-Derived Cardiomyocytes From Brugada Syndrome Patients With a Loss-of-Function SCN5A Mutation. *Front. cell Dev. Biol.* **8**, 592893 (2020).

239. Paci, M., Passini, E., Severi, S., Hyttinen, J. & Rodriguez, B. Phenotypic variability in LQT3 human induced pluripotent stem cell-derived cardiomyocytes and their response to antiarrhythmic pharmacologic therapy: An in silico approach. *Hear. Rhythm* **14**, 1704–1712 (2017).

240. Duncan, G. *et al.* Drug-Mediated Shortening of Action Potentials in LQTS2 Human Induced Pluripotent Stem Cell-Derived Cardiomyocytes. *Stem Cells Dev.* **26**, 1695–1705 (2017).

241. Minami, I. *et al.* A small molecule that promotes cardiac differentiation of human pluripotent stem cells under defined, cytokine- and xeno-free conditions. *Cell Rep.* **2**, 1448–60 (2012).

242. Burridge, P. W. *et al.* Chemically defined generation of human cardiomyocytes. *Nat. Methods* **11**, 855–60 (2014).

243. Kattman, S. J., Witty, A. D., Gagliardi, M., Dubois, N. C. & Niapour, M. Supplemental Information Stage-Specific Optimization of Activin / Nodal and BMP Signaling Promotes Cardiac Differentiation of Mouse and Human Pluripotent Stem Cell Lines. **8**,.

244. Parikh, S. S. *et al.* Thyroid and Glucocorticoid Hormones Promote Functional T-Tubule Development in Human-Induced Pluripotent Stem Cell-Derived Cardiomyocytes. *Circ. Res.* **121**, 1323–1330 (2017).

245. El-Battrawy, I. *et al.* Hyperthermia Influences the Effects of Sodium Channel Blocking Drugs in Human-Induced Pluripotent Stem Cell-Derived Cardiomyocytes. *PLoS One* **11**, e0166143 (2016).

246. Steichen, C., Hannoun, Z., Luce, E., Hauet, T. & Dubart-Kupperschmitt, A. Genomic integrity of human induced pluripotent stem cells: Reprogramming,

differentiation and applications. *World J. Stem Cells* **11**, 729–747 (2019).

247. van den Brink, L. *et al.* Cryopreservation of human pluripotent stem cell-derived cardiomyocytes is not detrimental to their molecular and functional properties. *Stem Cell Res.* **43**, 101698 (2020).

248. Lewandowski, J. *et al.* The impact of in vitro cell culture duration on the maturation of human cardiomyocytes derived from induced pluripotent stem cells of myogenic origin. *Cell Transplant.* **27**, 1047–1067 (2018).

249. Verkerk, A. O. *et al.* Patch-Clamp Recording from Human Induced Pluripotent Stem Cell-Derived Cardiomyocytes: Improving Action Potential Characteristics through Dynamic Clamp. *Int. J. Mol. Sci.* **18**, (2017).

250. López-Redondo, F. *et al.* A distribution analysis of action potential parameters obtained from patch-clamped human stem cell-derived cardiomyocytes. *J. Pharmacol. Sci.* **131**, 141–5 (2016).

251. Fuerstenau-Sharp, M. *et al.* Generation of highly purified human cardiomyocytes from peripheral blood mononuclear cell-derived induced pluripotent stem cells. *PLoS One* **10**, e0126596 (2015).

252. Lin, B. *et al.* Culture in Glucose-Depleted Medium Supplemented with Fatty Acid and 3,3',5-Triiodo-l-Thyronine Facilitates Purification and Maturation of Human Pluripotent Stem Cell-Derived Cardiomyocytes. *Front. Endocrinol. (Lausanne).* **8**, 253 (2017).

253. Funakoshi, S. *et al.* Generation of mature compact ventricular cardiomyocytes from human pluripotent stem cells. *Nat. Commun.* **12**, 3155 (2021).

254. Goldfracht, I. *et al.* Generating ring-shaped engineered heart tissues from ventricular and atrial human pluripotent stem cell-derived cardiomyocytes. *Nat. Commun.* **11**, 75 (2020).

255. Lemoine, M. D. *et al.* Human iPSC-derived cardiomyocytes cultured in 3D

engineered heart tissue show physiological upstroke velocity and sodium current density. *Sci. Rep.* **7**, 5464 (2017).

256. Arking, D. E. *et al.* Genetic association study of QT interval highlights role for calcium signaling pathways in myocardial repolarization. *Nat. Genet.* **46**, 826–836 (2014).

257. Gauderman, W. & Morrison, J. QUANTO 1.2.4: A Computer Program for Power and Sample Size Calculations for Genetic-Epidemiology Studies. (2009).

258. Kim, S., Kim, D., Cho, S. W., Kim, J. & Kim, J. S. Highly efficient RNA-guided genome editing in human cells via delivery of purified Cas9 ribonucleoproteins. *Genome Res.* **24**, 1012–1019 (2014).

Appendices

Appendix 1: ECG trait GRSs in wild-type individuals

Variable	All WT individuals (n=104)		Caucasian (n=49)		Japanese (n=15)		Other/mixed ethnicity (n=40)		p-value
	Mean	SD	Mean	SD	Mean	SD	Mean	SD	
PR.GRS	4.51	2.10	5.24	2.13	2.67	0.58	3.81	1.83	0.0250
QRS.GRS	2.05	3.36	2.43	3.48	1.00	0.00	1.71	3.43	0.8403
QTc.GRS	3.50	1.81	3.68	1.49	4.50	0.71	3.22	2.15	0.7667
PR.wGRS	10.78	4.70	12.44	4.75	5.43	1.33	9.29	3.97	0.0145
QRS.wGRS	0.77	1.89	1.03	1.91	-0.18	0.26	0.57	1.95	0.6541
QTc.wGRS	5.93	3.13	6.39	2.73	7.13	0.62	5.31	3.58	0.7438

Appendix Table 1. Descriptive characteristics for unweighted and weighted genetic risk scores (GRS and wGRS respectively) in WT individuals from *SCN5A*-E1784K families (all *WT individuals* and separated by ethnicity).

GRS	B	SE	p-value	Cohort
PR.GRS	0.3	1.1	0.7934	All WT individuals
PR.GRS	-2.0	1.5	0.1933	Caucasian WT individuals
PR.GRS	2.7	1.5	0.0739	Other WT individuals
PR.wGRS	0.0	0.5	0.9390	All WT individuals
PR.wGRS	-1.0	0.7	0.1272	Caucasian WT individuals
PR.wGRS	1.1	0.7	0.1007	Other WT individuals

Appendix Table 2. Effects of unweighted and weighted genetic risk scores (GRS) on PR.age in WT individuals from *SCN5A*-E1784K families adjusted for male gender (and ethnicity for the total cohort). None were statistically significant.

GRS	B	SE	p-value	Cohort
QRS.GRS	1.4	0.4	0.0001	All WT individuals
QRS.GRS	1.4	0.6	0.0143	Caucasian WT individuals
QRS.GRS	1.3	0.4	0.0029	Other WT individuals
QRS.wGRS	2.4	0.7	0.0003	All WT individuals
QRS.wGRS	2.1	1.1	0.0464	Caucasian WT individuals
QRS.wGRS	2.5	0.8	0.0008	Other WT individuals

Appendix Table 3. Effects of unweighted and weighted genetic risk scores (GRS) on QRS.age in WT individuals from *SCN5A*-E1784K families. p<0.05 are highlighted in red and p-values that remained statistically significant after Bonferroni correction are highlighted in green.

GRS	B	SE	p-value	Cohort
QTc.GRS	2.7	1.3	0.0378	All WT individuals
QTc.GRS	-0.5	1.6	0.7447	Caucasian WT individuals
QTc.GRS	4.9	2.1	0.0225	Other WT individuals
QTc.wGRS	1.7	0.8	0.0276	All WT individuals
QTc.wGRS	-0.4	0.9	0.6482	Caucasian WT individuals
QTc.wGRS	3.4	1.2	0.0060	Other WT individuals

Appendix Table 4. Effects of unweighted and weighted genetic risk scores (GRS) on QTc.age in WT individuals from *SCN5A*-E1784K families. p<0.05 are highlighted in red and p-values that remained statistically significant after Bonferroni correction are highlighted in green.

Appendix 2: ECG trait GRS meta-analyses

GRS	I2 (Indicator of heterogeneity)	p-value
PR.GRS	51%	0.1309
PR.wGRS	50%	0.1359
QRS.GRS	75%	0.0186
QRS.wGRS	79%	0.0091
QTc.GRS	76%	0.0152
QTc.wGRS	68%	0.0423

Appendix Table 5. Meta-analysis for heterogeneity by ethnicity of the unweighted and weighted genetic risk scores (GRS) in all individuals from *SCN5A*-E1784K families (*SCN5A*-E1784K carriers and WT individuals). p<0.05 are highlighted in red and p-values that remained statistically significant after Bonferroni correction are highlighted in green.

GRS	I2 (Inidicator of heterogeneity)	p-value
PR.GRS	24%	0.2685
PR.wGRS	38%	0.1988
QRS.GRS	92%	0.0000
QRS.wGRS	83%	0.0032
QTc.GRS	0%	0.6416
QTc.wGRS	0%	0.5748

Appendix Table 6. Meta-analysis for heterogeneity by ethnicity of the unweighted and weighted genetic risk scores (GRS) in *SCN5A*-E1784K carriers. p-values that remained statistically significant after Bonferroni correction are highlighted in green.

GRS	I2 (Indicator of heterogeneity)	p-value
PR.GRS	79%	0.0288
PR.wGRS	80%	0.0251
QRS.GRS	0%	0.9382
QRS.wGRS	0%	0.7725
QTc.GRS	76%	0.0423
QTc.wGRS	84%	0.0120

Appendix Table 7. Meta-analysis for heterogeneity by ethnicity of the unweighted and weighted genetic risk scores (GRS) in WT individuals from *SCN5A*-E1784K families. p<0.05 are highlighted in red and p-values that remained statistically significant after Bonferroni correction are highlighted in green.

Appendix 3: Reagents

List of reagents

Accutase (A6964)

Acetone (67-64-1)

Activin A recombinant human (PHC9564)

Antibodies:

- Rabbit polyclonal Nav1.5 (custom-made antibody from Dr Angeliki Asimaki – Dr Hughes Ariel) - diluted 1:80
- Mouse TNNT2 (ab8295) - diluted 1:200
- Cy3-conjugated goat anti-rabbit (ab6939) - diluted 1:400
- Cy3-conjugated goat anti-mouse (A10521) - diluted 1:400

Antifade mounting medium with DAPI (H-1200)

B27 supplement (0080085-SA)

B27 supplement minus insulin (0050129SA)

Bovine serum albumin, BSA (A7030)

BMP4, recombinant human (314-BP)

BTS solution: N-benzyl-p-toluene sulphonamide (BTS) in 30 mM in DMSO (sterile-filtered using PTFE filters)

β-mercaptoethanol (21985-023)

Collagenase II solution: 200 U/ml in HBSS, sterile-filtered (17101015)

CytoTune® 2.0 Sendai reprogramming vectors (A16517)

Dexamethasone (11015)

DMEM (21969-035)

DMSO (D2650)

DNase (D8764)

Dulbecco's Phosphate Buffered Saline, DPBS (no $CaCl_2$ / $MgCl_2$) (14190-169)

EDTA 0.5M (15575020)

Essential 6 (E6) medium (A1516401)

Essential 8 medium (E8) medium (A1517001)

Fetal Bovine Serum (FBS) (F9665)

FGF (basic), recombinant human (PHG0264)

Glacial acetic acid (Fisher Chemical)

GlutaMAX™-I Supplement (100x) (35050-038)

KaryoMAX COLCEMID 10ug/mL (15212-012)

KnockOut™ Serum Replacement (KSR) (10828-028)

KY02111 (4731/10)

L-Glutamine 200mM (100x) (25030-024)

Matrigel, Corning Matrigel Basement Membrane Matrix (354234)

MEM Non-essential Amino Acids, NEAA (11140-035)

Methanol (HPLC grade, Fisher Chemical)

Normal goat serum (16210064)

Penicillin-Streptomycin (P0781)

Paraformaldehyde (PFA) 4% (SC-281692)

ROCK inhibitor Y-27632 (Y1000)

RPMI Medium 1640 (21875-034)

RPMI 1640 Medium, no glucose (11560406)

Sodium-L-Lactate (Sigma- 71718)

StemPro-34 (10639-011)

T3 (Sigma T2877)

Trypsin-EDTA 0.05% (25300)

Tri-sodium citrate (Fisher Chemical S/3320/53)

Triton X-100 (T8532)

TryplE (12563-029)

Tween (P5927)

Vitronectin (A14700)

XAV939 (3748/10)

Preparation of reagents

Activin A – 5ug/ml Recombinant human Activin A stock solution was prepared by reconstituting lyophilised powder using 0.1% BSA in distilled H_20 as per manufacturer's instructions and aliquoted.

B-GK medium – 85% DMEM + 15% KSR + 1% GlutaMAX + 1% NEAA + 100μM β-mercaptoethanol.

Blocking buffer for hiPSC-CM dissociation - 24 μg DNase/ml in RPMI

BMP4 – 10ug/ml recombinant human BMP4 stock solution was prepared by reconstituting lyophilised powder using 0.1% BSA in distilled H_20 as per manufacturer's instructions and aliquoted.

CDS – 40% RPMI +40% cell dissociation buffer + 20% TryplE.

Fibroblast Medium – 78% DMEM + 20% FBS + 1% GlutaMAX + 1% NEAA + 100 μM β-mercaptoethanol.

EDTA – 0.5µM EDTA in DPBS.

KY02111 - 10mM KY02111 stock solution was made up in DMSO at 55°C as per manufacturer's instructions and aliquoted.

Lactate enrichment medium - RPMI 1640 (no glucose) supplemented with sodium-L-Lactate (4mM final concentration)

ROCK (Rho-associated protein kinase) inhibitor – 10mM stock solution was prepared by dissolving in DPBS and aliquoted.

XAV939 – 10mM XAV939 stock solution was prepared by dissolving in DMSO at 55°C as per manufacturer's instructions and aliquoted.